DEVELOPING TEST PROTOCOLS TO DETERMINE GEOSYNTHETIC MATERIAL PROPERTIES THAT BETTER REPRESENT TRAFFIC LOADING CONDITIONS

Final Report

by

Eli Cuelho

&

Suresh Ganeshan

of the

Western Transportation Institute
College of Engineering
Montana State University - Bozeman

November 2004

ACKNOWLEDGEMENTS

The authors would like to extend their appreciation to the University Transportation Center at the Western Transportation Institute (WTI) for their sponsorship and participation in this project. Also, many thanks to Suresh Ganeshan who worked so diligently to complete the many tasks associated with this project. This project truly wouldn't have been successful without his dedication and hard work.

DISCLAIMER

ALTERNATIVE FORMAT STATEMENT

The Western Transportation Institute attempts to provide reasonable accommodations for any known disability that may interfere with a person participating in any service, program, or activity. Alternative accessible formats of this document will be provided upon request. Persons with disabilities who need an alternative accessible format of this information, or who require some other reasonable accommodation to participate, should contact Kate Heidkamp, Communications and Information Systems Manager, Western Transportation Institute, Montana State University-Bozeman, PO Box 174250, Bozeman, MT 59717-4250, telephone number 406-994-7018, e-mail: katel@coe.montana.edu.

ABSTRACT

Geosynthetics have been successfully used for filtration, separation, drainage, moisture barriers and reinforcement in flexible pavements. Using them to reinforce the base layer of flexible pavements may provide savings either by reducing the thickness of the base or extending the life of the road. To quantify their potential benefit, it is essential to evaluate their intrinsic material properties under conditions pertinent to pavements. Standard tension tests, such as ASTM D 4595 and D 6637, apply monotonic loads to the materials to determine elastic moduli in their two principal directions. However, the types of loading conditions prescribed by these tests do not reflect conditions experienced by geosynthetics used as reinforcement in flexible pavements. Even though multiple research studies have been carried out to determine the effects of load rate, type of load, temperature, sample size and configuration, and normal confinement on geosynthetic material properties, results to-date are either limited, not applicable, or conflicting according to literature reviewed as part of this study. Therefore, the purpose of this research was to develop test protocols that better describe the intrinsic material properties of geosynthetics pertinent to reinforced pavement design applications. Accordingly, cyclic loads and, to some extent, various strain rates and samples sizes were used to study their effect on these parameters.

Three geotextiles and four geogrids were tested to compare their unconfined load/strain properties under monotonic and cyclic loads. Monotonic test protocols were used to study the effects of strain rate and specimen size on material properties. Wide-width monotonic tests were compared to wide-width cyclic tests. All testing was conducted using a servo-hydraulic loading system equipped with Curtis GeoGrips.

Results from cyclic tests conducted on the geotextiles generally showed that the stiffness remained constant for all 1000 load cycles at a particular load level but that the stiffness increased significantly from one step to the next. Geogrids exhibited an opposite effect, in that the stiffness increased with increasing number of load cycles within a given load step, but did not change from step to step. Monotonic test results showed that the initial stiffness decreased as axial strain increased for geogrids, but remained constant for geotextiles.

In most cases, the geosynthetics tested in this research showed noticeable changes in stiffness when strained at rates varying between 0.03% and 20% per minute. As expected, in nearly all cases the material behaved more stiffly as the strain rate increased. Tests conducted using varying samples sizes revealed that both length and width have a significant effect on the stiffness for the Amoco 2006 and Tensar BX1100 materials, tested in the machine direction. Additional work is necessary to fully establish the influence of load type, strain rate, temperature and confinement on the measured elastic modulus for conditions pertinent in pavements.

TABLE OF CONTENTS

LIST OF TABLES

LIST OF FIGURES

1 INTRODUCTION

Geosynthetics have been successfully used for filtration, separation, drainage, moisture barriers and reinforcement in flexible pavements. Using them to reinforce the base layer of flexible pavements may provide savings either by reducing the thickness of the base or extending the life of the road. To quantify their potential benefit, it is essential to evaluate their intrinsic material properties under conditions pertinent to pavements. Standard tension tests, such as ASTM D 4595 and D 6637 (used for conducting tension tests on geotextiles and geogrids, respectively – ASTM, 2003) apply monotonic loads to the materials to determine elastic moduli in their two principal directions. However, the types of loading conditions prescribed by these tests do not reflect conditions experienced by geosynthetics used to reinforce flexible pavements. Even though multiple research studies have been carried out to determine the effects of load rate, type of load, temperature, sample size and configuration, and normal confinement on geosynthetic material properties, results to-date are either limited, not applicable, or conflicting. Therefore, the first objective of this project was to investigate test protocols that better describe the intrinsic material properties of geosynthetics pertinent to reinforced pavement design applications. To accomplish this, an extensive literature of past research was reviewed and summarized to evaluate the effect of temperature, strain rate, confinement, and load type (i.e., monotonic or cyclic) on geosynthetic material properties.

A new mechanistic-empirical design guide for flexible pavements is currently under development and review by American Association of State Highway and Transportation Officials (AASHTO) through the National Cooperative Highway Research Program (NCHRP) Project 1-37A (NCHRP, 2003). This new method, however, does not address geosynthetic reinforcement of the base layer. Perkins et al. (2004) has developed a design method for geosynthetic-reinforced pavements that is compatible with the methods developed in NCHRP Project 1-37A (NCHRP, 2003). A finite element model (FEM), developed by Perkins et al. (2004), uses structural membrane elements for the reinforcement. Mechanistic material models are an essential component; therefore, material models that describe the geosynthetic reinforcement layer needed to be developed. Therefore, the second objective of this research was to conduct laboratory tests that appropriately describe the constitutive material properties of geosynthetics to reinforce pavement structures, as input parameters into a FEM. Available time and resources permitted only load type and, to some extent, various strain rates to be conducted and studied with regard to their effect on geosynthetic material parameters. A side study of the effect of sample size was also conducted.

1.1 Background

It is well known that geosynthetic reinforcement materials exhibit direction dependent properties. Most notably, the elastic modulus differs between the machine and cross-machine direction of the material. An orthotropic material model best describes the direction dependent properties of reinforcement materials but cannot be used directly in a 2-D axisymmetric finite element model. An orthotropic linear elastic material model contains nine independent elastic constants, four of which describe the behavior within the plane of the material (E_{xm}, E_m, $\nu_{xm\text{-}m}$, $G_{xm\text{-}m}$) and are pertinent to a reinforcement sheet modeled by membrane elements. These parameters are defined as follows:

- E_{xm} is the elastic modulus in the cross-machine direction
- E_m is the elastic modulus in the machine direction
- $\nu_{xm\text{-}m}$ is the Poisson's ratio in the cross-machine/machine plane
- $G_{xm\text{-}m}$ is the shear modulus in the cross-machine/machine plane

The elastic moduli in the two principal directions are generally determined from tension tests, the in-plane Poisson's ratio can be determined from biaxial tension tests, and there is no current test to directly determine the in-plane shear modulus. Kinney and Xiaolin (1995) developed a test to determine a parameter called the aperture stability modulus, which can be related to the in-plane shear modulus of the material.

The response model used by Perkins et al. (2004) was a two-dimensional axisymmetric finite element model based on models contained in NCHRP Project 1-37A (NCHRP, 2003). Axisymmetric response models require that the reinforcement be described by an isotropic material model, which is incapable of distinguishing direction dependent material properties (i.e., machine versus cross-machine direction). Since the material models for the remaining pavement layers are elastic, a model of similar complexity was chosen for the reinforcement. Even though many reinforcement materials exhibit non-linear behavior, this behavior is ignored for the sake of simplicity when attempting to select properties pertinent to the stress or strain range anticipated for the material. Hence, an isotropic linear elastic model is used for the reinforcement within the finite element response model, where required input parameters consist of an elastic modulus, E, and a Poisson's ratio, ν. Equivalent isotropic elastic constants are calculated from orthotropic constants using a relationship derived from a work-energy approach described by Perkins et al. (2004). The work described in this report focuses on determining the elastic modulus in both principal strength directions, that is, E_m and E_{xm}, the elastic moduli in the machine and cross-machine directions, respectively.

1.2 Organization of This Report

Chapter 2 provides the results of an extensive literature review of various factors affecting geosynthetics testing. Load type, specimen size and aspect ratio, strain rate, and temperature are all considered. In addition, various strain measuring devices are discussed.

Chapter 3 describes the laboratory equipment used to test the various geosynthetics. Specifically, the loading system, gripping mechanism, and instrumentation are described. The seven geosynthetics used in this research are described in this section, as well as how individual samples were prepared for testing.

Chapter 4 details the two main test protocols used to test the geosynthetics. Monotonic tests were conducted to determine effects due to strain rate and specimen size. Cyclic tests were compared to standard monotonic tests.

Chapter 5 summarizes the analysis of the test results. Comparisons are made between cyclic and tangent modulus, and the effects of strain rate and specimen size on secant modulus are summarized.

Finally, **Chapter 6** summarizes and concludes all the work conducted as part of this research project, as well as provides suggestions for future research.

2 LITERATURE REVIEW

Traditionally, wide-width tension testing is used to determine material properties of geosynthetics. These tests use monotonic loads and are applied at relatively slow rates (10% axial strain per minute), representing situations where movements are slow and steady. However, when geosynthetics are used as reinforcement in the base layer of pavements, they experience cyclic loading from traffic. Other conditions pertinent to the reinforced pavement application that may not be accounted for in traditional wide-width tests include: variations in load type (cyclic or monotonic), specimen size and aspect ratio, strain rate, temperature, and normal stress confinement. In addition, various methods employed to measure strain during testing were also summarized. An extensive literature review examined test conditions that influence geosynthetic material properties. Following is a summary of all relevant literature collected as part of this work.

2.1 Cyclic and Monotonic Loads

Ashmawy and Bourdeau (1996) conducted simple tension tests to investigate the stress-strain behavior of two geotextiles under monotonic and cyclic loading conditions. A woven polyester and non-woven polypropylene were the two geotextile materials used in their testing program. During monotonic loading, the specimen was loaded at a constant rate of strain of 12 percent per minute until failure.

Cyclic testing was conducted by loading the specimens between zero and a maximum load ranging from 40 to 90 percent of its maximum breaking strength from the monotonic tests. For cycles with lower load levels, faster rates were used to shorten the test duration. A 2 Hz loading frequency was used to when the maximum load value was 40 percent monotonic strength and the remaining loading cycles were applied at a frequency of 1 Hz. Corresponding load and displacement data were collected from the testing machine's internal LVDT and a load cell.

Result showed that the strain at failure for the cyclically loaded specimens was lower than the monotonic test specimens. Cyclic tests using the non-woven geotextile (tested at a maximum load level of 40% monotonic load) were stopped at 1.2 million cycles to save time. From this, they predicted that the material would have failed at approximately 10 million cycles. These same samples were then subjected to monotonic loads. When the results were compared with the original monotonic test results, overall strength remained the same, but the strain at failure was significantly reduced. The strain at failure obtained only by the monotonic tests was 72 %, whereas the monotonic tests conducted after the cyclic testing was 53 %. For woven geotextiles, the magnitude of cyclic strain was comparable to the monotonic strain at corresponding load levels.

Raumann (1979) recommended studying differences between cyclic and monotonic test results, since the many field applications undergo dynamic rather than static loads. As such, Raumann (1979) conducted monotonic and cyclic tests on two types of woven geotextiles. For the cyclic tests, the geotextile was subjected to 500 cycles. The cyclic modulus was calculated at the 1st, 10th, 100th and 500th cycle. The initial modulus was calculated from the monotonic tests and compared with the cyclic modulus. It was concluded that for polyester fabric the cyclic modulus is much higher than the initial monotonic modulus. However, for the polypropylene material the cyclic modulus and initial monotonic modulus were the same. The ultimate failure strain was similar for both loading conditions, other than the polypropylene geotextile, where the ultimate failure strain during cyclic loading was considerably greater than the monotonic test results.

The effects of cyclic, monotonic and creep loading on a polymer geogrid was studied by Kongkitkul et al. (2002). They performed the monotonic testing at various strains rates from 0.01, 0.1, 1.0, 5.0, 10.0 and 20.0% per minute. Their cyclic testing program used seating strain rates of 1 and 5% per minute and load amplitudes of 10 and 20 kN/m. During the cyclic testing, the geogrid was initially exerted to a monotonic loading at a constant strain rate of 1% per minute until it reached 2.5% axial strain. Repeated cyclic loads were applied at load amplitude of 10kN/m for 100 cycles. At the end of 100th cycle, the geogrid was again exposed to the second level of seating strain and the cyclic load was also repeated at the same load amplitude. The geogrid was also tested at a higher load amplitude (20 kN/m) using the same initial strain levels. Similarly, the geogrid was also tested at a strain rate of 5% per minute and also at two different load amplitudes. Results from these two strain rates are shown in Figures 1 and 2.

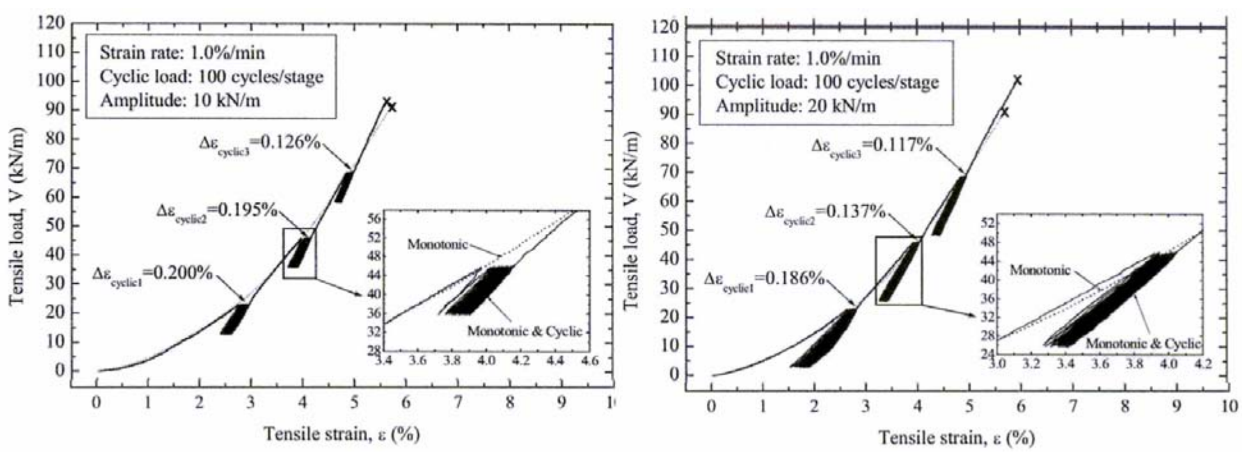

Figure 1: Load/Strain Relationships for Cyclic Loading Tests Conducted at a Strain Rate of 1 Percent per Minute (from Kongkitkul et al., 2002)

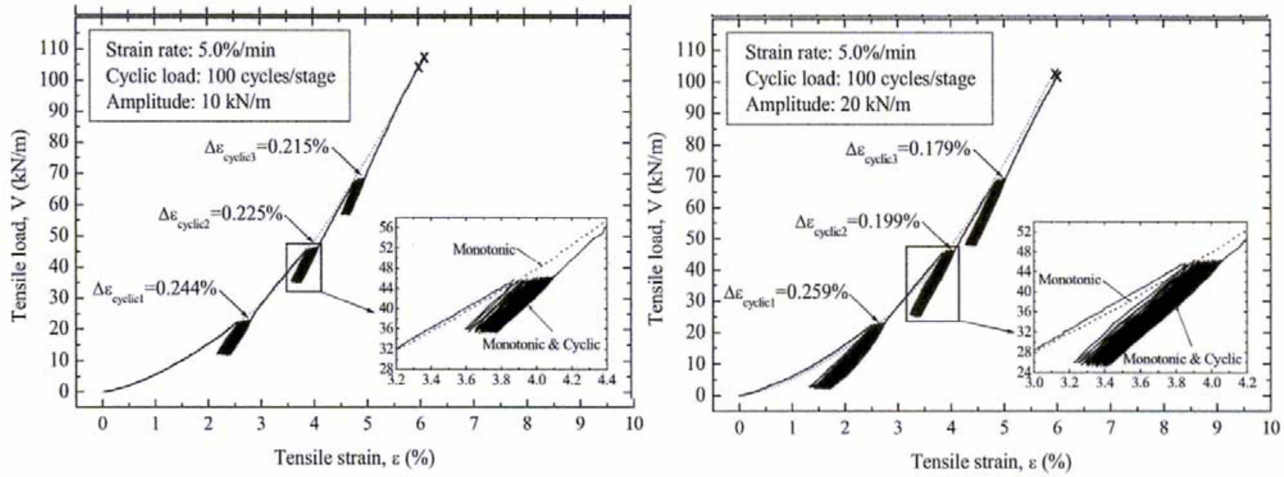

Figure 2: Load/Strain Relationships for Cyclic Loading Tests Conducted at a Strain Rate of 5 Percent per Minute (from Kongkitkul et al., 2002)

The authors concluded that the stiffness from the cyclic and monotonic test differed significantly, but the stiffness during the 100 load cycles remained constant. Nevertheless, the overall tensile strength was not significantly different. During the 100 load cycles, tensile strength of the cyclic test deviated from the tensile strength from the pure monotonic test. However, at the next step of initial strain, the cyclic test the tensile strength was again similar to the monotonic test results. From this they also concluded that cyclic loading does not necessarily degrade polymer geogrid materials.

Cyclic and monotonic behaviors of HDPE and PET geogrids were studied by Moraci and Montanelli (1997). Monotonic testing was performed at a strain rate of 10 percent per minute. Cyclic loading used repeated load amplitudes with a minimum load value of zero and a maximum load value in percentage of the maximum tensile strength (Tmax) from monotonic testing. The various maximum load percentages were 15, 25, 35, and 40% of the ultimate monotonic tensile strength. The secant modulus at 2% and 5% strain from the monotonic and cyclic tests were compared and, generally, the secant modulus obtained from the monotonic tests was greater than the cyclic results at a particular strain level (Table 1). Testing was also conducted at two different temperatures of 20° and 40° C. For HDPE geogrid at 20° C the secant modulus at 2% strain reduced by 20% and at 5% strain it reduced by 27%. Similarly, for the PET geogrid the secant modulus at 2% reduced by 38% and at 5% strain reduced by 19%.

Table 1: Comparison of Results from Cyclic and Monotonic Tests (after Moraci and Montanelli, 1997)

Material	Test Type	Secant Tensile Stiffness (kN/M)			
		@ 2% strain		@ 5% strain	
		20°C	40°C	20°C	40°C
HDPE Geo Grid	Monotonic	1507	928	1040	694
	Cyclic	1100	730	790	695
PET Geo Grid	Monotonic	803	---	465	---
	Cyclic	500	---	376	---

Moraci and Montanelli (1997) also investigated the behavior of cyclic tests conducted at different frequencies and load ratios. They cyclic tests were performed up to 10,000 load cycles. The entire cyclic testing program is shown in Table 2. Results showed, among other things, that the tensile modulus of the unloading/reloading curve is related more to the applied loads and secondarily of the frequency of the cycle. Generally, the cyclic tensile modulus increases with increasing frequency and as the applied load decreases. During testing it was noticed that the tensile modulus increases for the first 10 cycles or so, and remains constant for maximum loads less than or equal to 40 percent, but decreases for maximum loads greater than 40 percent. Finally, geogrid materials subjected to maximum load levels of 80% of the maximum tensile strength (Tmax) fail at an early stage of their testing program.

Table 2: Cyclic Testing Program for HDPE and PET Geogrid Materials (after Moraci and Montanelli, 1997)

Material	Load Range (% of Maximum Load)			
	@ 1.00 Hz	@ 0.50 Hz	@ 0.25 Hz	@ 0.1 Hz
HDPE	0 to 20 %	0 to 20 %	0 to 20 %	0 to 20 %
HDPE	0 to 40 %	0 to 40 %	0 to 40 %	0 to 40 %
HDPE	---	0 to 60 %	0 to 60 %	0 to 60 %
HDPE	---	---	0 to 80 %	0 to 80 %
HDPE	20 to 40 %	20 to 40 %	20 to 40 %	20 to 40 %
HDPE	40 to 60 %	40 to 60 %	40 to 60 %	40 to 60 %
HDPE	30 to 50 %	---	---	---
HDPE	60 to 80 %	---	---	---
PET	0 to 20 %	---	---	0 to 20 %
PET	0 to 40 %	---	---	0 to 40 %
PET	---	---	---	0 to 60 %

Similarly, Bathurst and Cai (1994) performed monotonic and cyclic tests on HDPE and PET polymer geogrids. Monotonic testing was performed at a strain rate of 10% per minute. The cyclic tests were conducted at five different loading frequencies of 0.1, 0.5, 1.0, 2.0, and 3.5 Hz over a range of load amplitudes. The cyclic and monotonic load-strain responses were significantly different for the two geogrids tested. In general, comparisons between PET and HDPE showed that HDPE was more sensitive to the loading frequency and the loading amplitude values (Figure 3).

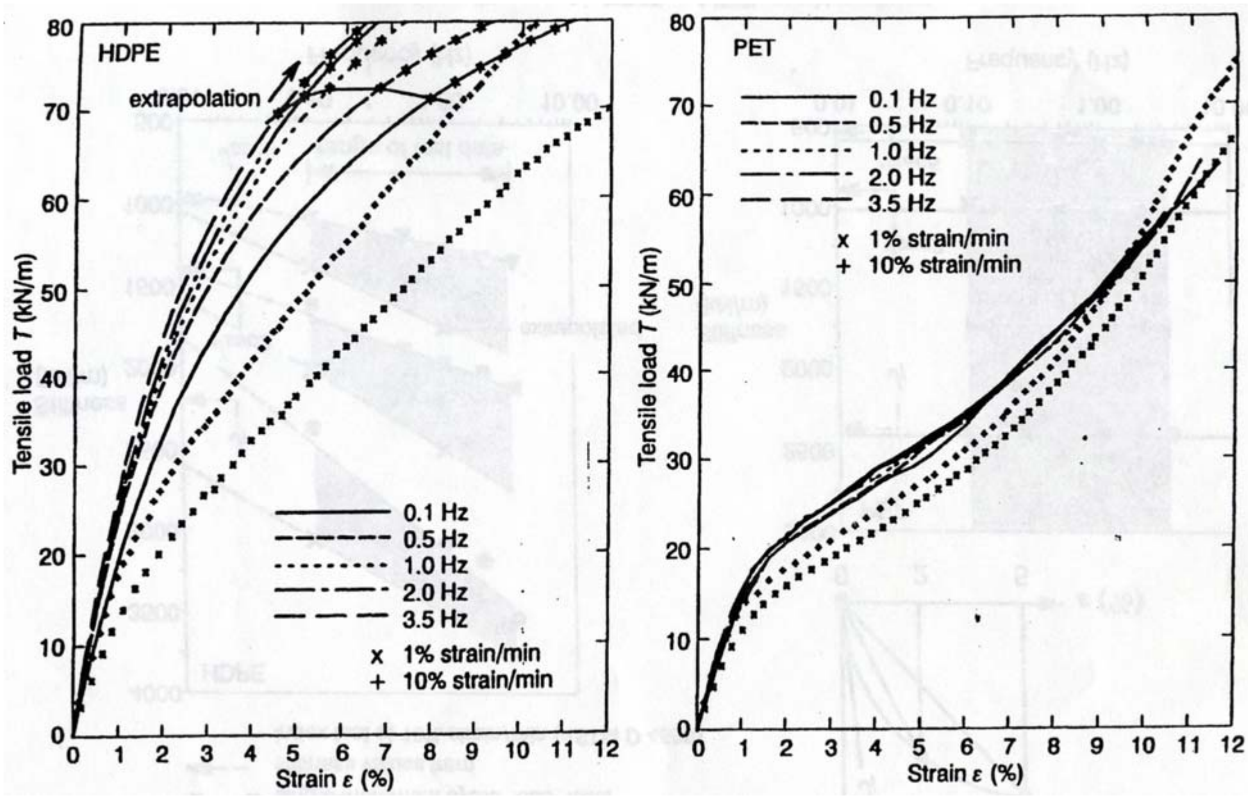

Figure 3: Load/Strain Curves for the Two Geogrids Tested at Different Load Frequencies and Two Monotonic Strain Rates (from Bathurst and Cai, 1994)

The initial modulus values of cyclic testing were similar to those from the monotonic testing. In general, the tangent modulus of the HDPE geogrid increased as frequency increase while that of PET remained constant. The initial secant modulus for those geogrids was shown in the Figure 4 below.

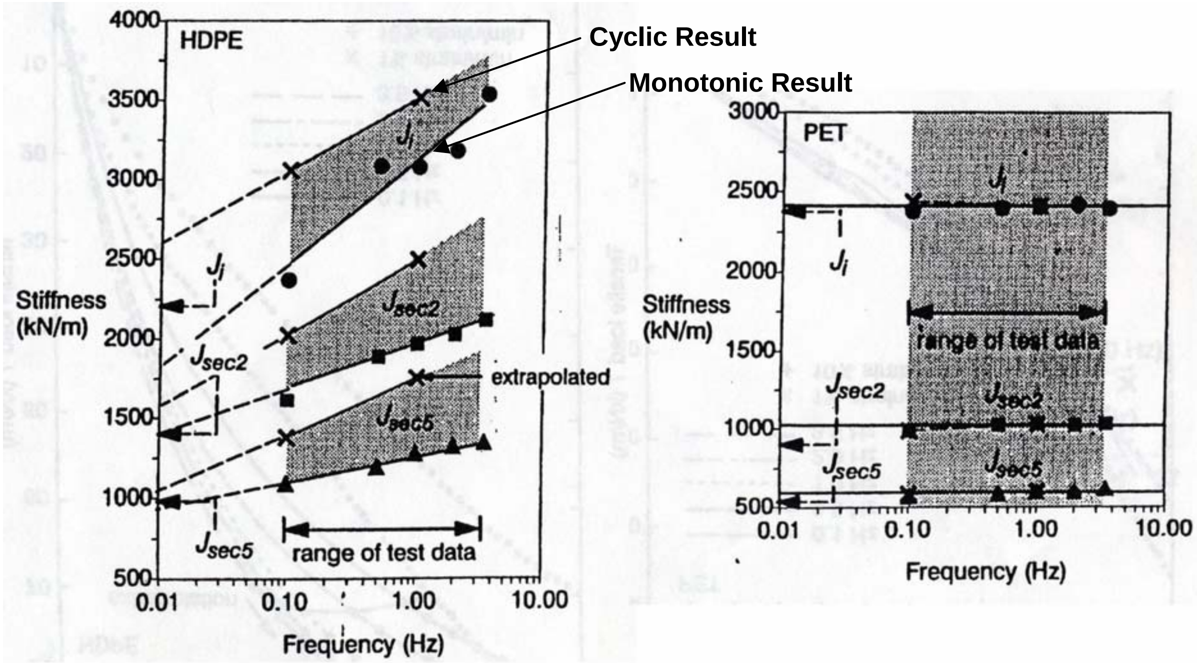

Figure 4: Stiffness versus Frequency of Cyclic Loading for HDPE and PET Geogrid Specimens (from Bathurst and Cai, 1994)

Ketchart and Wu (2001) also conducted monotonic (M) and cyclic (UR – unloading/reloading) testing on two different geosynthetics: Amoco 2044 a polypropylene woven geotextile and Typar 3301 a polypropylene non-woven geogrid. A strain rate of 10% per minute was used for the monotonic tests. Initially, the UR tests were conducted in a stress-controlled mode with various loading sequences at a constant loading rate of 1.75 kN/m per minute, then during the unloading/reloading sequence the load is cycled between zero and 2 kN/m for the Typar 3301 material, and zero and 10 kN/m for Amoco 2044 material. Prior to cyclic loading, the samples were preloaded by going through a single unloading/reloading cycle. Near the end of the UR test, a monotonic load was applied ad a strain rate of 10% per minute until the material failed. The details of this test protocol are illustrated in Figure 5.

The secant stiffness was calculated to examine the effects of preloading of the geosynthetics used in this study. The secant stiffness was determined at the maximum cyclic tensile load applied to the geosynthetic (2 kN/m for Typar 3301 and 10 kN/m for Amoco 2044). Using this, the authors also calculated a stiffness ratio defined as the ratio between the preloading secant stiffness and the UR secant stiffness. The stiffness ratio of both materials appeared to reduce with increasing preloading load levels. This behavior indicates that preloading can have a significant effect on the geosynthetics during the UR tests. They have also concluded that in UR tests preloading have reduced the ultimate strength of the geosynthetics by up to 5%.

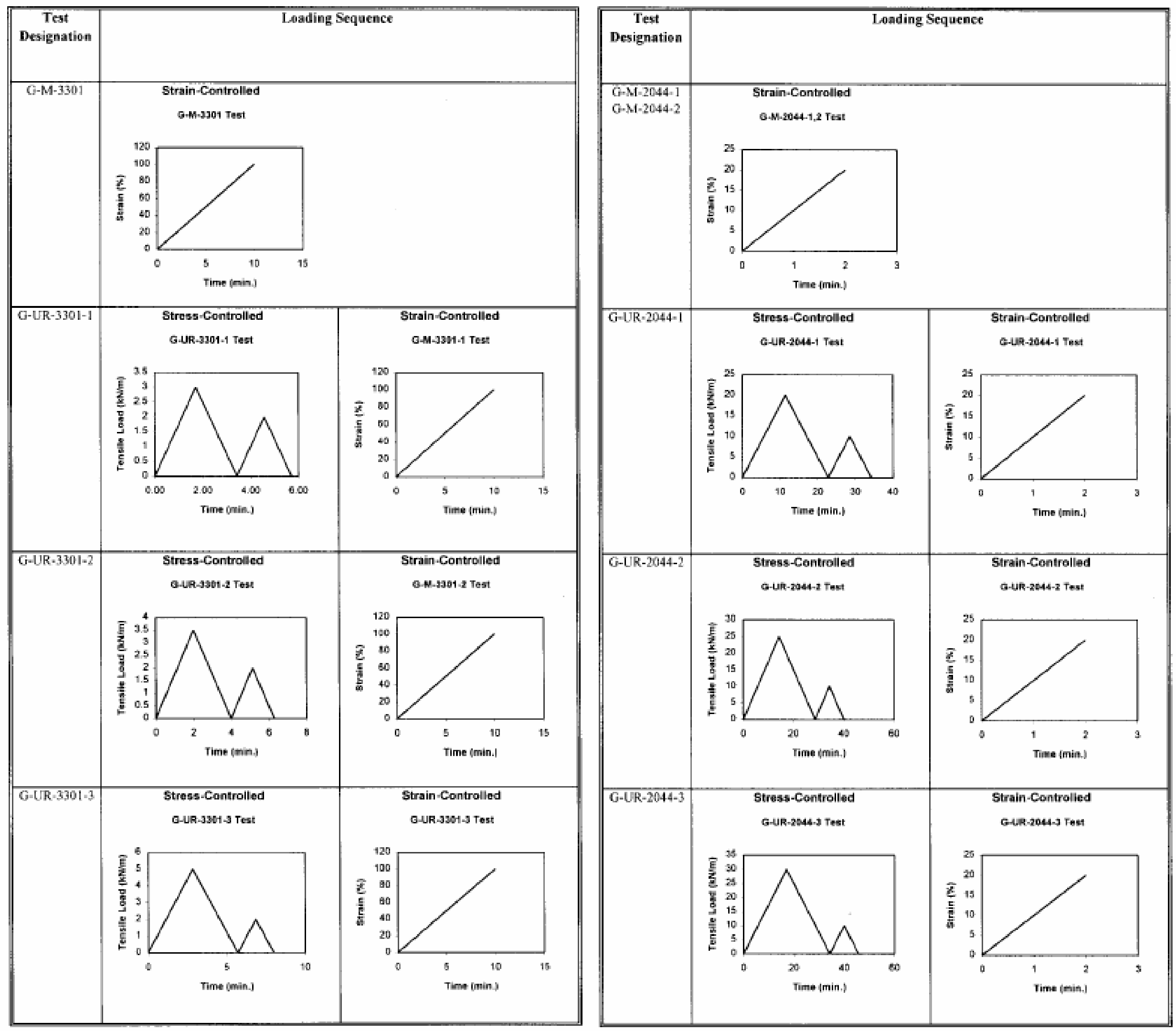

(a) (b)

Figure 5: Test Protocol for a) Typar 3301 and (b) Amoco 2044 (from Ketchart and Wu, 2001)

Various authors have conducted tests under both monotonic and cyclic loading conditions. Overall it is acknowledged that geosynthetics material properties are generally affected by the type of loading conditions. To determine the appropriate material properties, one must set up a testing regime to emulate loading conditions in the field. Cyclic loading conditions are appropriate for geosynthetics used in pavements since they experience repeated dynamic loads in the field, while monotonic loads generally appropriate for static structures. Overall, the authors reviewed as part of this study agreed that the ultimate strength of the geosynthetics is not significantly affected by the type of loading. However, strain at failure, secant modulus and strain behaviors are significantly affected by loading conditions.

2.2 Specimen Size and Aspect Ratio

The size and aspect ratio of standard laboratory test specimens used to determine geosynthetics materials properties may not always represent field conditions. The ASTM specification D 4595 for testing geotextiles (wide-width test for geotextiles) specifies using a specimen size of 200 mm wide by 100 mm long (8 in. wide by 4 in. long). For geogrids, the ASTM specification D6637 (wide-width test for geogrids) specifies using a sample size of 200 mm wide by 300 mm long (8 in. wide by 11.8 in. long). Therefore, it is necessary to verify whether specimen size and aspect ratio of the sample used during the laboratory tests has an impact on its intrinsic material properties. Several research studies were consulted and summarized to determine the effects of specimen size and aspect ratio on geosynthetic material properties such as ultimate strength, tangent and secant modulus and elongation at failure.

Shrestha and Bell (1982) conducted a research study to investigate whether the standard wide-width tensile test is appropriate for the routine laboratory measurement of tensile stress strain properties. A total of 383 tests were conducted on six different geotextiles. They concluded that the ultimate strength is not significantly affected by the specimen size but that strain levels at failure and the elastic modulus are significantly affected.

Wide-width tensile tests were conducted by Boyle et al. (1996) on two non-woven geotextiles to investigate the effect of gauge lengths on the material properties. For this purpose, six or less wide-width tests were conducted on 200 mm wide specimen using various gauge lengths of 25, 50, 56, 75, 100 and 115 mm. All these tests were conducted at constant strain rate of 10 percent per minute. Their research concluded that gauge length did not significantly increase its apparent strength. However, secant modulus at 5% strain had significantly increased as the gauge length decreased. As shown in Figure 6, the secant modulus decreased by 130% and 65% for the two non-woven materials as the lengths increased from 25 mm to 115 mm.

Gallagher (1995) also demonstrated similar work to that of Boyle et al. (1996). He concluded that the secant modulus at 5% and 10% strain is significantly affected by the gauge length for non-woven geotextiles. Similarly, the modulus decreased as gauge length increased (Figures 7 and 8).

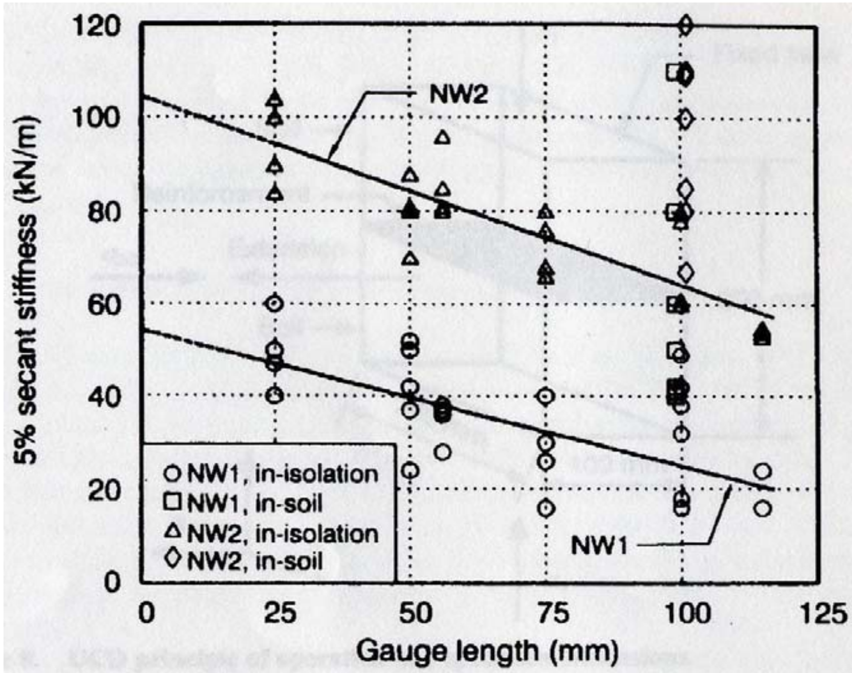

Figure 6: Secant Modulus versus Gauge Length from In-Isolation and In-Soil Tests for Non-Woven Geotextiles (from Boyle et al., 1996)

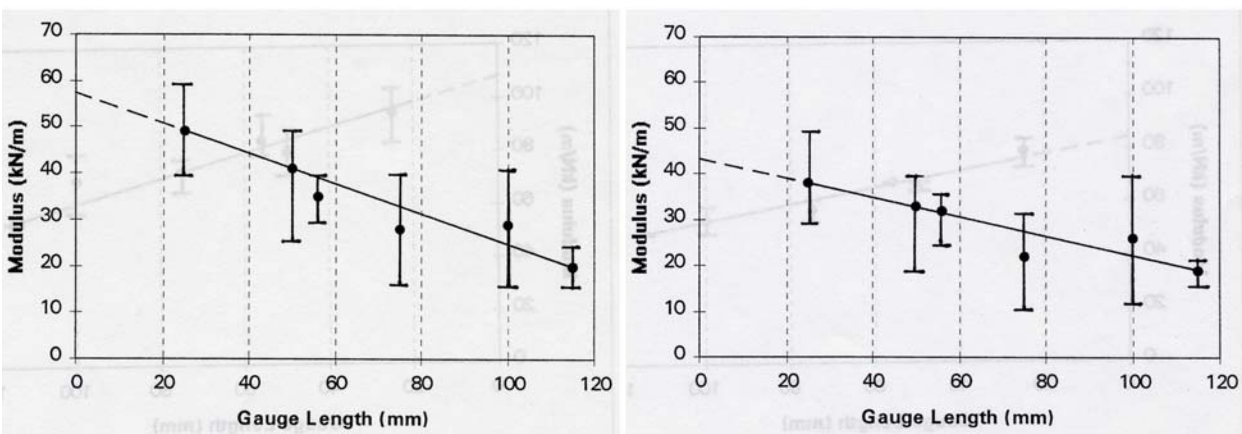

(a) (b)

Figure 7: Secant Modulus versus Gauge Length at a) 5% Strain and b) 10% Strain for Non-Woven Geotextile #1 (from Gallagher, 1995)

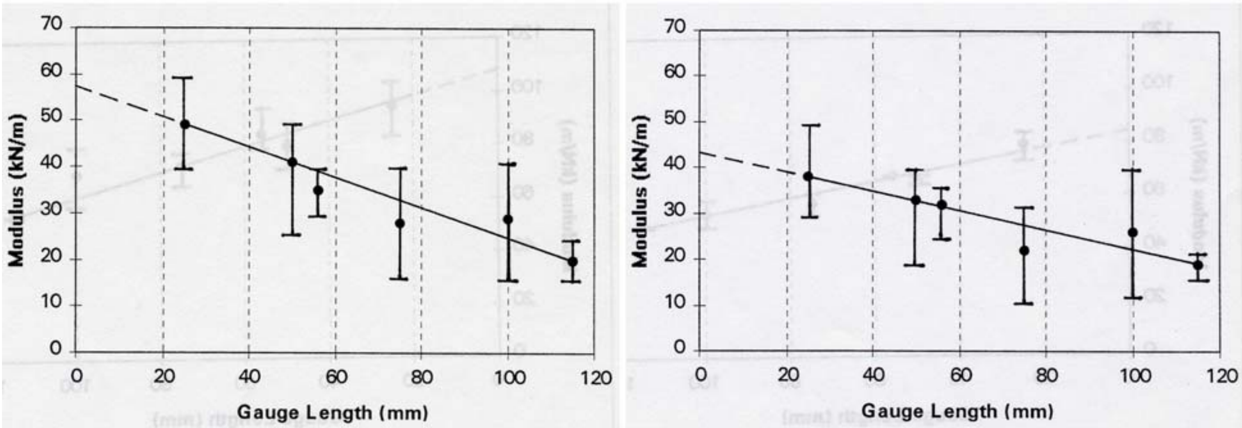

(a) (b)

Figure 8: Secant Modulus versus Gauge Length at a) 5% Strain and b) 10% Strain for Non-Woven Geotextile #2 (from Gallagher, 1995)

Wang et al. (1990) considered four different non-woven geotextile materials and concluded that the stress-strain properties are highly affected by the specimen width. Overall, they determined that strength increased with an increased specimen width. As the sample width increases, necking of the sample is reduced, which affects the stress/strain properties. Contrary to the conclusions of Shrestha and Bell (1982), Gallagher (1995) and Boyle (1996), Wang et al. (1990) had concluded that the strength values of non-woven geotextiles increased with decreasing the gauge length. Sample results are shown in Figure 9.

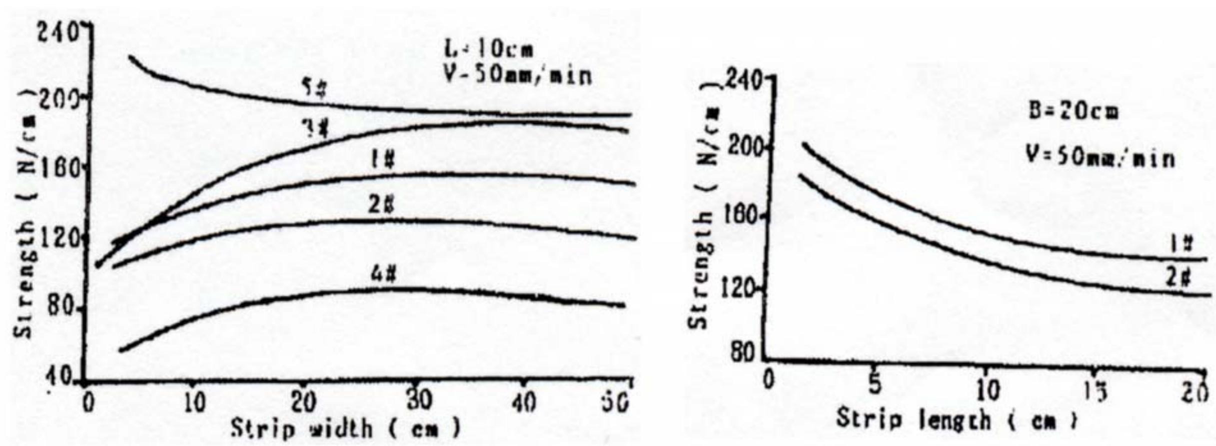

Figure 9: Effect of Specimen Width and Length on the Geotextile Tensile Strength (from Wang et al., 1990)

In a study conducted by Austin et al. (1993), single ribs of polypropylene geogrids were tested at two different specimen lengths (three and four junctions). The results showed that the tensile modulus increased as specimen length decreased but that the difference in modulus between the two gage lengths remained constant (Figure 10).

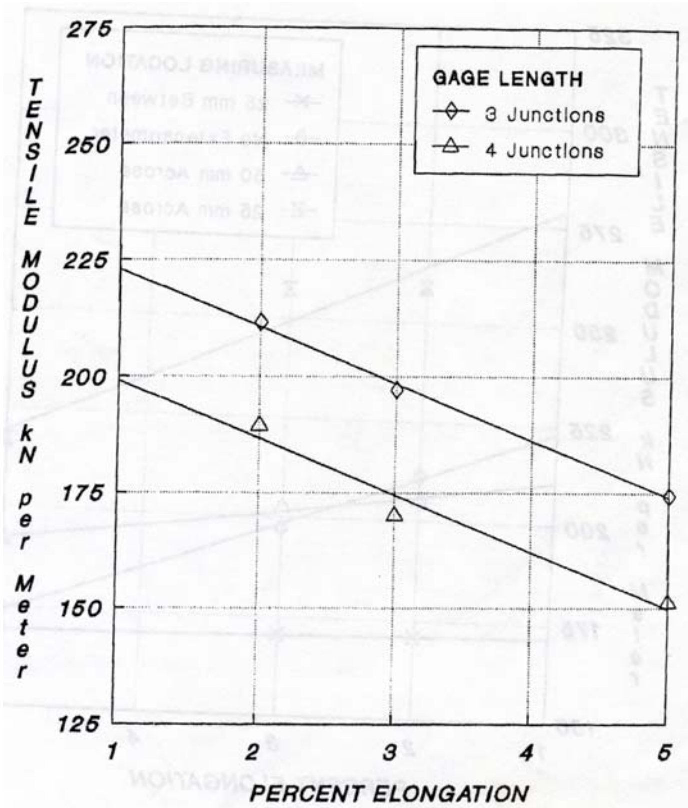

Figure 10: Gage Length Effects on Tensile Modulus (from Austin et al., 1993)

Haliburton et al. (1978) investigated the effect of specimen width on the stress-strain properties of various woven geotextiles. For this purpose, monotonic tests were conducted on 305 mm long specimen using widths of 25, 77 and 152 mm. They concluded that the tensile strength was not affected by changes in specimen width. Even so, the Poly-Filter X material fails at approximately 80 lb/in higher tensile stress when the width is increased from 1 inch to 6 inches. Similarly, the Permealiner M-1195 fails at approximately 50 lb/in under the same width difference. The results from their testing are shown in Figure 11.

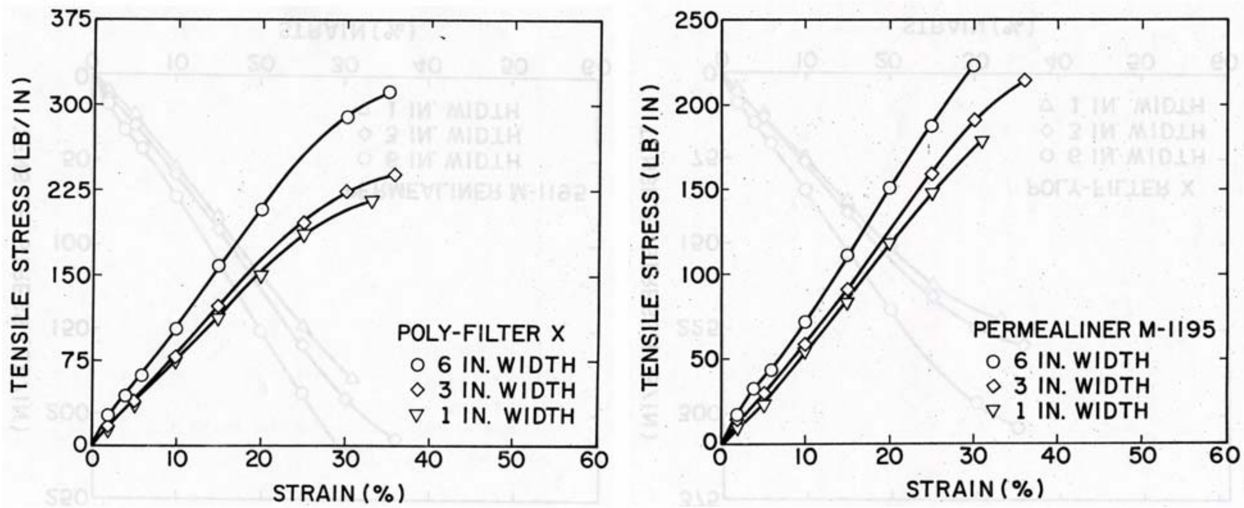

Figure 11: Effect of Specimen Widths on the Tensile Stress of Two Woven Geotextiles (from Haliburton et al., 1978)

Overall, it can be concluded that the measured ultimate load is less sensitive to change in specimen size and aspect ratio. However, the stiffness of non-woven geotextiles is more sensitive to the specimen size and aspect ratio. Woven geotextiles are also not as sensitive to changes in specimen size. The majority of the authors recommended using the standard specimen size from wide-width tensile test for the routine laboratory measurement of tensile stress strain properties, simply because they are easy to test and represents the bulk of field conditions under which geosynthetics are used. However, from the literature review, little work had been done to test very large sample sizes which better represent actual field conditions. More research is needed to determine the appropriate sample size to use in laboratory testing when values for the material's stiffness are needed.

2.3 Strain Rate

In general, geosynthetic material properties, like most plastics, have been shown to be sensitive to strain rate. As such, it is essential to test geosynthetics at a strain rate which represents strain rates experienced in the field. The current ASTM standard for wide-width tensile testing of geotextiles (ASTM D 4595) recommends that testing be conducted at a strain rate of 10% per minute. Myles and Carswell (1986) commented that a strain rate of 10% is generally higher than what most geosynthetics experience in static structures, but that it is low enough to be accepted by most practitioners. So, even though the recommended strain rate is convenient, it may not represent the true strain rate induced in geosynthetics in the field – especially in dynamic situations. In particular, when fabrics are used as reinforcement, it is prudent to fully understand the strain rate characteristics for the specific material (Rowe & Ho, 1986). Van Zanten (1986) encouraged engineers to specify the strain rate at which design strength was obtained. Several researchers still believe that additional research needs to be conducted to find a suitable strain rate for laboratory testing (Wang et al., 1990; Gallagher, 1995; Rowe & Ho, 1986). Several research studies were consulted and summarized to determine the effects of strain rate on geosynthetic material properties such as ultimate strength, tangent and secant modulus, and elongation at failure.

Results from Bell et al. (1980) showed that the ultimate tensile strengths of geotextiles are not sensitive to strain rate, but that the tensile modulus is significantly affected. Shrestha and Bell (1982) conducted a series of testing on five polypropylene materials and one polyester material at stain rates varying from 1.25 to 12.5 percent per minute. The results showed that changing the strain rate did not significantly affect ultimate strength and, as such, recommended using 10 percent per minute for routine laboratory tensile testing (Figure 12).

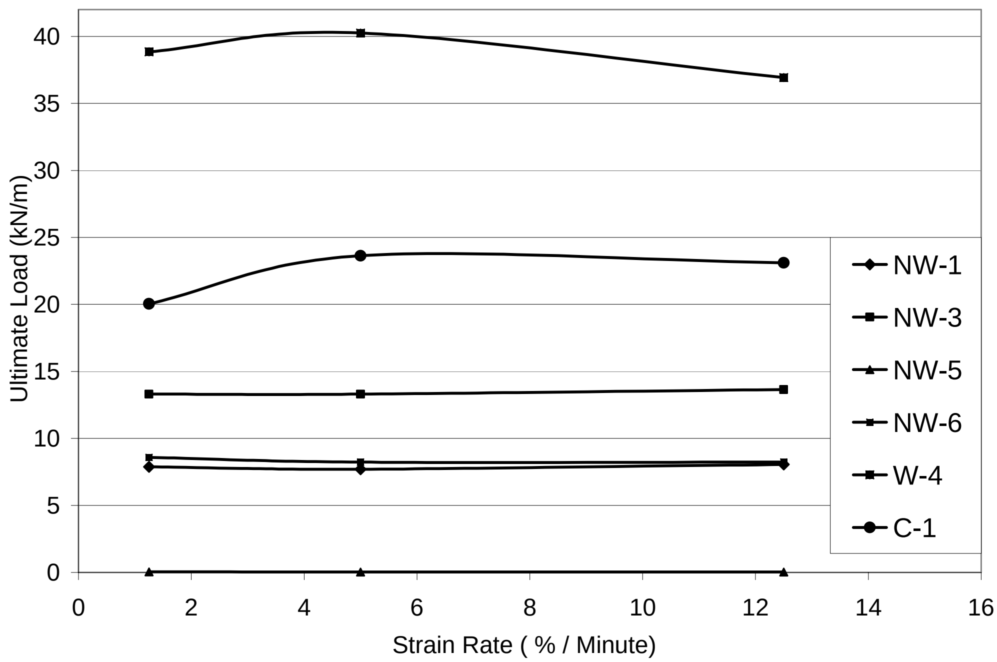

Figure 12: Effect of Strain Rates on the Ultimate Strength (after Shrestha & Bell, 1982)

Rowe and Ho (1986) conducted testing on seven different geosynthetics and found that the tensile moduli of geotextiles are quite sensitive to strain rate. The tests were conducted at strain rates ranging from 0.2 to 10 percent per minute. Figure 13 shows how maximum tensile strength changes for different strain rates. They recommended using a strain rate of 2 percent per minute to determine the design properties since the tensile modulus obtained from wide width tests conducted at that strain rate represented the strain rates experienced by most geotextiles in the field.

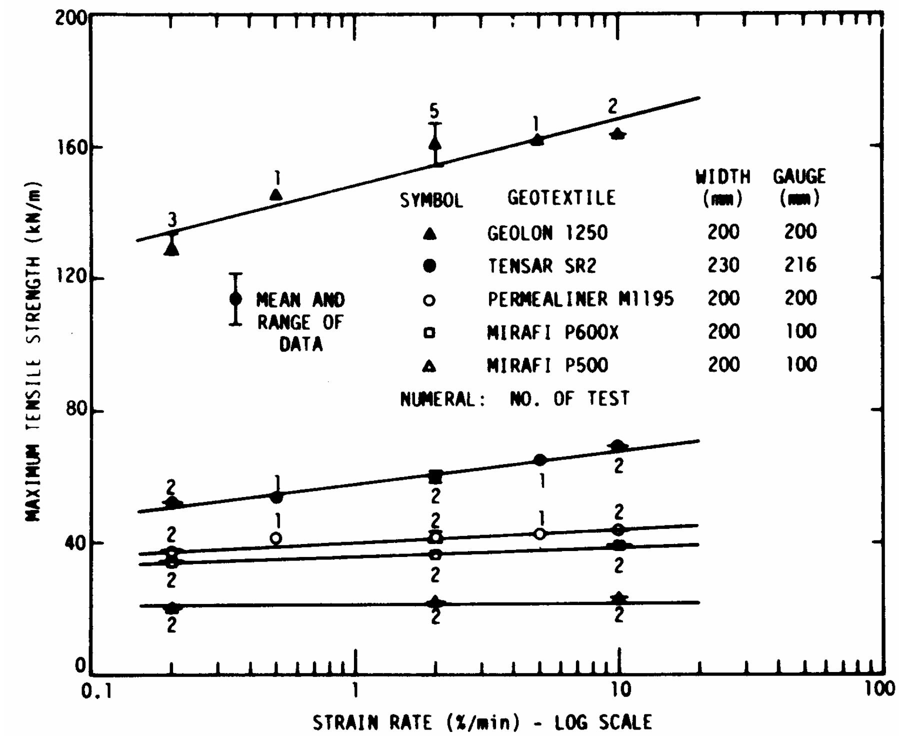

Figure 13: Variation of Tensile Modulus with Strain Rate (from Rowe & Ho, 1986)

Gallagher (1995) conducted wide-width tensile tests on three woven and two non-woven polypropylene materials. These tests were performed at strain rates of 0.01, 0.1, 1 and 10 percent per minute. Results showed that as the strain rate decreased, the secant modulus at 2% and 5% strain and ultimate strength at failure decreased, but that elongation at failure increased. Similar tests were conducted on woven polyester materials and resulted in minimal differences in modulus, strength and elongation with decreasing strain rates. It was concluded from this research that polypropylene materials were more sensitive than polyester materials to changes in strain rate (see Figure 14). Further analysis by Boyle et al. (1996) compared the secant modulus at 5% for three woven polypropylene materials (PP1, PP2 and PP3) to a woven polyester (PET4) and found that the polypropylene materials were more sensitive to changes in strain rate (Figure 15).

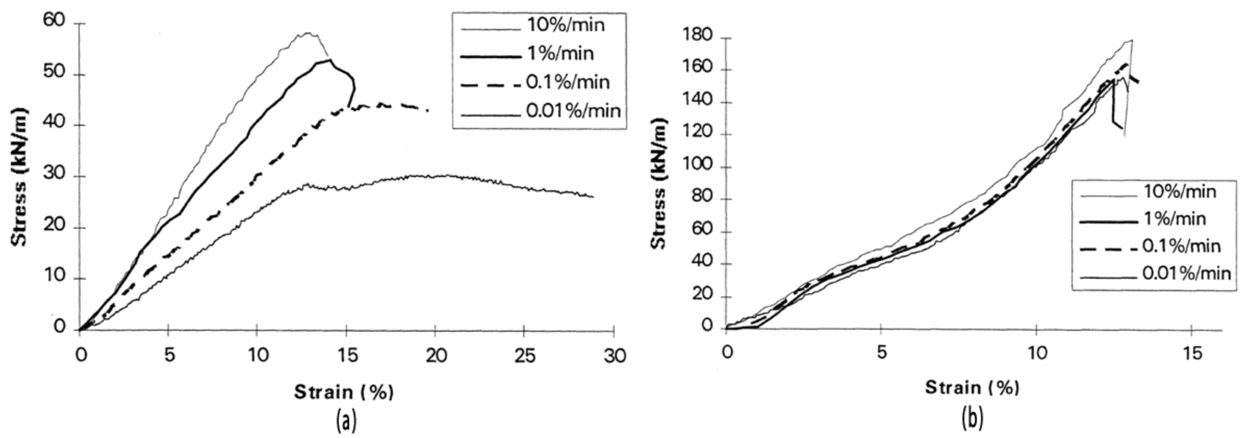

Figure 14: Comparison of the Effect of Strain Rate on Woven PP and PET Geosynthetics (from Gallagher, 1995)

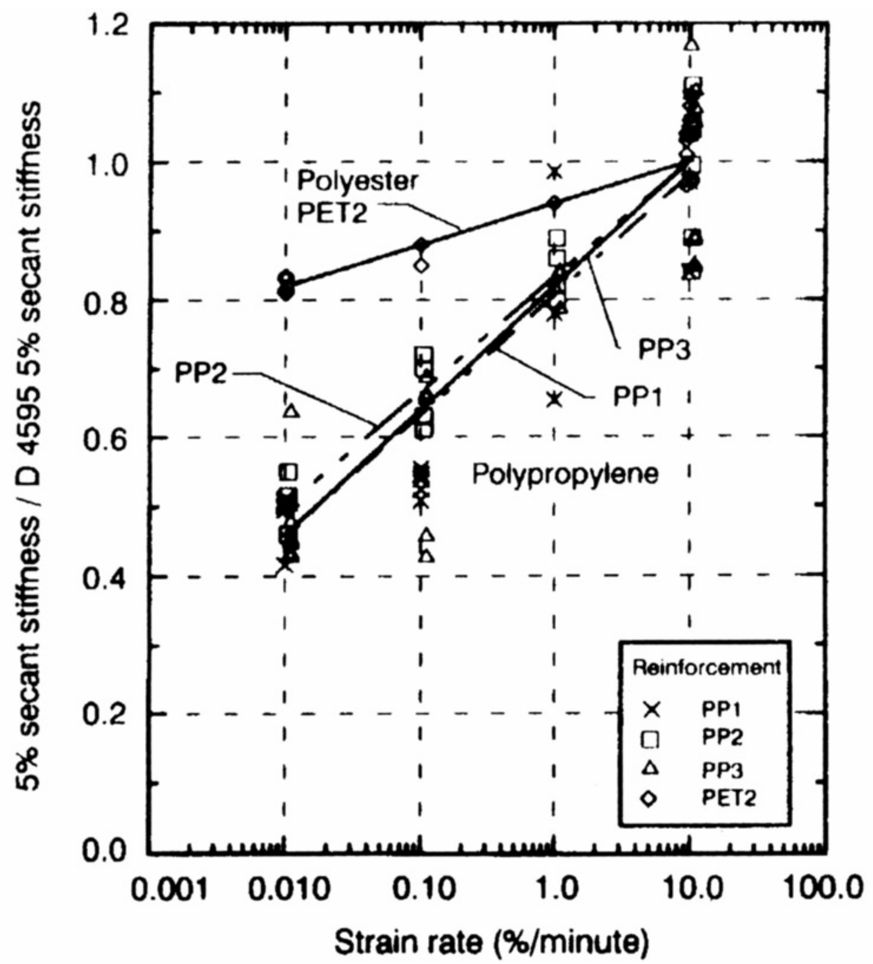

Figure 15: Normalized 5% Secant Modulus versus Strain Rate (from Boyle et al., 1996)

Van Zanten (1986) compared the tensile strength of four typical geosynthetic polymers (Nylon – PA, High Density Polyethylene – HDPE, Polyester – PET, and Polypropylene – PP) as strain rates increased. Strain rates from 0.2% per minute to 100% per minute were used. Results showed that all of the polymers are sensitive to changes in strain rate, with HDPE being the most sensitive and PET being the least (Figure 16).

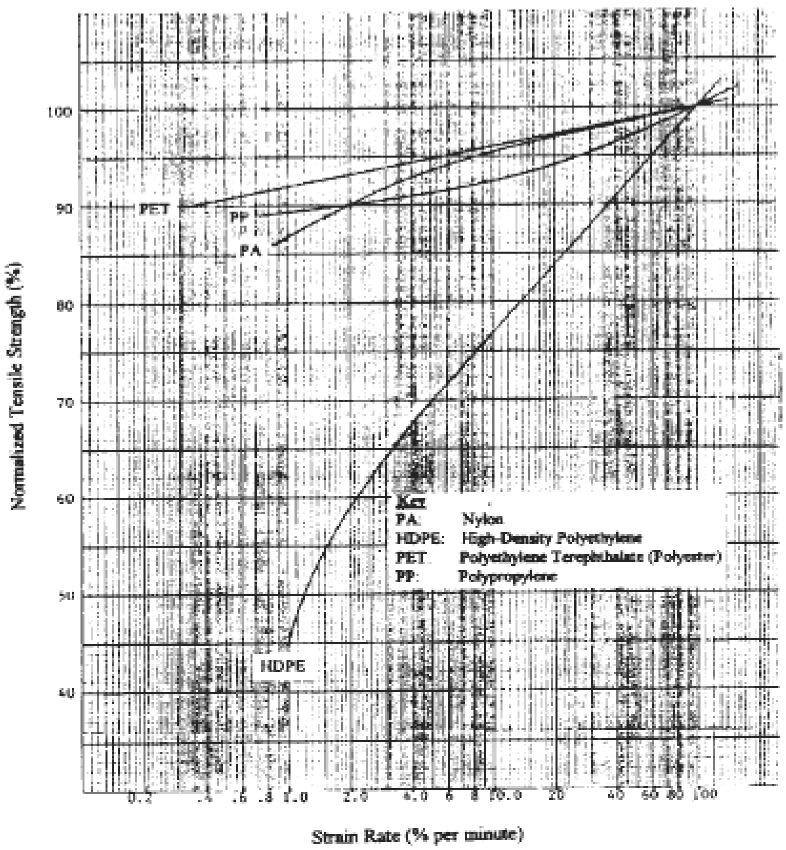

Figure 16: Variation of Tensile Strength with Strain Rate (from Van Zanten, 1986)

Bathurst and Cai (1994) conducted monotonic load-extension tests on HDPE and PET geogrids using the ASTM wide-width testing procedures (ASTM D 4595) to investigate the sensitivity of the HDPE and PET geogrid materials to changes in strain rate. Monotonic tests at slow rates of 1% per minute and 10% per minute were conducted, and faster strain rates were achieved using cyclic loads having ramp-up strain rates of 60% per minute and 300% per minute. The results showed that HDPE is more sensitive to changes in strain rate than polyester (Figure 17). More specifically, as the strain rate increased the initial secant and tangent modulus of the HDPE geogrid also increased. Differences in these properties for the PET materials were minimal.

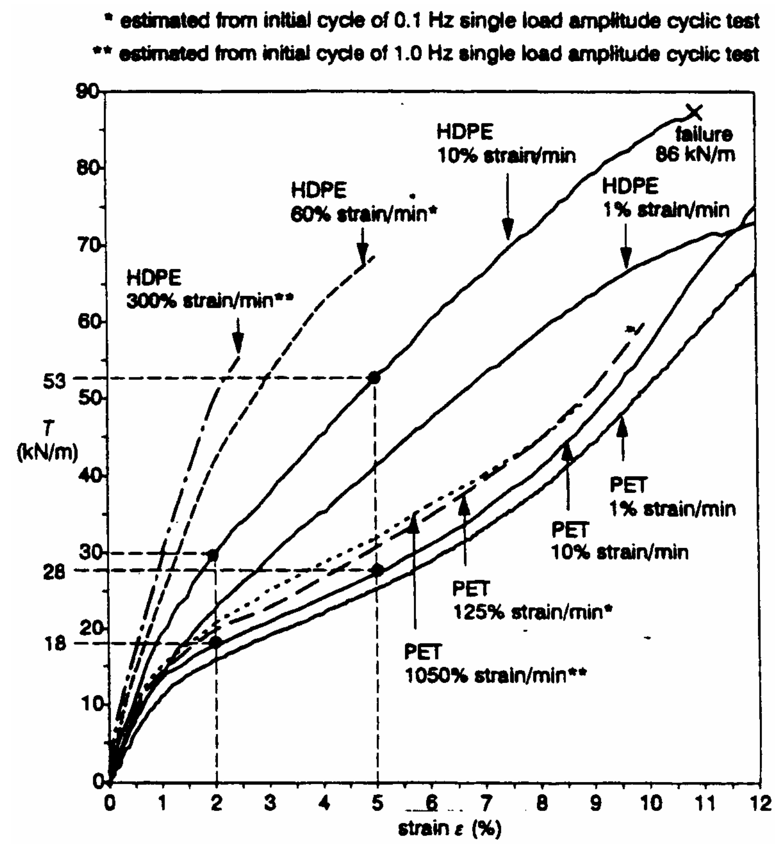

Figure 17: Changes in Load/Strain Properties for Different Loading Rates in HDPE and PET Geogrids (from Bathurst and Cai, 1994)

Haliburton et al. (1978) investigated the effect of strain rate on the stress-strain properties and uniaxial tensile strength of fifteen polypropylene, seven polyester, and five other types of geosynthetics. Strain rates of 0.5, 1.0 and 2.0 percent per minute were chosen because of their compatibility with the slower strain rates normally used in soil testing. Results from these tests did not show a significant correlation between strain rate and tensile modulus (Figure 18).

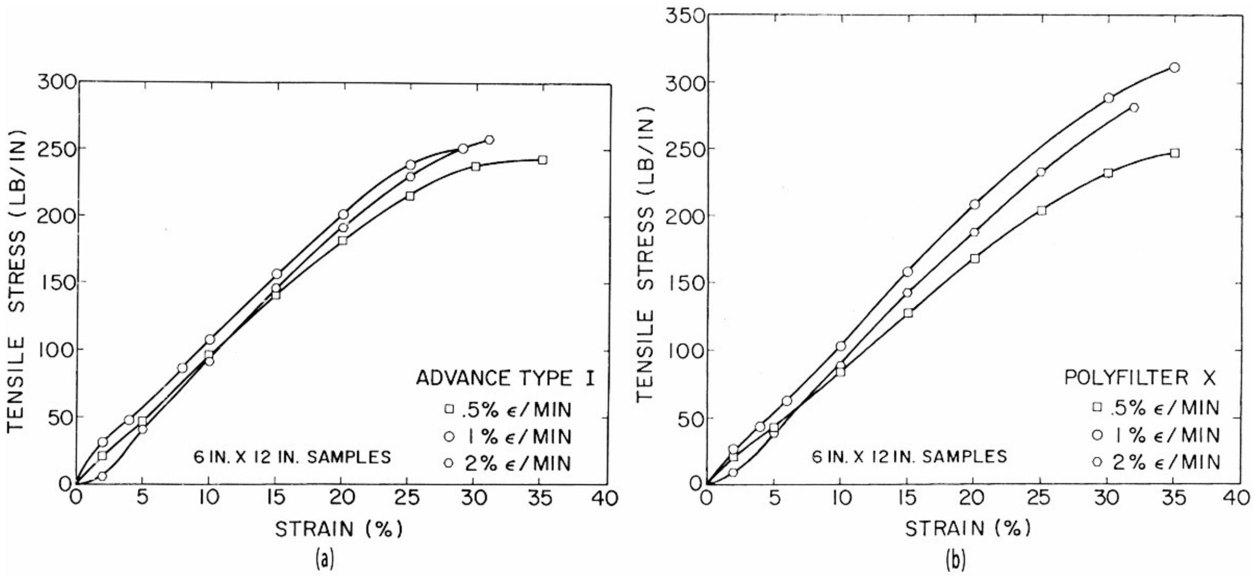

Figure 18: Effect of Varying Strain Rate on Tensile Stress (from Haliburton et al., 1978)

Five geotextiles and three strain rates (10, 50 and 100 percent per minute) were considered in a study conducted by Wang et al. (1990). Results showed that as strain rates increase, tensile strength also increase (Figure 19).

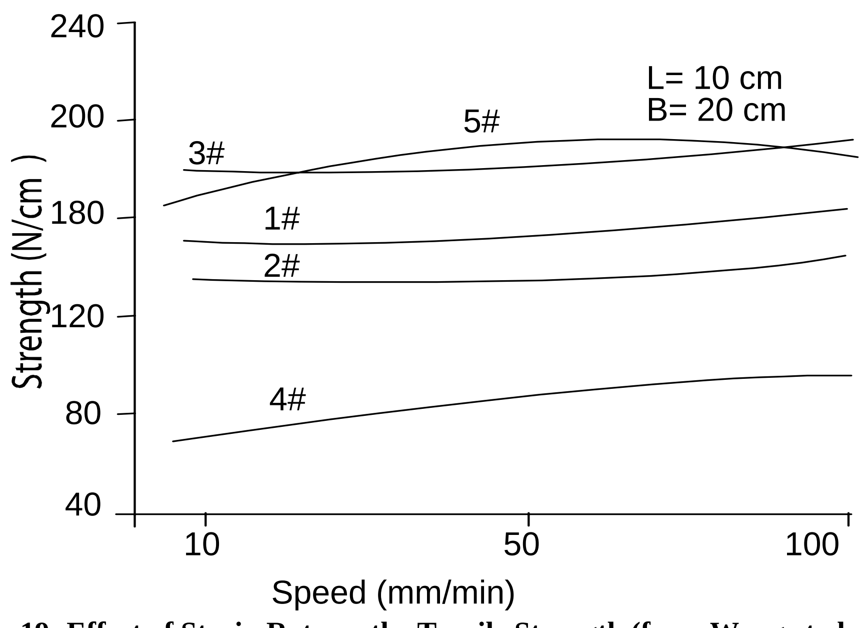

Figure 19: Effect of Strain Rate on the Tensile Strength (from Wang et al., 1990)

Raumann (1979) conducted tests on woven polypropylene and polyester materials at strain rates of 1 to 5 percent per minute and 50 to 100 percent per minute. From this research it was concluded that elongation at failure of polyester fabrics are not significantly affected by strain rate, but that polypropylene materials are highly affected.

Strain rate effects of HDPE and polypropylene geogrids were studied by McGown et al. (1985). They conducted tests on geogrids at strain rates of 0.001, 0.01, 1.0, 10, and 100 percent per minute. Their results were analogous to other authors (Raumann, 1979; Bathurst and Cai, 1994; Gallagher 1995) that is, both HDPE geogrids were found to be significantly affected by the strain rates. A summary of their results is shown in Figure 20.

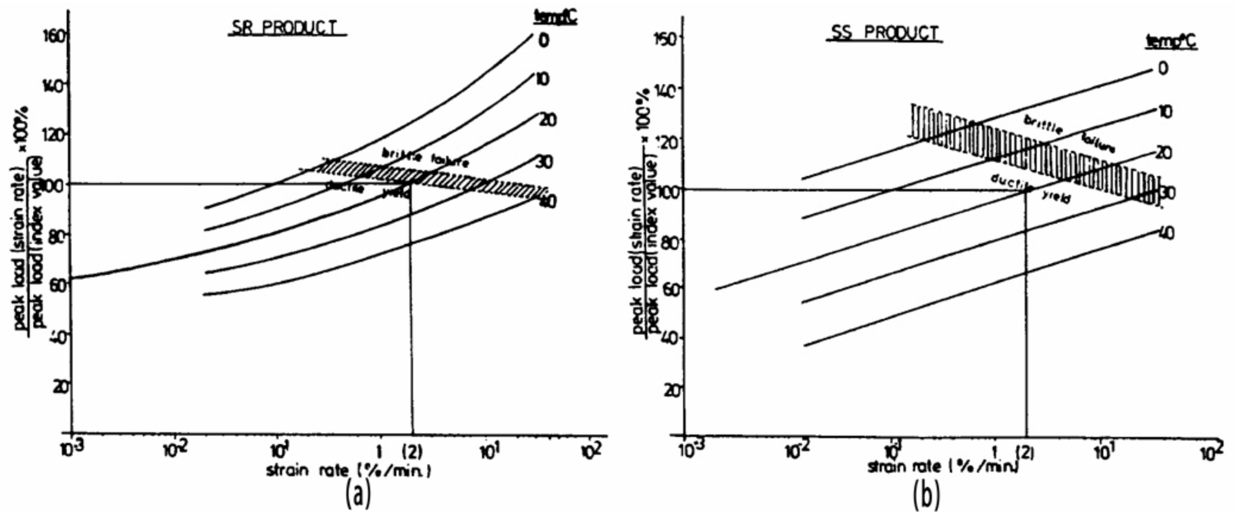

Figure 20: Effect of Strain Rate Ultimate Load (from McGown et al., 1985)

In a study conducted by Austin et al. (1993), polypropylene geogrids were tested at strain rates of 1.2, 12.5, 25, 50, and 125 mm per minute. Results did not show a clear trend, and several explanations were given to explain why tensile modulus generally decreased as strain rate increased (Figure 21). The first explanation was related to the non-uniform cross section of single ribs of geogrids and the second explanation was related to the internal friction causing viscous heating. Admittedly, these test results are somewhat difficult to understand since they do not show a pattern.

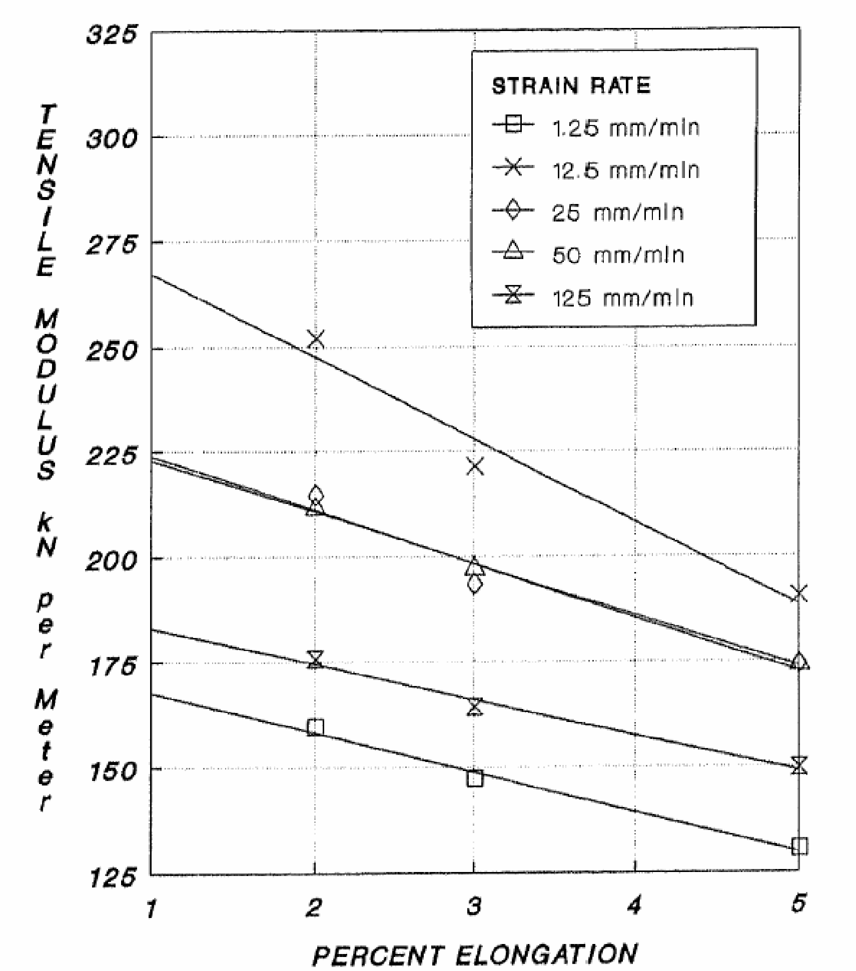

Figure 21: Strain effects on Tensile Modulus of Polypropylene Geogrids (from Austin et al., 1993)

It may be safely concluded that the geosynthetics are generally a strain rate dependent material. Among various geosynthetic polymers, HDPE was found to be highly sensitive, PP moderately sensitive and PET relatively insensitive to changes in strain rate. Therefore, depending on the type of material being considered, strain rate should be considered as an important factor when material properties are being determined. Accordingly, strain rates used during testing should simulate the strain rates experienced by the geosynthetic in the field.

A summary of all authors included in this section of the literature review is provided in Table 3. Sensitivity of various geosynthetics to changes in strain rate were assessed using subjective rating system ranging from 1 to 3, where 1 signifies that the material was insensitive, 2 as moderately sensitive, and 3 as highly sensitive. Ratings were assigned based on qualitative and quantitative information contained in each of the research papers considered.

Table 3: Summary of the Strain Rate Effects on Various Geosynthetics by Author

Author/Researcher	Strain Rate (%/minute)	Material Type	No. of Different Geosynthetics	Polymer Types*	Material Property of Interest	Effect on Properties[†]
Haliburton, et al. (1978)	0.5, 1, 2	Geotextile	15	PP	Tensile Modulus	2
			7	PET	Tensile Modulus	1
			5	Other	Tensile Modulus	---
Raumann (1979)	1 to 5 and 50 to 100	Geotextile	1	PET	Elongation at failure	1
		Geotextile	1	PP	Elongation at failure	2
Bell and Shrestha (1982), Bell et al.	1.25 to 12.5	Geotextile	5	PP	Tensile Modulus	2
		Geotextile	1	PET	Tensile Modulus	1
McGown et al. (1985)	0.001, 0.1, 1, 10, 100	Geogrid	1	HDPE	Tensile Strength	3
			2	PP	Tensile Strength	2
Van Zanten (1986)	0.2 to 100	Geosynthetic Polymers	---	HDPE	Tensile Strength	3
				PET	Tensile Strength	1
				PP	Tensile Strength	2
				Nylon	Tensile Strength	2
Myles and Carswell (1986)	1, 10, 50	Geotextile	6	PET	Stress/Strain Behavior	1
		Geogrid	1	PE	Stress/Strain Behavior	3
Rowe and Ho (1986)	0.2 to 10	Geotextile	4	PP & PET	Tensile modulus	2
		Geogrid	1		Tensile Modulus	
Austin et al. (1993)	1.2, 12.5, 25, 50, 125 mm/min	Geogrid	1	PP	Tensile Modulus	2
Bathurst and Cai (1994)	1, 10, 60, 300	Geogrid	1	HDPE	Tensile strength at 2% and 5% strain	3
	1, 10, 125, 1050	Geogrid	1	PET		1
Wang et al. (1994)	10, 50, 100	Geotextile	5	---	Tensile Strength	2
Gallagher (1995), Boyle et al. (1996)	0.01, 0.1, 1, 10	Geotextile	5	PP	Secant Modulus at 2% and 5%, ultimate strength, and elongation at failure	2
		Geotextile	1	PET		1

*HDPE – High Density Polyethylene
PP – Polypropylene
PET – Polyethylene

[†] 1 = low sensitivity
2 = moderate sensitivity
3 = high sensitivity

2.4 Temperature

Geosynthetics material properties can also be affected by changes in temperature. Depending on what material is being used, it may be necessary to study changes in material properties due to temperature changes experienced in the field. The ASTM D4595 standard for testing geosynthetics recommends testing geosynthetics at typical room temperature (21 ±1° C). This temperature, however, may not represent field conditions. Since geosynthetics may be used in various climates, material parameters must be determined that relate to their specific application. Several research studies were consulted and summarized to determine the effects of temperature on geosynthetic material properties such as ultimate strength, tangent and secant modulus, and elongation at failure and creep.

A research study conducted by Nothdurft and Janardhanam (1994) showed the importance of knowing the glass-rubber transition temperature (T_g) of geotextile materials to better understand changes in material properties due to temperature fluctuations. Their results showed that, generally, when the service temperature of any plastic rises above its T_g, strength properties may change significantly. Values of T_g for three commonly used geosynthetics polymers (polyester, polypropylene and polyethylene) were investigated in their study: polyester, 75° C (167° F); polypropylene, -100° C (-148° F); polyethylene, -100° C (-148° F). Polyester's T_g is greater than anticipated field temperatures so its material properties should not be greatly affected by temperature changes. Conversely, since T_g for polypropylene and polyethylene is lower than anticipated field temperatures, their material properties will most likely be affected by temperatures fluctuations.

In a study conducted by Allen et al. (1983) to understand the effect of temperature has on the load-strain and creep characteristics of polypropylene and polyester geotextiles. Three polypropylene and two polyester geotextiles were tested at -12° C (10° F) and 22° C (70° F). Results showed that temperature had very little effect on tensile strength of the geotextiles, but in general polypropylene geotextiles were found to be greatly affected by the temperature changes when compared to the polyester materials. The effect of temperature on breaking strength, strain at failure and secant modulus at 10% strain are summarized Table 4. For polyester, ultimate strength increased with increase in temperature where as for polypropylene strength decreased as temperature increased.

Table 4: Effect of temperature on the load-strain characteristics (after Allen et al., 1983)

Material Type	Breaking Strength (kN/m)		% Strain @ Failure		Normalized Secant Modulus (@ 10%)	
	22° C	-12° C	22° C	-12° C	22° C	-12° C
Polyester 1	18.5	17.5	53.2	60	33.5	20.3
Polyester 2	5.9	5.6	32.6	27.9	37.7	41
Polypropylene 1	8.9	10.3	53.3	31.3	56.9	75.2
Polypropylene 2	10.3	---	186	---	6.1	7.5
Polypropylene 3	24.2	23.7	21.2	18	151	163

The literature review conducted by Allen et al. (1983) summarized a list of all material properties which should be considered when studying temperature affects on geotextiles used as reinforcement. The importance of these properties were ranked in terms of their importance using an ordinal scale from 1 to 4, where "1" signified the least importance and "4" the greatest (Table 5).

Table 5: Importance of Temperature on Material Properties Used as Reinforcement (after Allen et al., 1983)

Geotextile Property	Importance
Tensile Strength	3
Modulus	3
Failure Elongation	4
Burst Strength	2
Durability	4
Puncture resistance	2
Static Creep Resistance	3
Dynamic Creep Resistance	2
Soil–Geotextile Friction	3
Permeability	N/A
Pore size	N/A

Calhoun (1972) investigated the effect of temperature on the load-strain characteristics of one vinylidene chloride and six polypropylene geotextiles. Tests were conducted at temperatures ranging from -18° C (0° F) to 82°C (180° F). Results showed that tensile strength was not significantly affected by changes in temperature (Figure 22), but that strain at failure and initial tensile modulus of all the geotextiles were significantly affected.

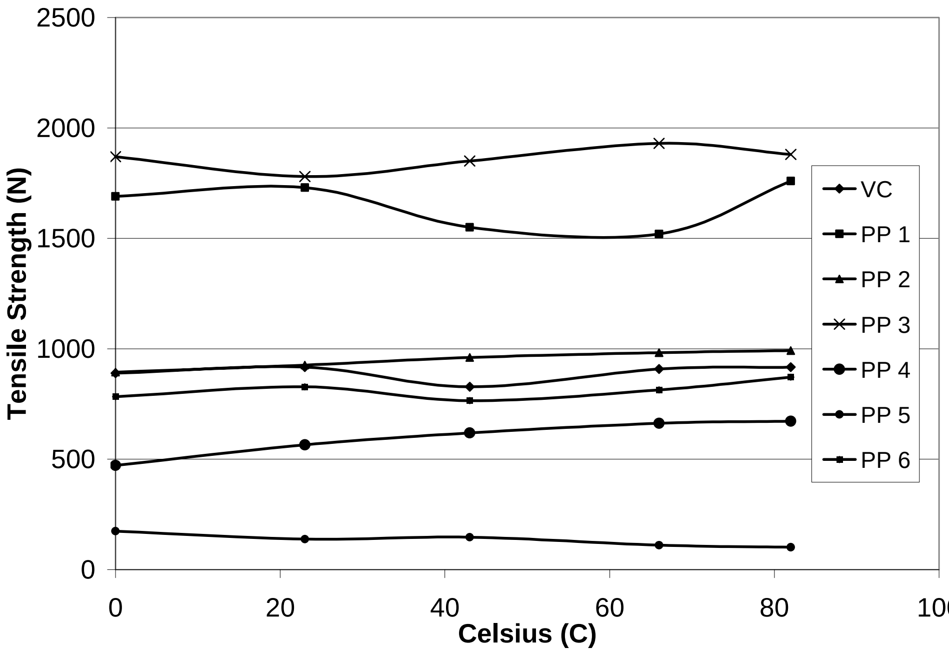

Figure 22: Effect of temperature on the tensile strength of seven woven geotextiles (after Calhoun, 1972)

Results from Austin et al. (1993) showed that the tensile modulus decreased as temperature increased from 23° C (73° F) to 32° C (90° F) for a polypropylene geogrid. The tensile modulus (secant) at lower strains (1 and 2 %) was sensitive to changes in temperature, but at 5% strain differences were negligible (Figure 23).

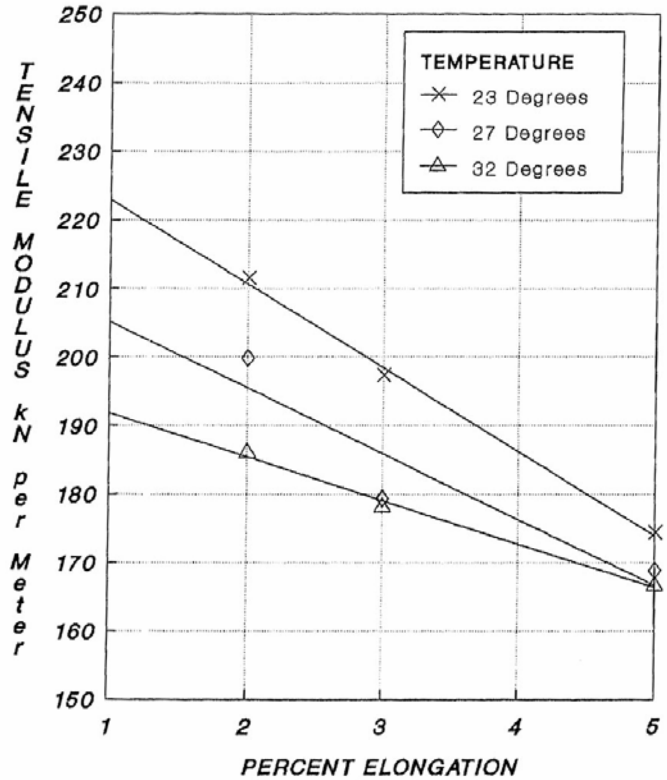

Figure 23: Effect of Temperature on Tensile Modulus (from Austin et al., 1993)

Effect of temperature on the tensile strength of single polypropylene geogrid was evaluated by McGown et al. (1985). Results showed that the tensile strength decreased as temperature increased for temperatures between 10 and 40° C (Figure 24).

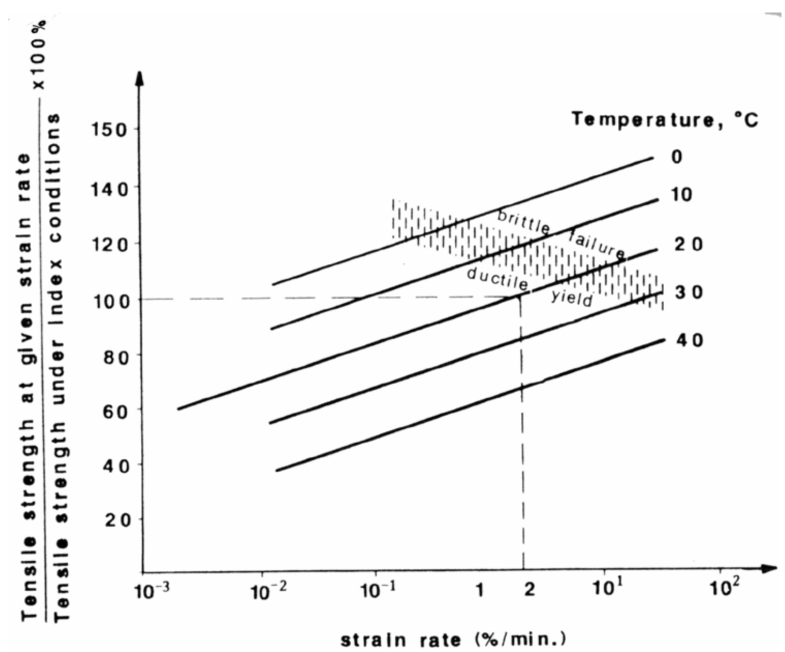

Figure 24: Effect of Temperature on a Polypropylene Geogrid (after McGown et al., 1985)

Effect of temperature on the long-term strength of HDPE geogrids was studied by Bush (1990). Three HDPE geogrids were tested at three service temperatures: 10° C (50° F), 20° C (68° F), and 40° C (104° F). Results showed that the long term strength of HDPE geogrids were relatively insensitive to changes within these temperature ranges (Figure 25).

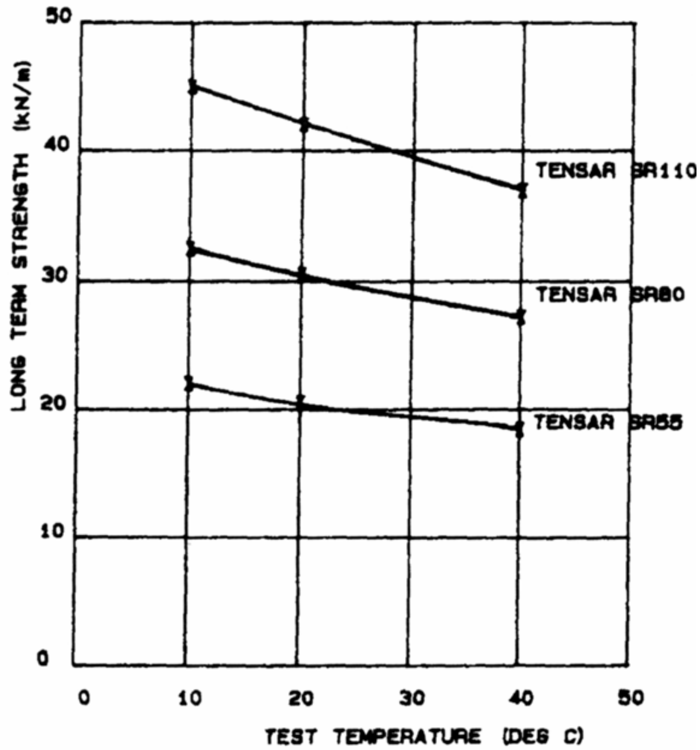

Figure 25: Effect of Temperature on Long-Term Strength of an HDPE Geogrid (from Bush, 1990)

Temperature effects on the tensile-creep behavior of three high-strength geosynthetics were investigated by Cazzuffi and Sacchetti (1999). A HDPE geogrid, a PET woven geogrid and a PP/PET woven/non-woven geotextile were tested at three temperatures: 10° C (50° F), 20° C (68° F) and 40° C (104° F). Results showed that temperature highly affects the tensile creep behavior of HDPE geogrids, has an intermediate affect on PP/PET geotextiles and little affect on PET geogrids (Figure 26).

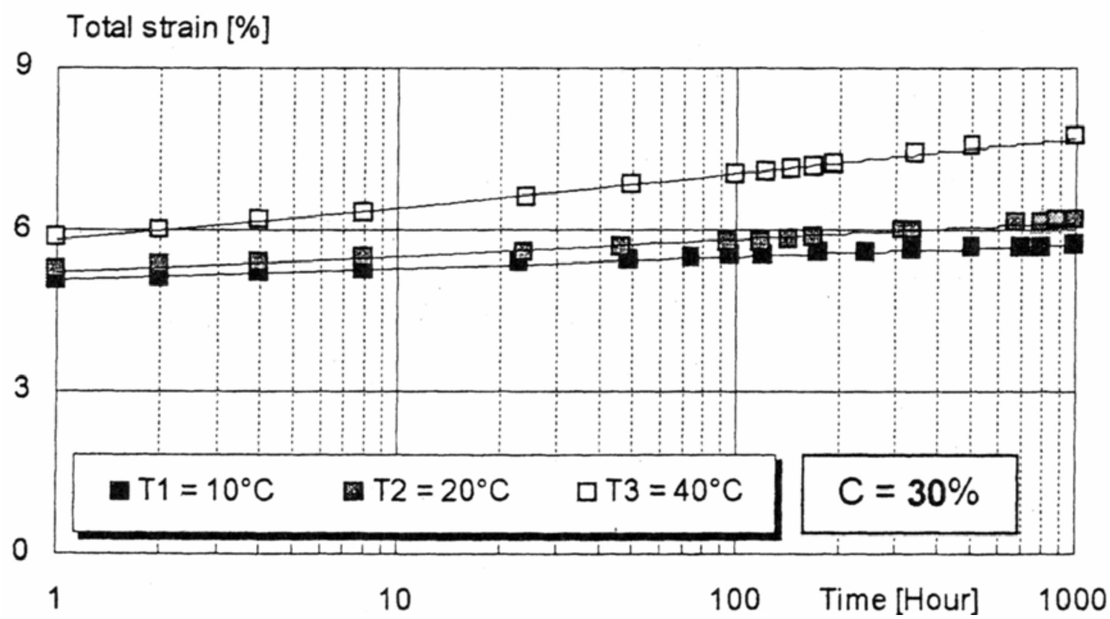

Figure 26: Effect of temperature on tensile creep behavior of PP/PET woven and non woven geotextile (from Cazzuffi and Sacchetti, 1999)

Effect of temperature on the tensile behavior of various geomembranes was studied by Tsuboi et al. (1998). The four geomembranes considered in their study were made up of high density polypropylene (HDPE), ethylene propylene diene methylene rubber (EPDM), thermo plastic olefin (TPO) and polyvinyl chloride (PVC). Tensile tests, using a dumbbell shaped specimen were conducted at temperatures ranging from -25° C to 60° C. Actual temperatures used in the study were -25° C (-13° F), 0° C (32° F), 20° C (68° F), 40° C (104° F) and 60° C (140° F). Results shows that the tensile strength increased as the temperature decreased. Additional testing using square shaped specimens tested at a constant rate of strain of 1% per minute showed that the secant modulus at 1.0% strain increased significantly as temperature decreased. Both results are shown in Figure 27.

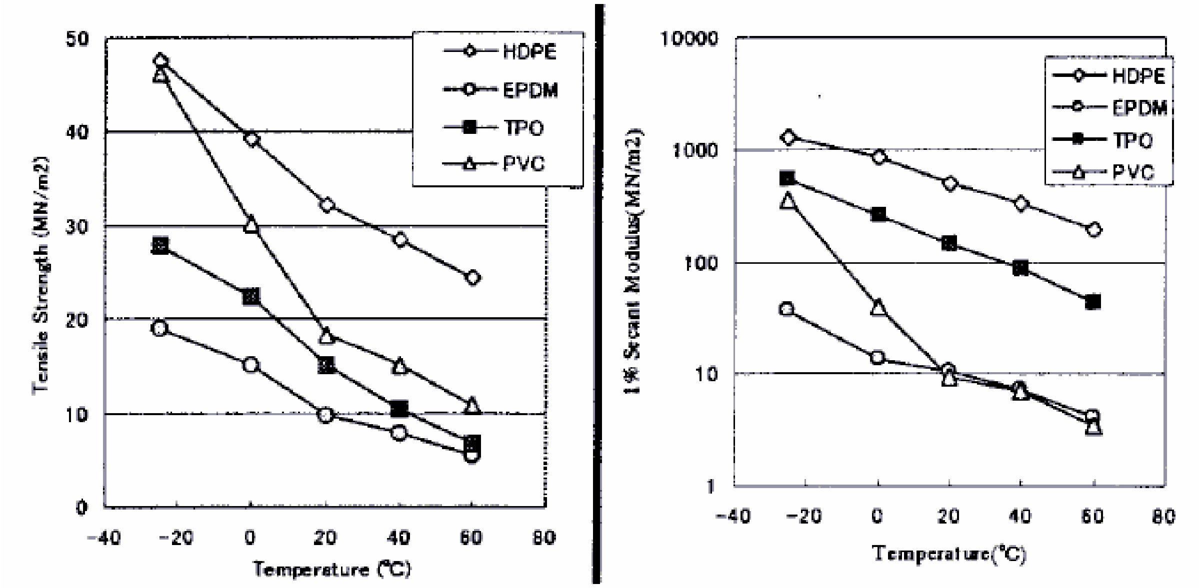

Figure 27: Temperature Effect on Tensile Strength and Secant Modulus (from Tsuboi et al., 1998)

Laboratory tests were conducted by Budiman (1994) to determine the impact of temperature fluctuations on the physical behavior of a HDPE geomembrane. The testing simulated actual field conditions by following temperature variations between the summer and winter. The temperature varied from -20° C (-4° F) to 60° C (140° F) and the specimens were subjected to 0, 1, and 120 temperature cycles. Temperature cycles had no significant effect on the stress-strain characteristics of the HDPE geomembrane, however, authors believed that higher number cycles may affect the geomembrane properties. After the temperature cycles, each specimen was tested at a particular temperatures, -20° C (-4° F), -10° C (14° F), 0° C (32° F), 20° C (68° F). Results showed that the HDPE geomembrane material exhibited increased stiffness as temperature decreased.

Soong and Lord (1998) also conducted laboratory tests to determine the design modulus of the HDPE geomembrane to use in their engineering design. For this purpose they conducted tests at temperatures of -10° C (14° F), 10° C (50° F), 30° C (86° F), 50° C (122° F), 70° C (158° F) and strain rates of 0.001, 0.01, 0.1, 1, 10, 100% per minute. Their results showed that the secant modulus at 0.3% strain did not change when the strain rates were lower than 0.01 percent per minute (Figure 28a). However, the secant modulus is significantly affected by temperature changes, as shown in Figure 28b, where the modulus decreased as temperature increased.

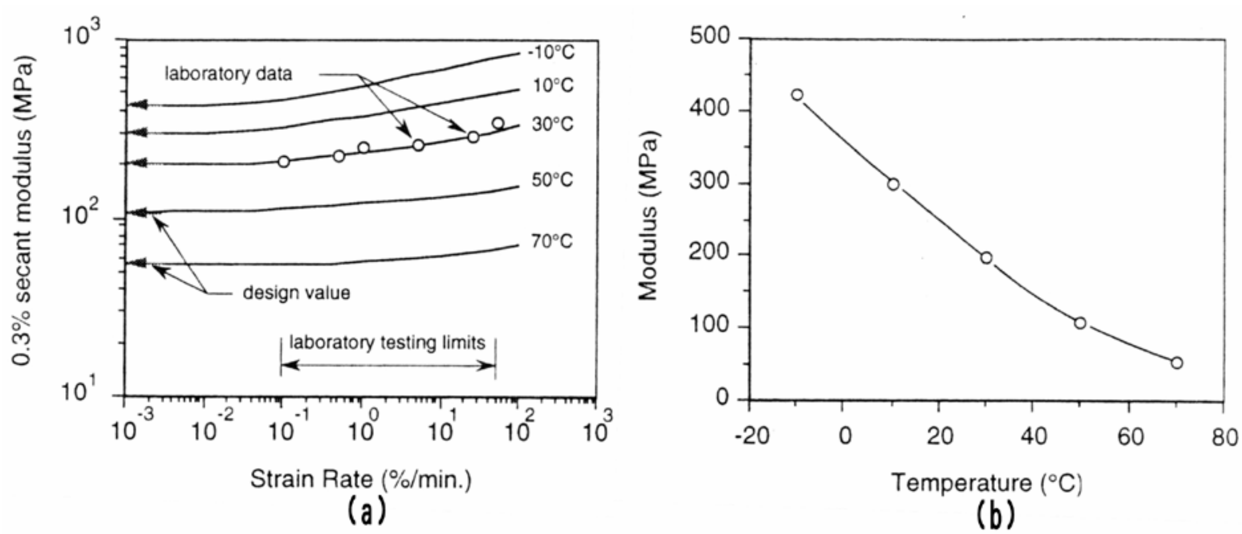

Figure 28: Effect of Temperature on Secant Modulus at 0.3% Strain (from Soong and Lord, 1998)

The effect of temperature on the stress relaxation behavior of HDPE geomembrane was studied using a commercially available HDPE geomembrane (Soong et al., 1994). The test was conducted by loading the specimen at a strain rate of 25% per minute until it reached 3% strain. At that point, the applied loads were stopped, strain was held constant and the material was allowed to relax. The test lasted at least 100 minutes and the stress induced on the material was monitored. Results indicated that the HDPE geomembrane was highly sensitive to change in temperature stress relaxation was more prominent at lower temperature than at higher temperature (Figure 29).

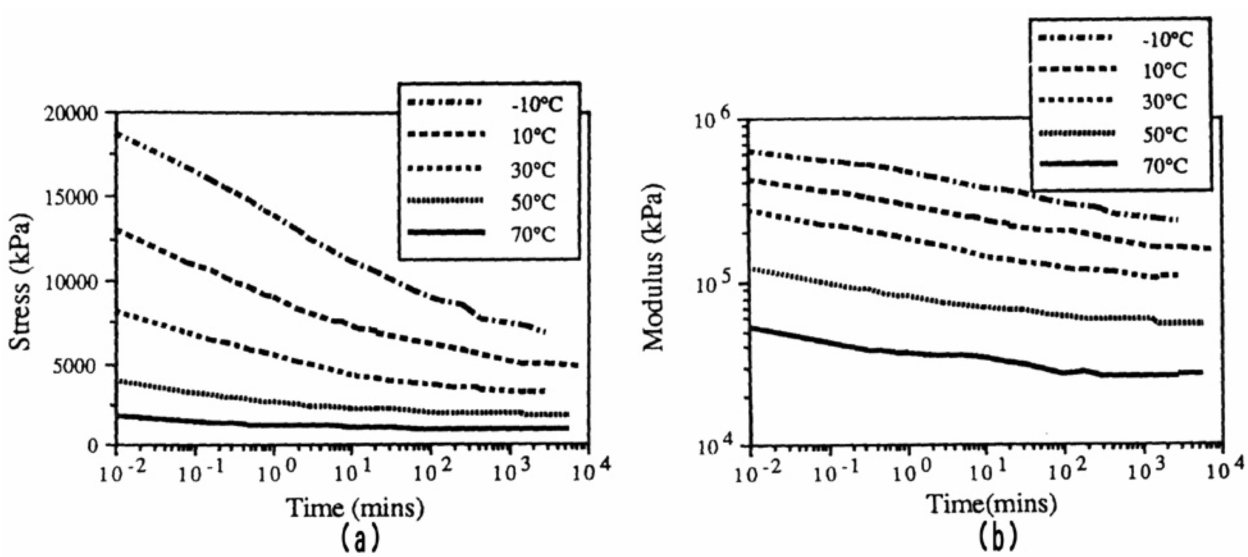

Figure 29: Effect of Temperature on Stress Relaxation and Stress Relaxation Modulus of a HDPE Geomembrane (from Soong et al., 1994)

Hsuan (1998) also studied the effect of temperature on the tensile yield behavior of two HDPE geomembranes. Tests were conducted at temperatures, 21° C (68° F) 30° C (86° F), 40° C (104° F), 50° C (122° F), 60° C (140° F), 70° C (158° F), and 80° C (176° F). The result showed that yield stress decreases as the temperature increases and that they follow a linear trend (Figure 30). It was also found that stress/strain behavior was also affected by temperature fluctuations (Figure 31).

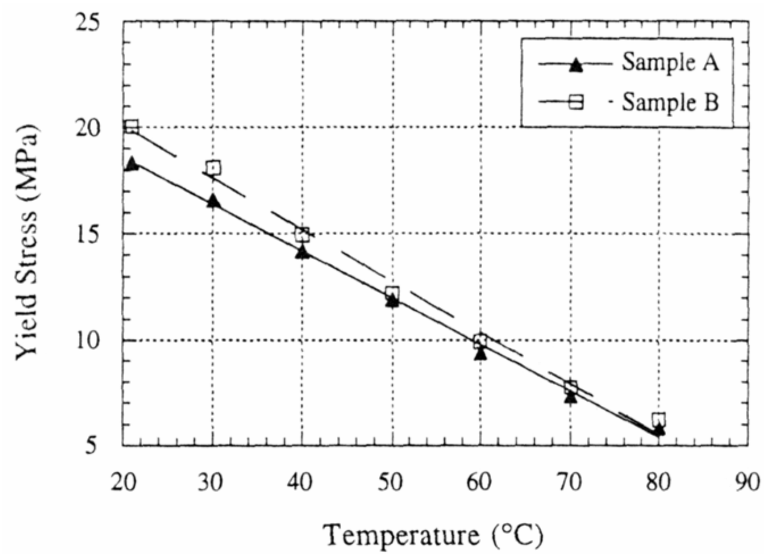

Figure 30: Changes in Tensile Yield Stress at Different Temperatures (from Hsuan, 1998)

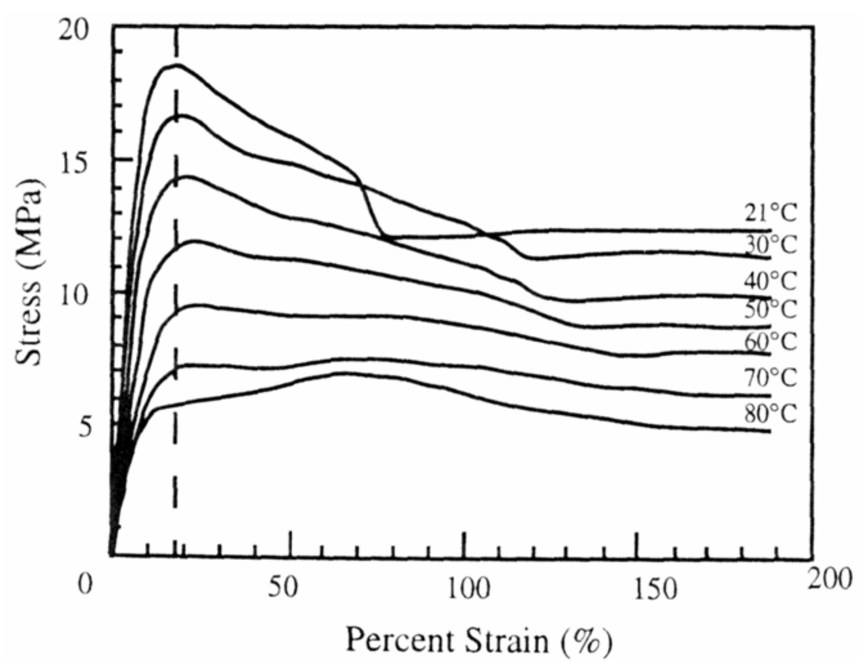

Figure 31: Temperature Effects on Stress/Strain Behavior (from Hsuan, 1998)

It is concluded that geosynthetic material properties are generally temperature dependent. Among various geosynthetic polymers, polypropylene (PP) and high density polyethylene (HDPE) materials are found to be highly sensitive to the temperature changes, while polyester (PET) is relatively insensitive. These results align well with the hypothesis that if the field temperatures are below T_g, it is unlikely their intrinsic material properties will be affected by the temperature variations. Therefore it is important to know the T_g of the geosynthetic or to conduct tensile tests on geosynthetics using a range of reasonable temperatures. It was also found that the initial tensile, secant and tangent modulus of geosynthetics are significantly affected by the temperature change in the field. Overall, the stiffness of the material decreases as temperature increases.

A summary of all authors included in this section of the literature review is provided in Table 6. Sensitivity of various geosynthetics to changes in temperature were assessed using subjective rating system ranging from 1 to 3, where 1 signifies that the material was insensitive to temperature, 2 as moderately sensitive, and 3 as highly sensitive. Ratings were assigned based on qualitative and quantitative information contained in each of the research papers considered.

Table 6: Summary of the Temperature Effects on Various Geosynthetics by Author

Author/Researcher	Temperature Range (°C)	Material Type	No. of Different Geosynthetics	Polymer Types*	Material Property of Interest	Effect on Properties[†]
Calhoun (1972)	-18 to 82	Geotextiles	6	PP	Tensile strength, Tensile modulus and strain at failure	2
			1	vinylidene chloride		2
Allen et al. (1983)	-12 to 22	Geotextiles	3	PP	Tensile strength, strain at failure, and secant modulus at 10% strain	2
			2	PET		1
McGown et al. (1985)	0 to 40	Geogrid	1	PP	Tensile strength	2
Bush (1990)	10 to 40	Geogrid	3	HDPE	Long-term strength	1
Austin et al. (1993)	23 to 32	Geogrid	1	PP	Tensile modulus at 1%, 2% and 5%	2
Budiman (1994)	-20 to 20	Geomembrane	1	HDPE	Stress/strain behavior	3
Soong et al. (1994)	-10 to 70	Geomembrane	1	HDPE	Stress relaxation and stress relaxation modulus	3
Soong and Lord (1998)	-10 to 70	Geomembrane	1	HDPE	0.3 % secant modulus	3
Hsuan (1998)	20 to 80	Geomembrane	2	HDPE	Tensile yield stress and stress/strain behavior	3
Tsuboi et al. (1998)	-25 to 60	Geomembrane	1	HDPE	Tensile strength,	2
			1		Secant modulus at 1%	3
			1	ethylene propylene diene methylene rubber	Tensile strength	2
			1		Secant modulus at 1%	2
			1	thermo plastic olefin	Tensile strength	2
			1		Secant modulus at 1%	2
			1	polyvinyl chloride	Tensile strength	3
			1		Secant modulus at 1%	2
Cazzuffi and Sacchetti (1999)	10 to 30	Geogrid	1	HDPE	Tensile creep behavior	3
			1	PET		1
		Geotextile	1	PP/PET		2

*HDPE – High Density Polyethylene
PP – Polypropylene
PET – Polyethylene

[†] 1 = low sensitivity
2 = moderate sensitivity
3 = high sensitivity

2.5 Normal Confinement

McGown et al. (1982) showed that the tensile modulus of certain geosynthetics increased as the normal stress confinement was increased. FHWA performed an extensive evaluation on the effects of confinement and developed protocols for evaluating confined extension and creep (Elias et al., 1998). In general, effects of confinement are most significant for nonwoven geotextiles, of some significance for woven geotextiles and woven geogrids, and insignificant for extruded geogrids.

2.6 Strain Measuring Instruments

It is essential to utilize stable and accurate instrumentation to measure strain induced during geosynthetics testing. Several literature sources were consulted to determine possible strain measuring devices currently available in the market, as well as those used in other similar material testing studies. Many researchers have spent significant time and money to develop and build appropriate measuring devices, and unfortunately, many of them were unsuccessful. In general, strain measuring instrumentation can be divided into two main categories: contacting and non-contacting. A summary of the available strain measuring instruments is presented below.

2.6.1 Contacting Type Instrumentation

Contacting type instrumentation is most widely used when testing geosynthetics. In this case, transducers are placed directly or indirectly on the specimen to measure strain. Bonded strain gages and Linear Variable Differential Transducers (LVDTs) are commonly used for this purpose. Various measuring techniques, advantages and problems associated with contacting type instrumentation are discussed below.

2.6.1.1 Strain Gages

Bonded strain gages are used extensively to measure strain. Essentially, strain gages detect changes in length through changes in electrical resistance. When compared to other technologies they are smaller and lighter. Strain gages must be bonded to the surface of the specimen being tested, so that strain induced in the material similarly deforms the strain gage. Special glues are used to affix the gages to the material surface. Glue type depends on the material and application. The bonding surface must be smooth to ensure accurate measurements.

Historically, strain gages are used to measure very small strains, generally less than two percent, but some types can measure up to 20+ percent. During a study conducted by Gallagher (1995) various problems were encountered when strain gages were used to measure strain in geotextiles. Unevenness of the fibers produced noticeable undulations in the strain gages, which resulted in uneven bonding to the material's surface. During testing, the bonded strain gages were not able to measure more than 80% of the total strain induced in the sample. Problems with the glue used in affixing the gages to the material also occurred. The gages also failed to remain bonded to the specimens for more than 3% strain. It was determined that strain rate during testing did not effect the bonding of the properties, nor did chemical conditioners used during bonding.

The strains induced during geosynthetic testing can easily exceed the limit of the strain gages. Because geosynthetics are made from inert polymers having low surface energy it is difficult to adhere strain gages to their surfaces. Chu et al. (1996) discussed various difficulties associated with bonding strain gages to polypropylene geosynthetics. Special strain gages types and bonding procedures must be used to ensure reliable results. They discovered that reliable bonding between strain gages and polypropylene could be achieved by first treating the surface using ultraviolet light.

Sluimer and Risseeuw (1982) summarized some of the advantages of using the appropriate strain-gages and bonding techniques as follows:

- registration of strains up to more then 10% is possible,
- there is little effects on the behavior of the geotextile,
- reading out at great distance is possible,
- it is independent of vertical pressures,
- reliability for long periods of service life, and
- handling is easy.

In their study they recommended a better method of gluing the strain gages to the geotextiles based on their results from strain gages bonded to polyester geotextiles.

Leshchinsky and Fowler (1990) used strain gages for all their tests and verified the output using photogrammetric measurements. They discussed the difficulties in attaching LVDTs and extensometers to geotextile and recommended taking extreme care when using those sensors so that geotextile behavior will not be affected. In their study they recommended a simple and inexpensive technique for measuring strains using the special type of strain gages.

Oglesby et al. (1992) attempted to develop a new protocol to successfully use strain gages on geogrids. Results from the bonded strain gages were compared to the cross head movement and extensometer results. In their study, the effects of various parameters such as strain rate, temperature and surface preparation on the measured strain using the strain gages were also studied. Using their specified gage, adhesive, surface preparation, and clamping and curing techniques, crosshead strain in the order of 25 to 30 percent were measured with excellent repeatability.

Cuelho (1998) successfully used strain gages to measure local strains induced during in-air testing. Strain gages were bonded to a geogrid and a woven geotextile using a high elongation epoxy and a silicone adhesive/sealants, respectively. The output from the strain gages were compared to externally measured displacements, and in general, the results were comparable for each of the materials. However, strain gages used on geotextiles showed larger differences than the geogrid. Specific guidelines for bonding strain gages to geosynthetics were established as part of his research.

2.6.1.2 Linearly Varying Differential Transducers (LVDTs)

Linearly Varying Differential Transducers (LVDTs) can be used as a displacement measuring instrument for wide range of displacements. Due to the limitations in the physical size and weight of LVDTs, researchers generally had difficulty attaching them to the geosynthetics. For this purpose various research projects have been done to determine how to successfully use LVDTs in geosynthetics testing.

Boyle et al. (1996) used a special setup called a "scissors" device. This device used an LVDT attached to a scissor device to transmit displacements from the material to the LVDTs (Figure 32). Needles mounted at the end of each scissor arm were used to attach the scissor mechanism to the geosynthetic. The authors found the scissors setup often gave erratic and unreliable results. In addition, they were not able to use this above setup on the specimen gage lengths less than 75 mm. In the end, they measured the observed strains using the crosshead displacement.

Bathurst and Cai (1994) used a pair of LVDTs attached directly to the material to measure its elongation. The LVDTs were attached to the specimen using two thin pieces of angled aluminum (Figure 33). Responses from each of the LVDTs were averaged to determine strain. The authors also believed that this method yields strains that are not affected by grip slippage. However, this setup will add additional weight to the specimen, which may change the behavior of the geotextile.

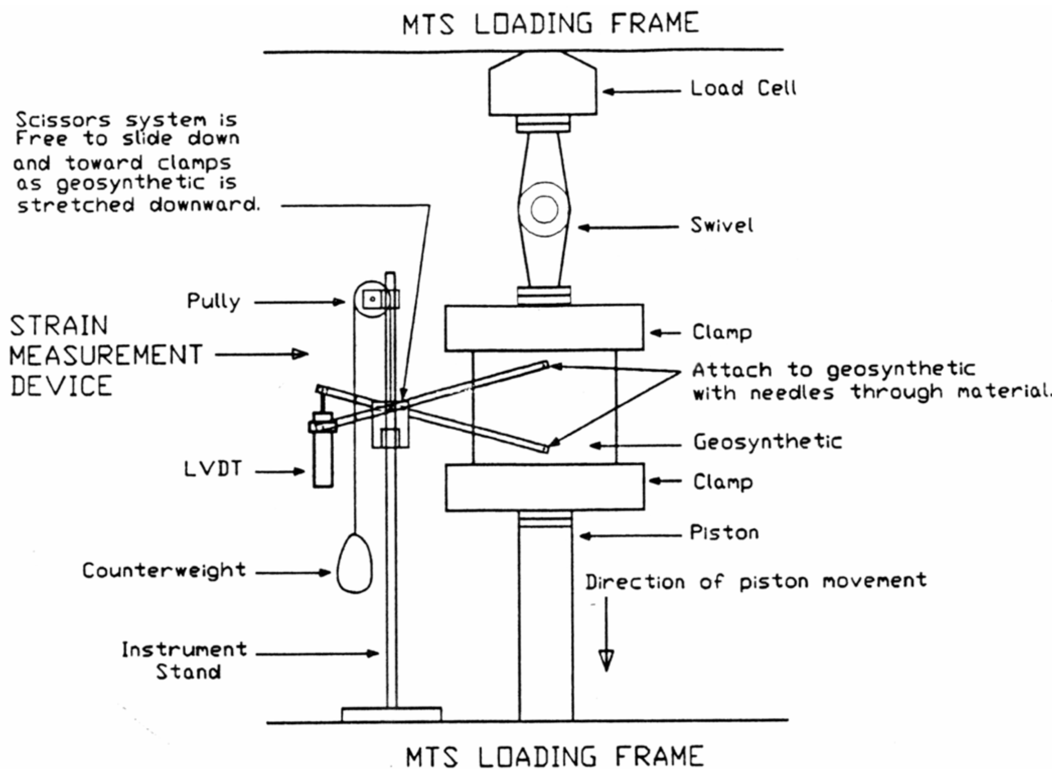

Figure 32: Schematic Diagram of the "Scissors" Device (from Boyle et al., 1996)

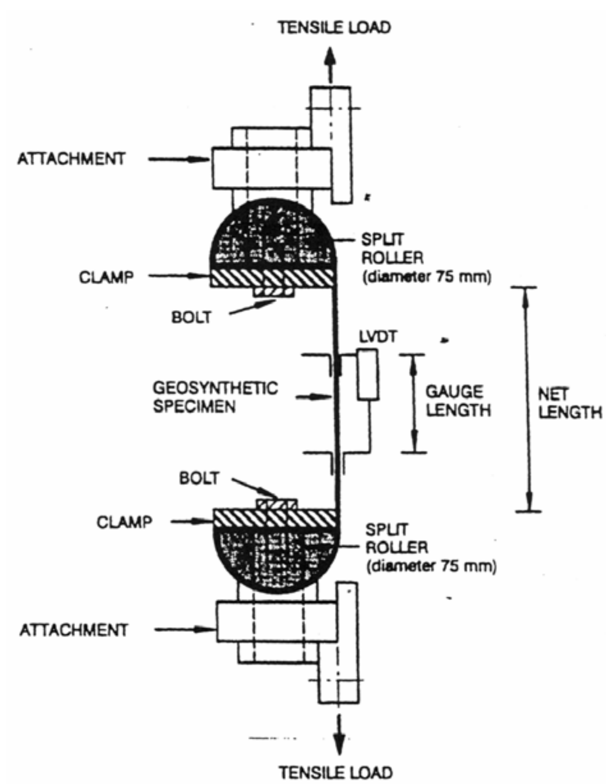

Figure 33: Direct Measurement of Displacement Using LVDTs (from Bathurst and Cai, 1994)

Ketchart and Wu (2001) developed a strain measuring technique (for geotextiles) using four LVDTs and two rows of angled plates. Both rows of small metal angles (25 mm by 25 mm) were glued to one side of the test specimen. The gage length between the two angled plates was 100 mm. Four LVDTs were mounted on the gripping system and the stylus of each LVDT was in contact with those angles glued to the specimen (Figure 34). Elongation of the specimen during the test was measured from the change in distance between the two rows of angle plates. The average elongation obtained between those two rows of angle plates were used to calculate axial strain.

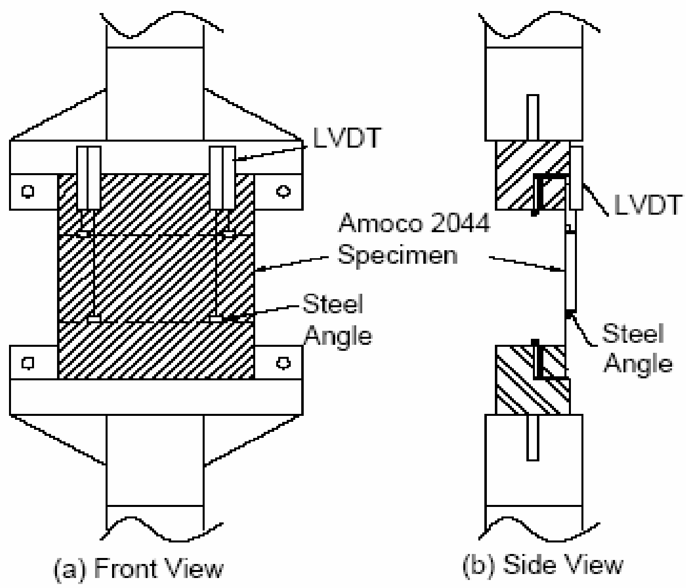

Figure 34: Strain Measuring Technique Used in Geotextile Testing (Ketchart and Wu, 2001).

2.6.1.3 Cross-Head Movement or Internal LVDT

Several researchers simply used the internal LVDT that measures the crosshead movement of the testing machine to determine overall displacement of the geosynthetic. Myles and Carswell (1986), Paulson (1993), and Allen et al. (1982) used the direct crosshead movement to measure displacement, and indirectly strain, during testing. Rowe and Ho (1986) used the travel of ram of the loading machine and the results were compared to the displacement measured by an optical measuring instrument.

Ashmawy and Bourdeau (1996) concluded that the effect of slippage on the measurement is relatively small and can be neglected for specimen lengths greater than or equal to 300 mm. They also concluded that using crosshead displacement for measuring strain is very economical since most load devices have an internal LVDT.

Austin et al. (1993) used an external strain extensometer to reduce the uncertainty in the measurement of strain using crossheads. An extensometer having a range of ±5.1 mm was mounted to the geosynthetic using a pair of small knife blades using rubber bands (Figure 35).

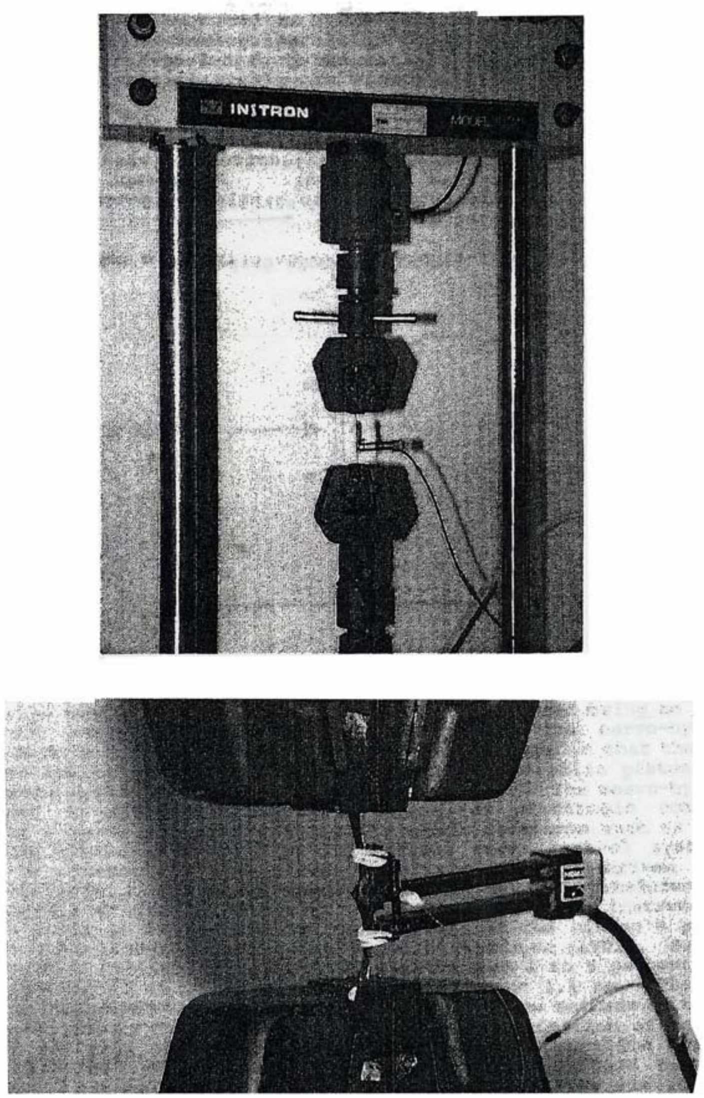

Figure 35: External Extensometer for Measuring Strain (from Austin et al., 1993)

2.6.2 Non-Contacting Type Instrumentation

More recently, the testing community has been offered a number of new optical, video and laser based devices to satisfy the need for non-contacting strain measurement. The non-contacting measuring devices are easy to setup, easy to use, are highly accurate and create no adverse affects on the behavior of the testing material. Many devices of this type are capable of measuring strain less than 1% to more than 1000% strain and also measures at a high accuracy of ±0.0001 in. The technical approach employed by these devices varies widely; from video image processing of gage marks to measuring lateral displacement at two gage locations using phase measurement of scattered laser light. One method uses speckle metrology to measure strain at a single specimen location. With respect to sample preparation, most methods require that gage marks, targets or flags be applied to the material. Cost for this type of extensometer varies from $5000 to $25,000.

Moracai and Montanelli (1997) successfully used a video extensometer to measure strain during cyclic and monotonic testing. They concluded that results from their testing were obtained at higher accuracy and found the results free of errors.

In general, contacting and non-contacting strain measuring instruments have their own advantages and disadvantages. Contacting type instruments are relatively inexpensive, but may affect readings depending on how they are attached to the geosynthetic during testing. In addition, heavy electronics hanging off of the sample can distort the geosynthetic, which affects the results. Moreover, if one wishes to bring the material to failure, they risk breaking the equipment in the process. Non-contacting instruments are accurate and easy to use but are expensive. For relatively low loads and cross-head displacement measurements can be used to determine strain, since very little slip between the grips and the geosynthetic occurs under small loads.

2.7 Synthesis and Implications of Literature Review

The results from the literature review suggested modest yet important effects due to temperature on modulus and significant effect of strain rate on modulus. However, the existing information is incomplete and does not allow general modifications to the tensile modulus values determined from standard tension tests to be adjusted so that material properties at temperatures and strain rates occurring in roadways are more characteristic. Although less work has been conducted to determine the effects of normal confinement, the literature suggested that the tensile modulus of certain geosynthetics can be significantly affected under these conditions. Finally, the load-strain behavior was significantly affected when cyclic loads were applied to geosynthetic material samples.

Based on these results, a matrix of laboratory tests using all of these test variables is necessary to better determine their effect on geosynthetic material properties. Unfortunately, time and resources constrained this research effort to experiments that studied the effects of load type, and to a lesser extent, strain rate and specimen size. Hopefully, future work will continue this endeavor to provide appropriate material properties and develop test protocols with respect to all of these test variables.

Literature reviewed with respect to strain measurement instrumentation revealed that there are monetary benefits when contacting-type instrumentation is used, but limited functionality. On the other hand, increased functionality, like that gained when non-contacting instrumentation is used, is offset by increased costs.

3 DESCRIPTION OF TEST EQUIPMENT

The apparatus used in this research consisted of four main components: a servo-hydraulic load frame, special grips, displacement and strain sensors and a data acquisition system. Each of these components is described in the following subsections.

3.1.1 Loading System

A servo-hydraulic loading system (MTS 8500 Plus) was used to apply load to the geosynthetics during testing (Figure 36). Special grips attached to the hydraulic actuator were used to deliver the load to the material. A programmable control unit coupled with an internal LVDT and load cell was used to regulate strain rates and load limits. The crosshead was able to move up and down on two vertical columns to accommodate various dimensions of the geosynthetic, but remained stationary during testing. The hydraulic actuator located in the base of the load frame provided the load during testing.

A programmable control unit was used to control the servo-hydraulic actuator using information from an internal lvdt and a load cell. Incidentally, the lvdt and load cell also provided measures of displacement of the load cylinder and the applied load, respectively. The load cell has a maximum capacity of 250 kN and an sensitivity of 0.00543 kN. The internal lvdt has a sensitivity of 0.0127 mm.

3.1.2 Gripping Mechanism

Special grips (Curtis "Geo-Grips") were used to transfer the load from the hydraulic actuator to the geosynthetic sample. These grips were specially designed to test planar synthetic materials such as geosynthetics. The grips have a maximum gripping force of 44.5 kN and can accommodate a test specimen up to 200 mm wide. Geo-Grips use hydraulic pressure to hold the geosynthetic in place. Two different grip facing materials could be used to minimize slip depending on which material was being tested.

Figure 36: MTS 8500 Plus Loading System

3.1.3 Instrumentation

Based on literature reviewed as part of this study, accurately measuring strain on geosynthetics during testing was of primary concern. Many methods currently available are either very expensive or are difficult to mount to geosynthetics. Many attempts were made to design an accurate, reliable, easy-to-use, universal strain measuring device. However, in this study, axial strains were calculated using displacement measurements from the lvdt internal to the load frame. One issue associated with using the internal lvdt for the strain calculation is slip between the grips and the material. An external lvdt and a device called a “clip gage” were used to determine whether appreciable slip was occurring between the geosynthetic and the grips. The sensitivities of the internal and external lvdts and the clip gage are 0.012 mm, 0.020 mm, and 0.022 mm, respectively. The entire experimental setup is shown in Figure 37.

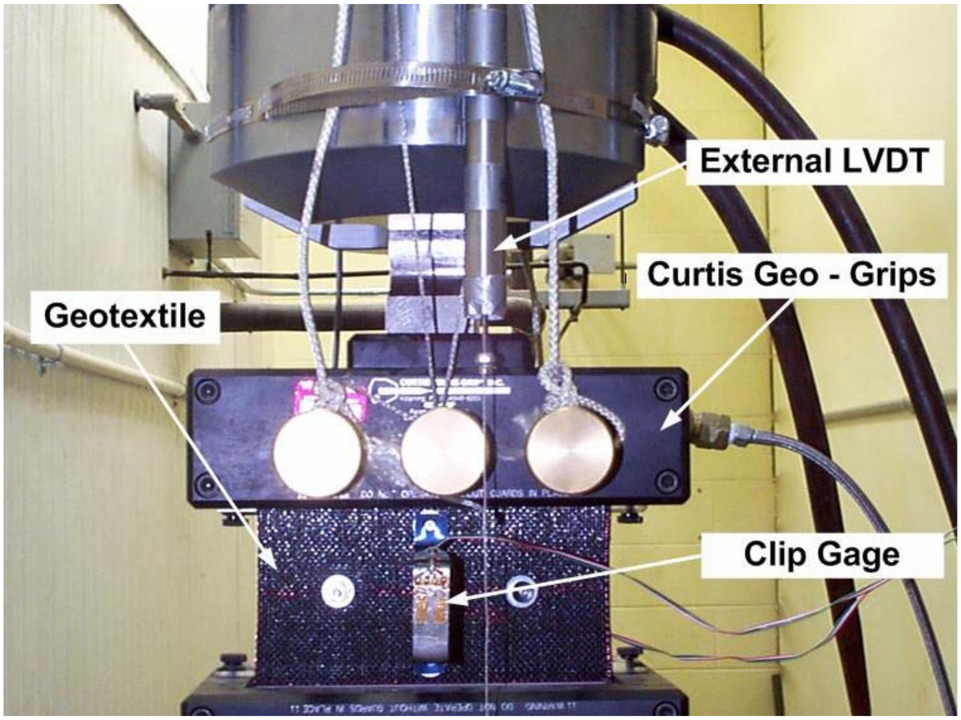

Figure 37: Experimental Set Up

The body of the clip gage was constructed from a piece of spring steel bent in the shape of a flat “U.” The bottom of the “U” was instrumented with four strain gages to measure flexure as the legs of the “U” are moved side to side. Hinges at the top of the “U,” where it attaches to the geosynthetic, kept the legs from buckling as they move. A picture of the clip gage is shown in Figure 38.

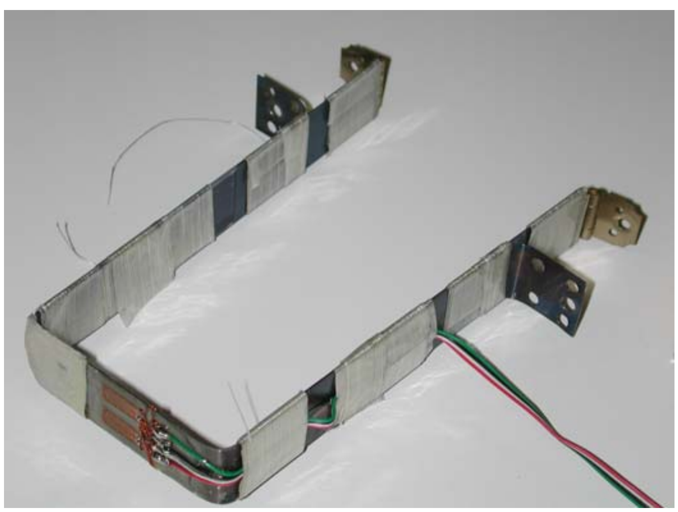

Figure 38: Clip Gage

The strain gages attached to the clip gage were arranged in a full bridge circuit configuration: two on the topside of the spring steel and two on the underside. Figure 39 illustrates the strain gage layout and corresponding circuit. This arrangement provided the greatest sensitivity, allowing the clip gage to measure displacements to the nearest 0.022 mm. The sensitivity of the clip gages was similar to the external lvdts, but it measured the displacement directly on the geosynthetic, thereby avoiding grip slip issues. The clip gage was calibrated using a special jig that produced a purely linear motion in the legs. From this a linear relationship between voltage and displacement was established. Strain can be calculated if the original distance between the legs is known. The clip gage can be used with either a convex or concave shape to the gaged portion of the spring steel, however, care was taken to ensure that the gage did not go through the "snap-through" portion (i.e., when the gage reverses from a concave shape to convex, or vice versa), because in that portion the voltage-displacement relationship is non-linear and cannot be easily predicted.

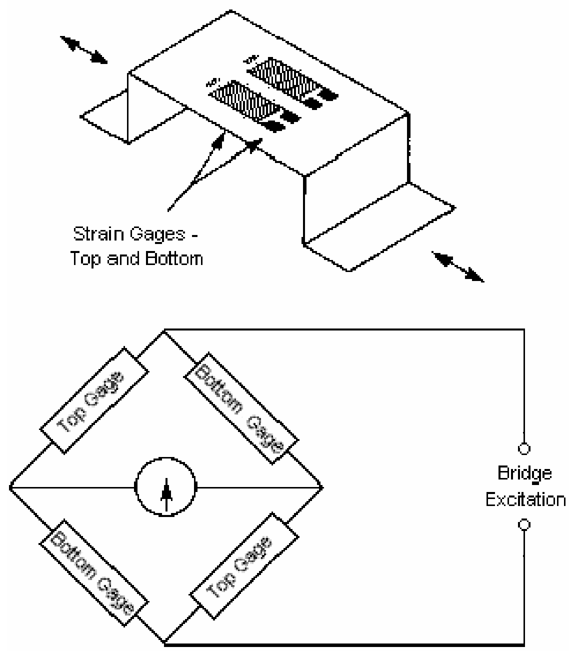

Figure 39: Clip Gage's Strain Gage Layout and Corresponding Circuit (from Vishay, 2004)

3.1.4 Materials/Sample Preparation

Seven polypropylene-based geosynthetics were tested throughout the course of this research project: four geogrids and three geotextiles. A basic description of their properties is provided in Table 7.

Geosynthetic samples were cut from manufacturer-supplied rolls in the two principle directions: machine direction (MD) and cross-machine direction (XMD). Final dimensions were approximately 200 mm wide by 125 mm long for geotextiles and approximately 200 mm wide by 300 mm long for geogrids. Approximately 50 mm of material was engaged by the grips on either side. Lines were drawn on the sample to ensure proper orientation during testing. Since the junctions on the geogrids were much thicker than the remaining material, the gage length was measured between the junctions within the grips.

Table 7: General Description of the Geosynthetics

Generic Name	Manufacturer & Brand Name	Geosynthetic Type	Polymer Type / Structure
Geosynthetic A	Amoco ProPex 2006	Geotextile	Polypropylene / Woven
Geosynthetic B	Colbond Enkagrid Max 20	Geogrid	Polypropylene / Welded grid
Geosynthetic C	Synthetic Industries Geotex 3×3	Geotextile	Polypropylene / Woven
Geosynthetic D	Ten Cate Nicolon Geolon HP570	Geotextile	Polypropylene / Woven
Geosynthetic E	Tenax MS220b	Geogrid	Polypropylene / Extruded, multi-layer
Geosynthetic F	Tensar BX1100	Geogrid	Polypropylene / Biaxial, punched, drawn
Geosynthetic G	Tensar BX1200	Geogrid	Polypropylene / Biaxial, punched, drawn

4 TEST PROTOCOLS

Three parameters were considered to help define the appropriate test protocols by which to test geosynthetic materials in air. The existing wide-width test protocols (ASTM D4595 for geotextiles, and ASTM D6637 for geogrids) were used as the basis for the tests conducted in this study. These standard protocols were modified to incorporate various load application types (i.e., monotonic loading or cyclic loading), various material load rates, and various sample sizes. The following subsections describe how the laboratory test equipment was used and the data that was collected during testing.

4.1.1 Monotonic Test Protocol

Control tests were conducted according to ASTM D4595 for geotextiles and ASTM D6637 for geogrids. These tests are monotonic or constant strain rate tests. They were conducted at a strain rate of 10% per minute to define the material's constitutive material parameters under this type of loading. In particular, the tensile properties up to approximately 5% strain were desired from these tests. The tests were conducted on both machine and cross-machine directions of the material and were repeated at least twice to verify the repeatability of the results. The load-strain curves for both the machine and cross-machine direction of the Amoco ProPex 2006 geotextile material is provided as an illustration of typical results in Figure 40. All monotonic load-strain relationships for each material are presented in Appendix A.

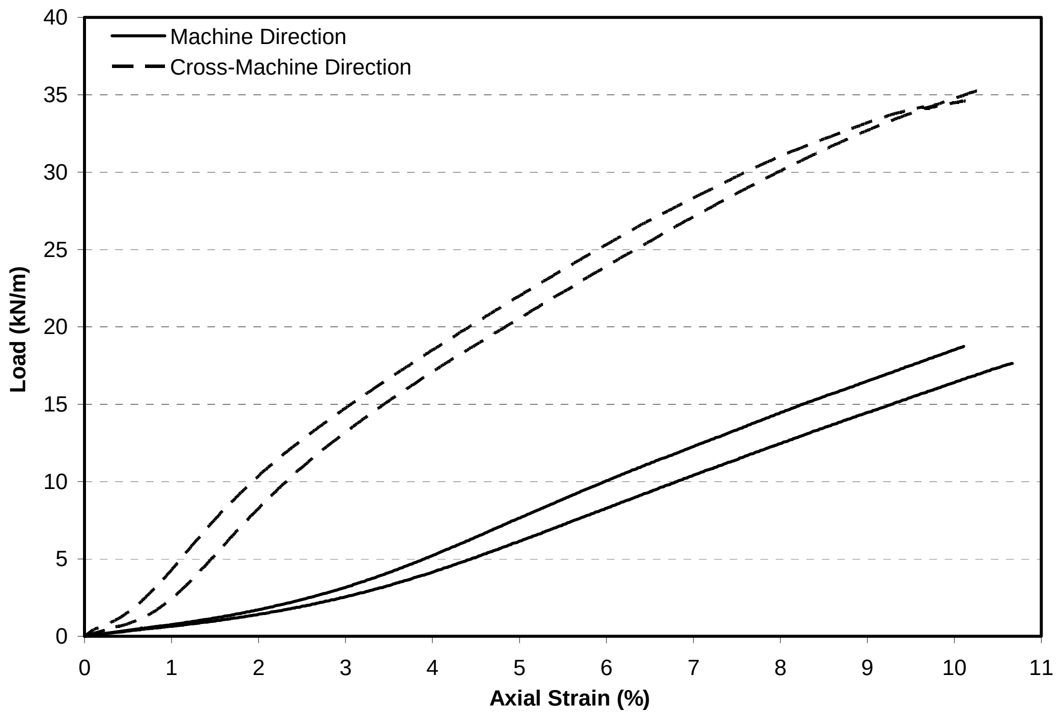

Figure 40: Monotonic, Load-Strain Curves for Amoco ProPex 2006 Geotextile in Both Principle Strength Directions

4.1.1.1 Strain Rate Effects

To determine the effect of strain rate on the material properties of the various geosynthetics, a series of monotonic tests were conducted using a modified monotonic testing procedure. Each geosynthetic material was pulled at three different strain rates: 0.03, 0.40 and 20.0% per minute. All geosynthetics were tested to failure in both the machine and cross-machine directions. An example of the results from these tests conducted on the Tensar BX1100 Geogrid in the Cross-Machine Direction is shown in Figure 41. The remaining results may be found in Appendix B. No tests were conducted on the Synthetic Industries Geotex 3x3 geotextile or the Tenax MS 220b geogrid. In addition, tests were not run in the cross-machine direction of the Tensar BX 1200 material.

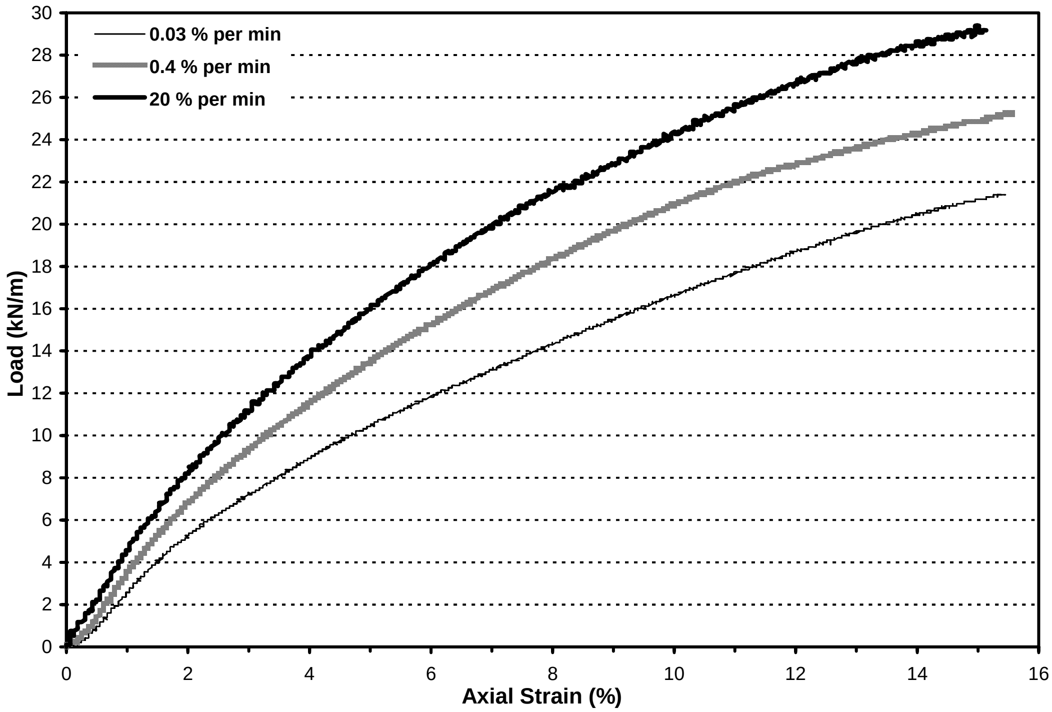

Figure 41: Load-Strain Curves for the Tensar BX1100 Geogrid in the Cross-Machine Direction at Three Strain Rates

4.1.1.2 Effects of Specimen Size

As indicated by the research in the literature review, changes in the sample size used during testing may affect the apparent material properties. Using the standard test protocol, length and width were varied for two of the materials (the Amoco 2006 geotextile and the Tensar BX1100 geogrid) to help identify any potential differences. Four widths 51, 102, 152, and 203 mm (2, 4, 6, and 8 inches) and six lengths 102, 203, 305, 406, 508, and 610 mm (4, 8, 12, 16, 20, and 24 inches) were considered for the Amoco 2006 material. Five widths and four lengths were used for the Tensar BX1100 geogrid. Because the dimensions in the geogrid were dependent on the spacing of the ribs, measurements of length and width were made from the nodes of the material. The widths of the geogrid considered in this study were based on 2, 3, 4, 5, and 6 longitudinal ribs, which corresponds to distances of 43, 81, 122, 160 and 201 mm (1.7, 3.2, 4.8, 6.3, and 7.9 inches), respectively. Likewise, the lengths of the geogrid, based on the number of transverse ribs, considered in this study were 5, 11, 16, and 24; which corresponded to distances of 114, 287, 429, and 627 mm (4.5, 11.3, 16.9, and 24.7 inches), respectively. Replicates were tested in all cases and, like the monotonic tests, the materials were pulled at a constant rate of strain of 10% per minute. A summary of the samples sizes is shown in Table 8. An example of the results from tests conducted on the Amoco 2006 geotextile samples, having a width of 102 mm and various lengths (DOE Levels 1 through 6), is shown in Figure 42. The remaining results of this testing are located in Appendix C.

Table 8: Material Sample Sizes Tested

DOE Level	Amoco 2006		Tensar BX 1100	
	Width (mm/in.)	Length (mm/in.)	Width (# of transverse ribs – mm/in.)	Length (# of longitudinal ribs – mm/in.)
1	52/2	102/4	2 – 43/1.7	5 – 114/4.5
2	52/2	203/8	2 – 43/1.7	11 – 287/11.3
3	52/2	305/12	2 – 43/1.7	16 – 429/16.9
4	52/2	406/16	2 – 43/1.7	24 – 627/24.7
5	52/2	508/20	3 – 81/3.2	5 – 114/4.5
6	52/2	610/24	3 – 81/3.2	11 – 287/11.3
7	102/4	102/4	3 – 81/3.2	16 – 429/16.9
8	102/4	203/8	3 – 81/3.2	24 – 627/24.7
9	102/4	305/12	4 - 122/4.8	5 – 114/4.5
10	102/4	406/16	4 - 122/4.8	11 – 287/11.3
11	102/4	508/20	4 - 122/4.8	16 – 429/16.9
12	102/4	610/24	4 - 122/4.8	24 – 627/24.7
13	152/6	102/4	5 – 160/6.3	5 – 114/4.5
14	152/6	203/8	5 – 160/6.3	11 – 287/11.3
15	152/6	305/12	5 – 160/6.3	16 – 429/16.9
16	152/6	406/16	5 – 160/6.3	24 – 627/24.7
17	152/6	508/20	6 – 201/7.9	5 – 114/4.5
18	152/6	610/24	6 – 201/7.9	11 – 287/11.3
19	203/8	102/4	6 – 201/7.9	16 – 429/16.9
20	203/8	203/8	6 – 201/7.9	24 – 627/24.7
21	203/8	305/12	---	---
22	203/8	406/16	---	---
23	203/8	508/20	---	---
24	203/8	610/24	---	---

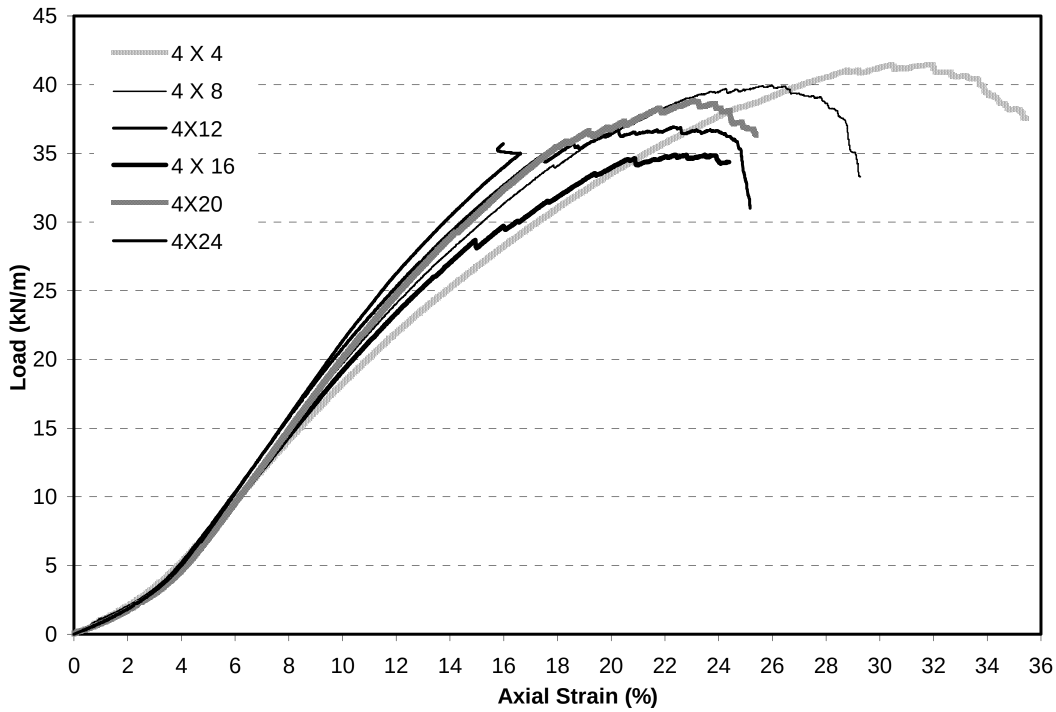

Figure 42: Load-Strain Curves for Amoco ProPex 2006 Geotextile with Constant Specimen width of 102 mm (4 inches) and Varying Specimen Length

4.1.2 Cyclic Test Protocol

In a reinforced pavement, permanent strain in the reinforcement material is seen to increase with increased traffic passes while dynamic strain for each traffic pass of constant load magnitude remains relatively constant. For non-linear reinforcement materials, the modulus will be dependent on the current strain or load at which a cycle of load is applied, which is in turn dependent on the number of traffic passes that have been applied. Creep and/or stress relaxation during repeated loading also leads to changes in material stiffness as the material is reloaded. Conditioning of the material during construction may also be a factor, especially for materials whose load-strain curve is convex.

In the cyclic tension tests, the geosynthetic was first loaded up to a prescribed axial strain, followed by the application of 1000 load cycles where the axial strain varied between prescribed limits, having a cyclic strain amplitude of 0.2%. The seating strain was applied at a rate of 50% per minute while the cyclic strain was applied at a rate of 16% per minute. The tests performed in this way were cyclic stress-relaxation tests, in that load was allowed to decrease as the strain was cycled between set limits. Table 9 shows the seating strain values for the six steps. Typical output from a cyclic test conducted on the Synthetic Industries Geotex 3×3 geotextile in the cross machine direction is illustrated in Figure 43. Similar to the monotonic tests, each test was repeated to verify the repeatability of the results. The remaining cyclic load-strain relationships for each material are presented in Appendix D.

Table 9: Seating Strain Levels for Each Step Used in the Cyclic Tests

Step	Seating Strain (%)	Cyclic Strain (%)
1	0.5	0.2
2	1.0	0.2
3	1.5	0.2
4	2.0	0.2
5	3.0	0.2
6	4.0	0.2

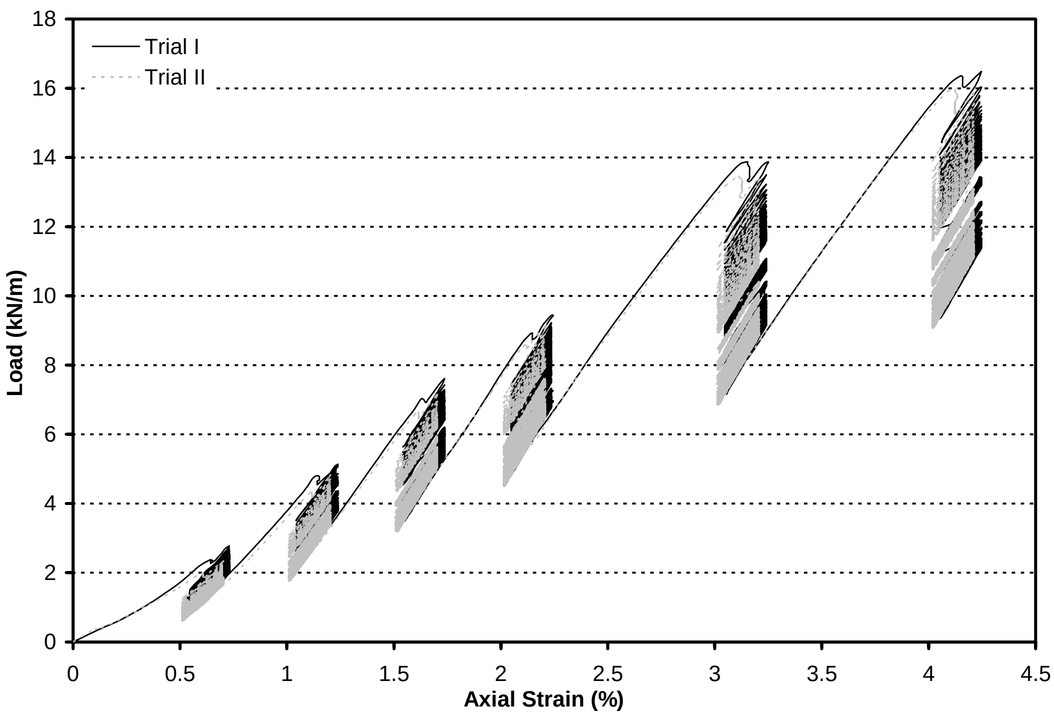

Figure 43: Cyclic, Load-Strain Curves for the Synthetic Industries Geotex 3×3 Geotextile in the Cross Machine Direction

5 ANALYSIS OF TEST RESULTS

5.1 Comparison of Cyclic and Tangent Modulus

Material stiffness in both principle strength directions, represented by the tangent and cyclic modulus, were calculated from the monotonic and cyclic tests, respectively. Tangent modulus was calculated using the monotonic test results by fitting a sixth-order polynomial curve to the monotonic load-strain curve. The derivative of the polynomial equation was taken to determine the slope of the curve at any strain level. Strain levels corresponding to the sequential steps used in the cyclic tests were used to determine corresponding tangent modulus values.

The cyclic modulus was determined at each of the six sequential load steps using the 1000th cycle. Recall that at each load step, 1000 load cycles were imparted to the material. A loading/unloading loop of load and strain is produced from each cycle. The cyclic modulus is defined as the straight line connecting the minimum and maximum load during a particular cycle. This procedure was used to calculate the cyclic modulus of all the six load steps. Differences in cyclic modulus were also investigated as the 1000 cycles were administered. As such, cyclic modulus was calculated at 30th, 500th, and 990th cycles. The average of the modulus from these three load cycles, at each of the six load steps were also calculated.

The cyclic and tangent moduli were calculated at similar strain levels to make comparisons between the two loading conditions. The results for the individual materials are shown and discussed below.

For the geotextiles used in this study (Amoco 2006, Synthetic Industries 3×3, and Geolon HP570) the initial load-strain behavior is generally the least stiff part of the curve, meaning the initial modulus is the lowest of all cyclic or tangent values, thereby showing a hardening effect. This is illustrated in Figure 44, a comparison of the monotonic and cyclic curves for Amoco 2006 in the machine direction. The other geotextiles, with the exception of Amoco 2006 and Geolon HP570 in the cross-machine direction, show this trend. In most cases, little stress-relaxation is observed for the lower steps and less is observed in the machine direction as compared to the cross-machine direction. This results in cyclic modulus values for the lower steps that are closer to the tangent modulus values. As stress-relaxation increases the higher steps, the cyclic modulus becomes greater. On the other hand, for the geogrids tested in this study (Tensar BX1100, Tensar BX1200, Enkagrid Max20, and Tenax MS220b), the initial load-strain behavior is generally the stiffest portion of the curve, thereby showing a softening effect. The results of Tensar BX1100 geogrid in the machine direction, which are similar to the other geogrids and the anomalous geotextile materials previously mentioned, are shown in Figure 45. The remaining cyclic and monotonic curves for each of the materials in each of the principle strength directions are located in Appendix E.

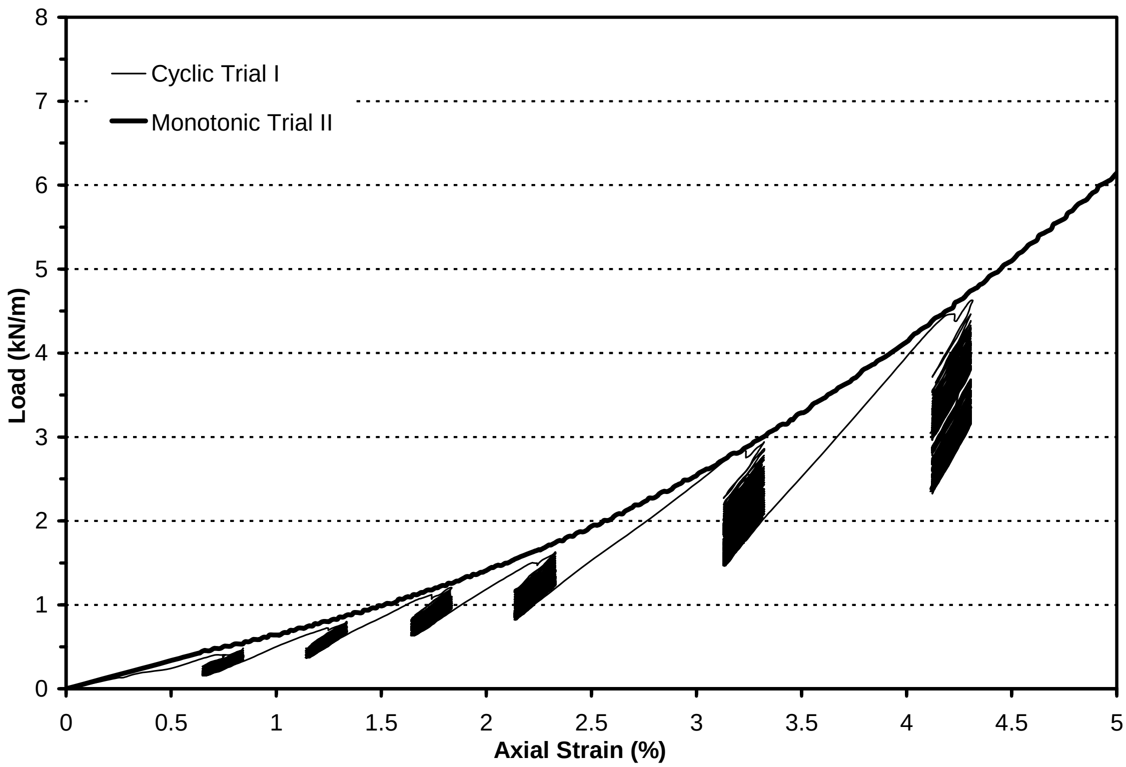

Figure 44: Cyclic and Monotonic Wide-Width Tests on Amoco 2006, Machine Direction

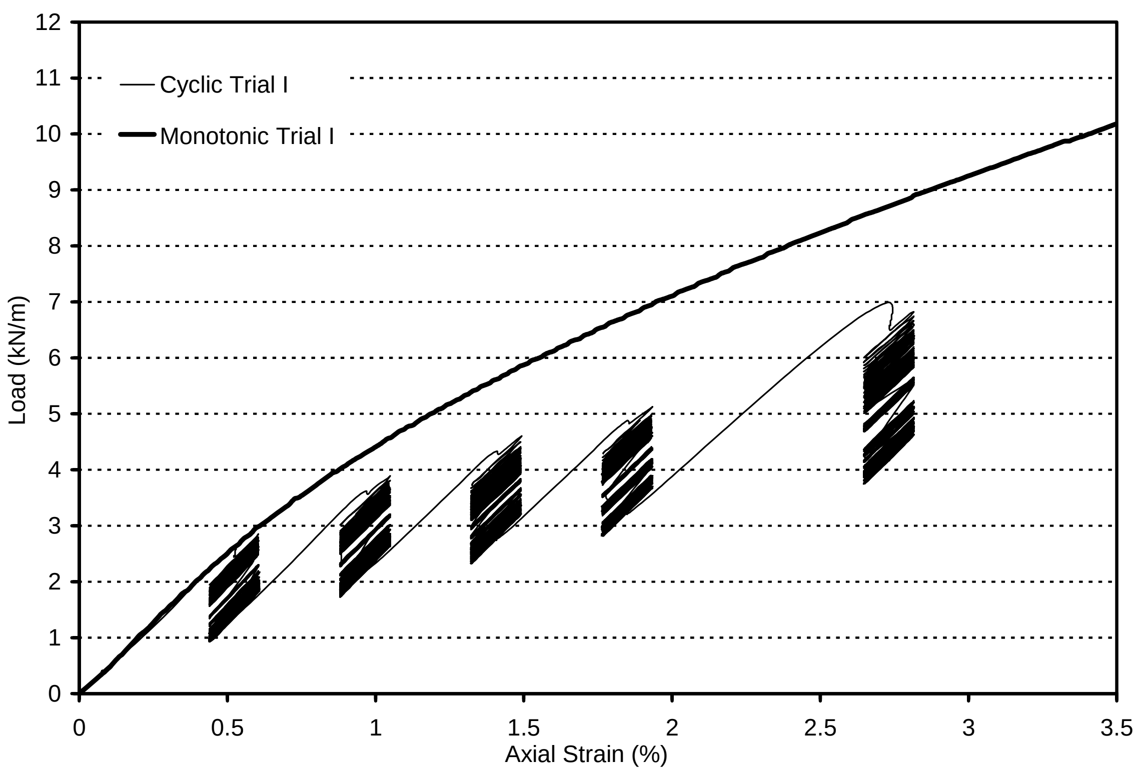

Figure 45: Cyclic and Monotonic Wide-Width Tests on Tensar BX1100, Machine Direction

For the geotextile materials, the cyclic modulus tends to increase significantly with increased strain level, as shown in Figures 46 and 47 – plots of the cyclic modulus as a function of permanent strain for all the materials oriented in the machine and cross-machine directions, respectively. Conversely, the cyclic modulus of the geogrids remains relatively constant for all levels of permanent strain. The points at zero strain were determined from the initial modulus of the monotonic curves. In the absence of strain induced in the material during compaction, these results would suggest that the values at zero strain be used for early load applications. It might also be argued that values for the early load cycles be evaluated for a small value of strain (e.g., 0.2%) to represent the dynamic strain in the material during load application.

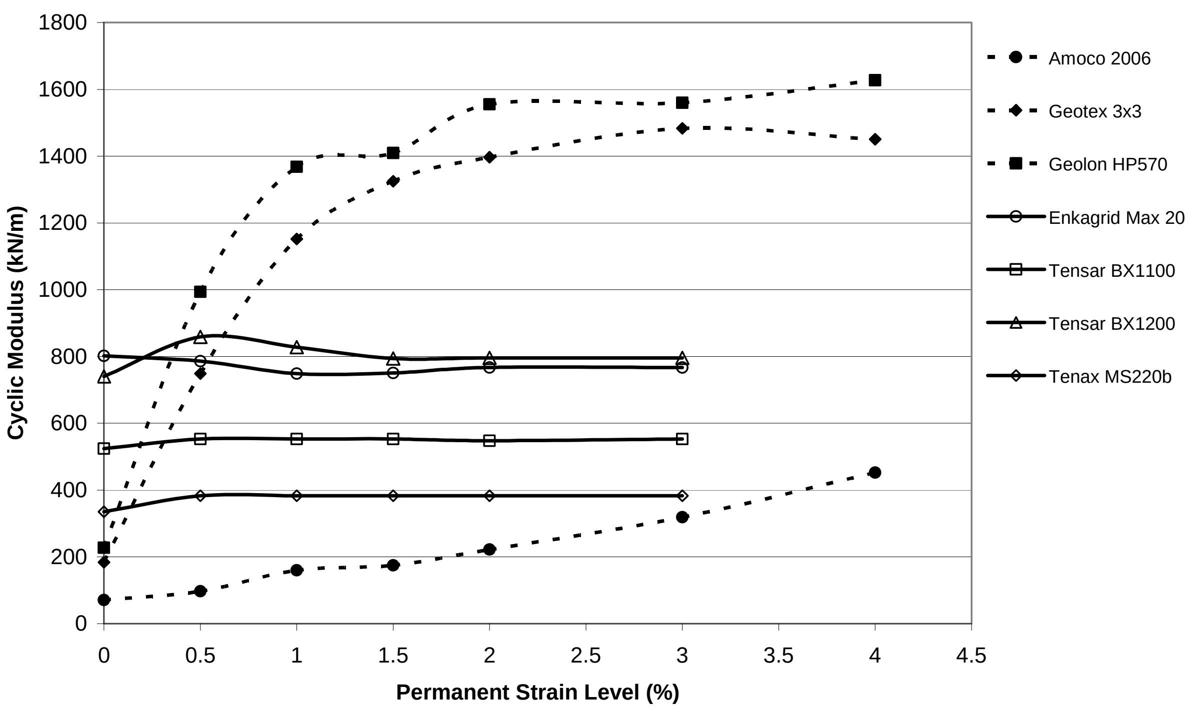

Figure 46: Cyclic Tensile Modulus versus Permanent Strain for All Geosynthetics, Machine Direction

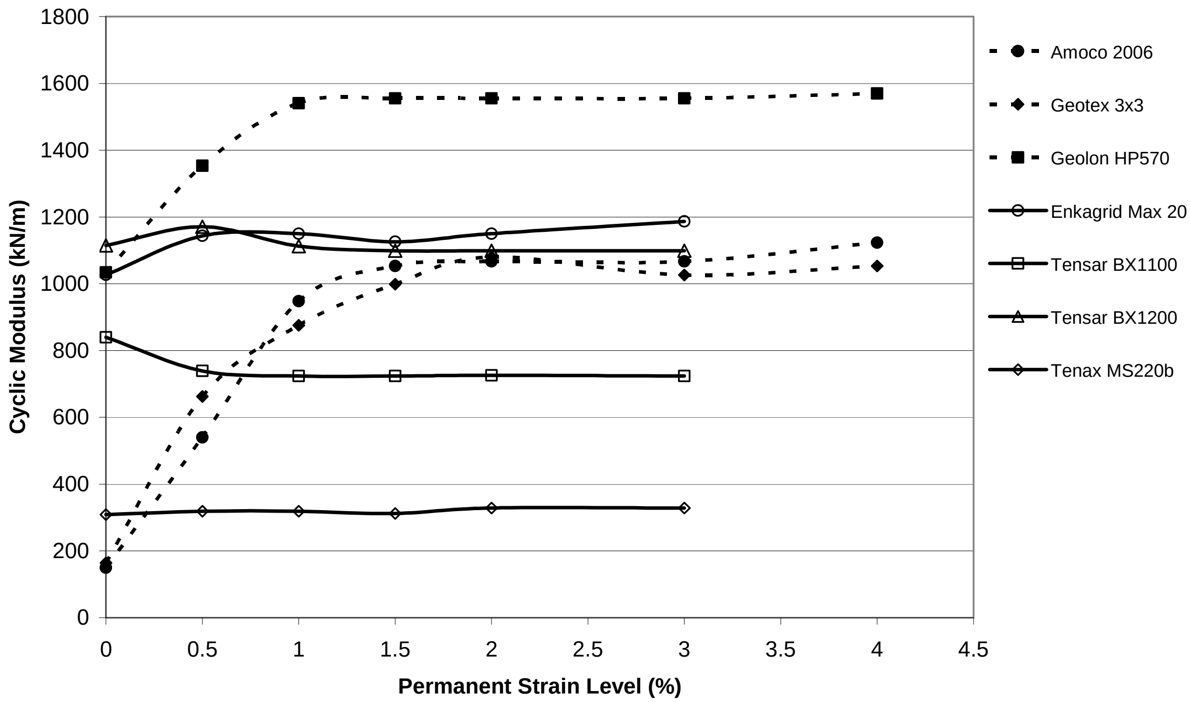

Figure 47: Cyclic Tensile Modulus versus Permanent Strain for All Geosynthetics, Cross-Machine Direction

5.1.1 Amoco ProPex 2006

In general, in both machine and cross-machine directions of Amoco 2006, the strength values from the monotonic test are higher than the cyclic test for all levels of axial strain. Overall, strength is greater in the cross-machine direction than in the machine direction. Initially, however, both monotonic and cyclic tests exhibit similar strength values. In the machine direction, both cyclic and tangent modulus increases as axial strain increases (Figure 48). In the cross-machine direction, the cyclic modulus increases and levels off while the monotonic modulus at first increases and later decreases as strain increases (Figure 49). Overall, modulus values from cyclic test were larger than the monotonic test and modulus in the cross-machine direction was approximately twice the machine direction.

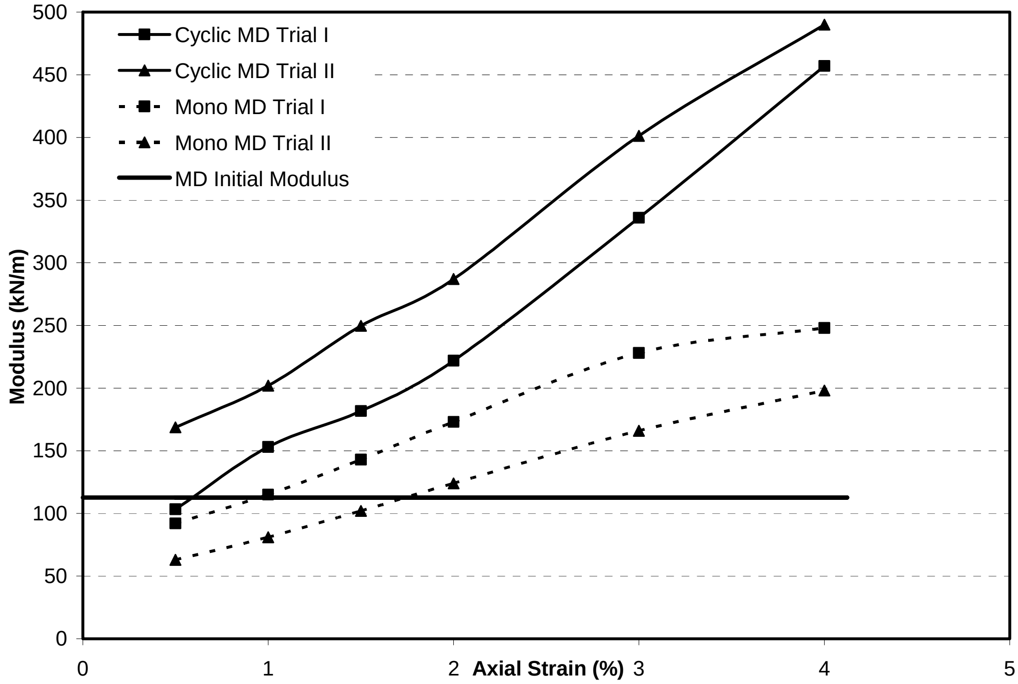

Figure 48: Modulus versus Axial Strain for Amoco ProPex 2006, Machine Direction

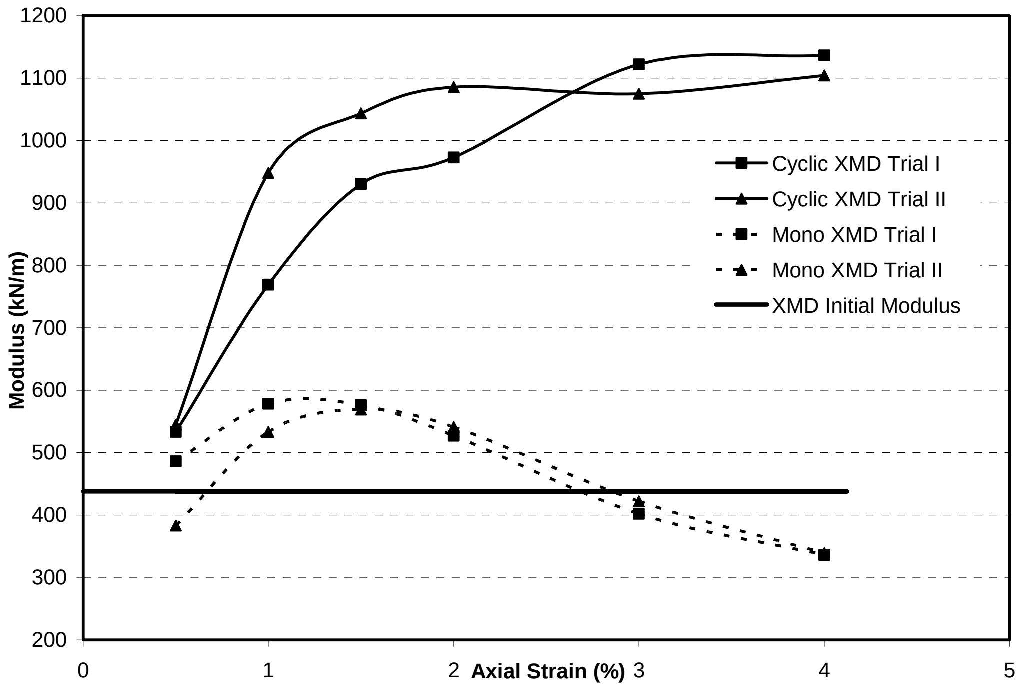

Figure 49: Modulus versus Axial Strain for Amoco ProPex 2006, Cross-Machine Direction

Differences in the cyclic modulus for increasing cycle numbers were small. Differences between the two trials are most likely due to inconsistent material properties between subsequent samples. Figures 50 and 51 show the cyclic modulus for specific cycle numbers for the Amoco 2006 geotextile.

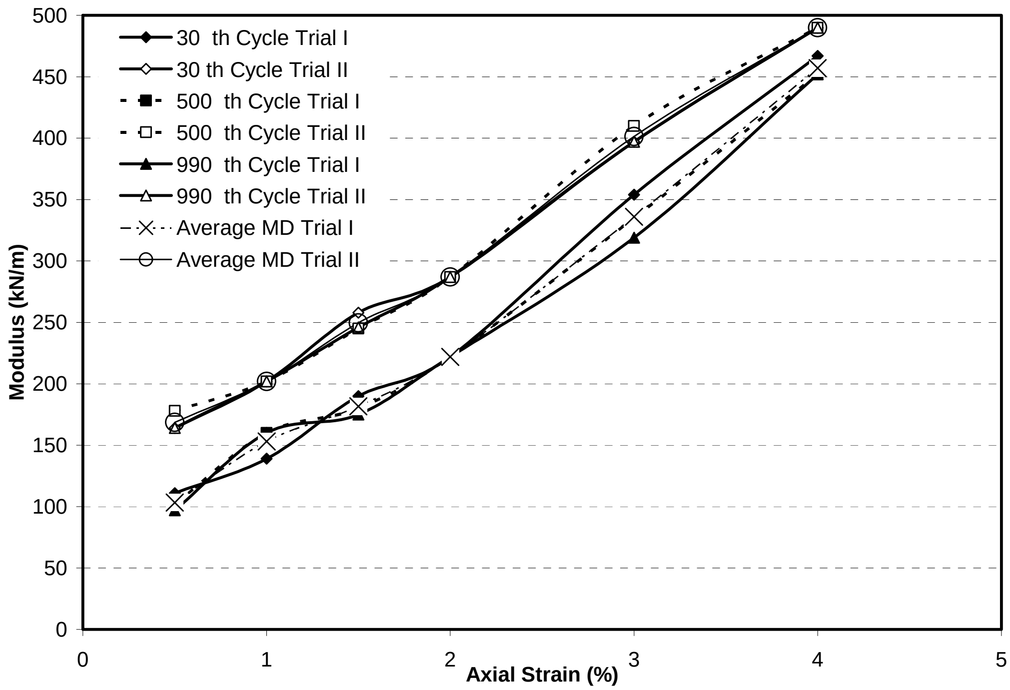

Figure 50: Cyclic Modulus versus Axial Strain for Amoco ProPex 2006 at Various Cycle Numbers, Machine Direction

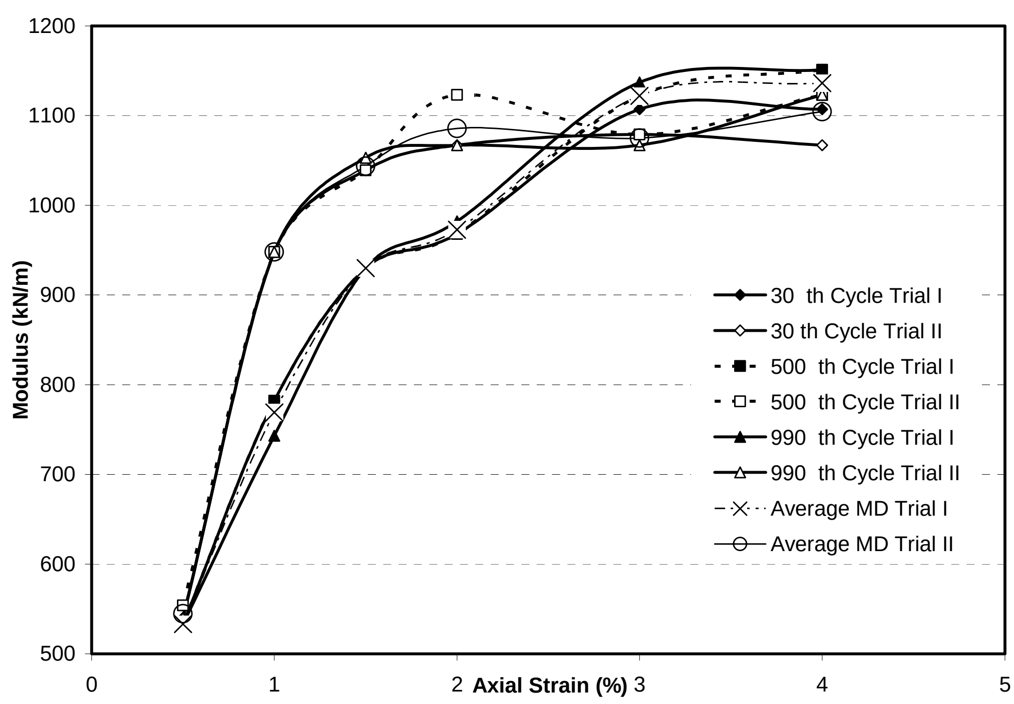

Figure 51: Cyclic Modulus versus Axial Strain for Amoco ProPex 2006 at Various Cycle Numbers, Cross-Machine Direction

5.1.2 Synthetic Industries Geotex 3×3

Results from monotonic and cyclic tests on Geotex 3×3 were similar to the cross-machine direction of the Amoco 2006 geotextile, where the cyclic modulus increased as axial strain increased but leveled off at approximately 2% axial strain. Unlike the Amoco 2006 material, most of the modulus values for the Geotex 3×3 geotextile were greater than the initial moduli. Modulus versus axial strain is shown in Figures 52 and 53 for the machine and cross-machine directions, respectively. Differences in the cyclic modulus for successive cycle numbers were small (Figures 54 and 55 for the machine and cross-machine directions, respectively).

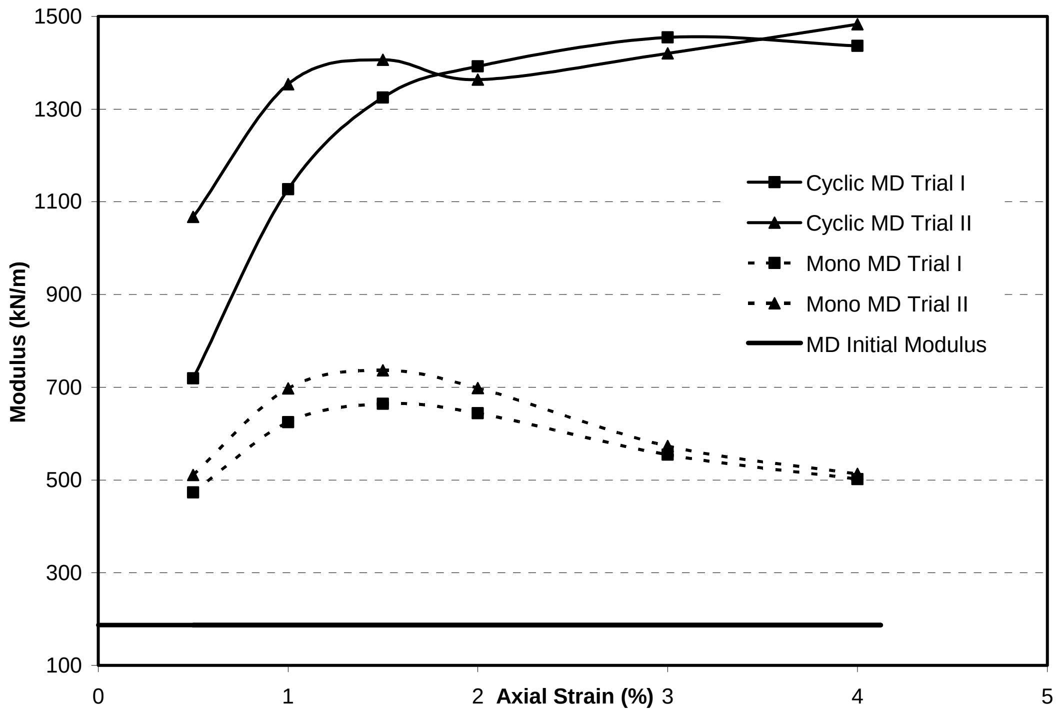

Figure 52: Modulus versus Axial Strain for Synthetic Industries Geotex 3×3, Machine Direction

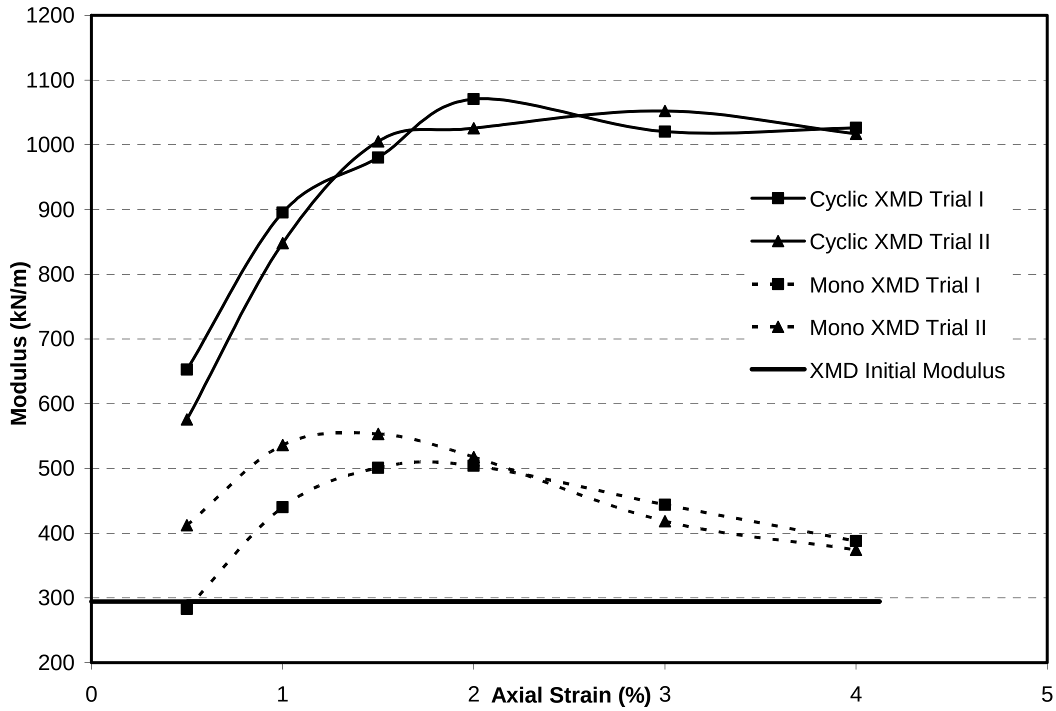

Figure 53: Modulus versus Axial Strain for Synthetic Industries Geotex 3×3, Cross-Machine Direction

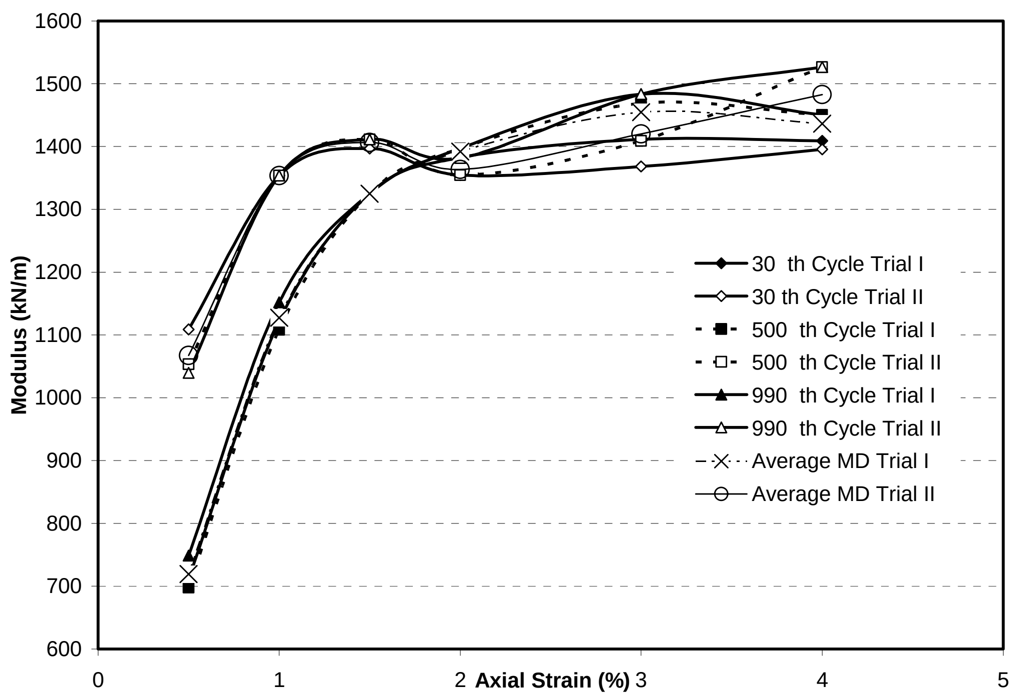

Figure 54: Cyclic Modulus versus Axial Strain for Synthetic Industries Geotex 3×3 at various Cycle Numbers, Machine Direction

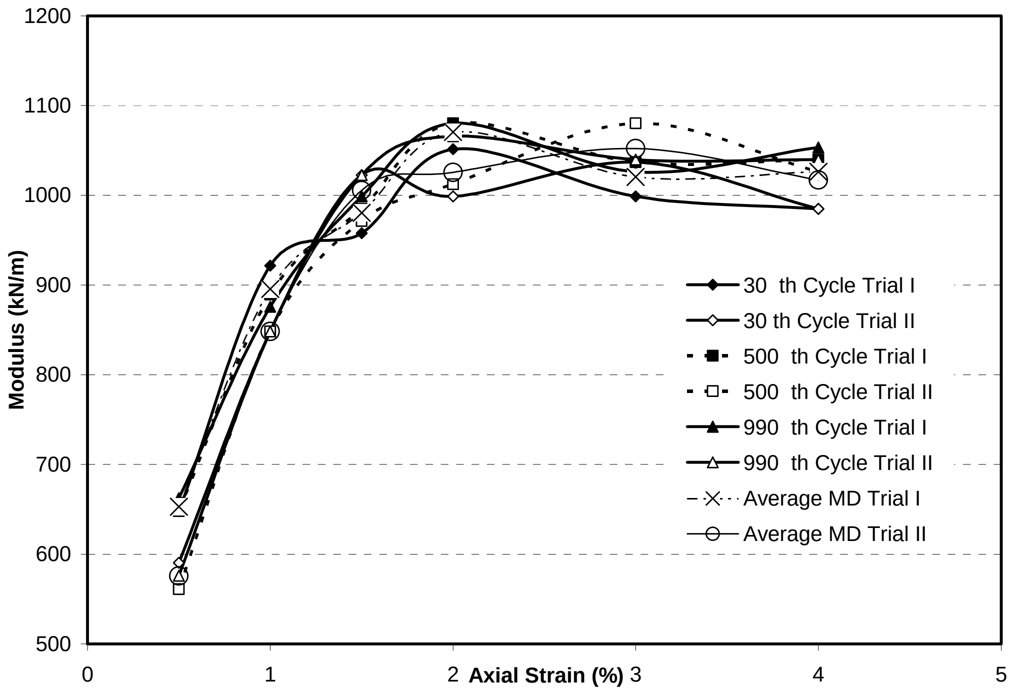

Figure 55: Cyclic Modulus versus Axial Strain for Synthetic Industries Geotex 3×3 at various Cycle Numbers, Cross-Machine Direction

5.1.3 Ten Cate Nicolon Geolon HP570

Monotonic and cyclic behavior of Geolon 570 is similar to the other two geotextiles (Amoco 2006 and Geotex 3×3). The strength behavior of the Geolon 570 geotextile for the machine and cross-machine directions is shown in Figures 56 and 57, respectively. However, in the cross-machine direction the monotonic tangent modulus is less than the initial modulus and decreases for increasing axial strains. This behavior was found only in this geotextile in the cross-machine direction, but is a common behavior in the geogrids.

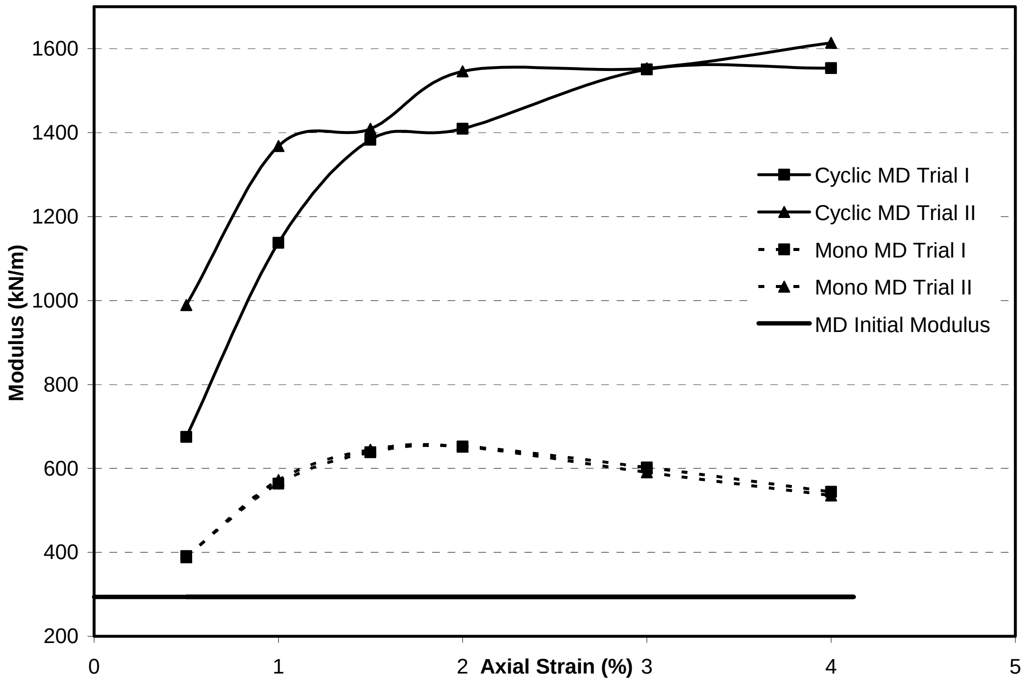

Figure 56: Modulus versus Axial Strain for Geolon HP570, Machine Direction

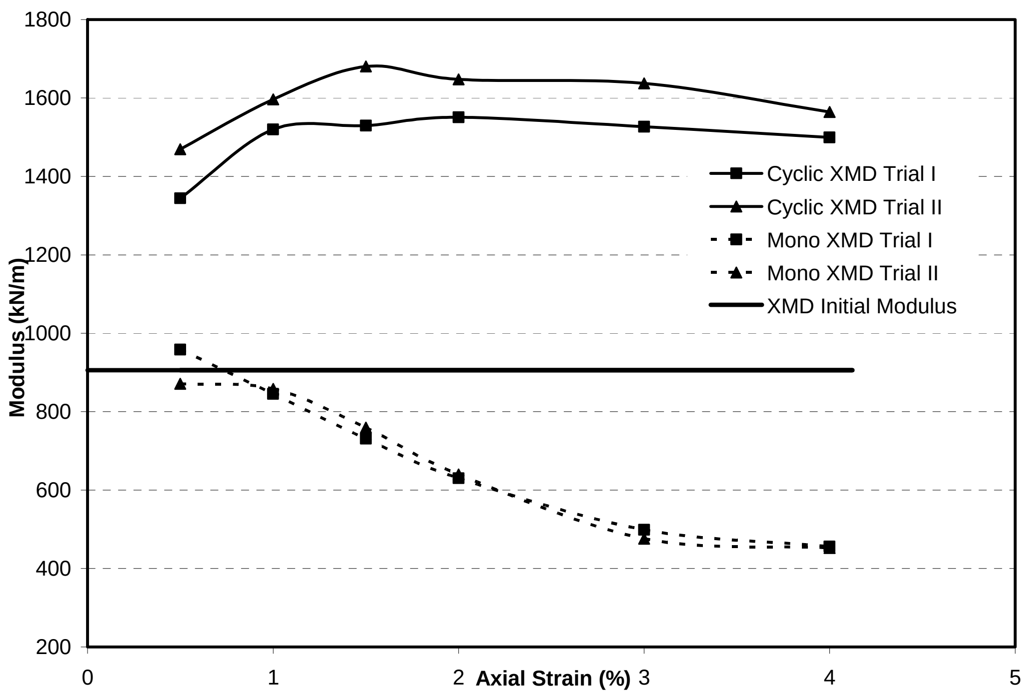

Figure 57: Modulus versus Axial Strain for Geolon HP570, Cross-Machine Direction

The cyclic moduli for successive cycles were very similar in the machine direction for both trials (Figure 58). However, in the cross-machine direction, differences were more pronounced for higher axial strain levels (Figure 59).

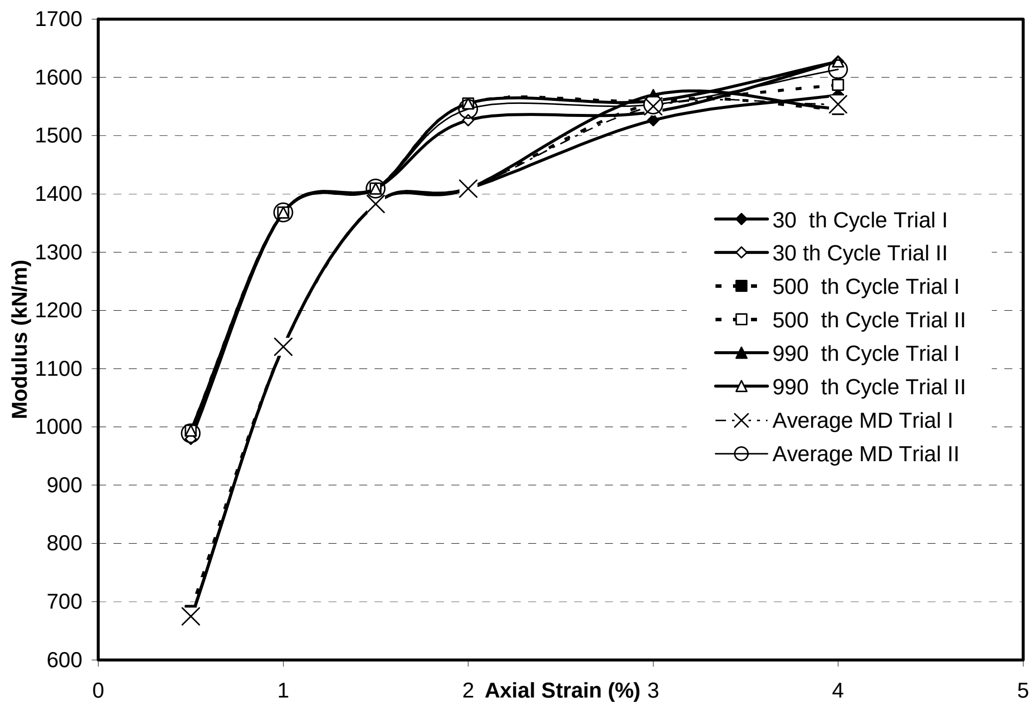

Figure 58: Cyclic Modulus Vs Axial Strain for Geolon HP570 at various Cycle Numbers, Machine Direction

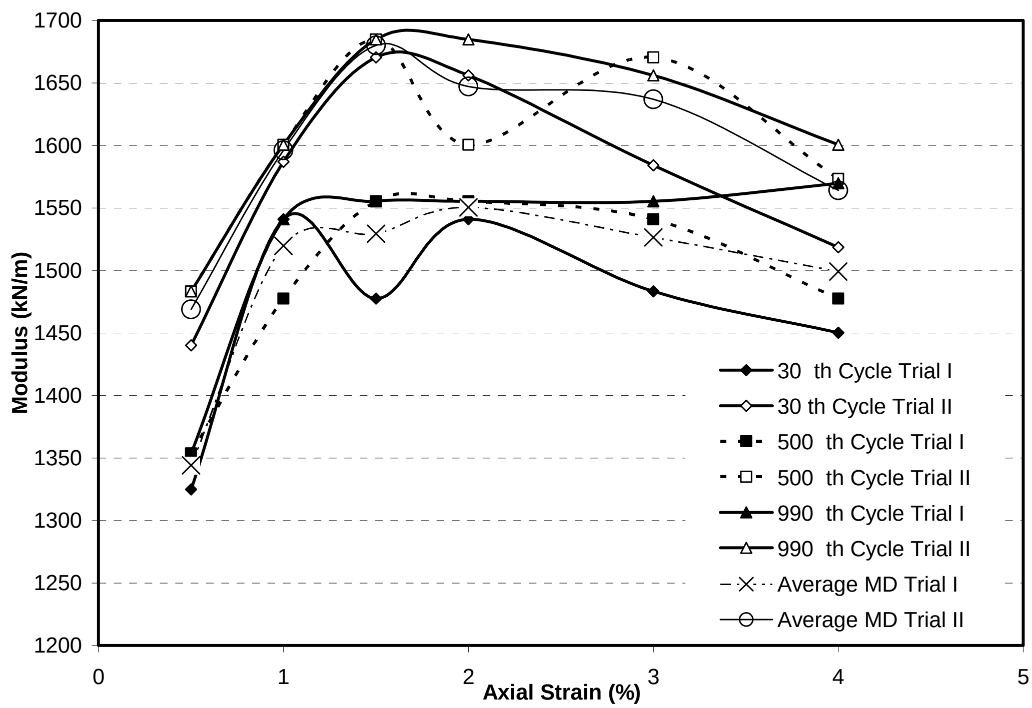

Figure 59: Cyclic Modulus Vs Axial Strain for Geolon HP570 at various Cycle Numbers, Cross-Machine Direction

5.1.4 Tensar BX1100

The stiffness in both machine and cross-machine directions of the BX1100 is significantly affected by the type of loading. In the machine direction, the cyclic moduli at all levels of axial strain are greater than the initial modulus and the tangent moduli are less than the initial modulus (Figure 60). The cyclic modulus essentially remains constant for all levels of axial strain. The cross-machine direction of BX1100 shows similar behavior, in the cross-machine direction, both tangent and cyclic modulus are less than the initial modulus (Figure 61). In both cases, the cyclic modulus remains constant and the tangent modulus decreases with increasing axial strain.

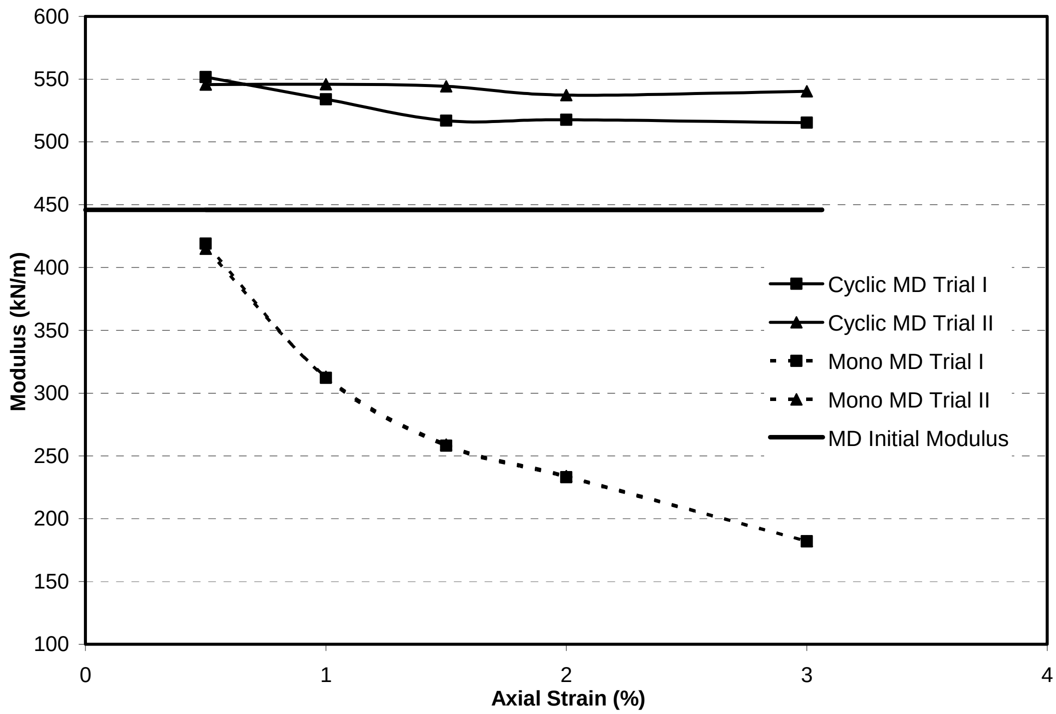

Figure 60: Modulus versus Axial Strain for Tensar BX 1100, Machine Direction

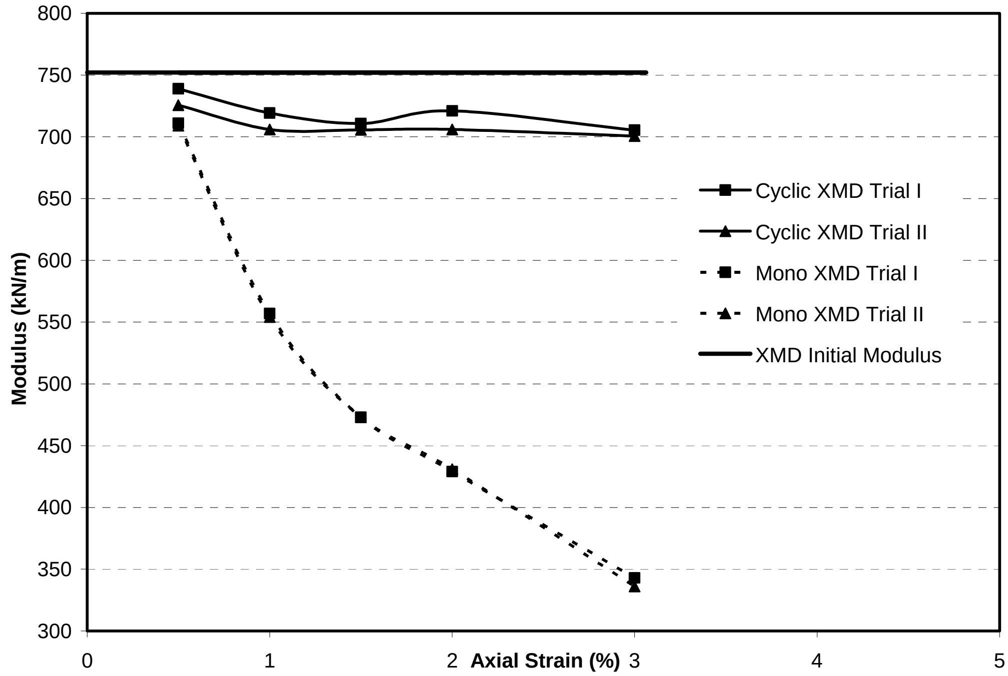

Figure 61: Modulus versus Axial Strain for Tensar BX 1100, Cross-Machine Direction

The cyclic modulus in both principle strength directions did not deviate much for increasing numbers of applied cycles (Figures 62 and 63 for the machine and cross-machine directions, respectively). Differences between trials were also negligible.

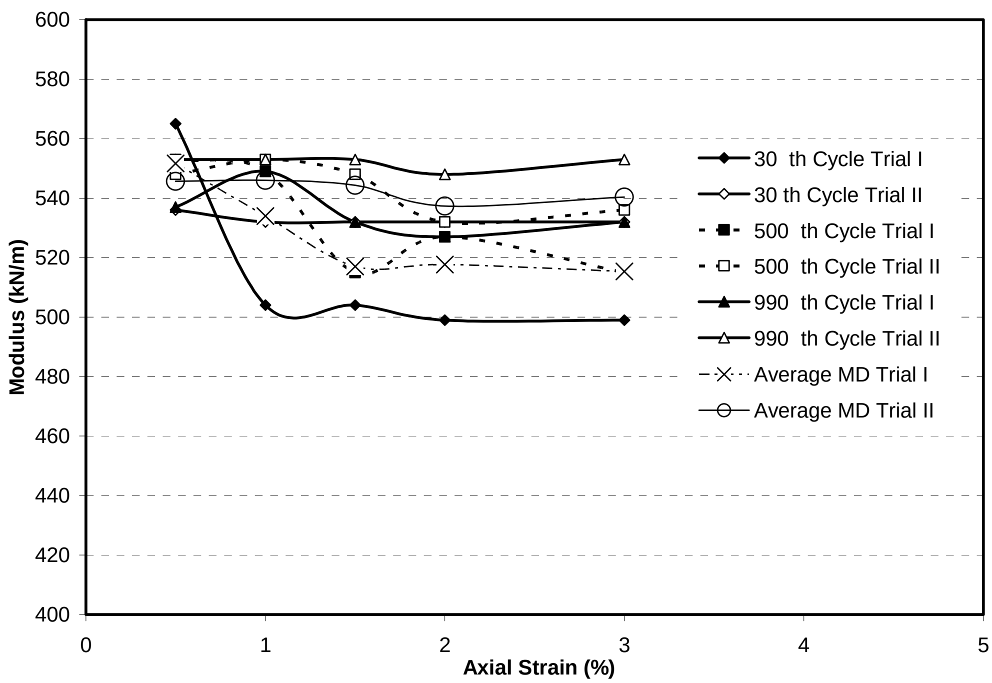

Figure 62: Cyclic Modulus Vs Axial Strain for BX 1100 at various Cycle Numbers, Machine Direction

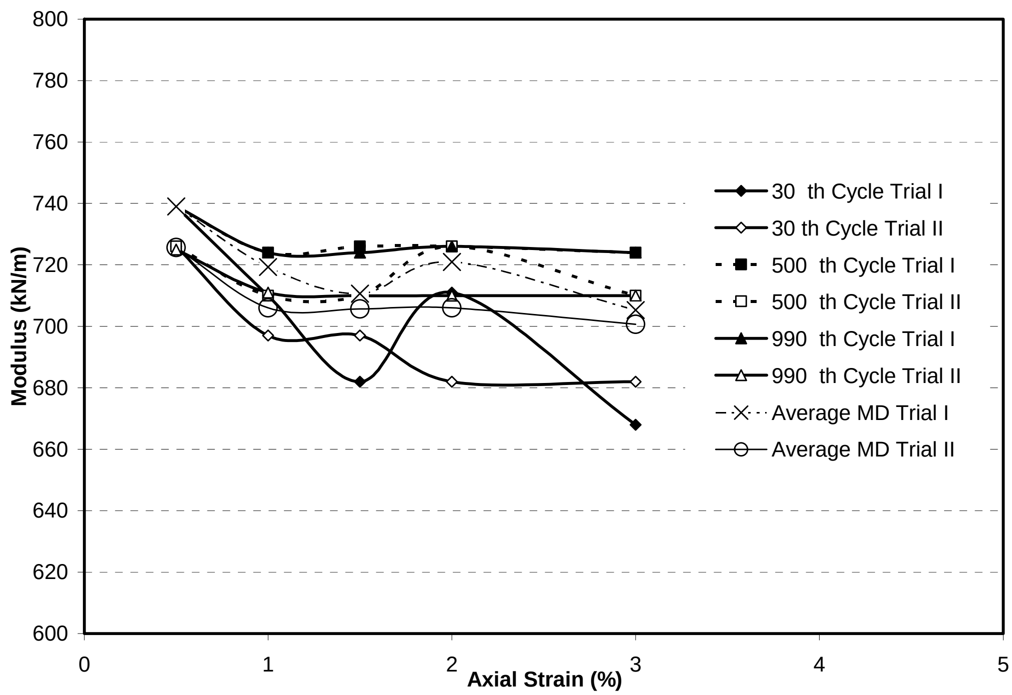

Figure 63: Cyclic Modulus Vs Axial Strain for BX 1100 at various Cycle Numbers, Cross-Machine Direction

5.1.5 Tensar BX1200

The stiffness of BX1200 geogrid in the machine and cross-machine directions is significantly affected by the type of loading. The shape and structure of both BX1100 and BX1200 are similar except for the thickness (BX1200 is thicker and stronger). Likewise, the behavior of the two materials is also very similar, as shown by comparing the stiffnesses in the machine direction (Figures 60 and 64). The results in the cross-machine direction are also similar between products, but the cyclic modulus for the BX1200 is greater than the initial modulus (Figure 65). The cyclic modulus essentially remains constant for all levels of axial strain.

The cyclic modulus remains relatively constant during the cyclic loading for each of the five load steps. Variations generally are less than 100 kN/m. The cyclic modulus at various cycle numbers for the BX1200 material in the machine and cross-machine directions are shown in Figures 66 and 67, respectively. The results are similar to the BX1100 material.

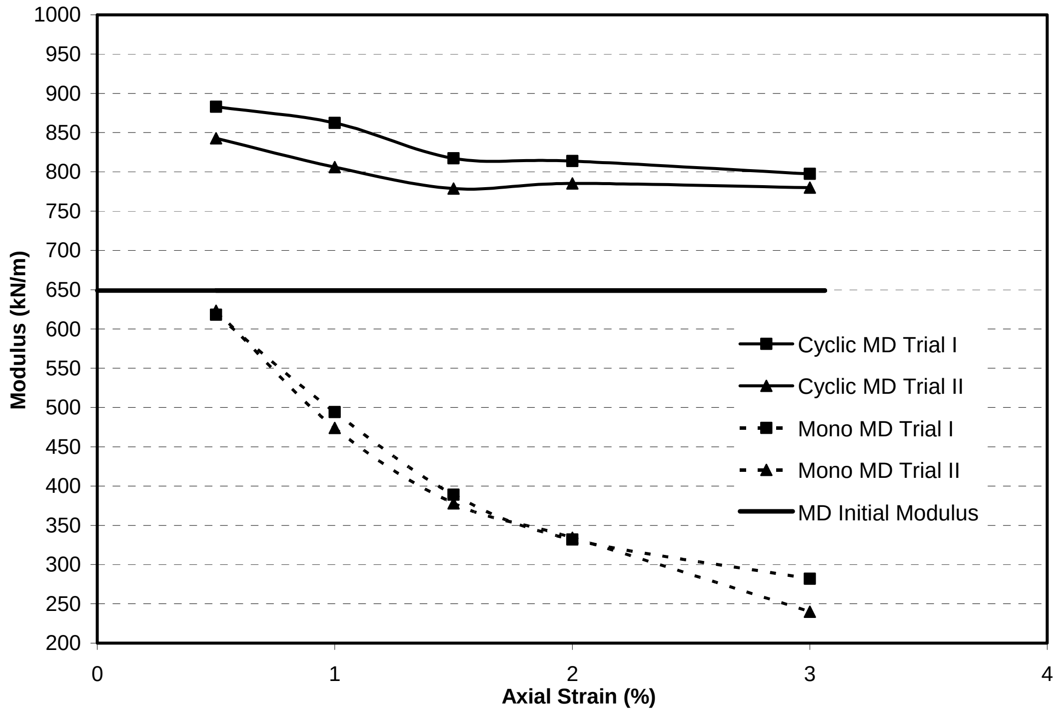

Figure 64: Modulus Vs Axial Strain for BX 1200, Machine Direction

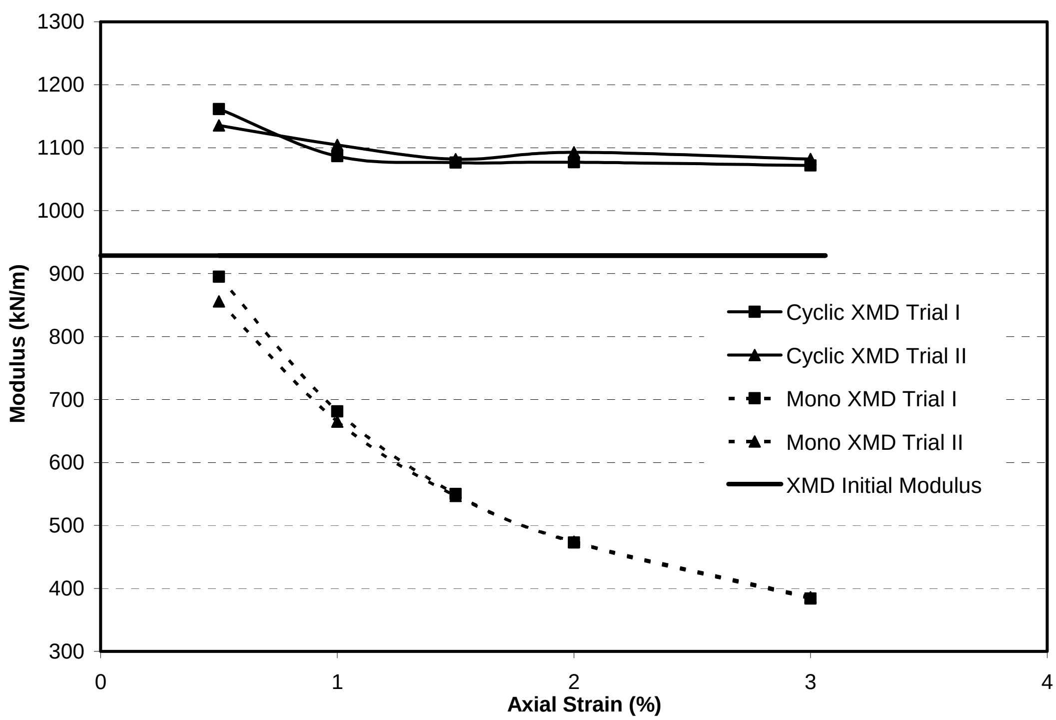

Figure 65: Modulus Vs Axial Strain for BX 1200, Cross-Machine Direction

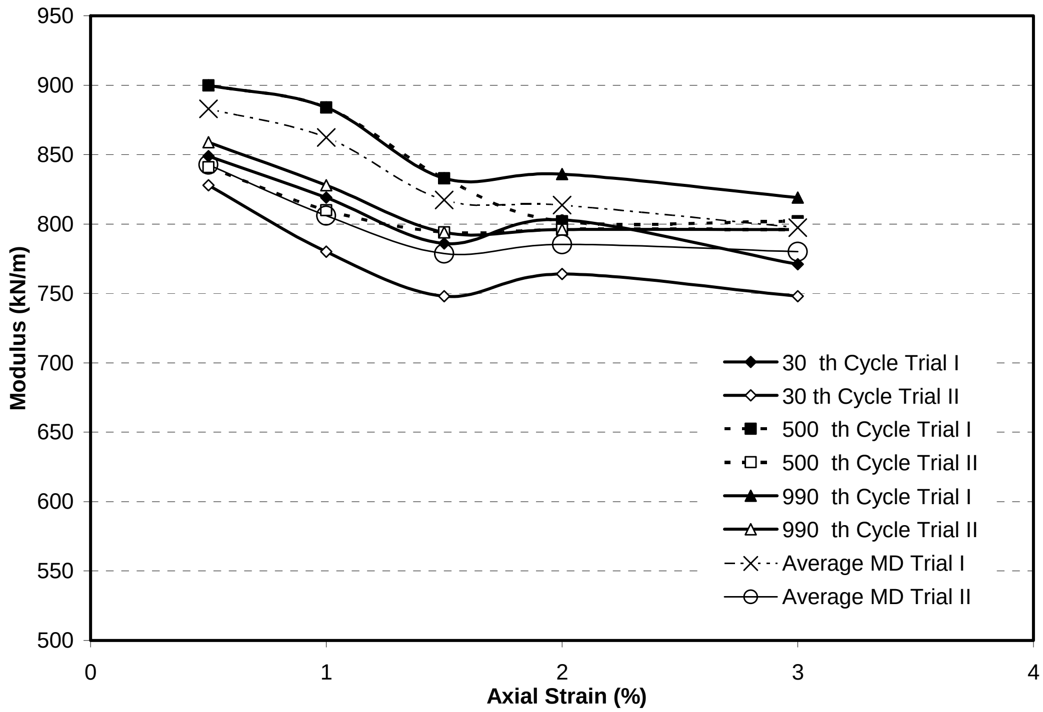

Figure 66: Cyclic Modulus Vs Axial Strain for BX 1200 at various Cycle Numbers, Machine Direction

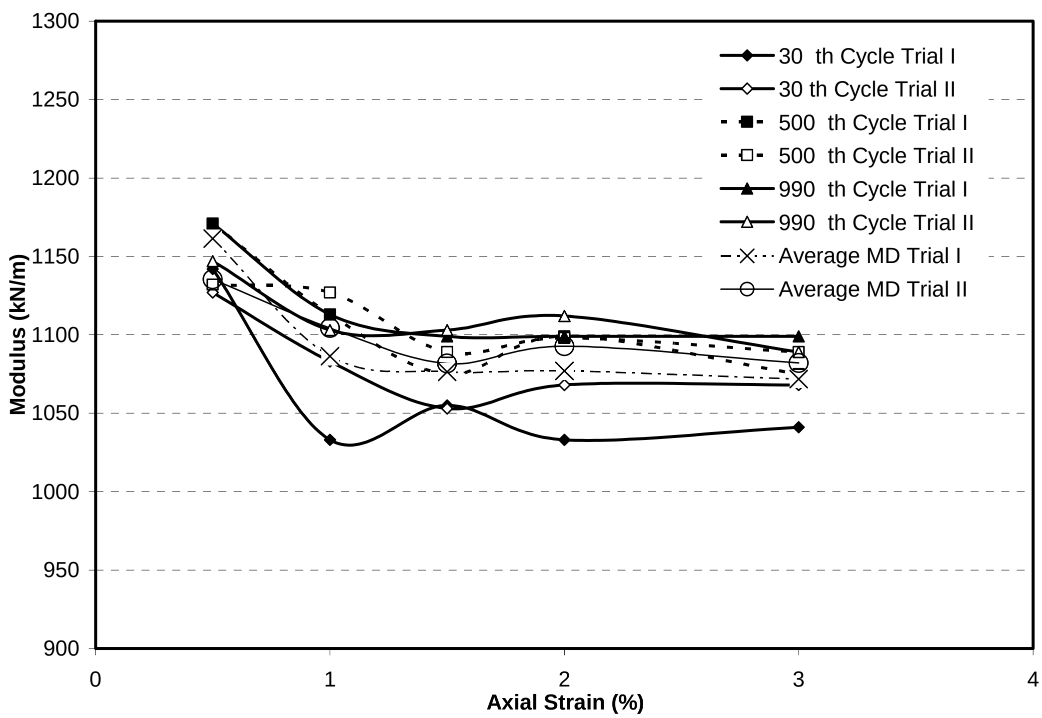

Figure 67: Cyclic Modulus Vs Axial Strain for BX 1200 at various Cycle Numbers, Cross-Machine Direction

5.1.6 Tenax MS220b

Among the seven geosynthetics involved in our testing program, Tensar MS220b material was the only material which consists of two layers of geogrid. Tests were conducted to verify that the two layers of the geogrids share load equally. Monotonic tests were conducted with single and double layers of MS220b material. The load-strain curves of the monotonic tests are shown in the Figures 68 and 69 for the machine and cross-machine directions, respectively. The results verified that doubling the layer simply doubles the load carrying capacity. Therefore, for simplicity, a single layer of Tenax MS220b was used for the cyclic tests.

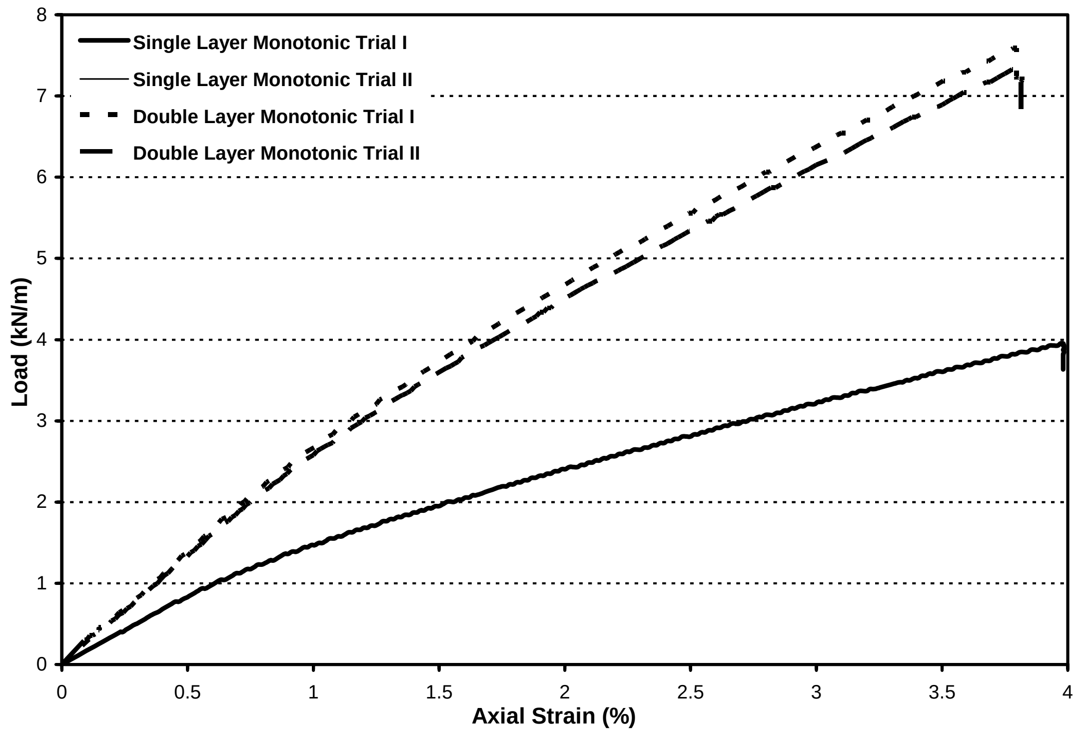

Figure 68: Comparison of Load-Strain Curves from Monotonic Test of Single and Double Layer Tensar MS220b Geogrid, Machine Direction

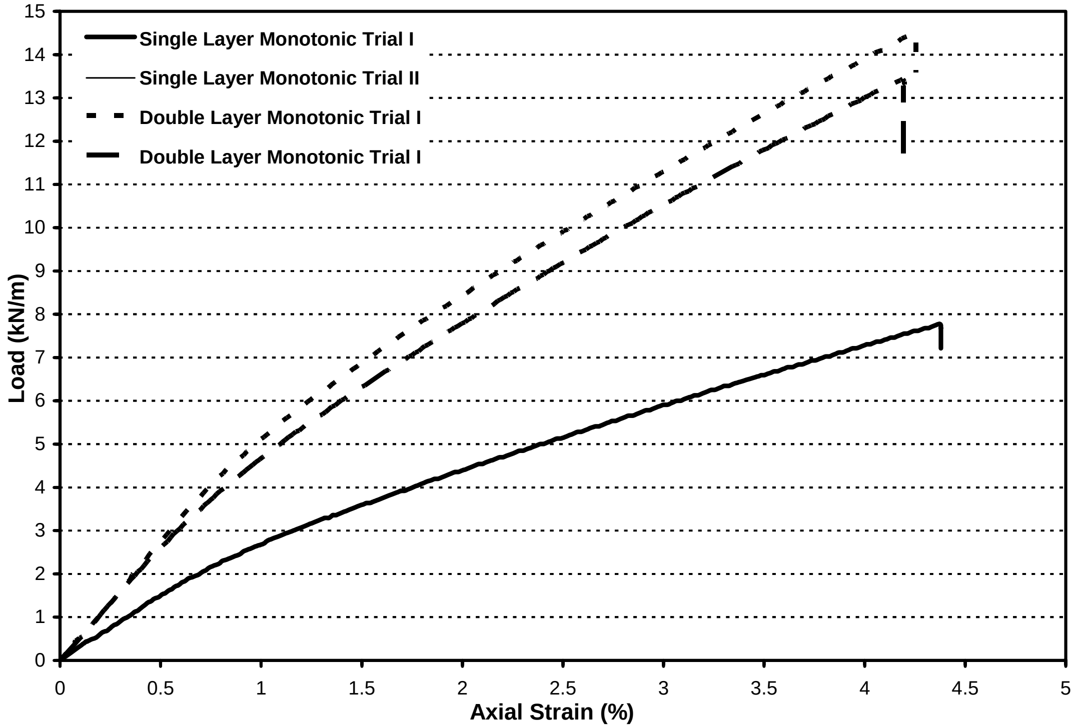

Figure 69: Comparison of Load-Strain Curves from Monotonic Test of Single and Double Layer Tensar MS220b Geogrid, Cross-Machine Direction

Both the machine and cross-machine directions of Tenax MS220b are significantly affected by the type of loading (Figures 70 and 71). Unlike the Tensar geogrids, the tangent modulus does not change as significantly for higher axial strains. The cyclic modulus remains relatively constant as axial strains increased. Similar results are obtained for the machine and cross-machine directions of the material. The tangent modulus is less than initial modulus value and cyclic modulus is greater.

The cyclic modulus remained relatively constant for various cycle numbers, fluctuating no more than 40 kN/m throughout all the tests. The cyclic modulus versus axial strain for various cycle numbers is shown in Figures 72 and 73 for the machine and cross-machine directions, respectively.

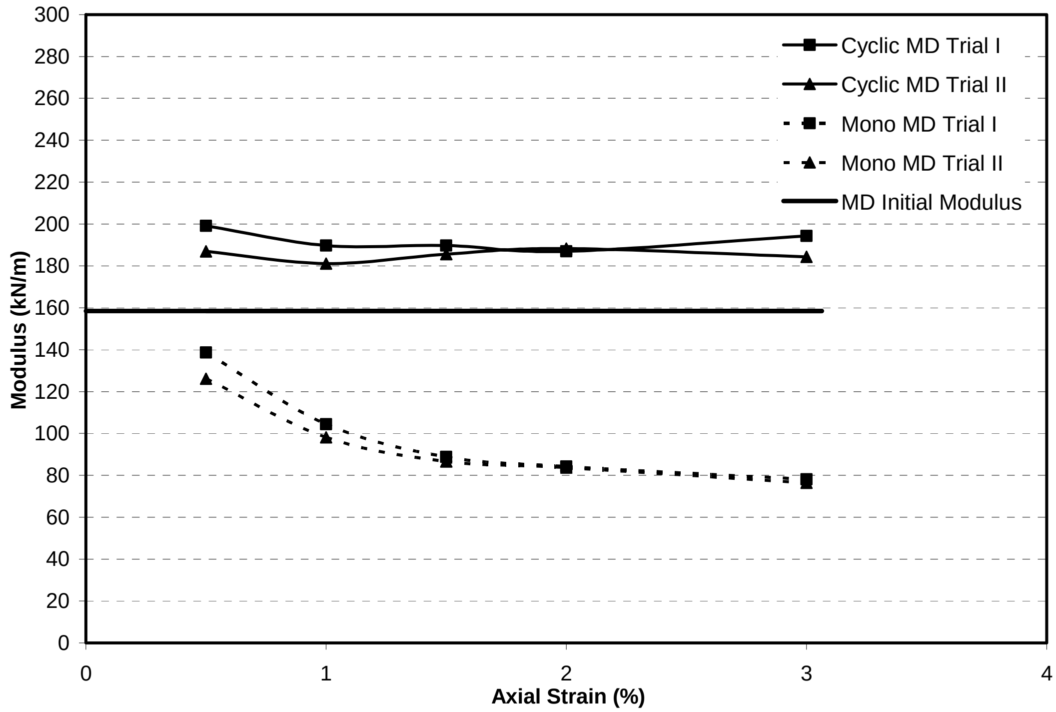

Figure 70: Modulus versus Axial Strain for Tenax MS220b, Machine Direction

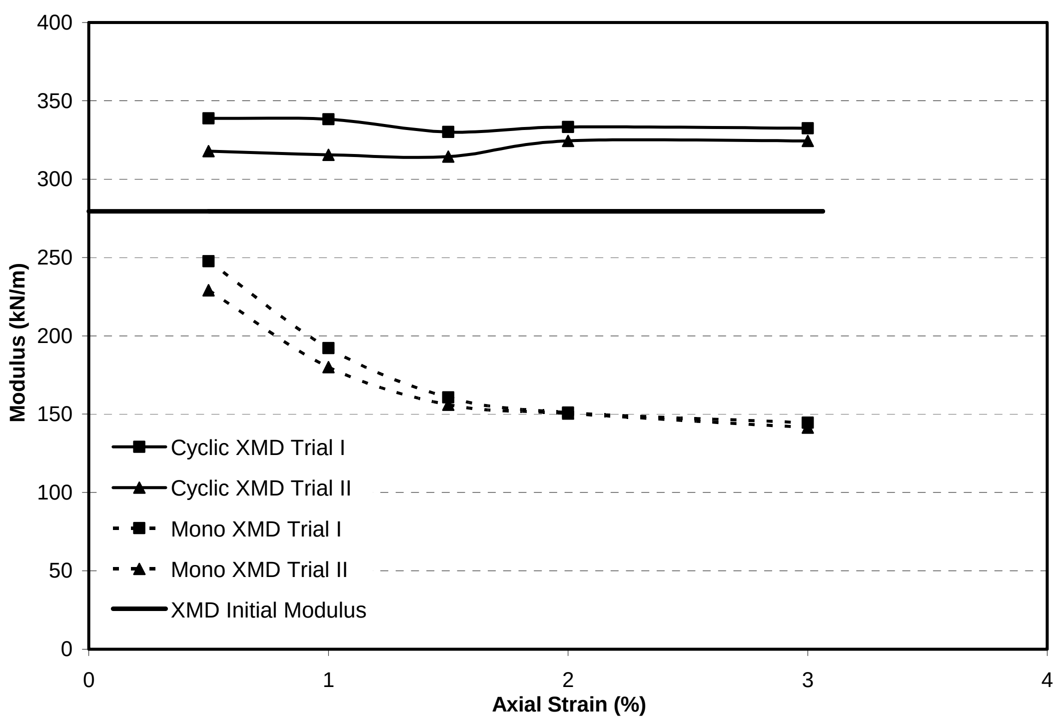

Figure 71: Modulus versus Axial Strain for Tenax MS220b, Cross-Machine Direction

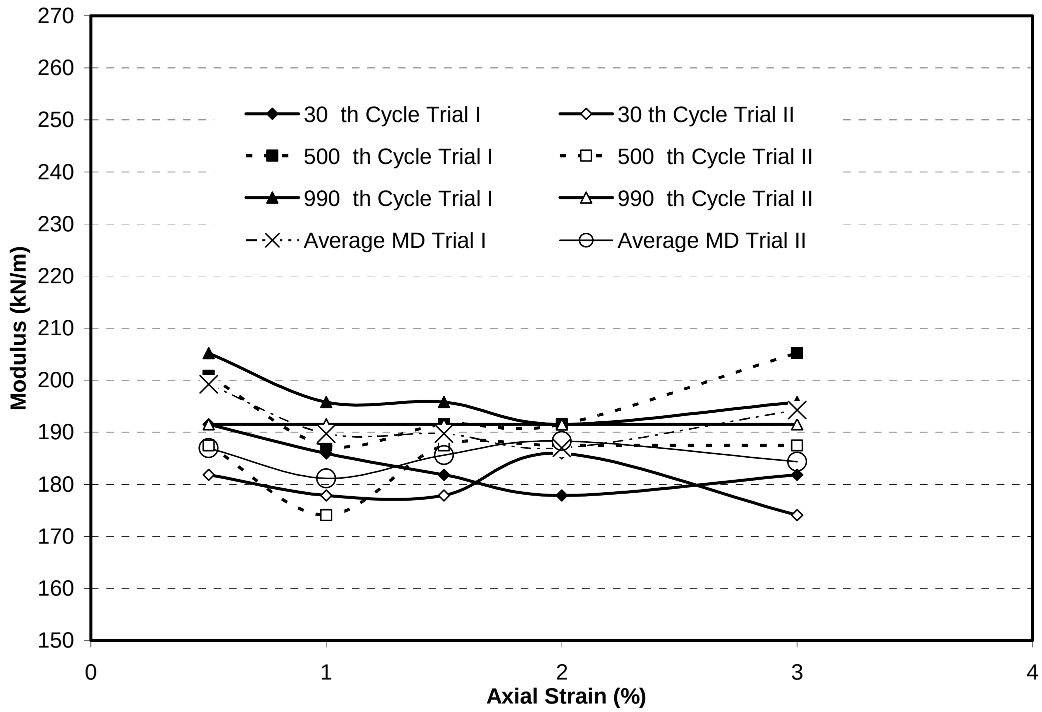

Figure 72: Cyclic Modulus versus Axial Strain for Tenax MS220b at various Cycle Numbers, Machine Direction

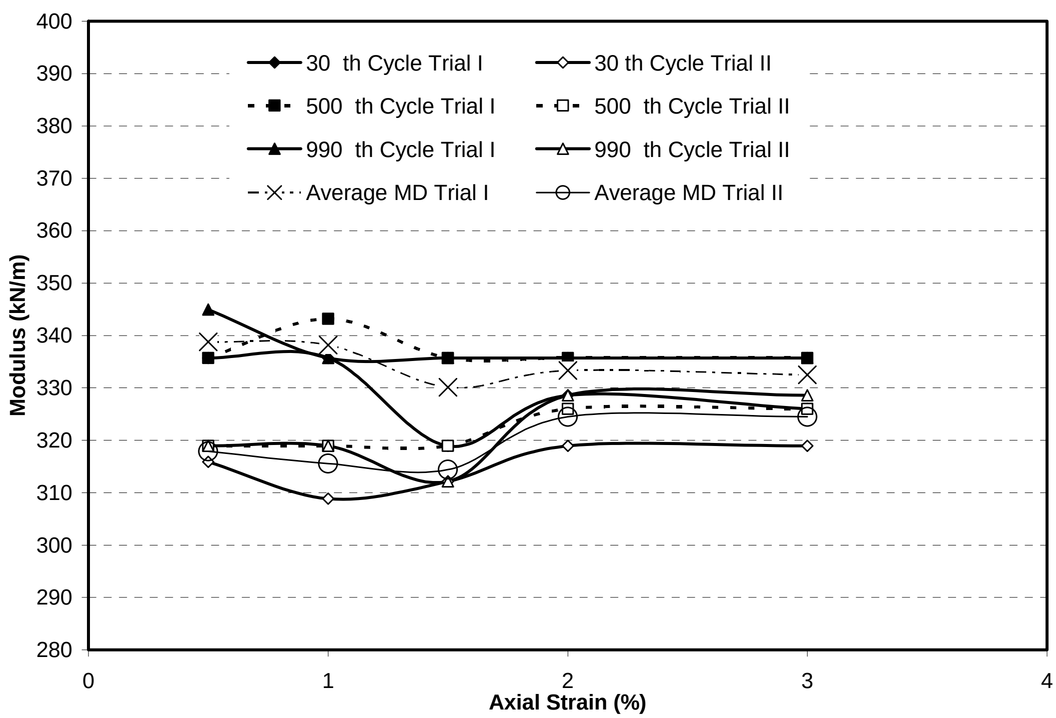

Figure 73: Cyclic Modulus versus Axial Strain for Tenax MS220b at various Cycle Numbers, Cross-Machine Direction

5.1.7 Colbond Enkagrid Max 20

The machine and cross-machine directions of Colbond Enkagrid Max 20 are significantly affected by the type of loading, as shown in Figures 74 and 75, respectively. Like most of the geogrids, the cyclic modulus is greater than the tangent modulus and the tangent modulus decreass for increasing axial strains. Likewise, the cyclic modulus remains relatively stable for all axial strain levels.

Variations in the modulus for increasing cycle numbers is greater in the cross-machine direction than in the machine direction, as illustrated in Figures 76 and 77, respectively. Even so, differences are relatively small: less than 75 kN/m in the machine direction and less than 125 kN/m in the cross-machine direction.

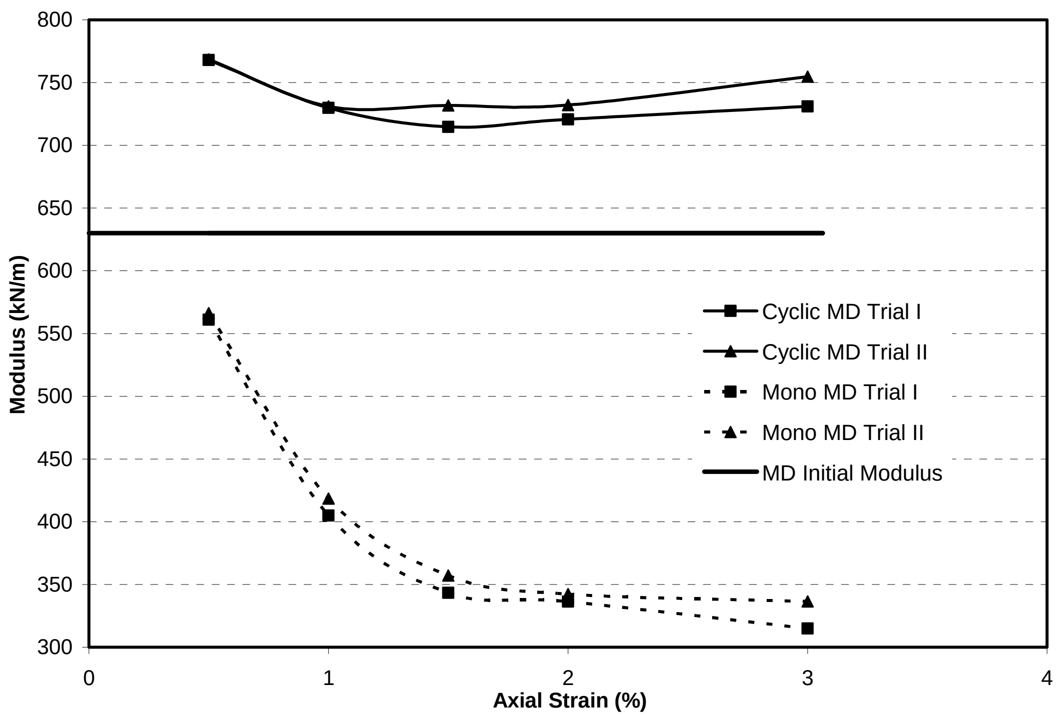

Figure 74: Modulus versus Axial Strain for Colbond Enkagrid Max 20, Machine Direction

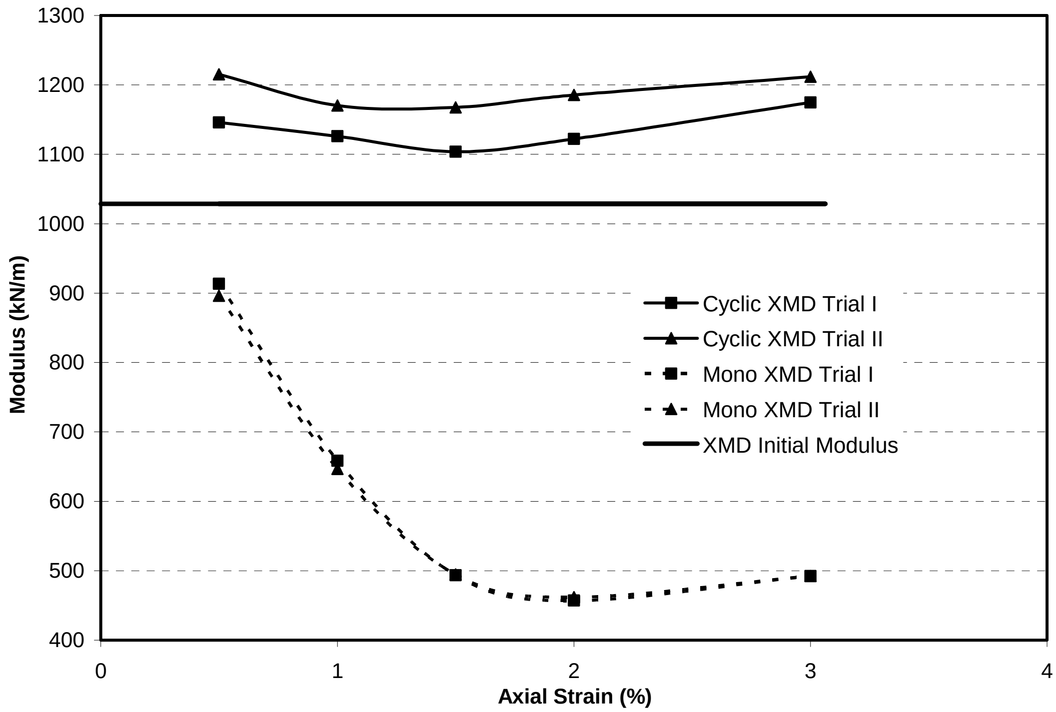

Figure 75: Modulus versus Axial Strain for Colbond Enkagrid Max 20, Cross-Machine Direction

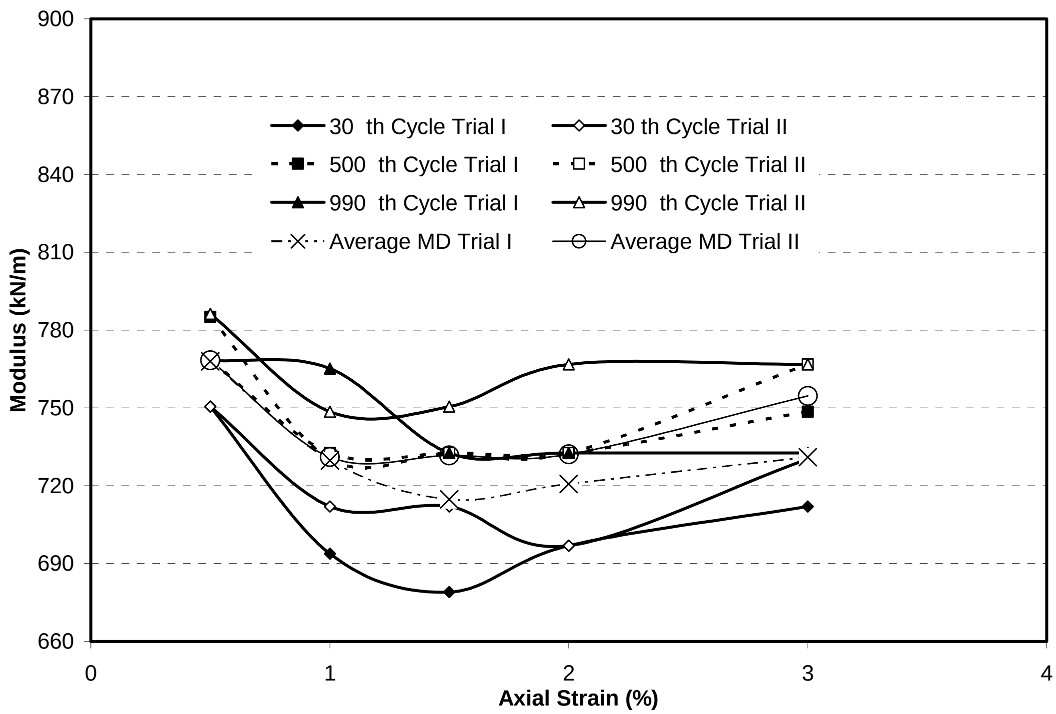

Figure 76: Cyclic Modulus versus Axial Strain for Colbond Enkagrid Max 20 at various Cycle Numbers, Machine Direction

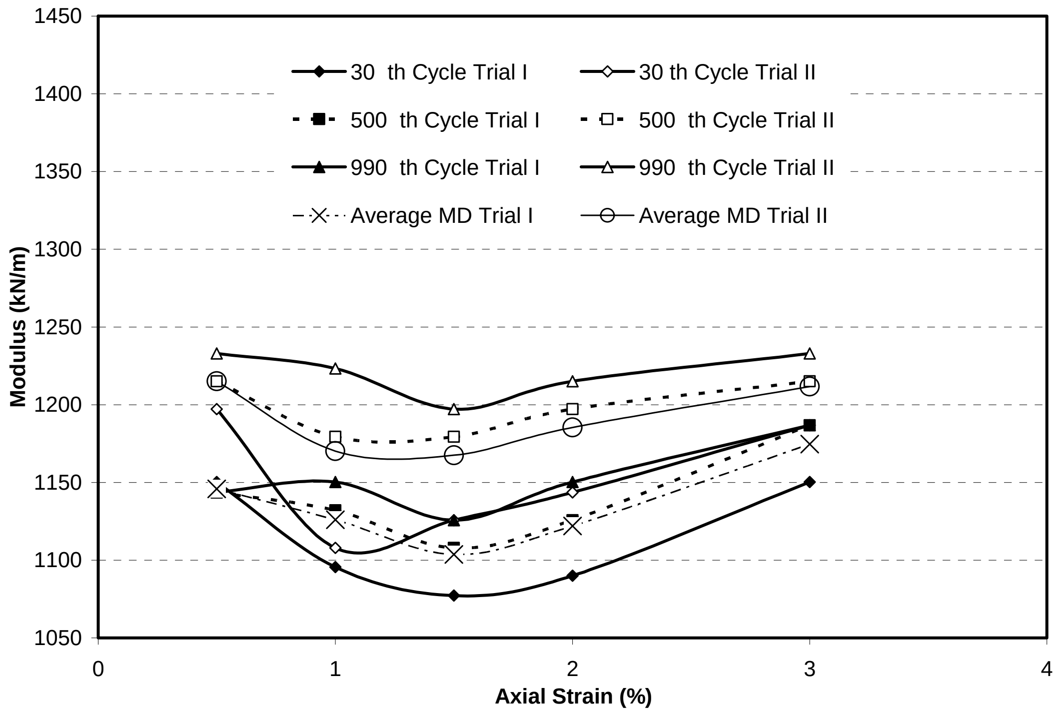

Figure 77: Cyclic Modulus versus Axial Strain for Colbond Enkagrid Max 20 at various Cycle Numbers, Cross-Machine Direction

5.1.8 Summary

The cyclic modulus increases with increases in axial strain for all the three geotextile materials, both in machine and cross-machine directions. Generally, the tangent and cyclic moduli of the geotextiles are greater than the initial modulus. One exception is the Geolon HP570 geotextile, where the tangent modulus from the monotonic tests in the cross-machine direction is less than the initial modulus, and it decreases instead of increases with higher axial strains. In this way, the Geolon HP570 material behaves more like a geogrid.

For the geogrids, the cyclic modulus remains relatively constant as axial strain increases in the machine and cross-machine directions. Tangent modulus decreases with increasing axial strain for all the four geogrids in their two principal directions. In all cases, the tangent modulus is less than the initial modulus for the geogrid materials.

During cyclic testing, the cyclic modulus remains relatively constant during the 1000 cycles at a particular permanent strain level for all geosynthetics tested. However, differences are greatest in the geotextiles.

These results have the following implications for reinforced pavement modeling. For stiffer materials like the geogrids, cyclic loading tends to create a state in the material where the stiffness of small-strain amplitude load cycles is equal to a constant for any level of permanent strain. These results suggest that a constant elastic modulus should be used for the reinforcement for any level of pavement load application. This constant modulus value can be approximated by averaging the cyclic modulus values. However, for softer materials like the geotextiles, modifications to the material models are required to incorporate this non-linear behavior.

5.2 Effect of Strain Rate on Secant Modulus

Based on the literature review, geosynthetics properties can be significantly affected by the strain rate at which they were tested. Generally, when geosynthetics are tested at higher rates of strain the materials stiffen and rupture at lower strain values. Conversely, materials tested at slower rates tend to creep and rupture at higher strain rates. To further understand the behavior of geosynthetics at various strain rates, five of the seven materials in this study were subjected to various strain rates (0.03, 0.4 and 20.0% per minute). The secant moduli were compared at 1, 2, 3, 4 and 5% axial strain. Individual test results are provided in Appendix B. The results of each of the material tests are discussed in the following subsections.

5.2.1 Amoco ProPex 2006

Softer materials such as the Amoco 2006 geotextile tend to creep when loaded slowly. This will also result in lower load carrying capacity at a particular strain level. Figures 78 and 79 show the effect of strain rates on the secant modulus of Amoco 2006 in its machine and cross-machine directions, respectively. At higher strain rates the modulus drastically increases in the machine direction, but less in the cross-machine direction. Therefore, the Amoco 2006 geotextile material is considered strain-rate dependent. Small differences in modulus were found between different axial strain points. In general, the secant modulus increased slightly with increase in axial strain in the machine direction but decreased more significantly in the cross-machine direction. The results from the slowest rate (0.03 %/minute) were invalid in the cross-machine direction.

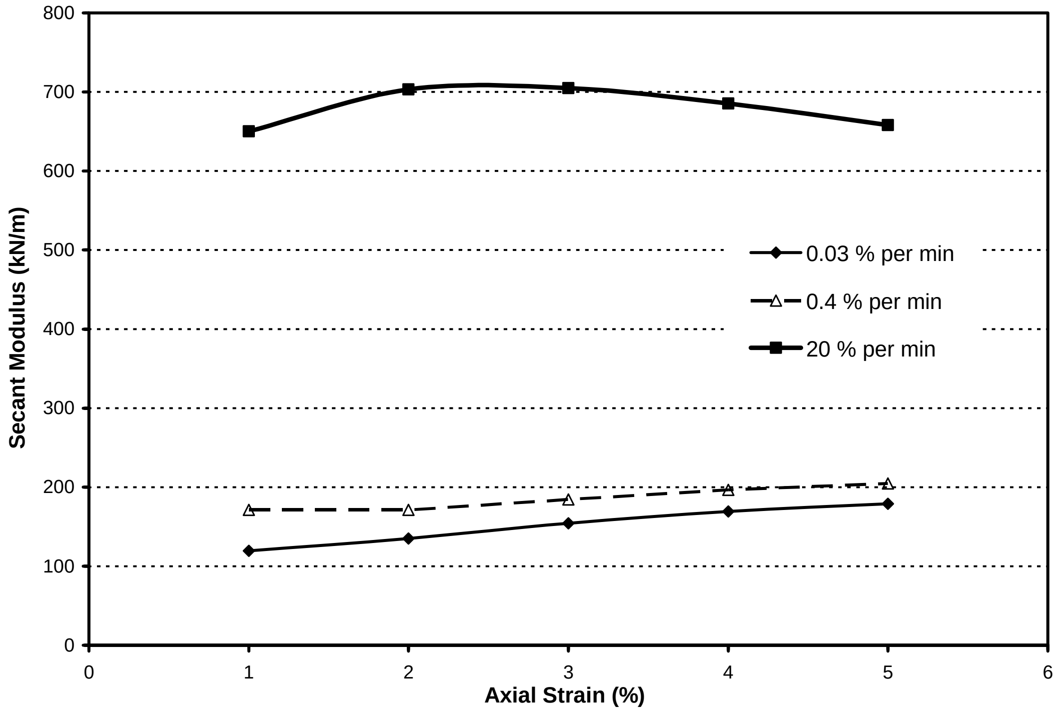

Figure 78: Secant Modulus versus Axial Strain for Amoco ProPex 2006, Machine Direction

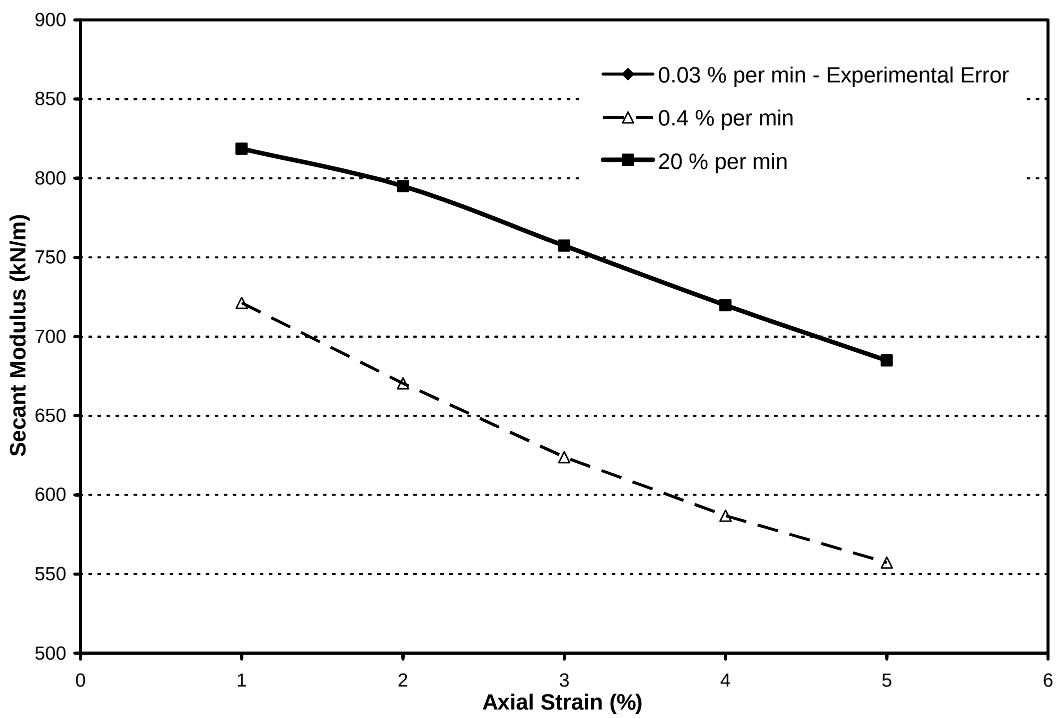

Figure 79: Secant Modulus versus Axial Strain for Amoco ProPex 2006, Cross-Machine Direction

5.2.2 Ten Cate Nicolon Geolon HP570

The secant modulus in the machine direction is not sensitive to changes in strain rate, but is very sensitive in the cross-machine direction (Figures 80 and 81). Interestingly, the results from the fastest rate in the machine direction are smaller for lower levels of strain rate. In the machine direction, secant modulus increases as axial strain increases, but behaves oppositely in the cross-machine direction.

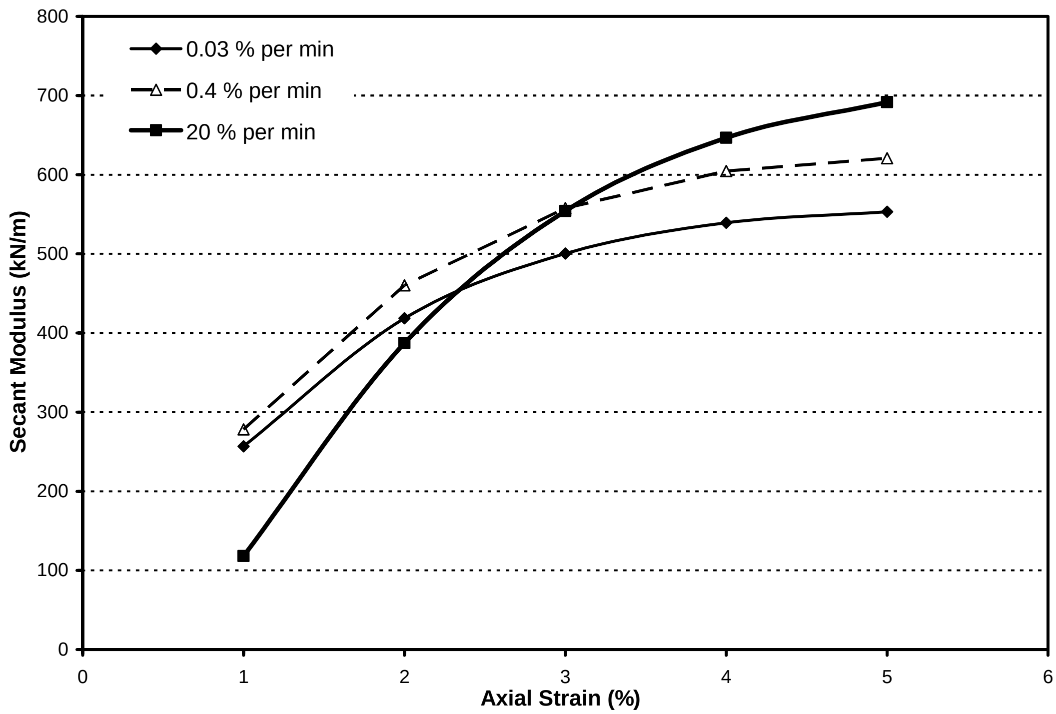

Figure 80: Secant Modulus versus Axial Strain for Geolon HP570, Machine Direction

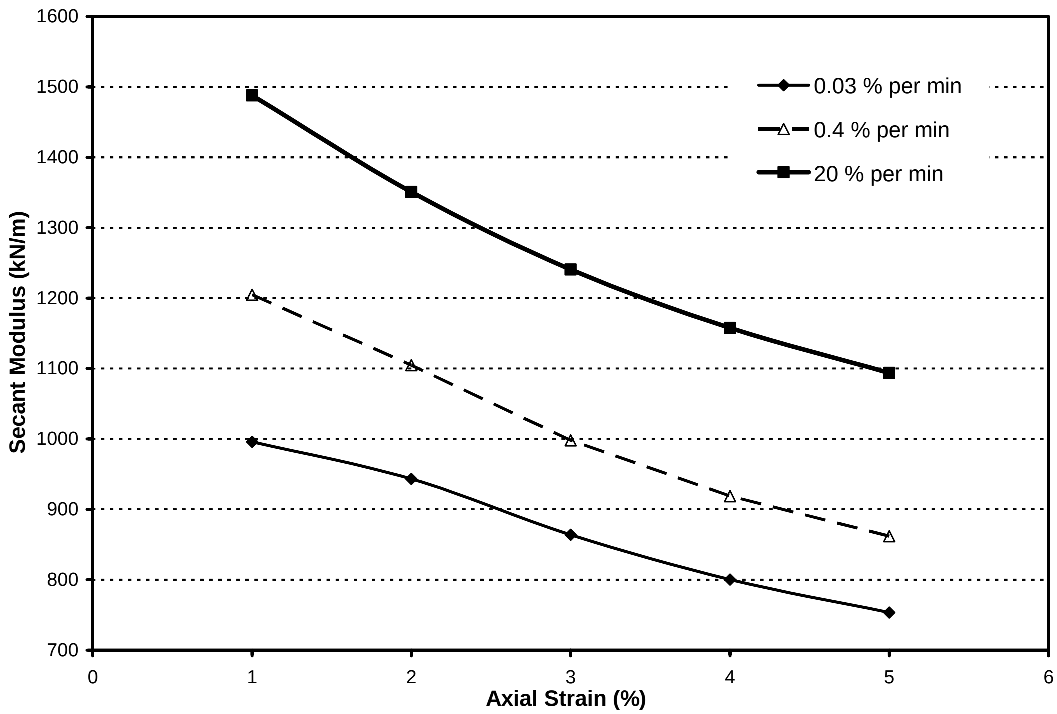

Figure 81: Secant Modulus versus Axial Strain for Geolon HP570, Cross-Machine Direction

5.2.3 Tensar BX1100

The Tensar BX1100 geogrid is similar to the Geolon HP570 product, because it is less sensitive to strain rate in the machine direction than in the cross-machine direction (as shown in Figures 82 and 83, respectively). Both the machine and cross-machine direction show decreasing secant modulus for increasing axial strains.

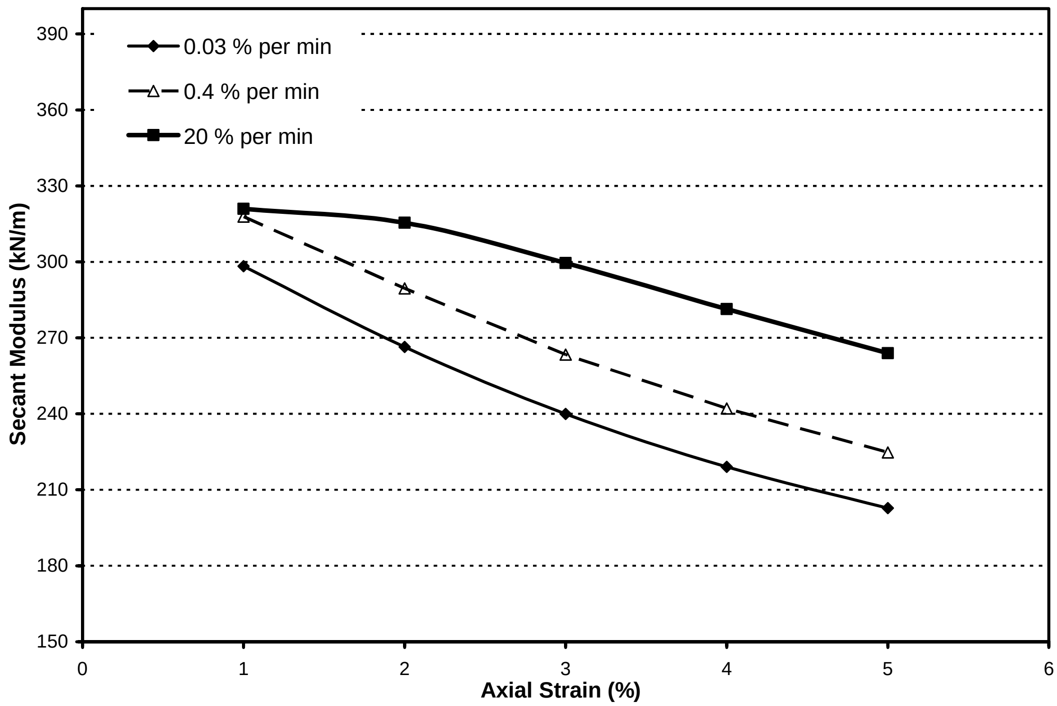

Figure 82: Secant Modulus versus Axial Strain for Tensar BX1100, Machine Direction

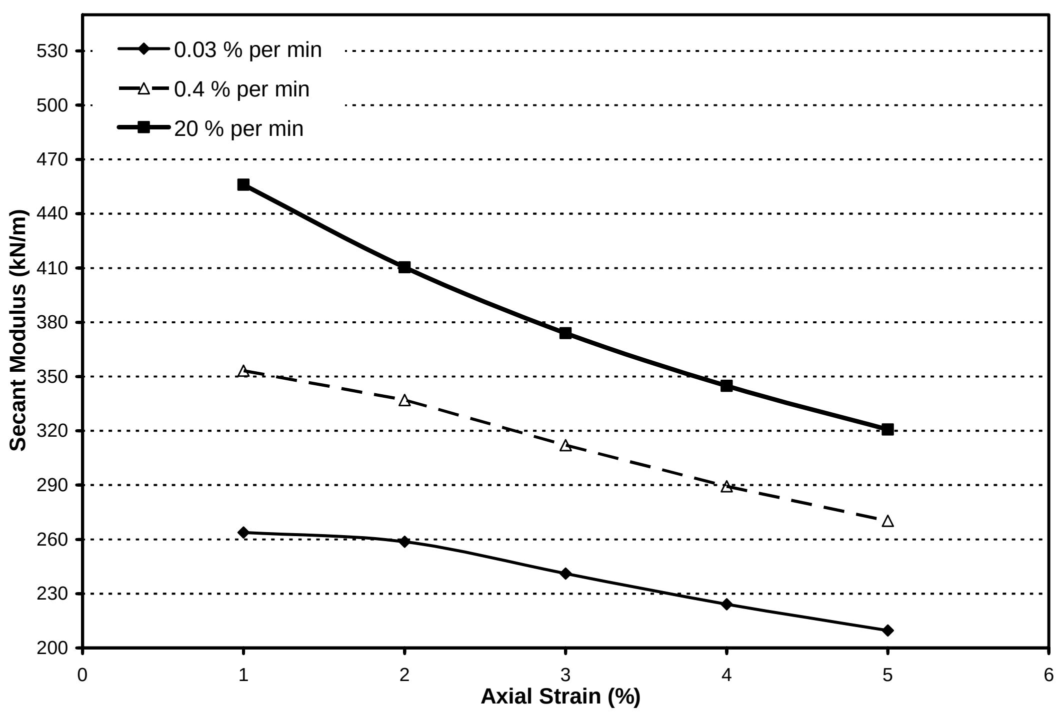

Figure 83: Secant Modulus versus Axial Strain for Tensar BX1100, Cross-Machine Direction

5.2.4 Tensar BX1200

Tensar BX1200 is relatively insensitive to strain rate in the machine direction (Figure 84). The results from the cross-machine direction were unacceptable and are therefore not shown. Like the other stiffer materials, the secant modulus decreases with increasing axial strains.

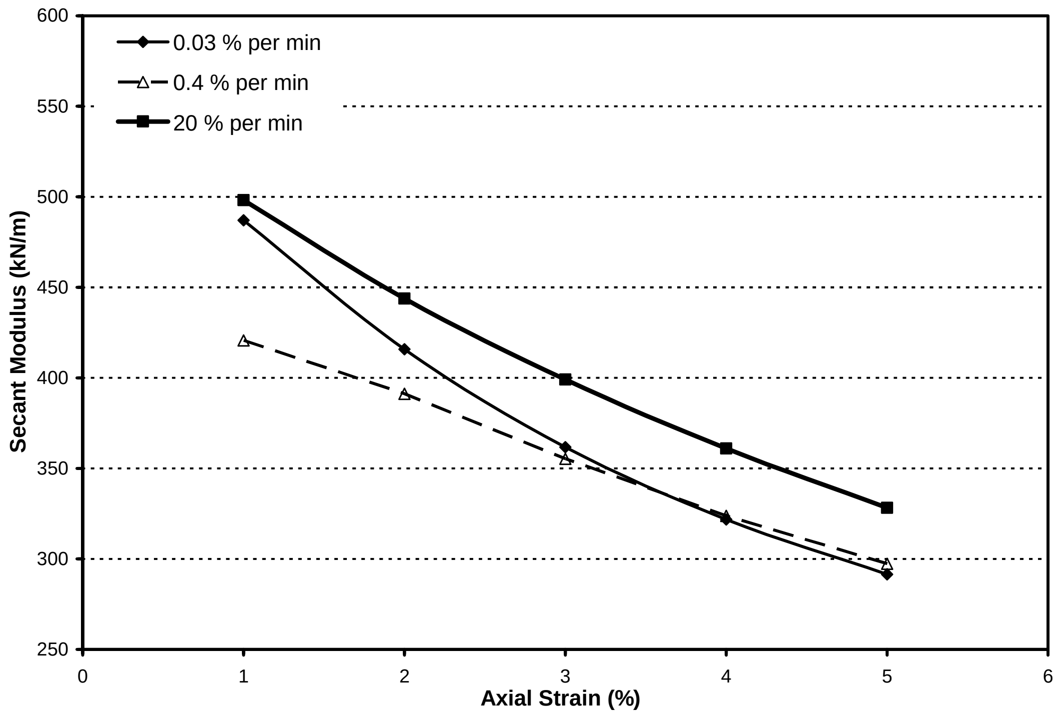

Figure 84: Secant Modulus versus Axial Strain for the Tensar BX1200 Geogrid, Machine Direction

5.2.5 Colbond Enkagrid Max 20

Enkagrid Max 20 is the weakest geogrid tested, therefore, secant moduli are only calculated up to three percent axial strain. It is moderately sensitive to strain rate in the machine direction (Figure 85) and mildly sensitive in the cross-machine direction (Figure 86). The secant modulus at 1% in the cross-machine direction is questionable since it is much smaller than anticipated. The shapes of the trends in both directions of this material are similar to the machine direction of Geolon HP570.

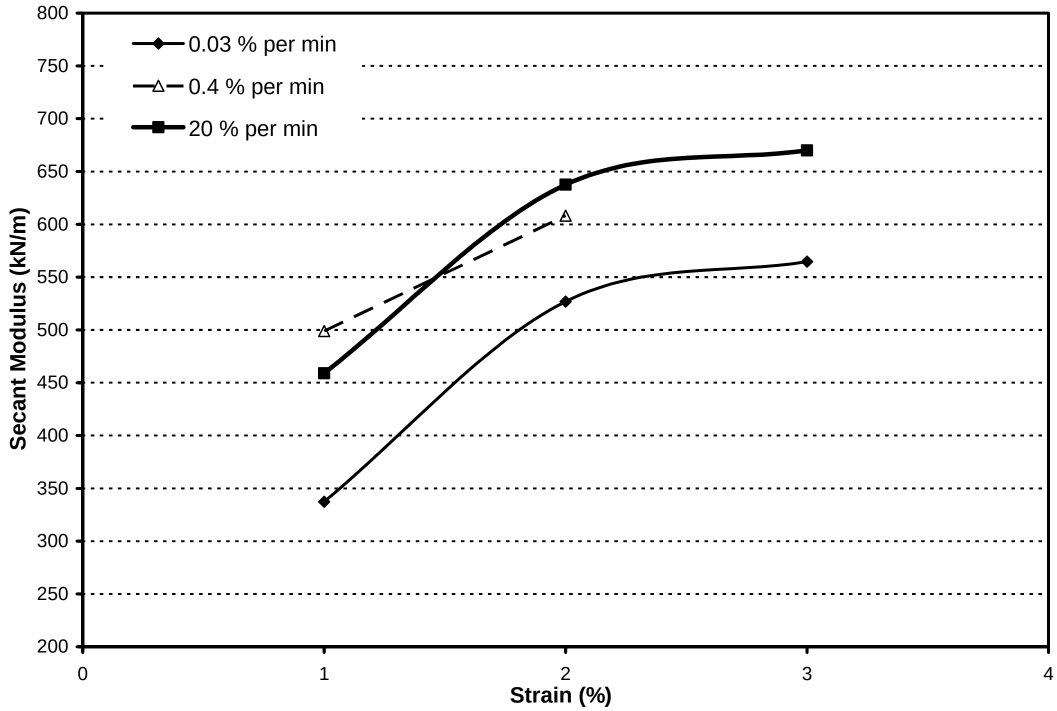

Figure 85: Secant Modulus versus Axial Strain for Enkagrid Max 20, Machine Direction

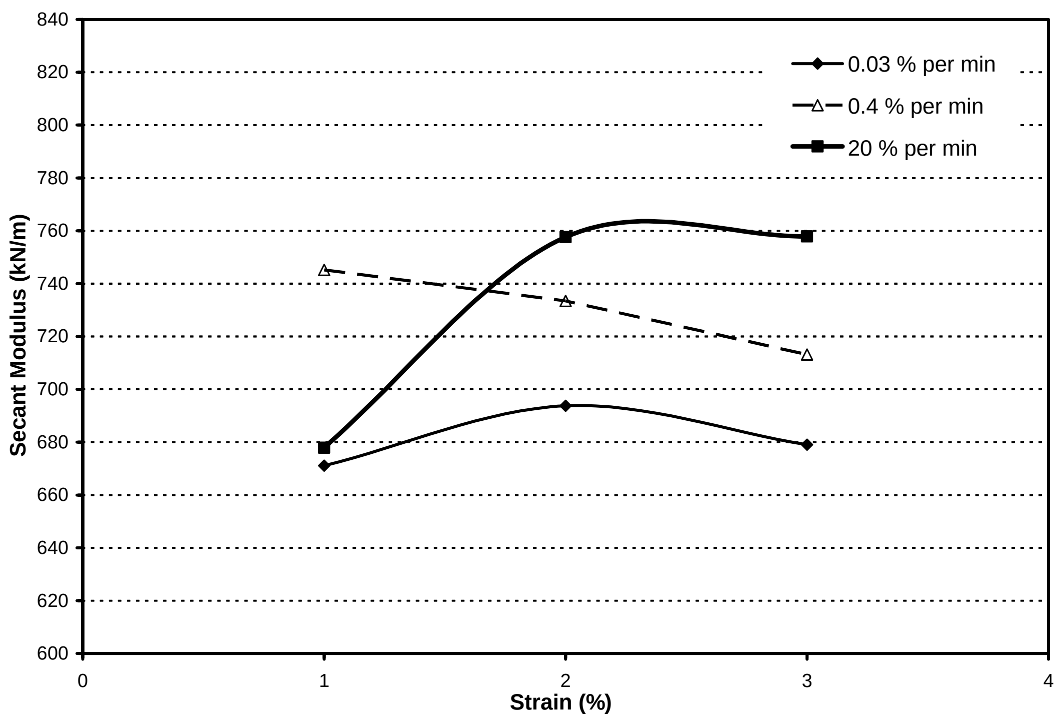

Figure 86: Secant Modulus versus Axial Strain for Enkagrid Max 20, Cross-Machine Direction

5.2.6 Summary

In most cases, the geosynthetics used in this research showed noticeable changes in stiffness when strained at rates varying between 0.03% and 20% per minute. In nearly all cases, the material behaved more stiffly (i.e., secant modulus increased) as the strain rate was increased – as expected. Stiffer materials, like the geogrids, were less sensitive to rate changes. Conversely, softer materials, like the geotextiles, were more sensitive to rate changes.

The overall stiffness of the material also influenced whether the secant modulus increased or decreased for higher levels of axial strain. Less stiff materials (such as the geotextiles) showed increasing stiffness for higher axial strains, while stiffer materials (such as the geogrids) showed decreased stiffness for higher axial strains. However, these trends were not as apparent for all materials.

5.3 The Effect of Specimen Size on Secant Modulus

To determine the effect of specimen size on geosynthetic material properties, a method called Design of Experiments (DOE) was used. DOE refers to the process of planning an experiment so that appropriate data will be obtained and analyzed using statistics, thereby yielding statistically valid and objective conclusions. The two basic steps in DOE are 1) designing suitable laboratory experiments or test methods, and 2) analyzing the results obtained from these experiments.

In the design phase, variables which can affect the output (*factors*) are determined. During testing, each factor is varied within a specific range to determine how it affects the output. Subdivisions within these ranges are called *levels*. Once an appropriate range of variability for each factor is defined, testing may begin. During testing multiple factors may be varied simultaneously or a single factor may be independently varied. Data from these experiments can be analyzed to determine how a particular factor, or combination of factors, affects the *output*.

The second step of the DOE is to analyze the results obtained from these experiments. The analysis is conducted using one, or a combination of three analysis methods: the ANOVA test, Tukey's test, or a graphical method.

5.3.1 Analysis Of Variance (ANOVA)

ANOVA is a statistical technique used to make objective comparisons between various factors to determine their effect on the output. The results from this analysis indicate whether a particular factor statistically affects the output. When a factor shows significance, it should be given due consideration when conducting the experiment. On the contrary, if a particular factor does not have significant effect on the output, it is unnecessary to consider that particular factor when conducting the experiment. ANOVA is the first step in testing for significance. If a particular factor shows significance, it might be necessary to determine what output level was responsible for the differences found. This can be accomplished using Tukey's test or the graphical method.

5.3.2 Tukey's Test

Tukey's test is used to determine significance between various levels of a particular factor. This test is more sophisticated than the ANOVA analysis since it is able to determine significance of a particular factor level for multiple factors simultaneously. Using this test, specific levels are compared to one another to determine whether there are significant differences between them. When individual levels are considered, all other levels are held constant, thereby eliminating their interference on the result. Results from this analysis statically show which levels of a factor are significant.

5.3.3 Graphical Method

Like Tukey's test, this method helps us to interpret significance of individual factor levels, but it does so visually using graphs. Using the graphical method positive or negative effects of particular factor levels can be revealed. Graphs are plotted for all output levels of a given factor and visually compared to other factor's levels. In general, the graphs describe trends of the output when levels are varied within a particular factor. One main advantage of this method is that it is easy to use.

5.3.4 Defining Factors Related to DOE

Overall, it was determined that of the many factors that could possibly affect the output, only the length of the sample and the width of the sample were considered. Obviously, there are a variety of factors that are omitted, for instance, the material's composition, structure, and the direction of loading. These are factors which are inherent in any material. In this analysis, materials were considered independently, so to a certain extent, differences between materials are ignored. Considering DOE for all the seven geosynthetics is very expensive and time consuming, so only two of the seven materials were studied – the Amoco 2006 geotextile and Tensar BX1100 geogrid. Future research can be planned to study the effect of remaining factors for all the seven geosynthetic materials.

5.3.5 Analysis and Results

Data collected were used to determine the material's load-strain characteristics. Load has the units of kN/m. An elastic secant modulus was determined from the initial portion of the load-strain curve for each test conducted. The geosynthetics were tested in the machine direction for all of these tests. Tests conducted on the geogrid were repeated once and repeated twice for the geotextile to ensure repeatability. Secant modulus values at 1% strain are shown in Tables 10 and 11.

At times it was necessary to correct the raw data due to initial loads placed on the material prior to testing. This problem was more pronounced for the Amoco 2006 material since more load was needed initially to straighten it between the grips, thereby producing some initial strain in the material. The correction consisted of extending the starting point of the plotted stress-strain curve towards the origin and calculating the 1% modulus using the corrected curve.

Table 10: Secant Modulus for BX1100 Oriented in the Machine Direction

Test #	Width (# of ribs)	Length (mm/in)	Secant Modulus (kN/m)		
			Test 1	Test 2	Avg.
1	2	114/4.5	477	487	482
2	2	28711.3	524	587	556
3	2	429/16.9	549	612	581
4	2	627/24.7	604	530	567
5	3	114/4.5	367	403	385
6	3	28711.3	491	491	491
7	3	429/16.9	531	482	507
8	3	627/24.7	509	466	488
9	4	114/4.5	307	291	299
10	4	28711.3	428	423	426
11	4	429/16.9	485	464	475
12	4	627/24.7	458	458	458
13	5	114/4.5	382	305	344
14	5	28711.3	426	426	426
15	5	429/16.9	473	446	460
16	5	627/24.7	471	475	473
17	6	114/4.5	324	339	332
18	6	28711.3	379	426	403
19	6	429/16.9	429	439	434
20	6	627/24.7	436	391	414

Table 11: Secant Modulus for Amoco 2006 Oriented in the Machine Direction

Test #	Width (mm/in)	Length (mm/in)	Secant Modulus (kN/m)			
			Test 1	Test 2	Test 3	Avg.
1	102/4	51/2	133	141	126	133
2	203/8	51/2	125	126	107	119
3	305/12	51/2	75	85	85	82
4	406/16	51/2	116	118	95	110
5	508/20	51/2	74	96	74	81
6	610/24	51/2	85	74	74	78
7	102/4	102/4	103	102	106	104
8	203/8	102/4	84	101	100	95
9	305/12	102/4	74	75	80	76
10	406/16	102/4	100	100	95	98
11	508/20	102/4	75	96	69	80
12	610/24	102/4	85	84	80	83
13	102/4	152/6	89	85	85	86
14	203/8	152/6	92	96	96	95
15	305/12	152/6	91	77	85	85
16	406/16	152/6	92	95	98	95
17	508/20	152/6	78	68	82	76
18	610/24	152/6	75	82	67	75
19	102/4	203/8	77	89	67	78
20	203/8	203/8	85	77	109	91
21	305/12	203/8	74	77	74	75
22	406/16	203/8	90	82	80	84
23	508/20	203/8	64	72	77	71
24	610/24	203/8	66	66	63	65

5.3.5.1 ANOVA Analysis

ANOVA was used to do determine whether length or width had a significant effect on the modulus. From this analysis, it was found that both length and width both have a significant effect on the modulus for both materials tested in the machine direction. Therefore, sample length and width should be considered when determining the constitutive material properties.

5.3.5.2 Tukey's Test

To determine potential *simultaneous* relationships between the length and width and the modulus, Tukey's test and the Graphical Method were used. Specifically, Tukey's test was used to determine specific cases where the secant modulus was significantly affected by varying sample lengths. Two separate Tukey's tests were used to accomplish this. In the first test the width was held constant and in the second the length was held constant. Individual comparisons between two different lengths or widths (A and B) were made to determine differences for a particular width or length, respectively. Results for the BX1100 tested in the machine direction are shown in Tables 12 and 13, and the results for the Amoco 2006 tested in the machine direction are shown in Tables 14 and 15. Generally, the results from Tukey's analysis showed that most of the significant differences were found when the shortest lengths and widths were compared to longest lengths and widths, respectively. For the Amoco 2006 product, lengths over 203 mm did not show much difference.

Table 12: Results from Tukey's Test on BX1100 Holding Width Constant

Length A (mm/in)	Length B (mm/in)	Width (# of ribs)				
		2	3	4	5	6
114/4.5	287/11.3		✓	✓		
114/4.5	429/16.9	✓	✓	✓	✓	✓
114/4.5	627/24.7	✓	✓	✓	✓	
287/11.3	429/16.9					
287/11.3	627/24.7					
429/16.9	627/24.7					

✓ = significant differences found

Table 13: Results from Tukey's Test on BX1100 Holding Length Constant

Width A (# of ribs)	Width B (# of ribs)	Length (mm/in)			
		114/4.5	287/11.3	429/16.9	627/24.7
2	3	✓			✓
2	4	✓	✓	✓	✓
2	5	✓	✓	✓	✓
2	6	✓		✓	✓
3	4				
3	5		✓		
3	6				
4	5				
4	6				
5	6				

✓ = significant differences found

Table 14: Results from Tukey's Test on Amoco 2006 Holding Width Constant

Length A (mm/in)	Length B (mm/in)	Width (mm/in)			
		51/2	102/4	152/6	203/8
102/4	203/8				
102/4	305/12	✓	✓		
102/4	406/16	✓			
102/4	508/20	✓	✓		
102/4	610/24	✓	✓		
203/8	305/12	✓	✓		
203/8	406/16				
203/8	508/20	✓			✓
203/8	610/24	✓		✓	✓
305/12	406/16	✓			
305/12	508/20				
305/12	610/24				
406/16	508/20	✓	✓	✓	
406/16	610/24	✓		✓	
508/20	610/24				

✓ = significant differences found

Table 15: Results from Tukey's Test on Amoco 2006 Holding Length Constant

Width A (mm/in)	Width B (mm/in)	Length (mm/in)					
		102/4	203/8	305/12	406/16	508/20	610/24
51/2	102/4	✓	✓				
51/2	152/6	✓	✓				
51/2	203/8	✓	✓		✓		
102/4	152/6	✓					
102/4	203/8	✓					
152/6	203/8						

✓ = significant differences found

5.3.5.3 Graphical Method

Using the Graphical method, plots for specific lengths and widths were generated showing trends of secant modulus to widths and lengths, respectively. These figures helped highlight visual relationships that exist between sample lengths and widths and the corresponding values of initial secant modulus. Figure 87 shows that the modulus decreases when the sample widths increase and that as sample lengths increase differences in moduli values are less when compared to longer lengths. Figure 88 shows that as the length increases, modulus increases and begins to level off, and that as widths increase overall values of modulus tend to decrease. So, for BX1100 in the machine direction, increasing lengths and widths work against each other, in that, increasing the length tends to increase the modulus and increasing the width tends to decrease the modulus.

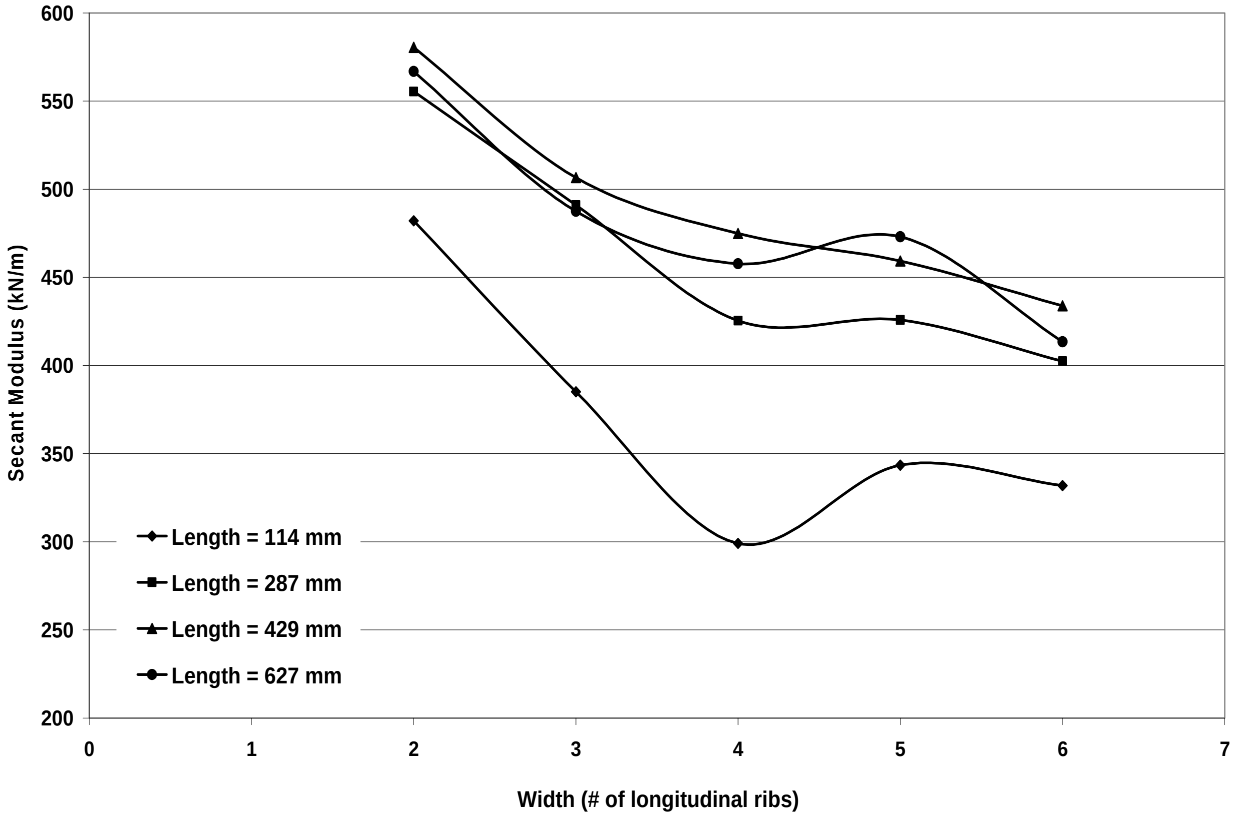

Figure 87: Modulus versus Width for Various Lengths of BX 1100

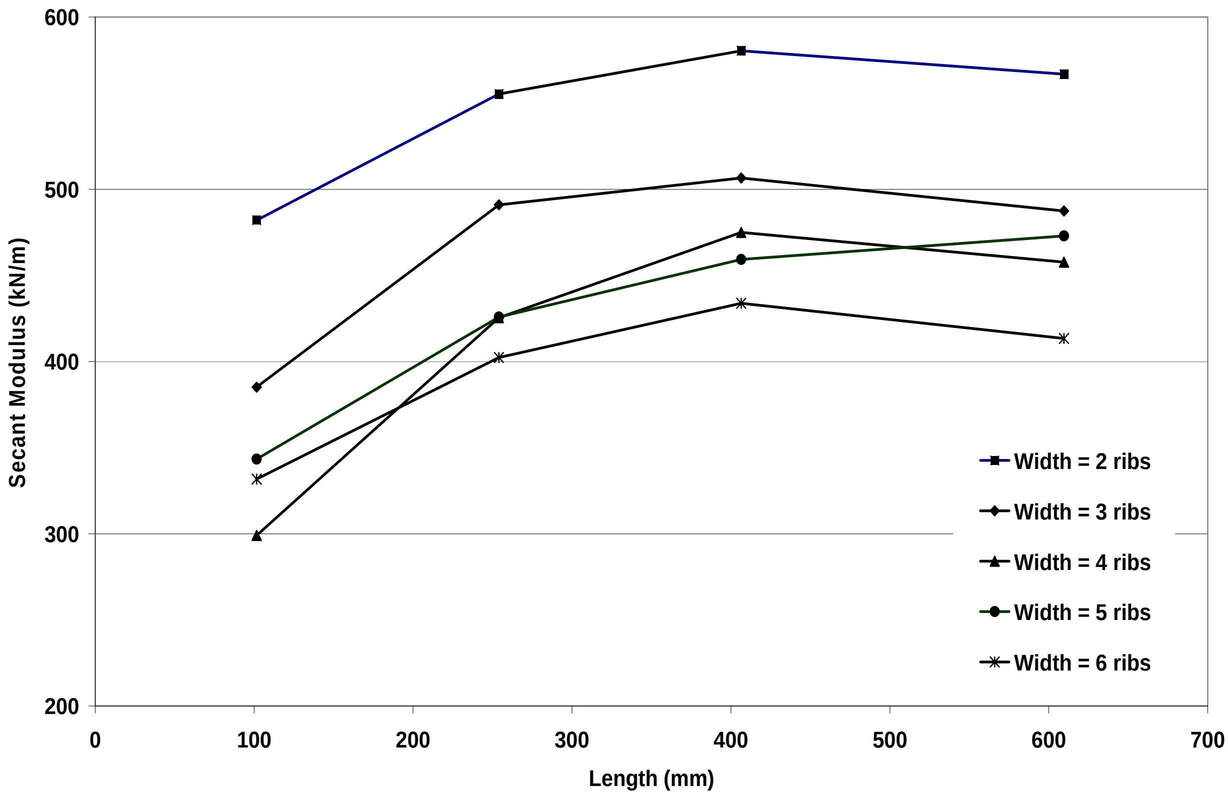

Figure 88: Modulus versus Length for Various Widths of BX 1100

For the Amoco 2006 material, as width increases, the secant modulus decreases, as shown in Figure 89. In addition, as width increases, there are less overall differences between the secant moduli for the lengths studied. For the 508 and 610 mm lengths, there are less overall differences on the secant modulus. Curiously, the 305 and 406 mm lengths don't seem to fit this trend as expected.

Comparing the secant modulus to sample width generally shows that as length increases the secant modulus tends to decrease (Figure 90). It is also much easier to see the differences in modulus for the 305 and 406 mm lengths as mentioned previously. Also, as the length increases, the differences between the moduli values for a particular length tend to decrease with the exception of the 406 mm length. The 102, 152 and 203 mm lengths closely followed one another, showing that as width increases, secant modulus changes less. Overall, for Amoco 2006, length and width have a similar effect on the output, that is, when either the length or width is increased, modulus decreases.

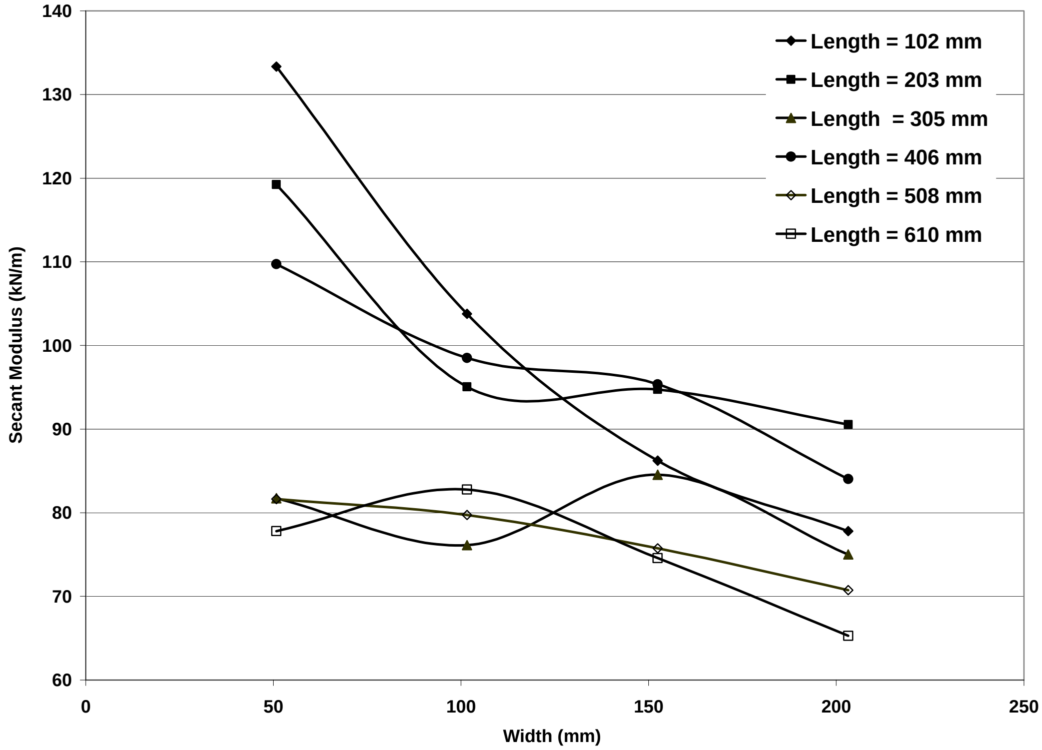

Figure 89: Modulus versus Width for Various Lengths of Amoco 2006

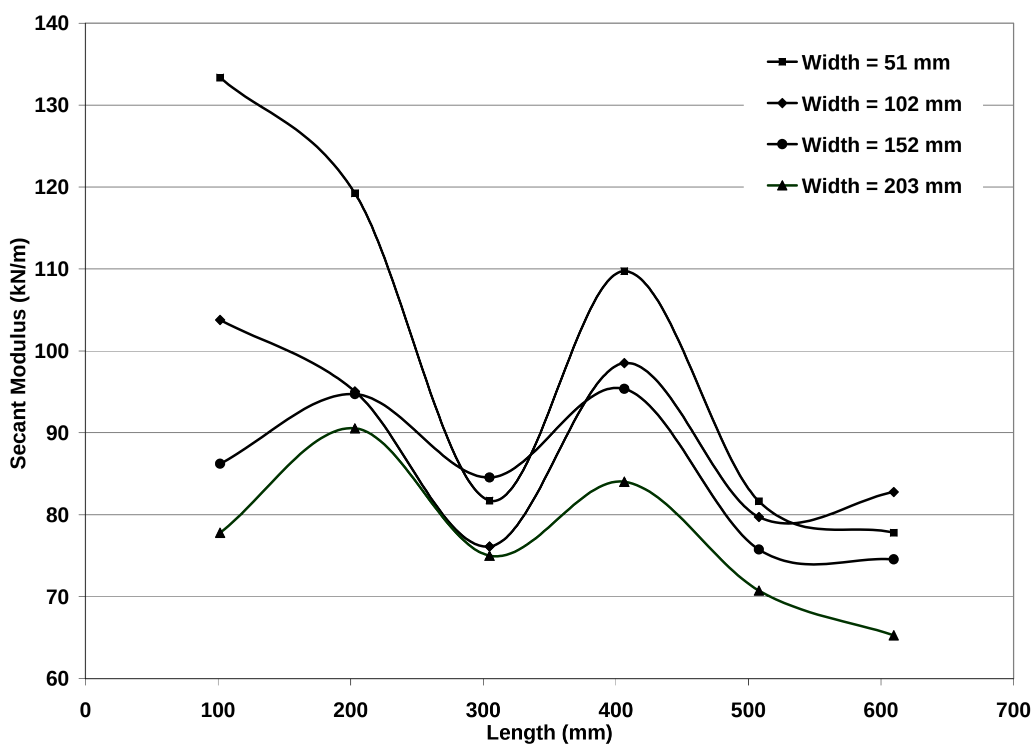

Figure 90: Modulus versus Length for Various Widths of Amoco 2006

5.3.6 Summary

The purpose of these tests was to investigate whether the initial secant modulus was affected by changing the length and width of samples of Tensar BX1100 geogrid and Amoco 2006 geotextile. Using ANOVA, Tukey's test and the Graphical method, it was determined that sample length and width had a significant affect on the initial secant modulus for both of these materials. Using the ANOVA analysis, it was found that both length and width both have a significant effect on the modulus for both materials tested in the machine direction. Generally, the results from Tukey's analysis showed that most of the significant differences were found when the shortest lengths and widths were compared to longest lengths and widths, respectively.

For the Amoco 2006 product, increasing either length or width decreases the initial secant modulus; and lengths over 203 mm did not show much difference. For the BX1100 material:

- increasing the width of the material decreases the initial secant modulus,
- increasing the length of the material increases the initial secant modulus,
- length and width have the opposite affect on the secant modulus, and
- increasing the length decreases differences in secant modulus, for a variety of widths.

6 SUMMARY, CONCLUSIONS AND FUTURE RECOMMENDATIONS

6.1 Summary

The purpose of this research was to develop test protocols that better describe the intrinsic material properties of geosynthetics pertinent to reinforced pavement design applications. In the past, standard tension tests such as ASTM D 4595 and D 6637 have been used to provide material properties for geosynthetic design. These tests apply monotonic loads to the materials to determine elastic moduli in their two principal directions. However, the types of loading conditions prescribed by these tests do not reflect conditions experienced by geosynthetics used as reinforcement in flexible pavements. Traffic loading is cyclic and may be better represented by laboratory tests that are also cyclic. In addition, other factors such as load rate, type of load, temperature, sample size and configuration, and normal confinement have been studied to determine their effect on measured material properties. The results from the literature review suggested modest yet important effects due to temperature on modulus and significant effect of strain rate on modulus. However, the existing information is incomplete and does not allow general modifications to the tensile modulus values determined from standard tension tests to be adjusted so that material properties at temperatures and strain rates occurring in roadways are more characteristic. Although less work has been conducted to determine the effects of normal confinement, the literature suggested that the tensile modulus of certain geosynthetics can be significantly affected under these conditions. Finally, the load-strain behavior was significantly affected when cyclic loads were applied to geosynthetic material samples. Based on this literature review, cyclic loads, and to a lesser extent, various strain rates and sample sizes were used to study their effect on these parameters.

Three geotextiles and four geogrids were tested to compare their unconfined load/strain properties under monotonic and cyclic loads. Tests were also conducted to study the effects of various strain rates and samples sizes. A servo-hydraulic loading system equipped with Curtis GeoGrips was used to load the geosynthetics. Axial and lateral strains were measured using a device called a “clip gage” and lvdts. All tests were conducted on standard sized, wide-width specimens except for tests used to study various sample sizes. For the cyclic tests, geosynthetics were loaded up to six predetermined levels of axial strain and cycled 1000 times at a strain amplitude of 0.2 percent at 0.67 Hz. This protocol simulates a static prestressed condition of the geosynthetic due to either accumulated load or construction, and then cycles the load representative of traffic. The load-strain curves from the monotonic and cyclic tests were used to calculate the tangent and cyclic modulus, respectively, at the six predetermined levels of axial strain.

6.2 Conclusions

Results from cyclic tests conducted on the geotextiles generally showed that the stiffness remained constant for all 1000 load cycles at a particular load level but that the stiffness increased significantly from one step to the next. Geogrids exhibited an opposite effect, in that the stiffness increased with increasing number of load cycles within a given load step, but did not change from step to step. Monotonic test results showed that the initial stiffness decreased as axial strain increased for geogrids, but remained constant for geotextiles. These intrinsic material parameters were used as inputs into a finite element model of a geosynthetic-reinforced pavement structure to study the effects various geosynthetics have on pavement performance.

These results have the following implications for reinforced pavement modeling. For stiffer materials like the geogrids, cyclic loading tends to create a state in the material where the stiffness of small-strain amplitude load cycles is equal to a constant for any level of permanent strain. These results suggest that a constant elastic modulus should be used for the reinforcement for any level of pavement load application. This constant modulus value can be approximated by averaging the cyclic modulus values. However, for softer materials like the geotextiles, modifications to the material models are required to incorporate this non-linear behavior.

When tested at various strain rates, the geosynthetics used in this research showed noticeable changes in stiffness when strained at rates varying between 0.03% and 20% per minute. As expected, the material behaved more stiffly (i.e., secant modulus increased) as the strain rate was increased. Stiffer materials, like the geogrids, were less sensitive to rate changes. Conversely, softer materials, like the geotextiles, were more sensitive to rate changes. The overall stiffness of the material also influenced whether the secant modulus increased or decreased for higher levels of axial strain. Less stiff materials (such as the geotextiles) showed increasing stiffness for higher axial strains, while stiffer materials (such as the geogrids) showed decreased stiffness for higher axial strains. However, these trends were not as apparent for all materials.

Tests conducted using various sample sizes of the Amoco 2006 geotextile and Tensar BX1100 geogrid showed that sample length and width had a significant affect on the initial secant modulus for both of these materials. Generally, the results from Tukey’s analysis showed that most of the significant differences were found when the shortest lengths and widths were compared to longest lengths and widths, respectively. Overall, the results from the Amoco 2006 geotextile showed that increasing either length or width decreases the initial secant modulus, and for lengths over 203 mm did not show much difference. For the BX1100 material, increasing the width of the material decreases the initial secant modulus, increasing the length of the material increases the initial secant modulus, length and width have the opposite affect on the secant modulus, and increasing the length decreases differences in secant modulus, for a variety of widths.

6.3 Recommendations for Future Research

Additional work is needed to establish the most efficient cyclic loading protocol and to evaluate this test for other reinforcement products. Loading of geosynthetics in pavement applications may be cyclic stress relaxation (like those conducted as part of this study), cyclic creep, relaxation-cyclic relaxation, creep-cyclic creep, or some combination of these conditions. In particular, it may be discovered that loading to a particular permanent strain, followed by stress relaxation or creep and subsequent reloading, provides the same information without applying multiple load cycles. Since it is unclear which loading case predominates in reinforced pavement applications, tests should be performed for each of the four basic dynamic cases. Additional testing should also be performed to establish the influence of strain rate, temperature and confinement on the measured elastic modulus for conditions pertinent in pavements, as indicated in the literature review.

7 REFERENCES

1. Allen, T., Bell, J.R. and Vinson, T.S. (1983). "Properties of Geotextiles in Cold Regions Applications", *Transportation Research Record,* Report No. 83-6, Transportation Research Institute, Oregon State University, Corvallis, Oregon.

2. Ashmawy, A.K. and Bourdeau, P.L. (1996). "Response of a Woven and a Nonwoven Geotextile to Monotonic and Cyclic Simple Tension", *Geosynthetics International*, Vol. 3, No. 4, pp. 493-515.

3. ASTM (2003), Annual Book of ASTM Standards, Vol. 04.13, West Conshohocken, PA, USA.

4. Austin, D.N., Wu, K.J. and White, D.F. (1993). "The Influence of Test Parameters and Procedures on the Tensile modulus of Stiff Geogrids", *Geosynthetic Soil Reinforcement Testing Procedures,* STP 1190, S.C. Jonathan Cheng, Ed., ASTM, Philadelphia, PA, pp. 90-110.

5. Bathurst, R.J. and Cai, Z. (1994). "In-Isolation Cyclic Load-Extension Behavior of Two Geogrids", *Geosynthetics International*, Vol 1, No. 1, pp. 1-19.

6. Bell, J.R., Hicks, R.G., Copeland, J., Evans, G.L., Cogne, J.J., Mallard, P., Jahn, S. and Lewis, M. (1980). "Evaluation of Test Methods and Use Criteria for Geotechnical Fabrics in Highways Applications", Federal Highway Administration, Washington, D.C., FHWA Report 80-021.

7. Boyle, S.R., Gallagher, M., and Holtz, R.D. (1996). "Influence of Strain Rate, Specimen Length and Confinement on Measured Geotextile Properties", *Geosynthetics International*, St. Paul, Minnesota, Vol. 3, No. 2, pp. 205-225.

8. Budiman, J., "Effects of Temperature on Physical Behaviour of Geomembranes", *Proceedings: Fifth International Conference on Geotextiles, Geomembranes and Related Products*, Singapore, September 1994, pp. 1093-1096.

9. Bush, D.I. (1990). "Variation of Long Term Design Strength of Geosynthetics in Temperatures up to 40° C", *Proceedings: Fourth International Conference on Geotextiles, Geomembranes and Related Products*, The Hague, Netherlands, pp.673-676.

10. Calhoun, C.C. (1972) "Development of Design Criteria and Acceptance Specifications for plastic Filter Cloths", Army Engineer Waterways Experiment Station, Vicksburg, Mississippi. Technical Report No. S-72-7.

11. Cazzuffi, D. and Sacchetti, M. (1999). "Temperature Effects on Tensile-Creep behavior of High-Strength Geosynthetics", *Proceedings: Geosynthetics' 99 Conference*, 723-733.

12. Chu, T., Gent, S. Suthankar., and N.P. Reddy. (1996). "Bonding methods for strain gages on polypropylene material". *Experimental Techniques*, pp.29.

13. Cuelho. E.V. (1998). "Determination of Geosynthetics Constitutive Parameters and Soil/Geosynthetic Interaction by In-Air and In-Soil Experiments", *Thesis presented to the Montana State University*, Bozeman, Montana, in partial fulfillment of the requirements for the degree of Master of Science in Civil Engineering.

14. Elias, V., Yuan, A., Swan, R. and Bachus, R. (1998) "Development of Protocols for Confined Extension/Creep Testing of Geosynthetics for Highway Applications," U.S. Department of Transportation, Federal Highway Administration, Washington, D.C., Report No. FHWA-RD-97-143, 211p.

15. Gallagher, M. (1995), "In-Isolation Wide Width Test on Geotextiles", *Thesis presented to the University of Washington*, Seattle, Washington, in partial fulfillment of the requirements for the degree of Master of Science in Civil Engineering.

16. Haliburton, T.A., Anglin, C.C. and Lawmaster, J.D. (1978). "Selection of geotechnical Fabrics for Embankment Reinforcement", *U.S. Army Engineer District, Mobile, Alabama,* Contract No. DACW01-78-C-0055.

17. Hsuan, Y.G. (1998). "Temperature Effect on the Stress Crack Resistance of High Density Polyethylene Geomembranes", *Proceedings: Sixth International Conference on Geosynthetics*, Denver, CO, pp. 371-374.

18. Ketchart, K and Wu, J. T. H. (2001). "Performance test for geosynthetic-reinforced soil including effects of preloading". Federal Highway Administration, McLean, VA, FHWA Report RD-01-018.

19. Kinney, T.C. and Xiaolin, Y. (1995) "Geogrid Aperture Rigidity by In-Plane Rotation," *Proceedings of the Geosynthetics '95 Conference*, Nashville, TN, Vol. 2, pp. 525-538.

20. Kongkitkul, W., Hirakawa, D. and Tatsuoka, F. (2002). "Viscous Deformation During Cyclic Loading of Geosynthetics Reinforcement", *Proceedings: 7th International Conference on Geosynthetics*, Nice, Vol.1, pp.129-132.

21. Leshchinsky, Dov and Fowler, Jack. (1990). "Laboratory measurement of load-elongation relationship of high-strength geotextiles". *Geotextiles and Geomembranes*, Vol. 9, pp.145-164

22. McGown, A.; Andrawes, K.Z. and Kabir, M.H. (1982). "Load Extension Testing of Geotextiles Confined In Soils." *Proceedings: Second International Conference on Geotextiles*, Las Vegas, Nevada, Vol. 3, Industrial Fabrics Association International, St. Paul, Minnesota, pp. 793-798.

23. McGown, A.; Andrawes, K.Z. and Yeo, K.C. (1985). "The Load-Strain-Time Behaviour of Tensar geogrids", *Proceedings: Polymer Grid Reinforcement*, pp. 11-17.

24. Moraci, N. and Montanelli, F. (1997). "Behavior of Geogrids Under Cyclic and Dynamic Loads", *Proceedings: Geosynthetics' 97 Conference*, Long Beach California, pp.961-977.

25. Myles, B. and Carswell, I.G. (1986). “Tensile Testing of Geotextiles”, *Proceedings: Third International Conference on Geotextiles*, Vol. 3, Vienna, Austria, pp. 713-718.

26. NCHRP (2003), NCHRP Project 1-37A, Development of NCHRP 1-37A Design Guide, Using Mechanistic Principles to Improve Pavement Design.

27. Nothdurft, D.B. and Janardhanam, R. “Influence of Polymer Viscoelasticity in Reinforcement Soil Structure Design”, *Proceedings: Fifth International Conference on Geotextiles, Geomembranes and Related Products*, Singapore, September 1994, pp. 247-250.

28. Oglesby, John W.; Mahmoodzadegan, Behnam; Griffin, Paul M. (1992). Evaluation of methods and materials used to attach strain gages to polymer grids for high strain conditions”. *Transportation Research Report*, Report No. FHWA/LA-92/265, Louisiana Department of Transportation and Development.

29. Perkins, S.W.; Christopher, B. R.; Cuelho, E.V.; Eiksund, G.R.; Hoff, I.; Schwartz, C.W.; Svanø, G.; and Watn, A. (2004) “Development of Design Methods for Geosynthetic Reinforced Flexible Pavements.” Final report to the Federal Highway Administration, Document Reference No. DTFH61-01-X-00068.

30. Raumann, G. (1979). “A Hydraulic Tensile test with Zero Transverse Strain for Geotechnical Fabrics”, *Geotechnical Testing Journal*, Vol. 2, No.2, pp. 69-76.

31. Rowe, R.K. and Ho, S.K. (1986) “Determination of Geotextile Stress-Strain Characteristics Using a Wide Strip Test”, *Proceedings: Third International Conference on Geotextiles*, Vienna, Austria, pp. 885-890.

32. Shrestha, S.C. and Bell, J.R. (1982) “A Wide Strip Tensile Test of Geotextiles”, *Proceedings: Second International Conference on Geotextiles*, Vol. 3, pp. 739-744.

33. Sluimer, G and Risseeuw, P. (1982). “A strain-gauge technique for measuring deformations in geotextiles”. *Proceedings: Second international conference on geotextiles,* Las Vegas, Nevada, pp.835-838.

34. Soong T.Y. and Lord, A.E. “Slow Strain Rate Modulus Assessment Via Stress Relaxation Experiments”, *Proceedings: Sixth International Conference on Geosynthetics*, Denver, CO, 1998, pp. 711-715.

35. Soong, T.Y., Lord, A.E. and Koerner, R.M. (1994) “Stress Relaxation Behavior of HDPE Geomembranes”, *Proceedings: Fifth International Conference on Geotextiles, Geomembranes and Related Products*, Singapore, September 1994, pp. 1121-1124.

36. Tsuboi, M., Imaizumi, S. and Miyaji, H. (1998). “Effect of the temperature on Tensile Behavior of Geomembranes”, *Proceedings: Sixth International Conference on Geosynthetics*, Denver, CO, 1998, pp. 201-204.

37. Van Zanten, ed. (1986). "Geotextiles and Geomembranes in Civil Engineering", A.A. Balkema.

38. Vishay (2004) http://www.vishay.com/brands/measurements_group/guide/tt/tt605/605j.htm. From the Vishay Measurements Group, Inc. website.

39. Wang, A., Zang, B. and Lu, L. (1990). "Research Influence of Test Conditions on the Tensile Strength of Geotextiles", *Proceedings: Fourth International Conference on Geotextiles, Geomembranes and Related Products*, Hague, Netherlands, May 1990, pp. 782-782.

APPENDIX A – MONOTONIC TEST RESULTS

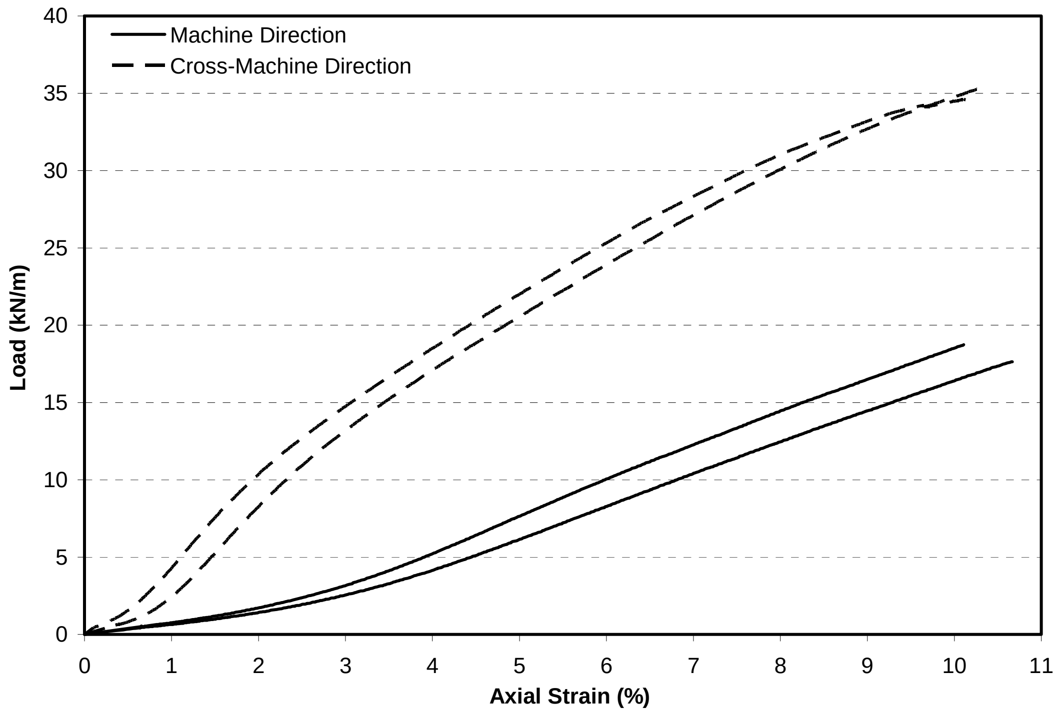

Figure A-1: Monotonic, Load-Strain Curves for Amoco ProPex 2006 Geotextile in Both Principle Strength Directions

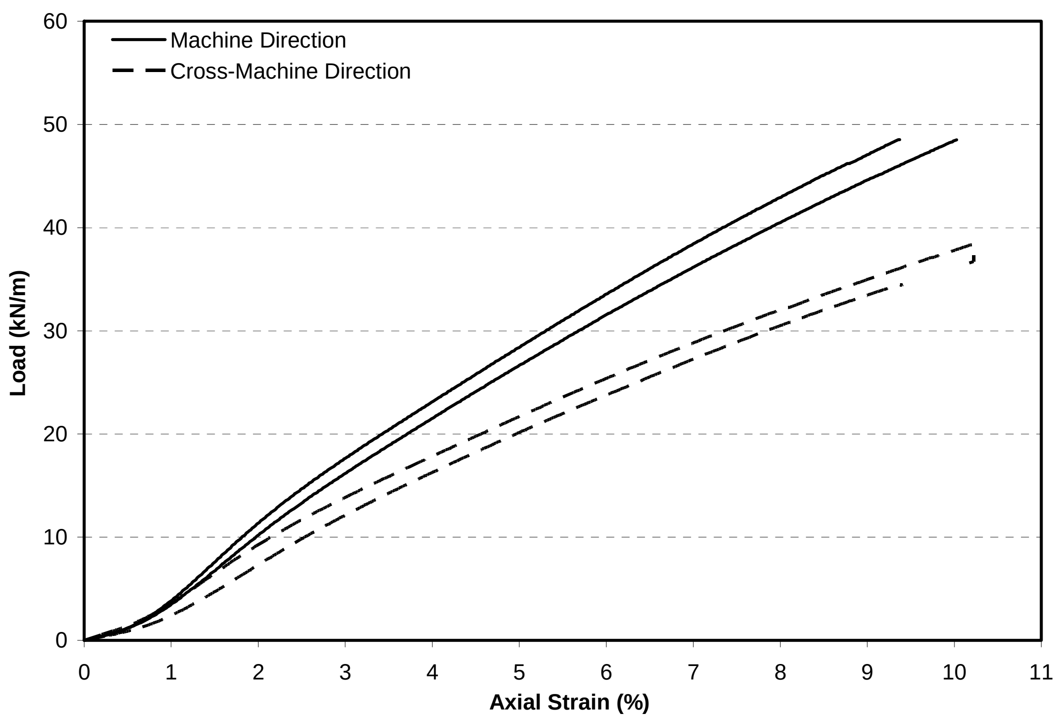

Figure A-2: Monotonic, Load-Strain Curve for Synthetic Industries Geotex 3×3 Geotextile in Both Principle Strength Directions

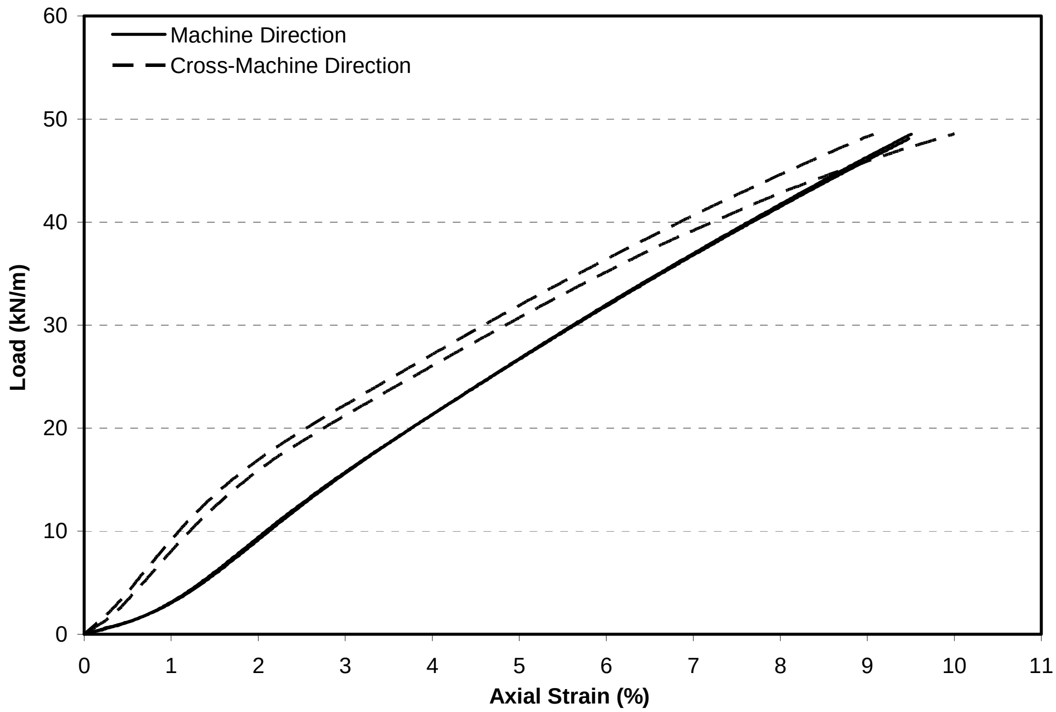

Figure A-3: Monotonic, Load-Strain Curve for Ten Cate Nicolon Geolon HP570 Geotextile in Both Principle Strength Directions

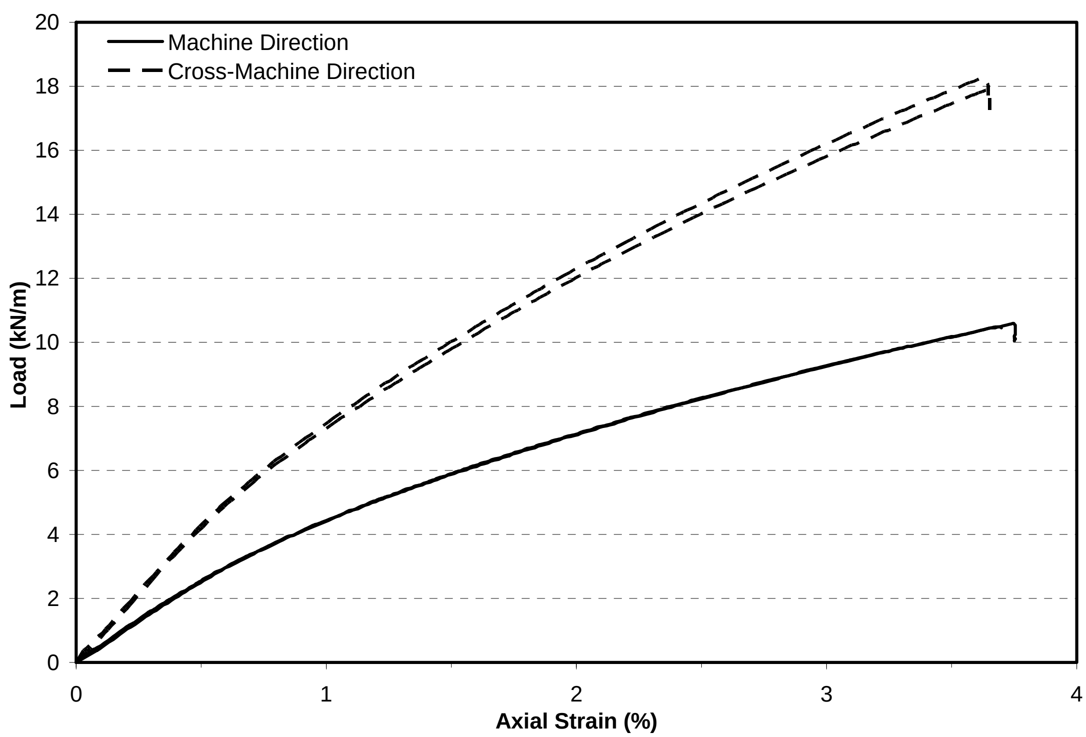

Figure A-4: Monotonic, Load-Strain Curve for Tensar BX 1100 Geogrid in Both Principle Strength Directions

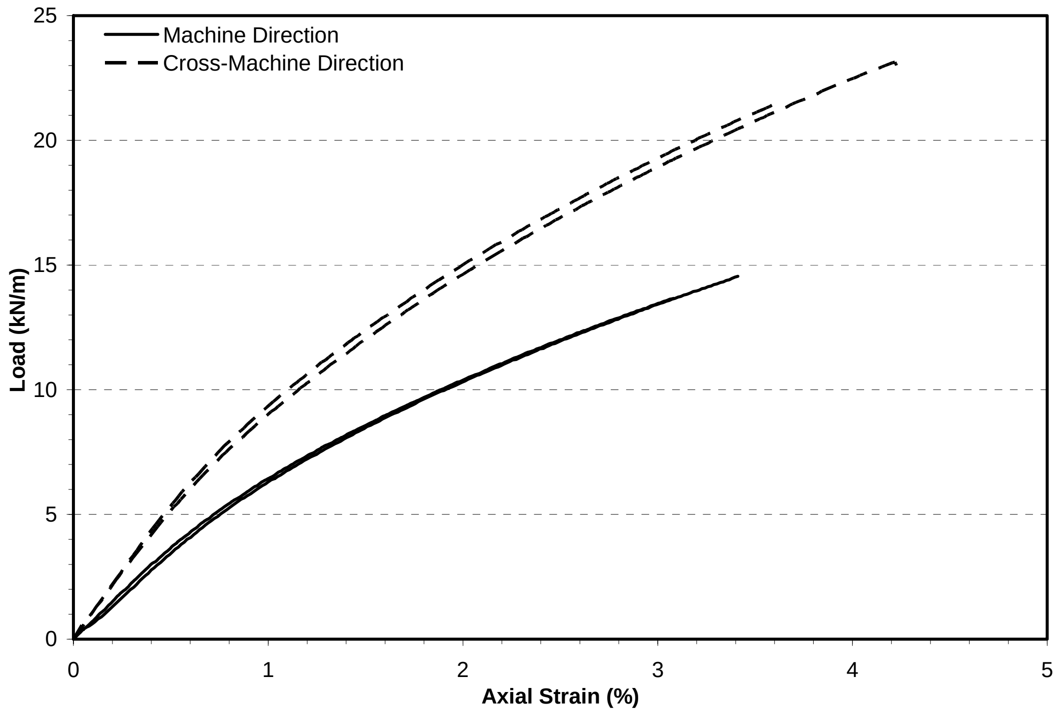

Figure A-5: Monotonic, Load-Strain Curve for Tensar BX 1200 Geogrid in Both Principle Strength Directions

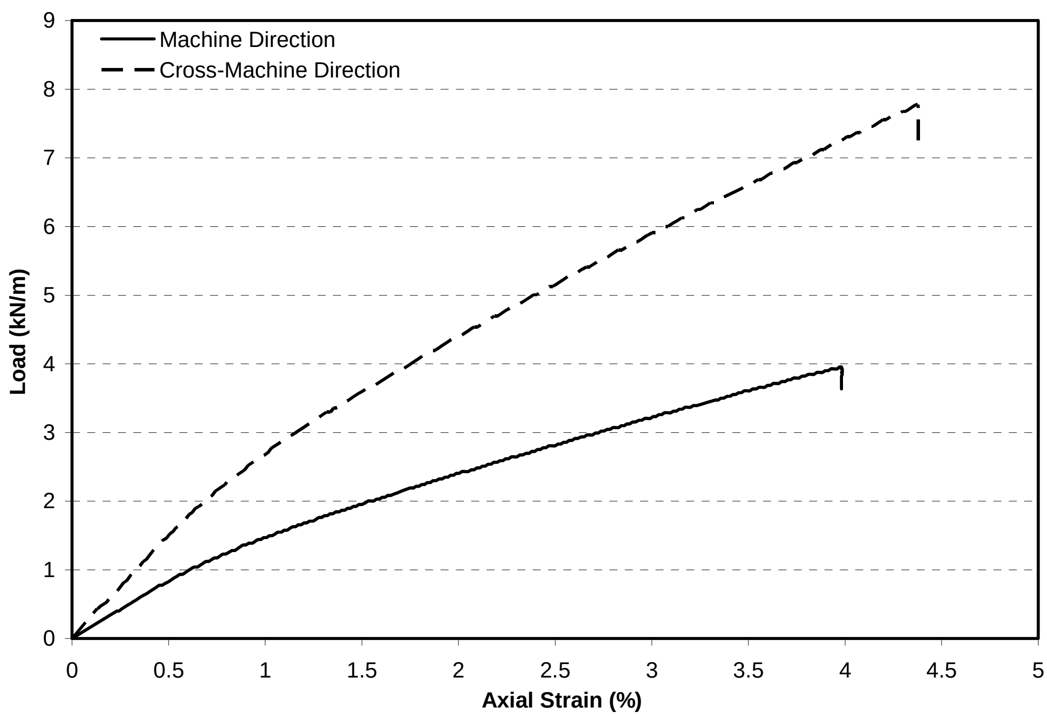

Figure A-6: Monotonic, Load-Strain Curve for Tenax MS220b Geogrid in Both Principle Strength Directions

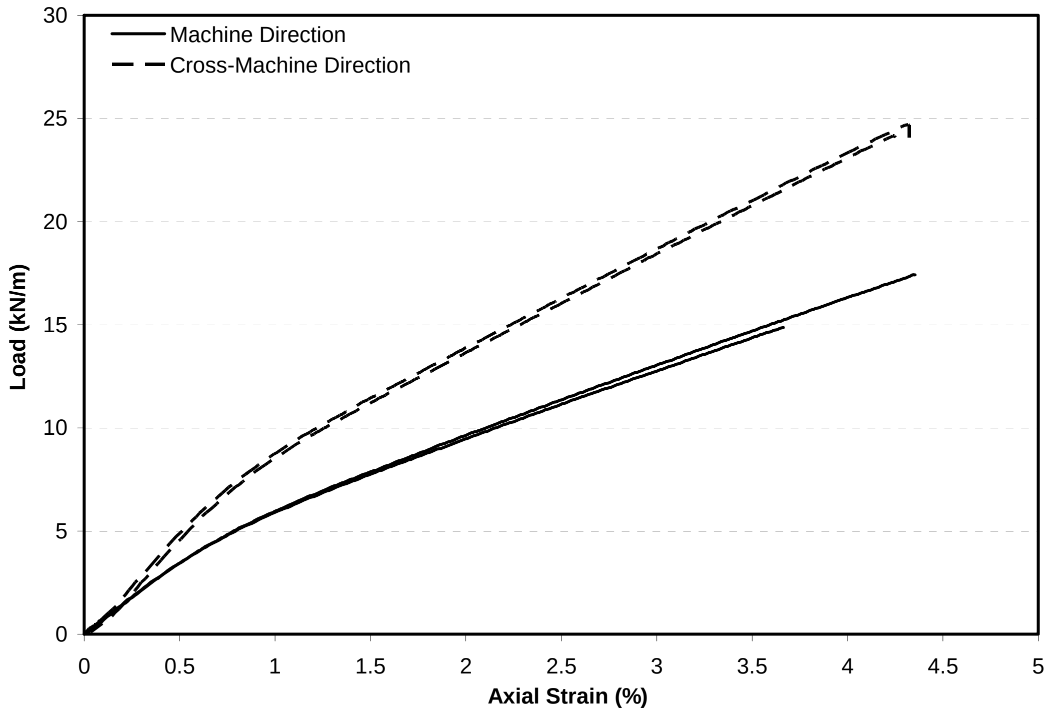

Figure A-7: Monotonic, Load-Strain Curves for Colbond Enkagrid Max 20 Geogrid in Both Principle Strength Directions

APPENDIX B – RESULTS OF TESTS AT VARIOUS STRAIN RATES

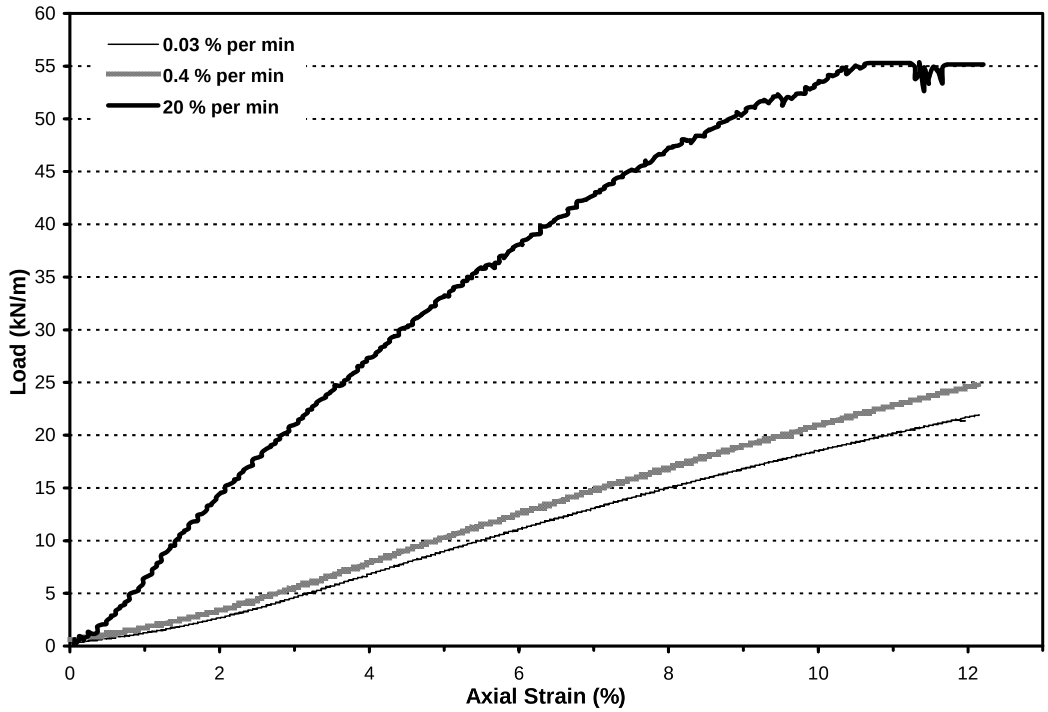

Figure B-1: Load-Strain Curves for the Amoco 2006 Geotextile in the Machine Direction at Three Strain Rates

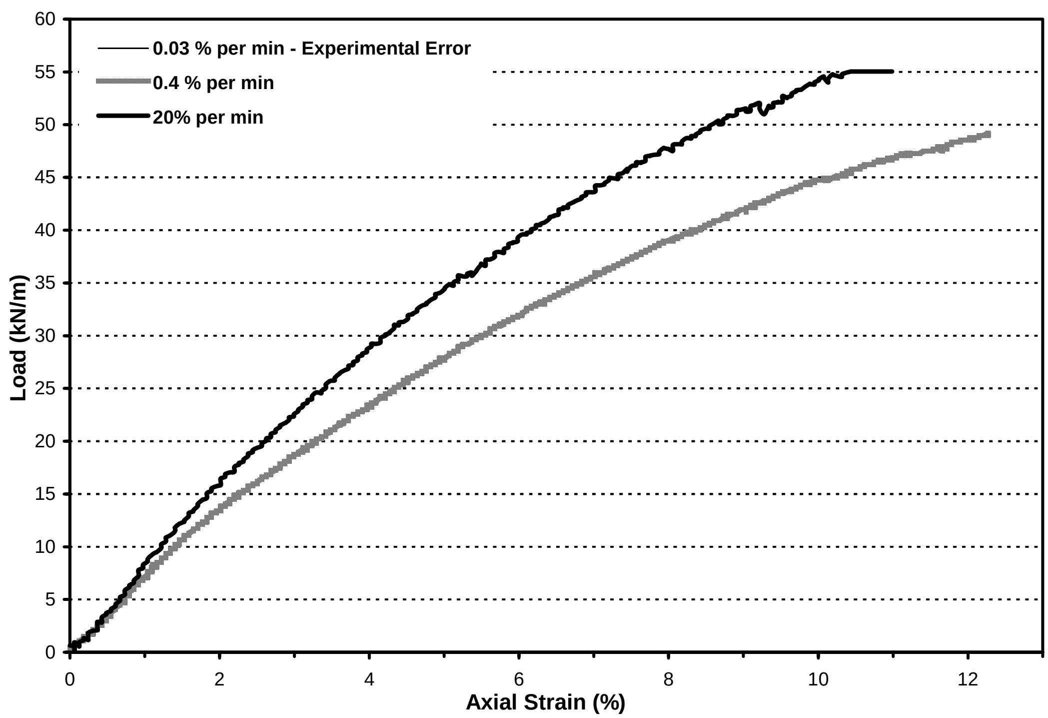

Figure B-2: Load-Strain Curves for the Amoco 2006 Geotextile in the Cross-Machine Direction at Three Strain Rates

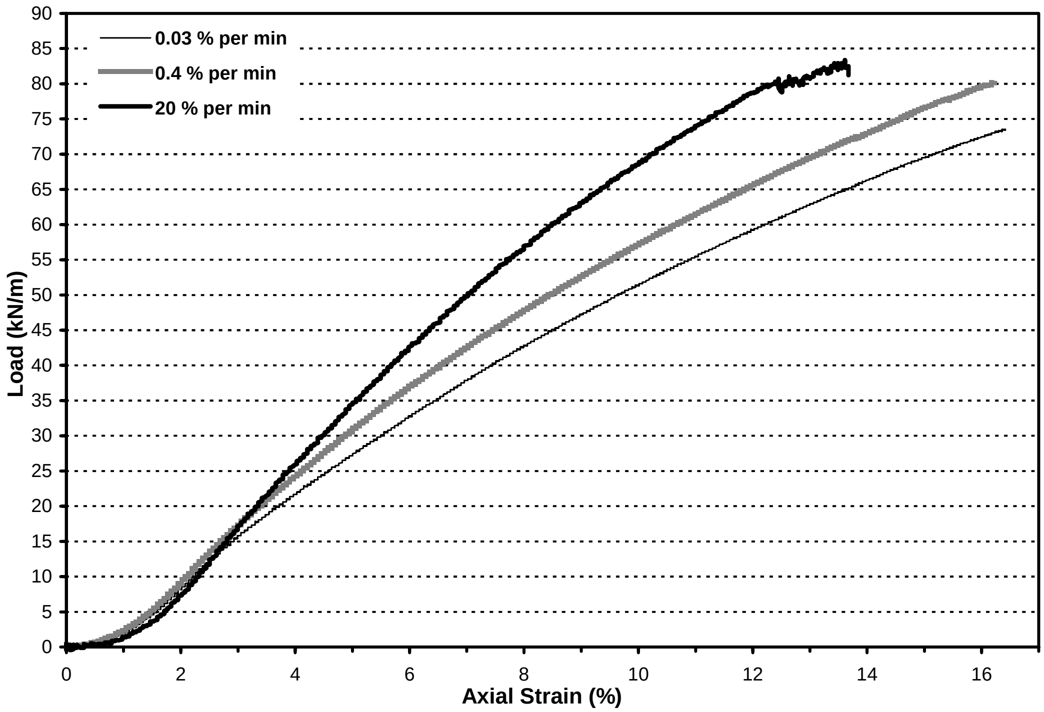

Figure B-3: Load-Strain Curves for the Ten Cate Nicolon Geolon HP570 Geotextile in the Machine Direction at Three Strain Rates

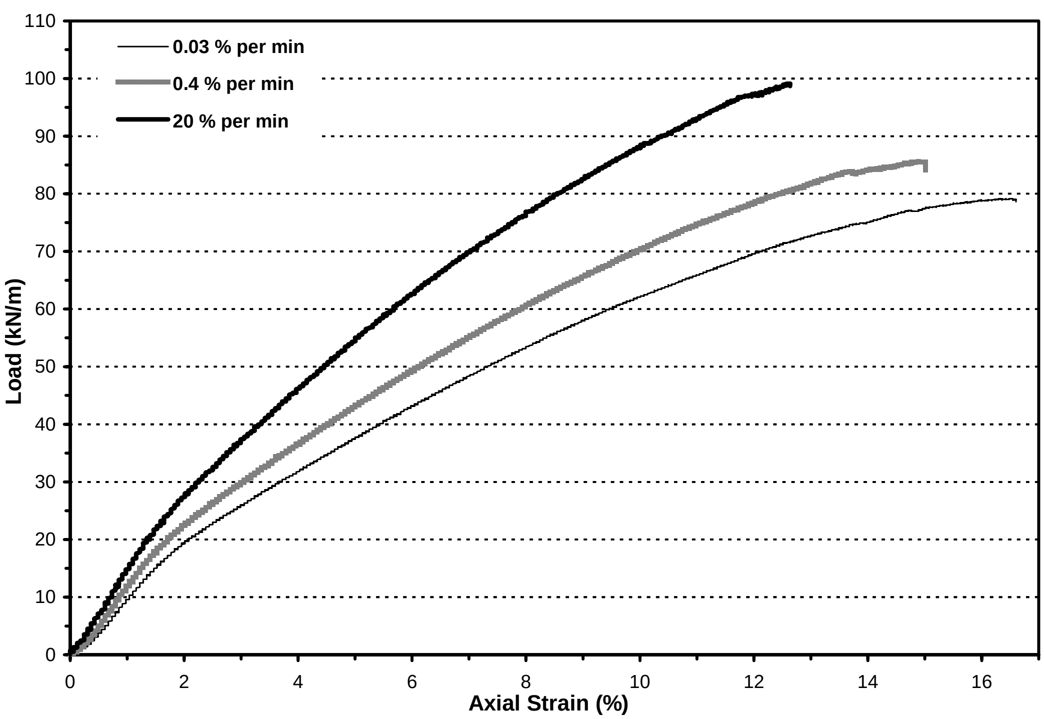

Figure B-4: Load-Strain Curves for the Ten Cate Nicolon Geolon HP570 Geotextile in the Cross-Machine Direction at Four Strain Rates

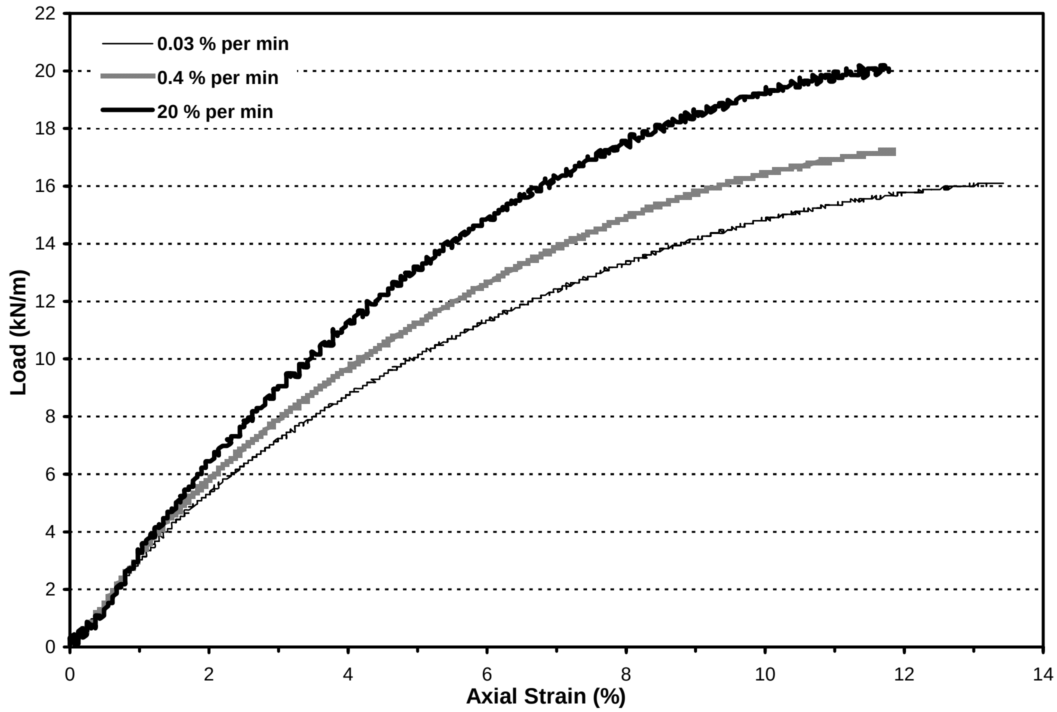

Figure B-5: Load-Strain Curves for the Tensar BX1100 Geogrid in the Machine Direction at Three Strain Rates

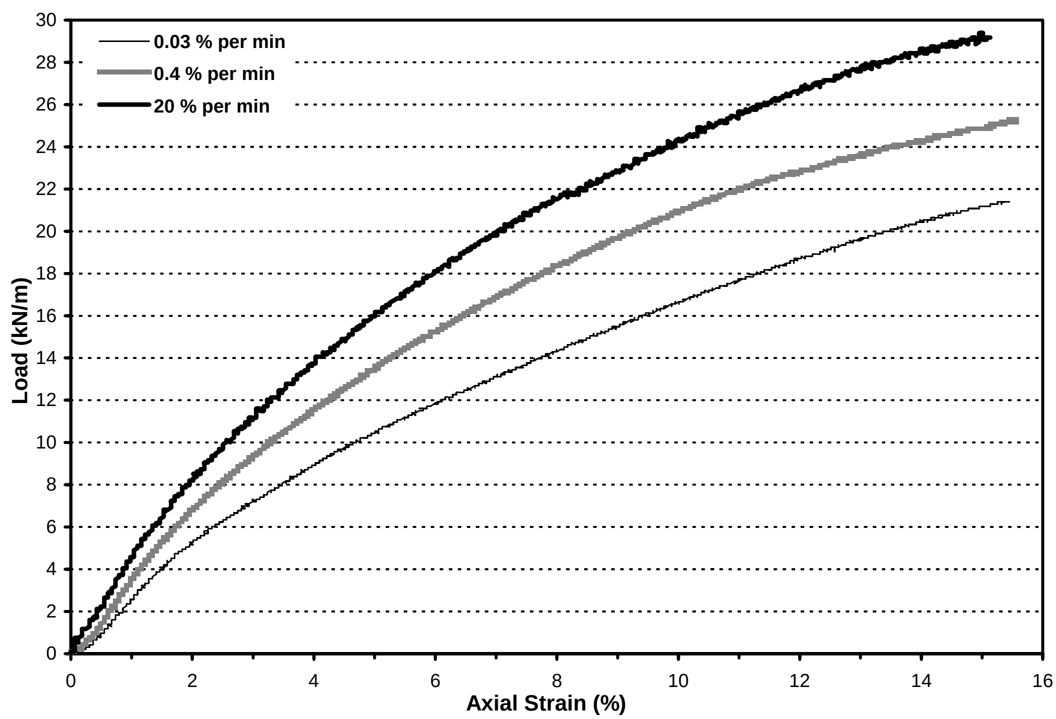

Figure B-6: Load-Strain Curves for the Tensar BX1100 Geogrid in the Cross-Machine Direction at Three Strain Rates

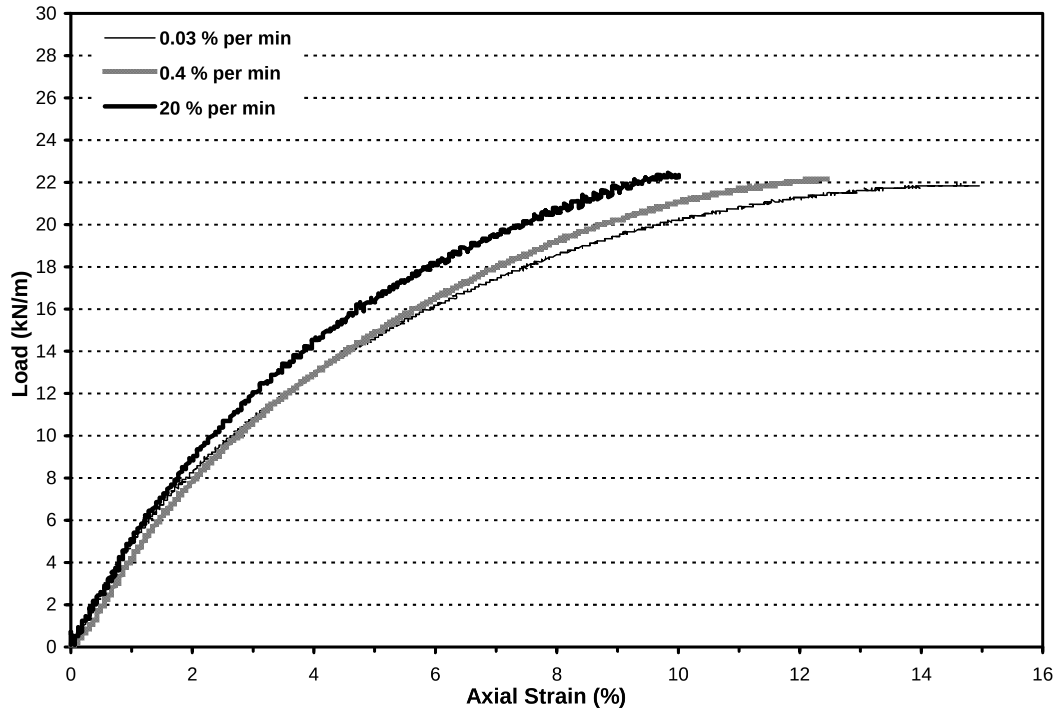

FigureB-7: Load-Strain Curves for the Tensar BX1200 Geogrid in the Machine Direction at Three Strain Rates

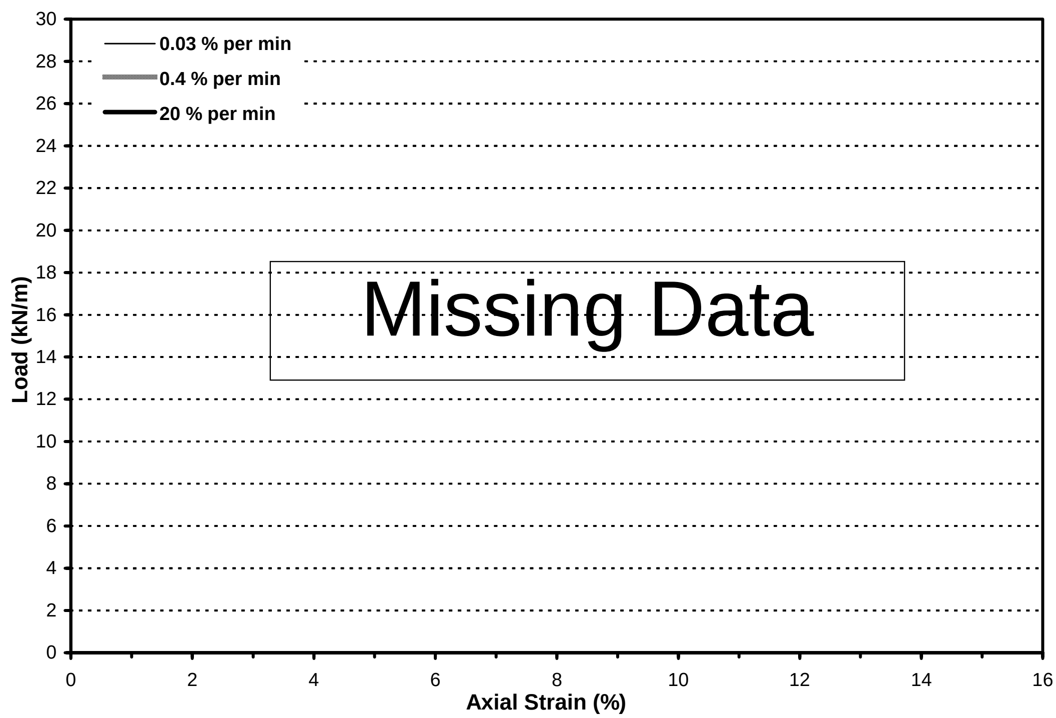

Figure B-8: Load-Strain Curves for the Tensar BX1200 Geogrid in the Cross-Machine Direction at Three Strain Rates

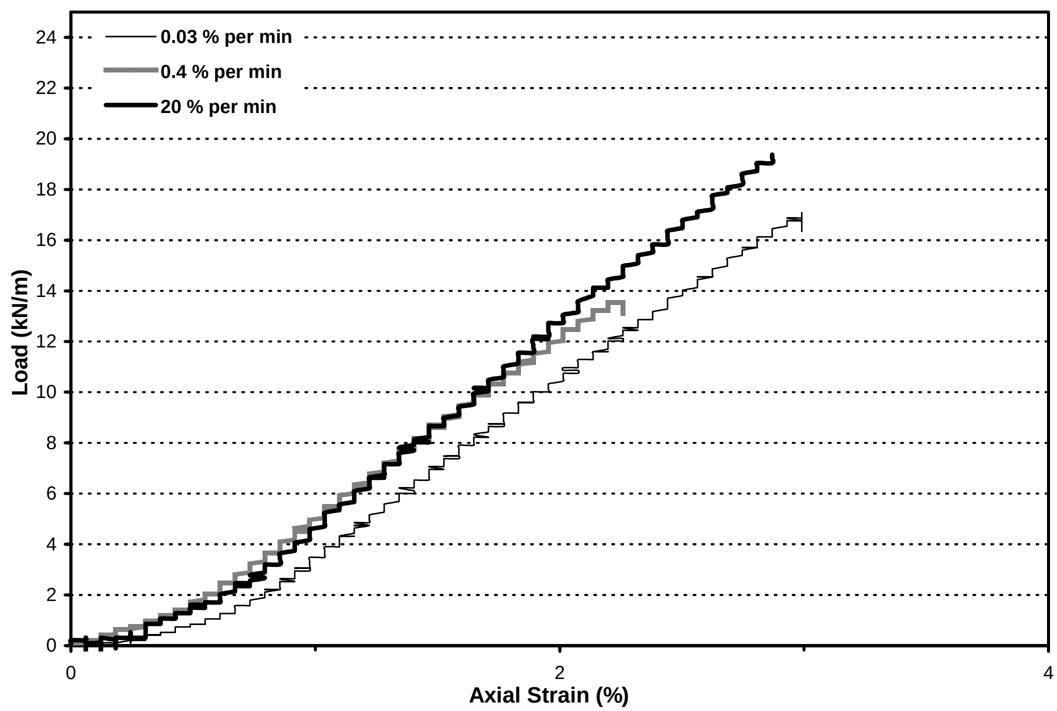

Figure B-9: Load-Strain Curves for the Colbond Enkagrid Max20 Geogrid in the Machine Direction at Three Strain Rates

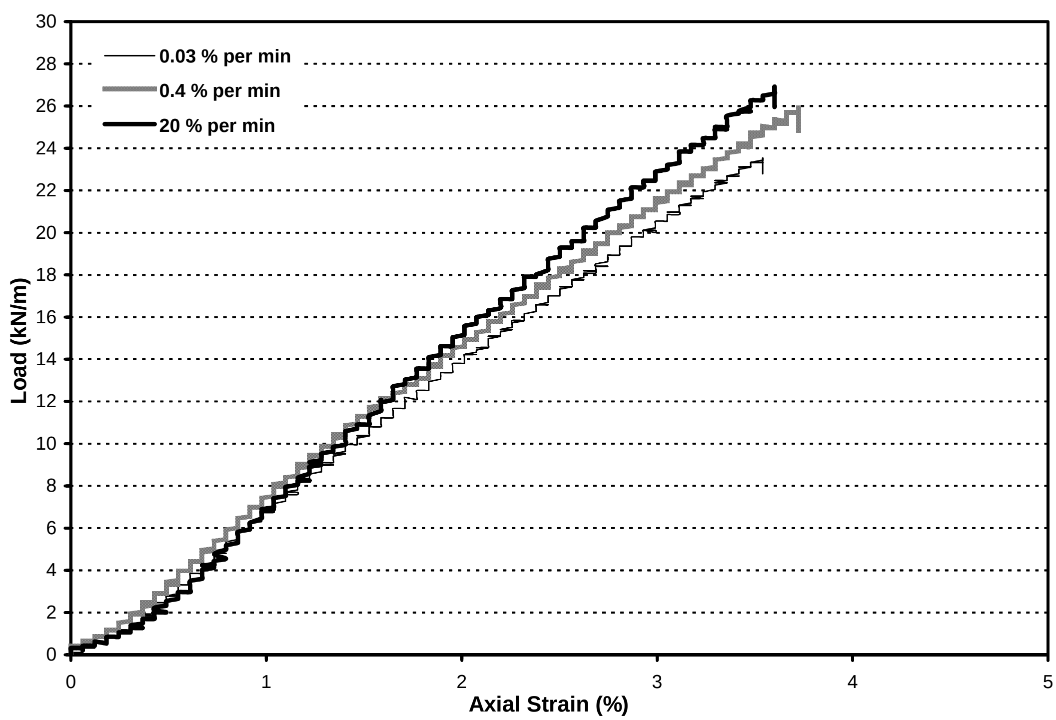

Figure B-10: Load-Strain Curves for the Colbond Enkagrid Max20 Geogrid in the Cross-Machine Direction at Three Strain Rates

APPENDIX C - RESULTS OF TESTS USING VARIOUS SAMPLE SIZES

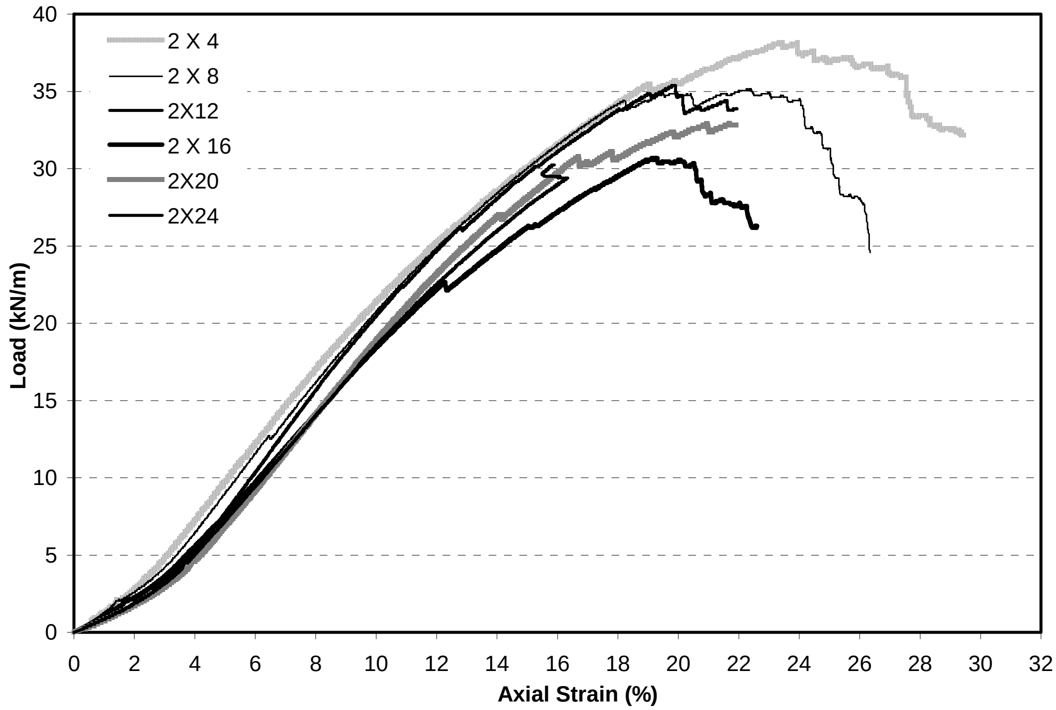

Figure C-1: Load-Strain Curves for Amoco ProPex 2006 Geotextile with Constant Specimen width of 2 Inches and Varying Specimen Length

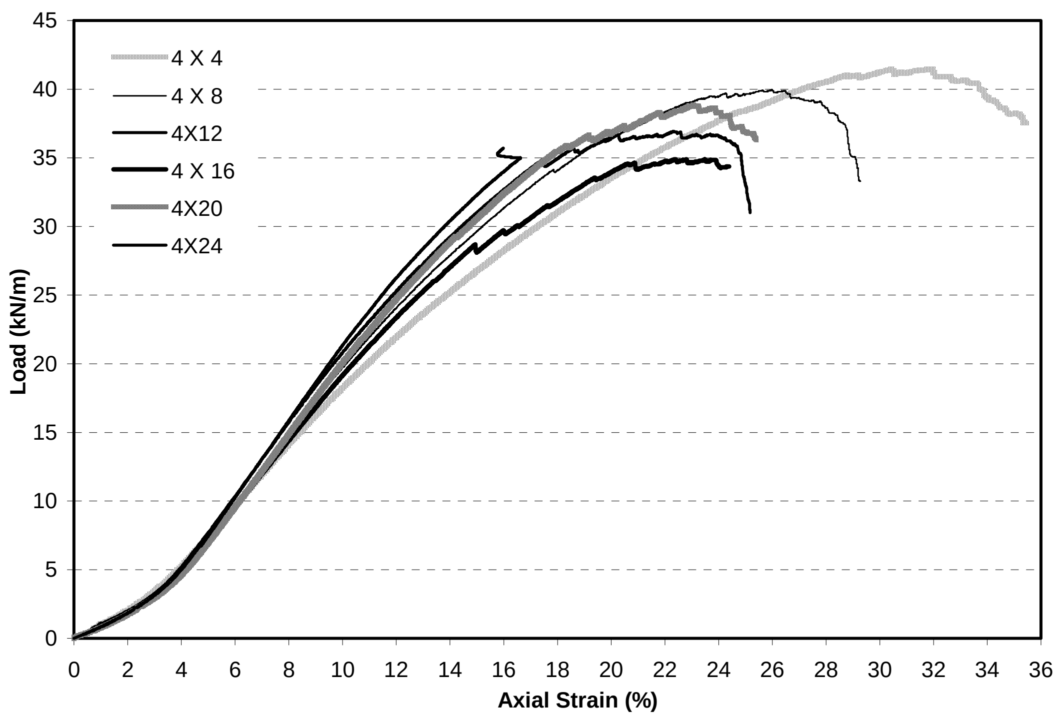

Figure C-2: Load-Strain Curves for Amoco ProPex 2006 Geotextile with Constant Specimen width of 4 Inches and Varying Specimen Length

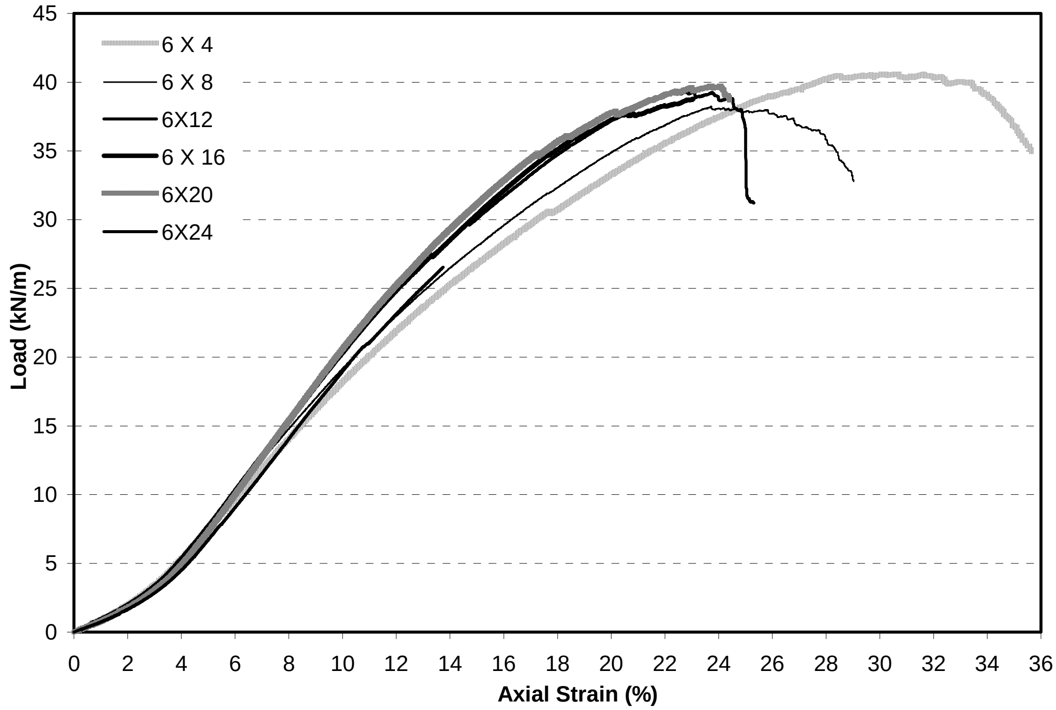

Figure C-3: Load-Strain Curves for Amoco ProPex 2006 Geotextile with Constant Specimen width of 6 Inches and Varying Specimen Length

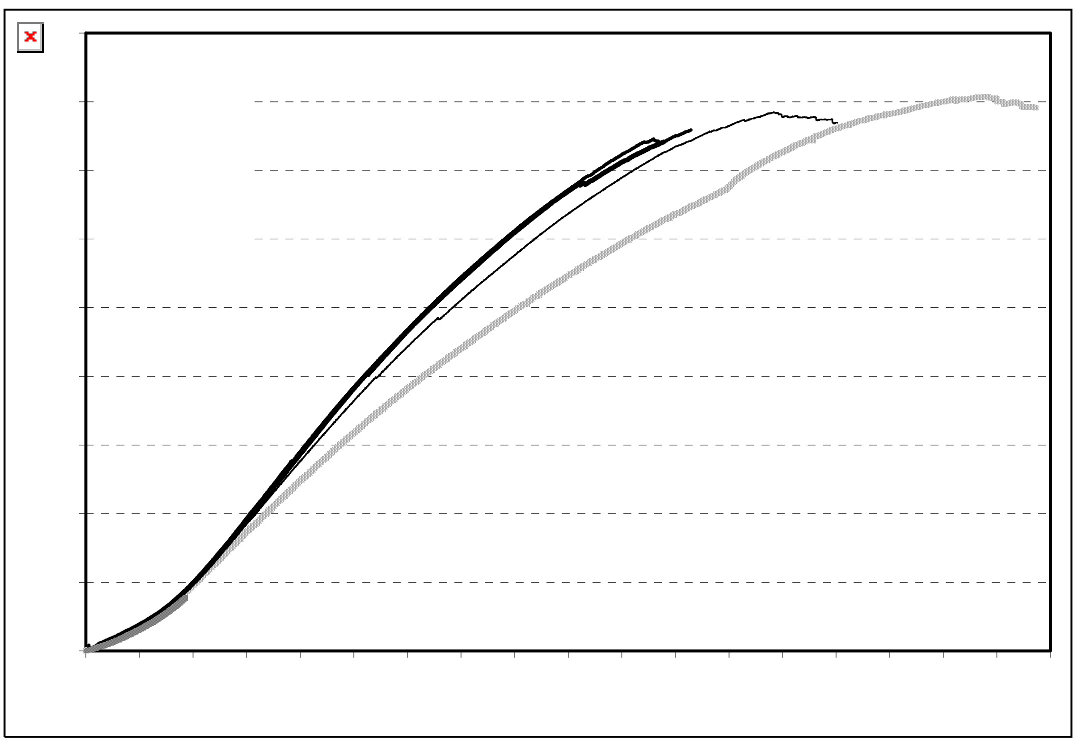

Figure C-4: Load-Strain Curves for Amoco ProPex 2006 Geotextile with Constant Specimen width of 8 Inches and Varying Specimen Length

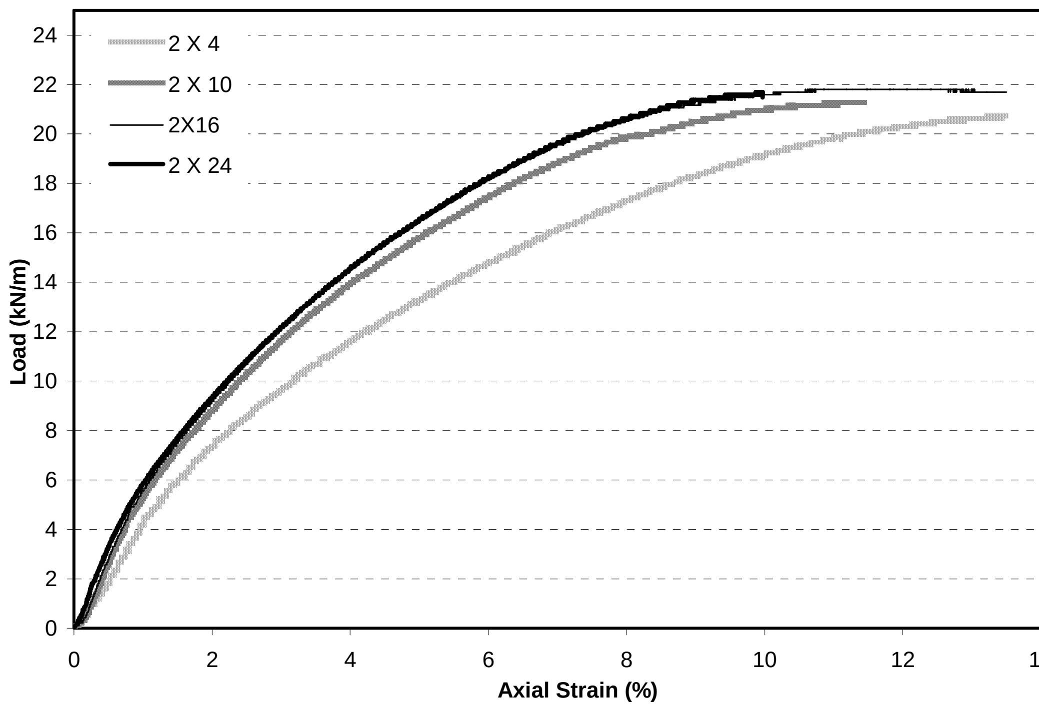

Figure C-5: Load-Strain Curves for Tensar BX1100 Geogrid with Constant Specimen width of 2 Longitudinal Ribs and Varying Number of Transverse Ribs

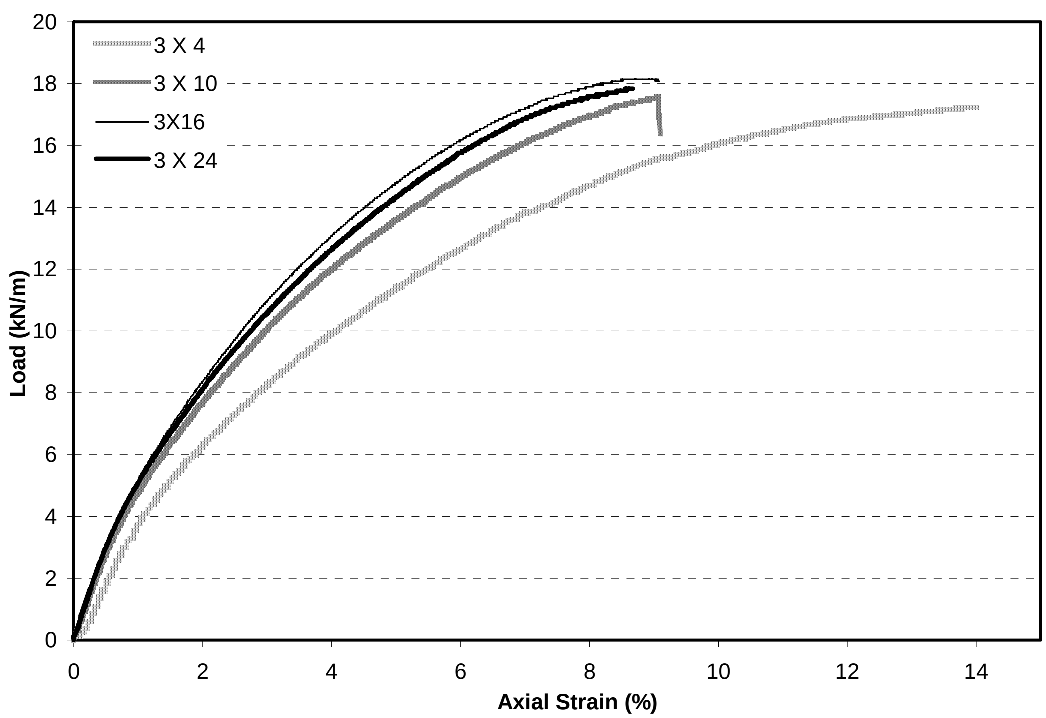

Figure C-6: Load-Strain Curves for Tensar BX1100 Geogrid with Constant Specimen width of 3 Longitudinal Ribs and Varying Number of Transverse Ribs

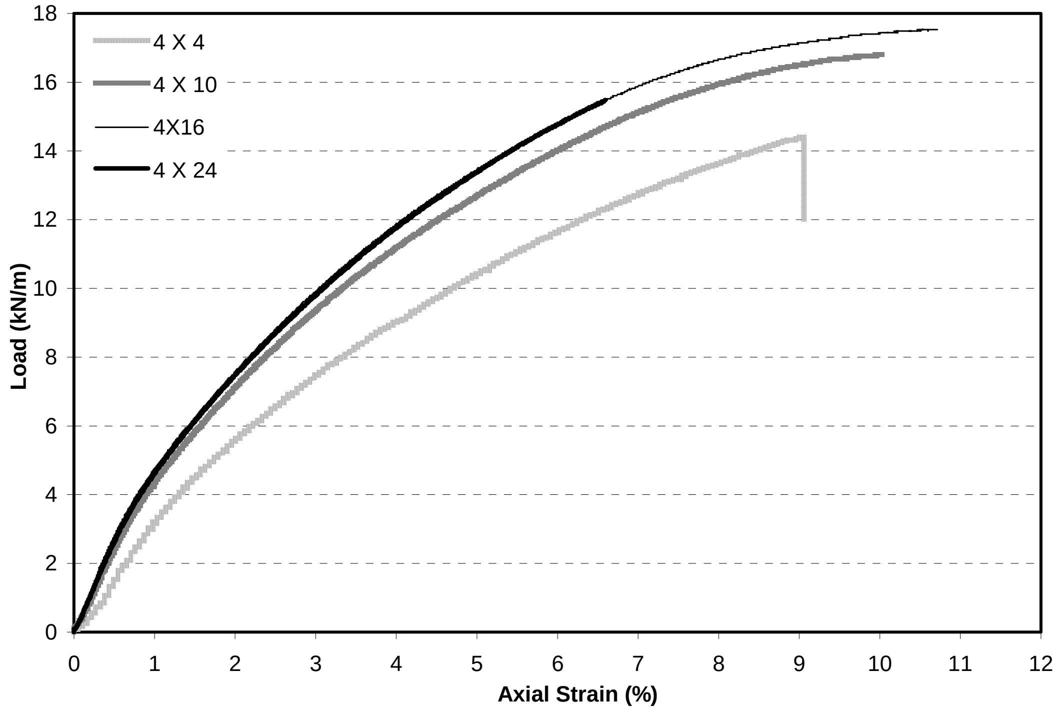

Figure C-7: Load-Strain Curves for Tensar BX1100 Geogrid with Constant Specimen width of 4 Longitudinal Ribs and Varying Number of Transverse Ribs

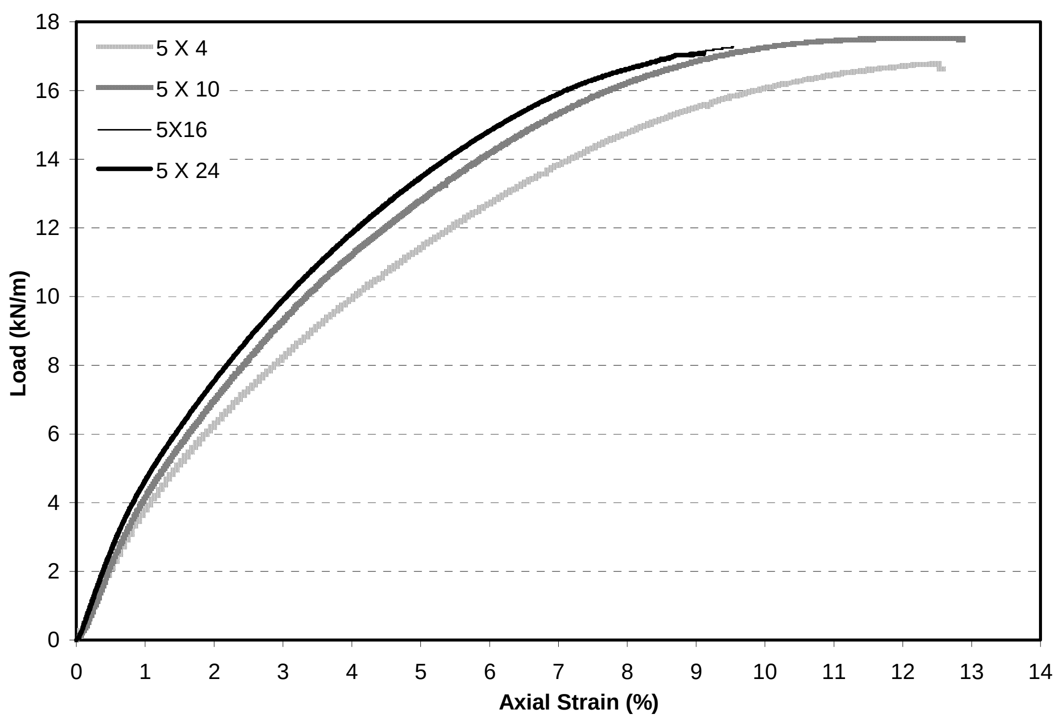

Figure C-8: Load-Strain Curves for Tensar BX1100 Geogrid with Constant Specimen width of 5 Longitudinal Ribs and Varying Number of Transverse Ribs

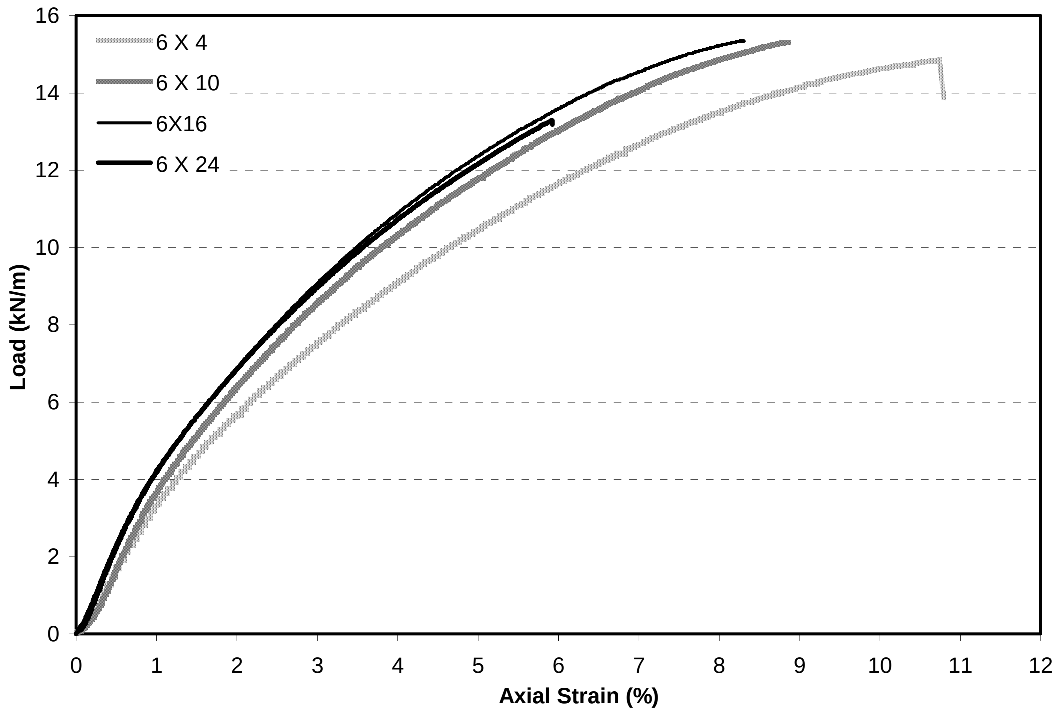

Figure C-9: Load-Strain Curves for Tensar BX1100 Geogrid with Constant Specimen width of 6 Longitudinal Ribs and Varying Number of Transverse Ribs

APPENDIX D – CYCLIC TEST RESULTS

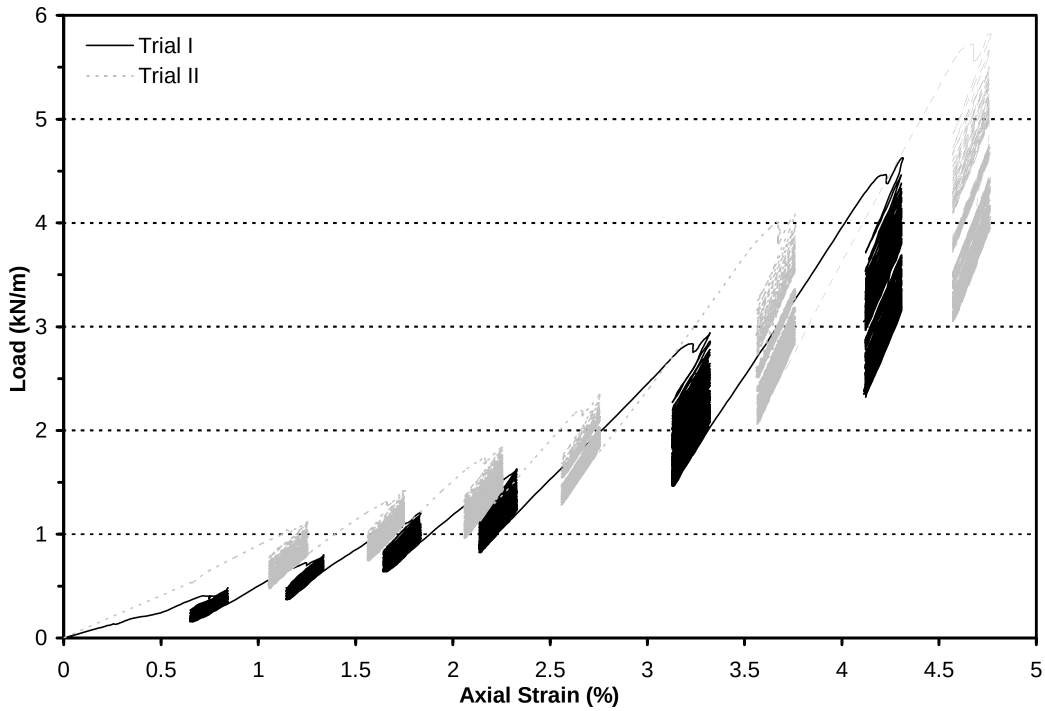

Figure D-1: Cyclic, Load-Strain Curves for the Amoco ProPex 2006 Geotextile in the Machine Direction

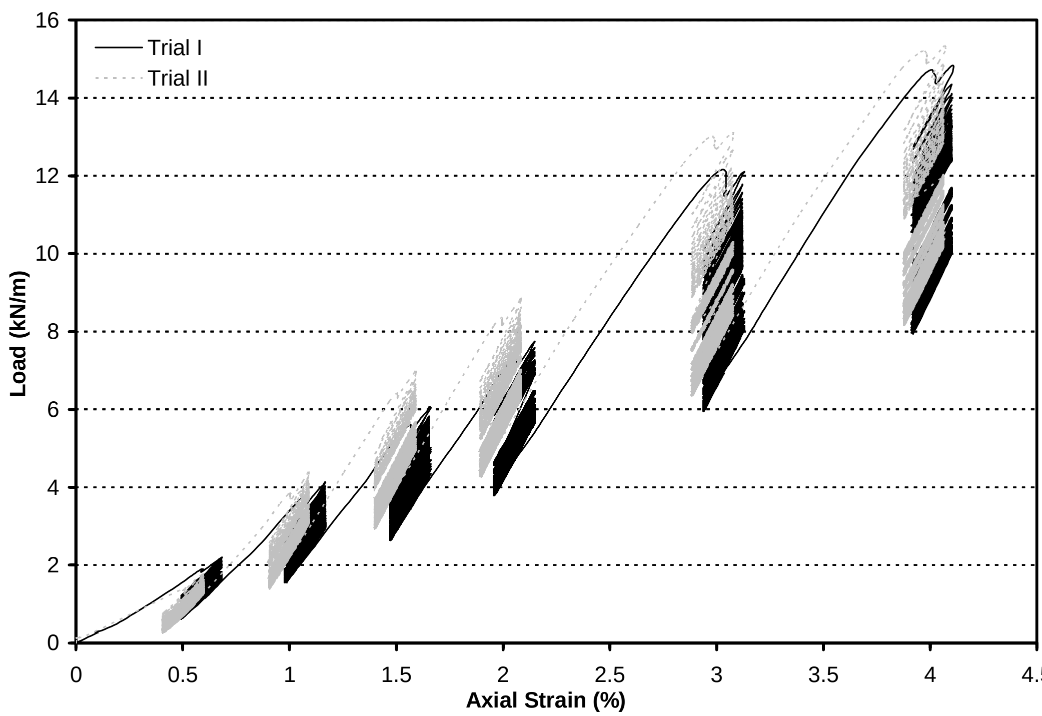

Figure D-2: Cyclic, Load-Strain Curves for the Amoco ProPex 2006 Geotextile in the Cross Machine Direction

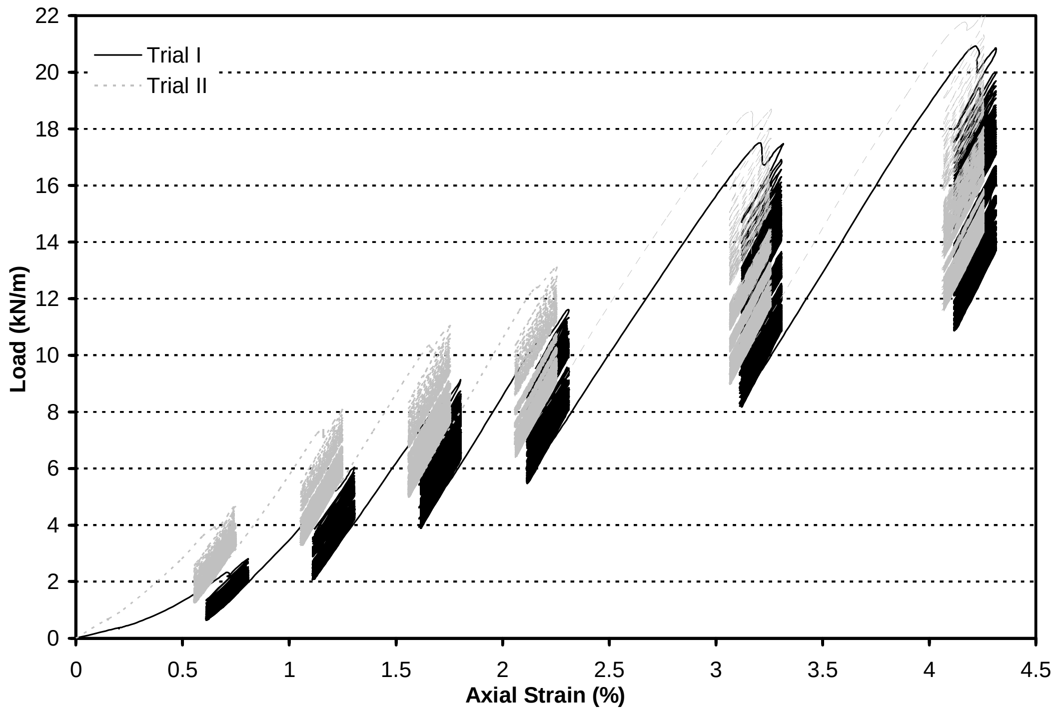

Figure D-3: Cyclic, Load-Strain Curves for the Synthetic Industries Geotex 3×3 Geotextile in the Machine Direction

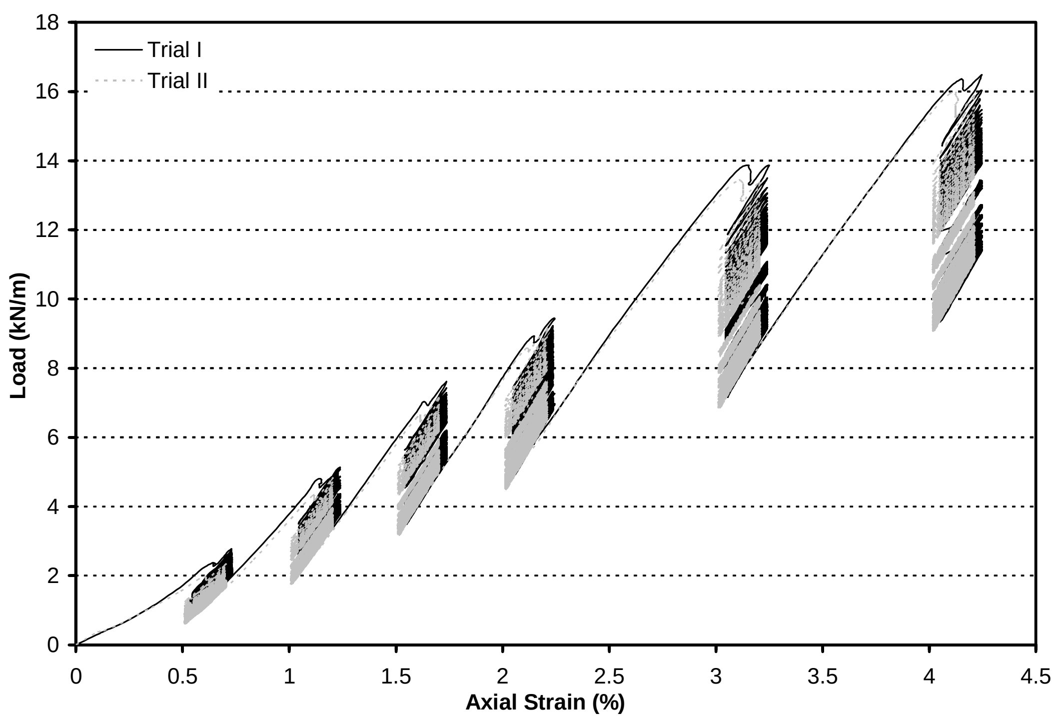

Figure D-4: Cyclic, Load-Strain Curves for the Synthetic Industries Geotex 3×3 Geotextile in the Cross Machine Direction

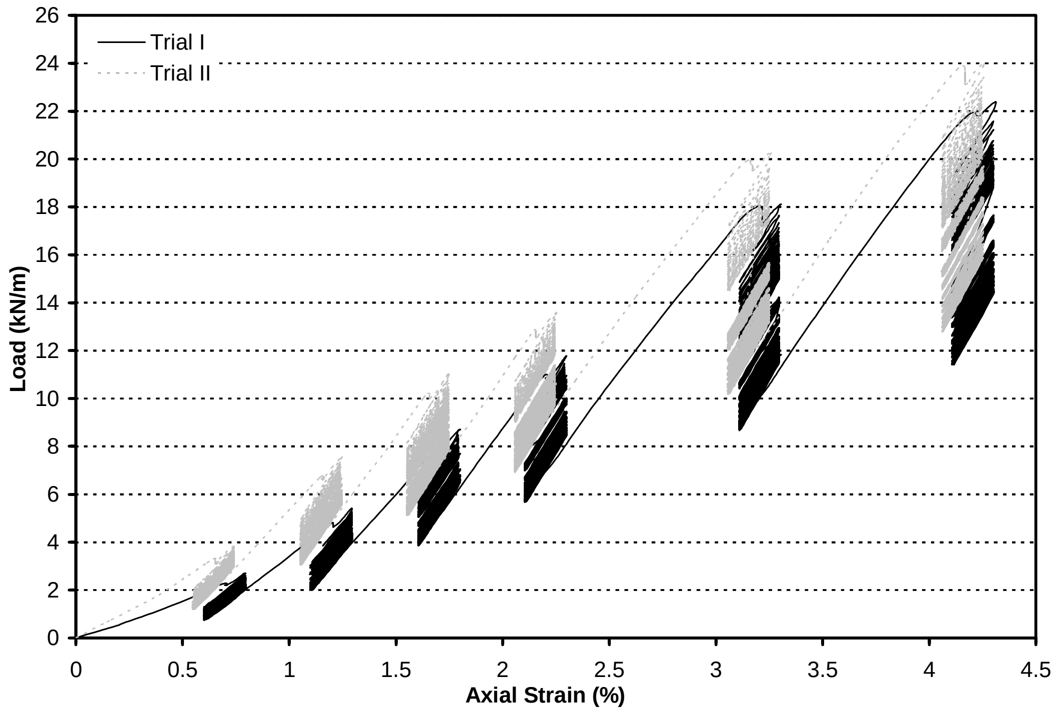

Figure D-5: Cyclic, Load-Strain Curves for the Ten Cate Nicolon Geolon HP570 Geotextile in the Machine Direction

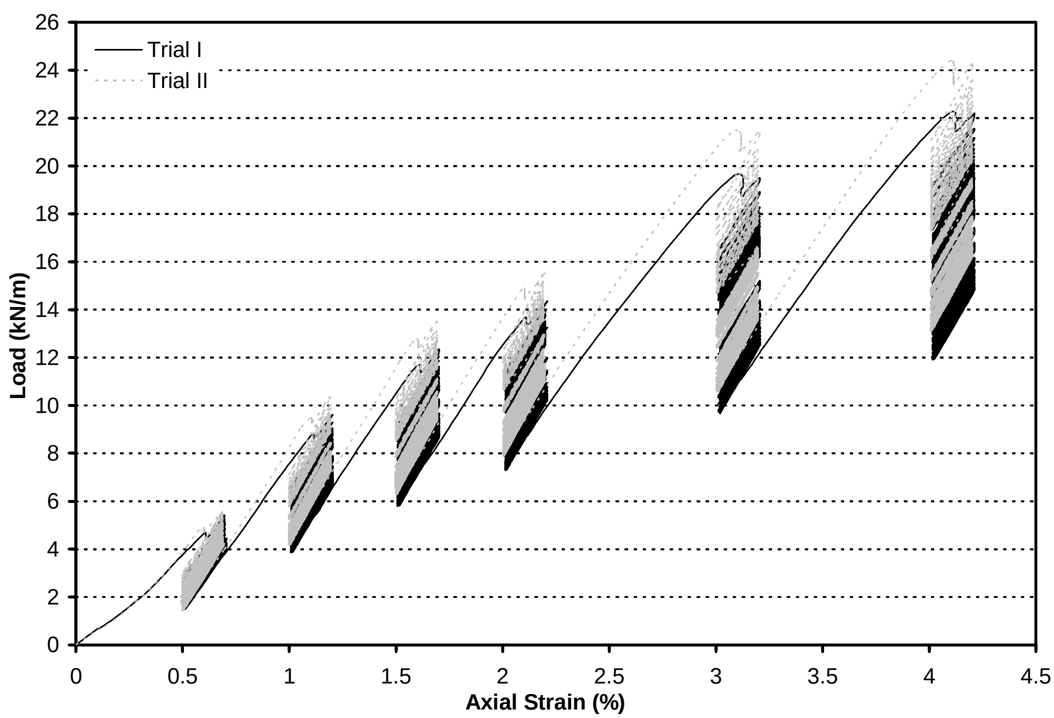

Figure D-6: Cyclic, Load-Strain Curves for the Ten Cate Nicolon Geolon HP570 Geotextile in the Cross Machine Direction

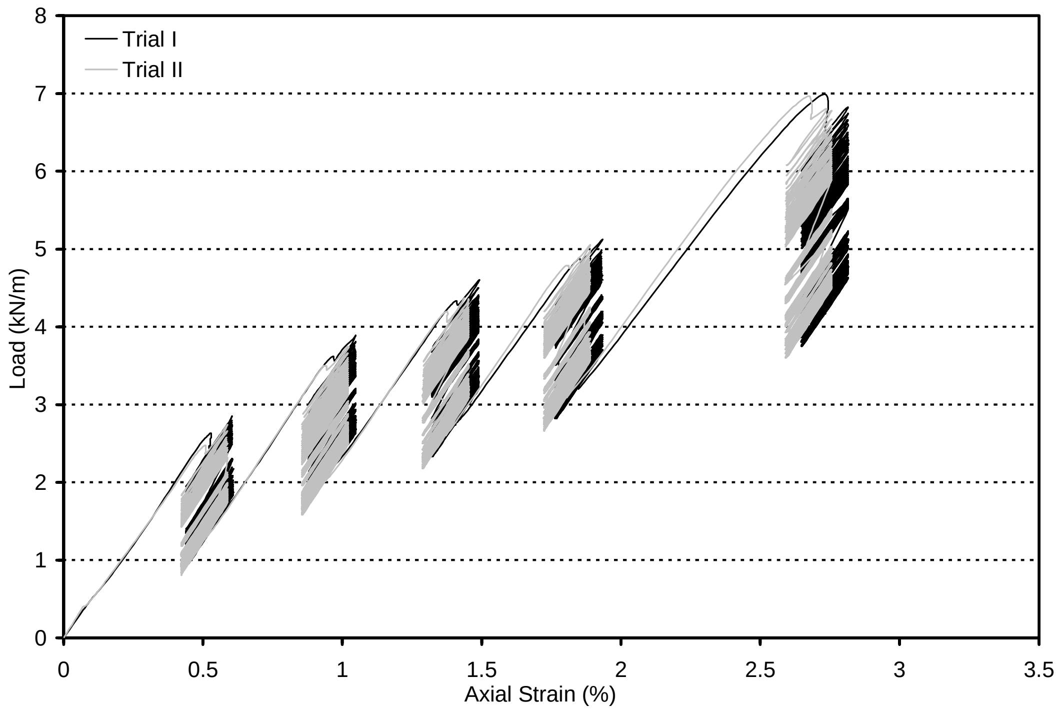

Figure D-7: Cyclic, Load-Strain Curves for the Tensar BX1100 Geogrid in the Machine Direction

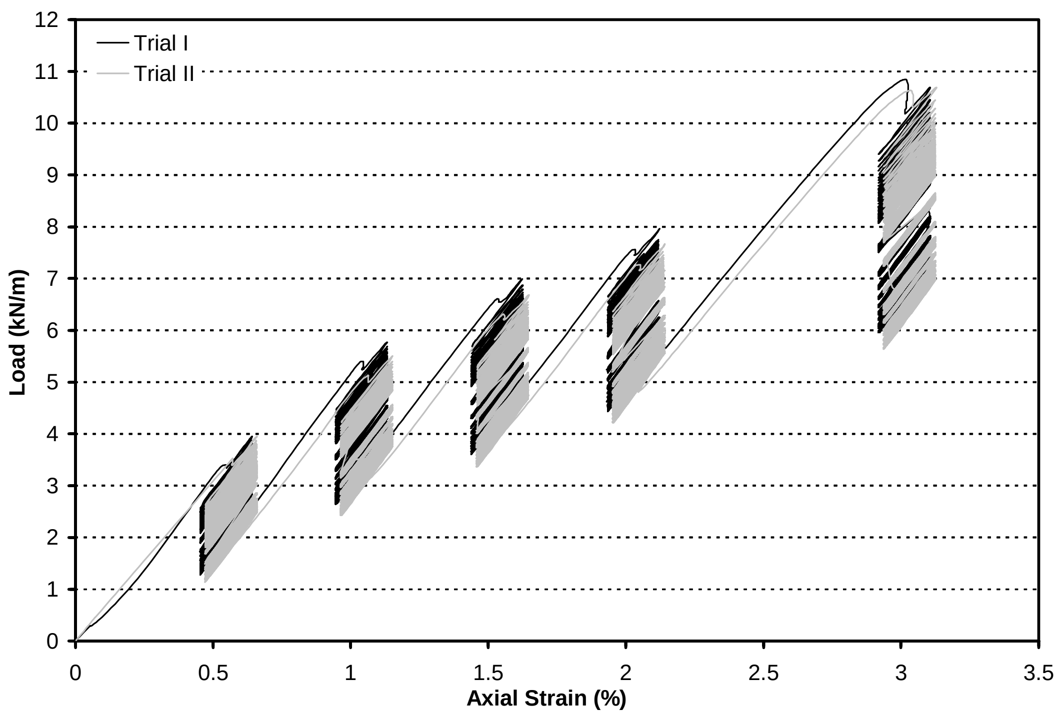

Figure D-8: Cyclic, Load-Strain Curves for the Tensar BX1100 Geogrid in the Cross Machine Direction

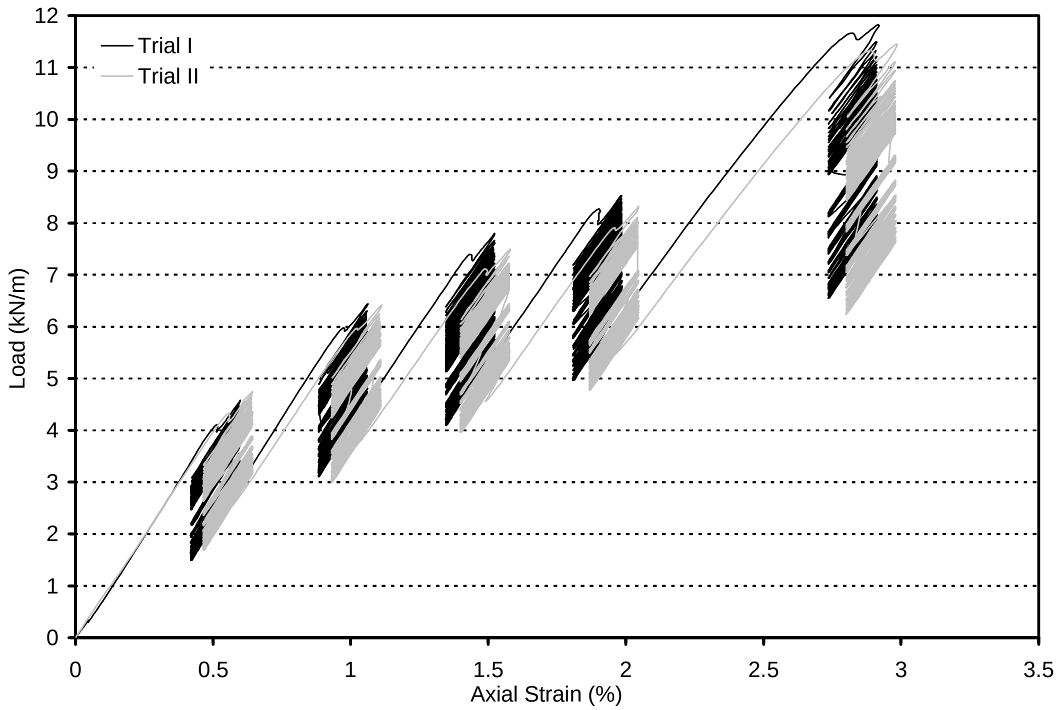

Figure D-9: Cyclic, Load-Strain Curves for the Tensar BX1200 Geogrid in the Machine Direction

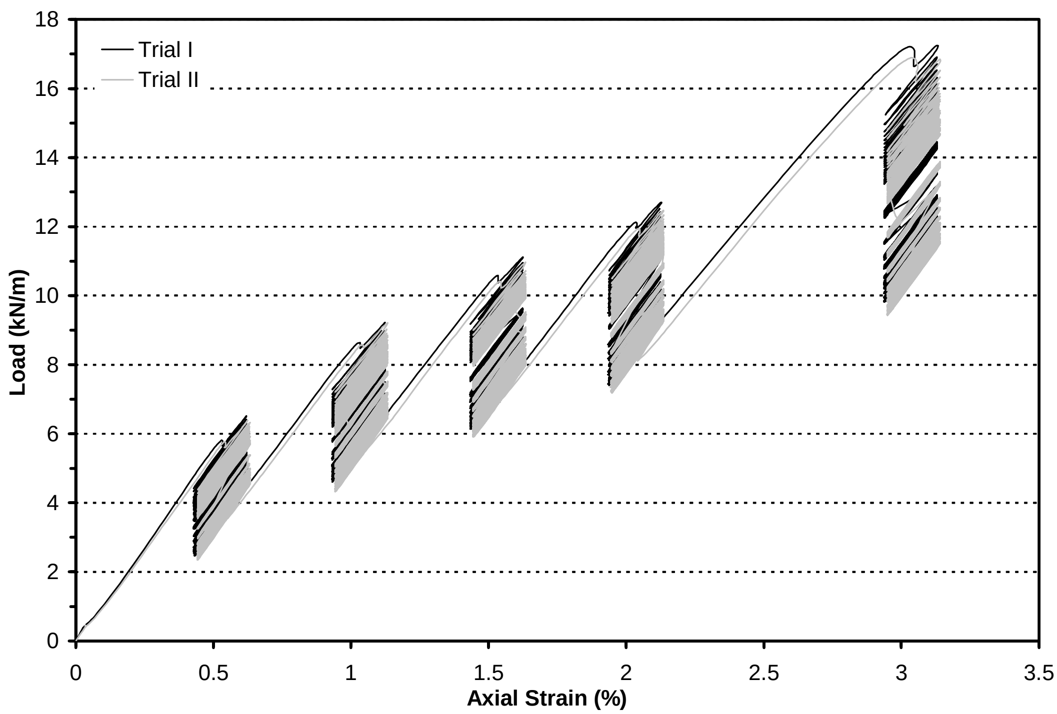

Figure D-10: Cyclic, Load-Strain Curves for the Tensar BX1200 Geogrid in the Cross Machine Direction

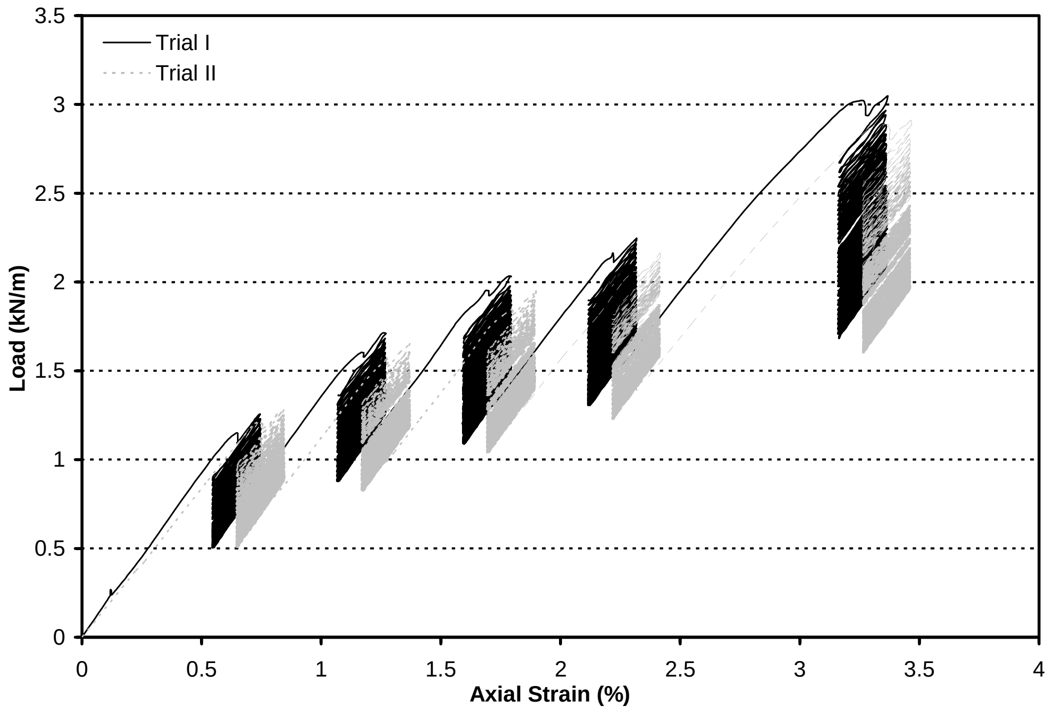

Figure D-11: Cyclic, Load-Strain Curves for the Tenax MS220b Geogrid in the Machine Direction

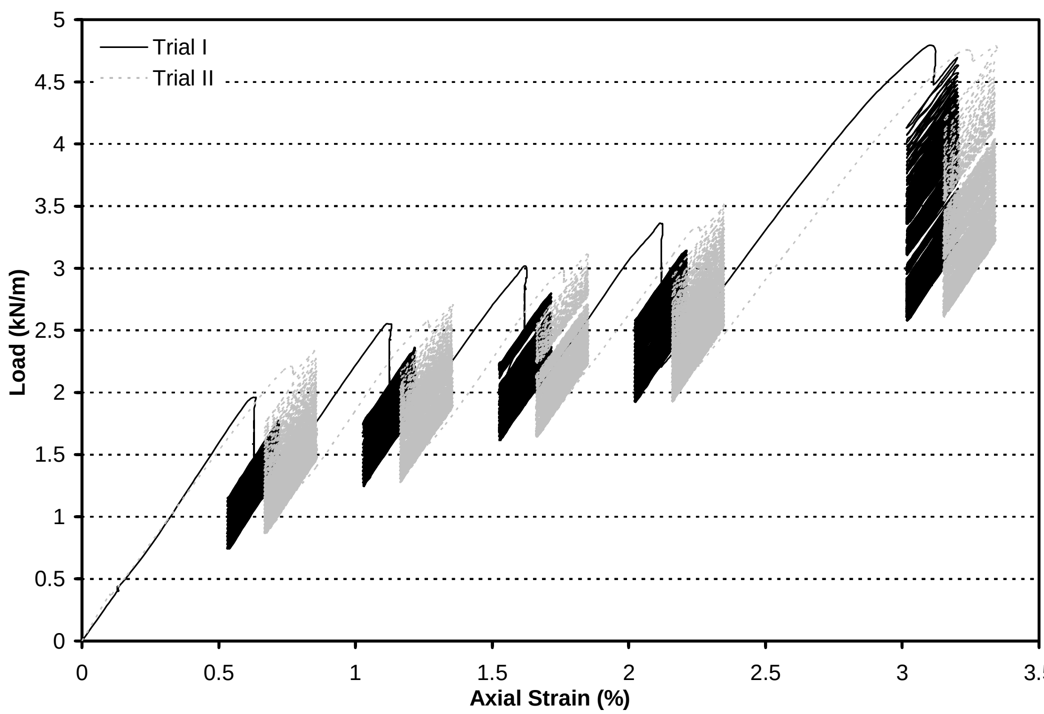

Figure D-12: Cyclic, Load-Strain Curves for the Tenax MS220b Geogrid in the Cross Machine Direction

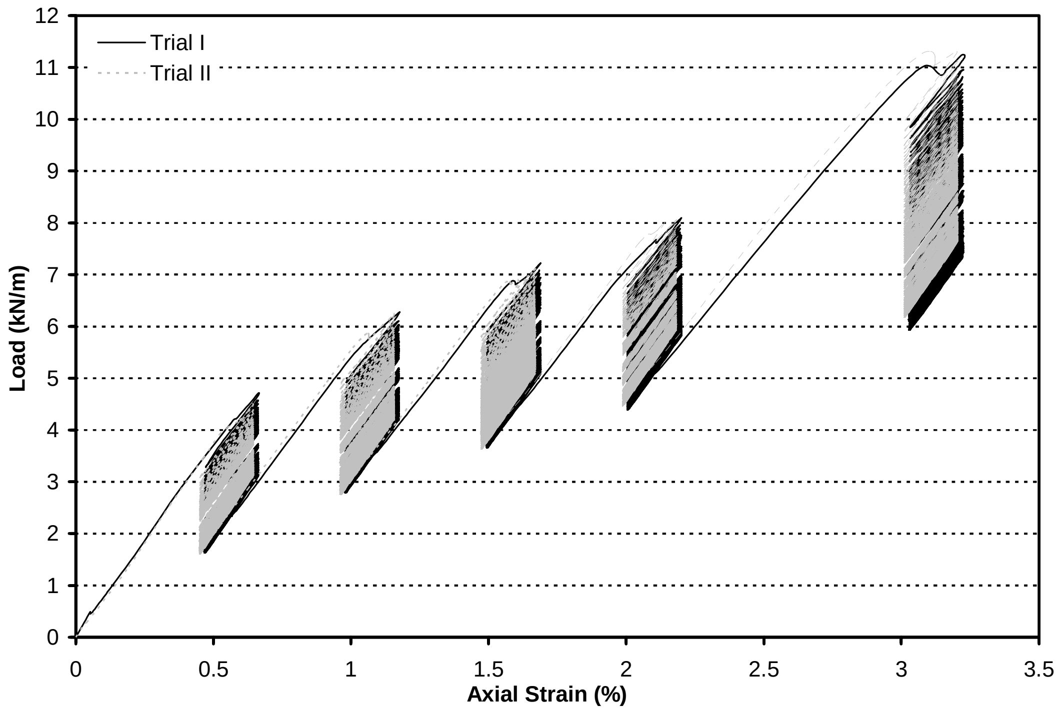

Figure D-13: Cyclic, Load-Strain Curves for the Colbond Enkagrid Max 20 Geogrid in the Machine Direction

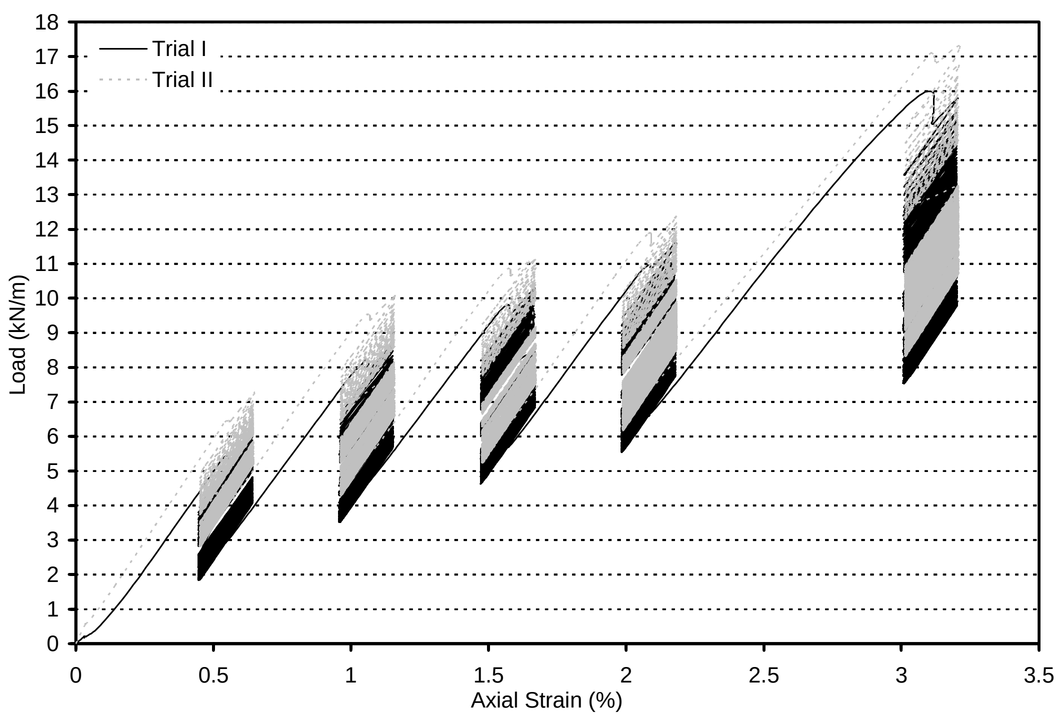

Figure D-14: Cyclic, Load-Strain Curves for the Colbond Enkagrid Max 20 Geogrid in the Cross Machine Direction

APPENDIX E – COMBINED MONOTONIC AND CYCLIC RESULTS

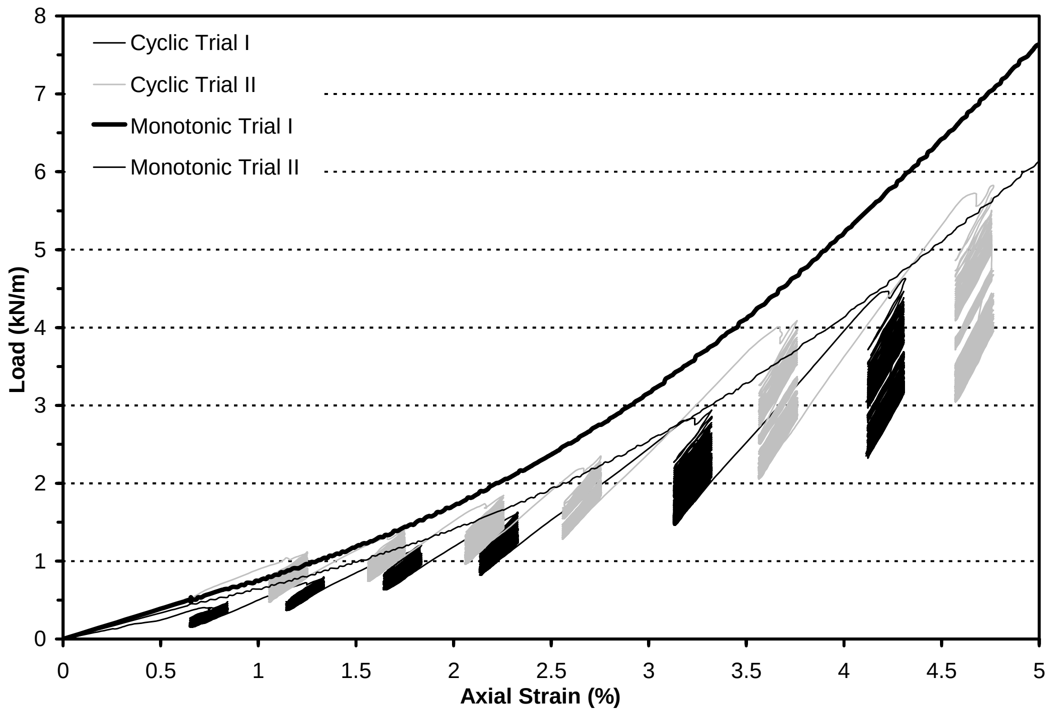

Figure E-1: Load-Strain Curves for Amoco ProPex 2006 Geotextile from Monotonic and Cyclic Tests in the Machine Direction

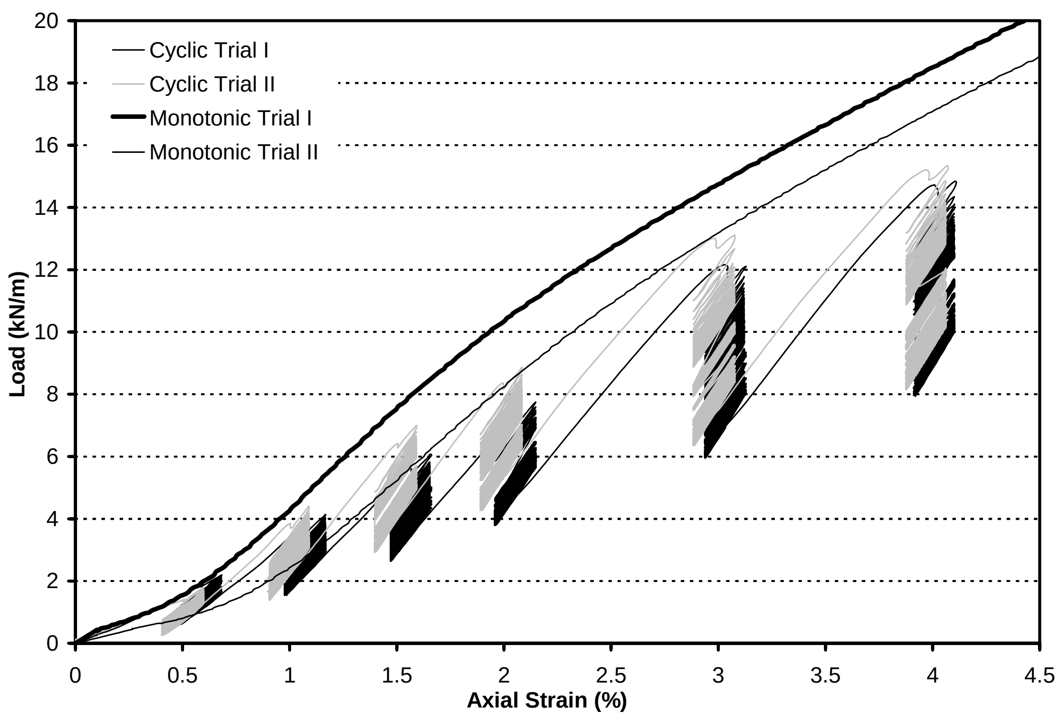

Figure E-2: Load-Strain Curves for Amoco ProPex 2006 Geotextile from Monotonic and Cyclic Tests in the Cross-Machine Direction

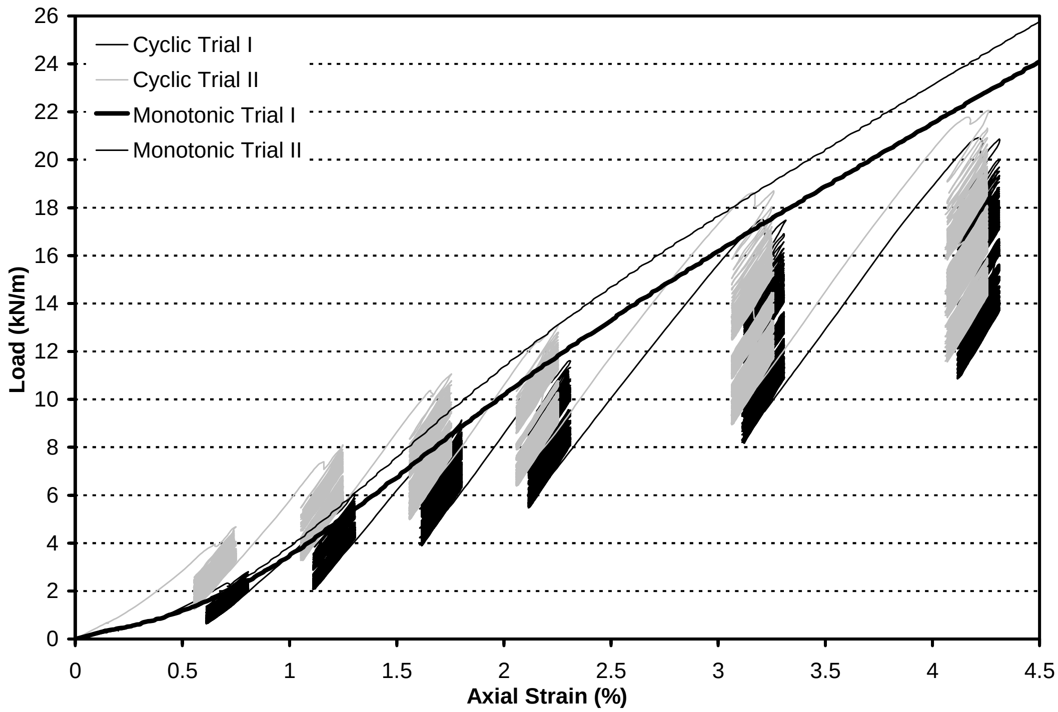

Figure E-3: Load-Strain Curves for Synthetic Industries Geotex 3x3 Geotextile from Monotonic and Cyclic Tests in the Machine Direction

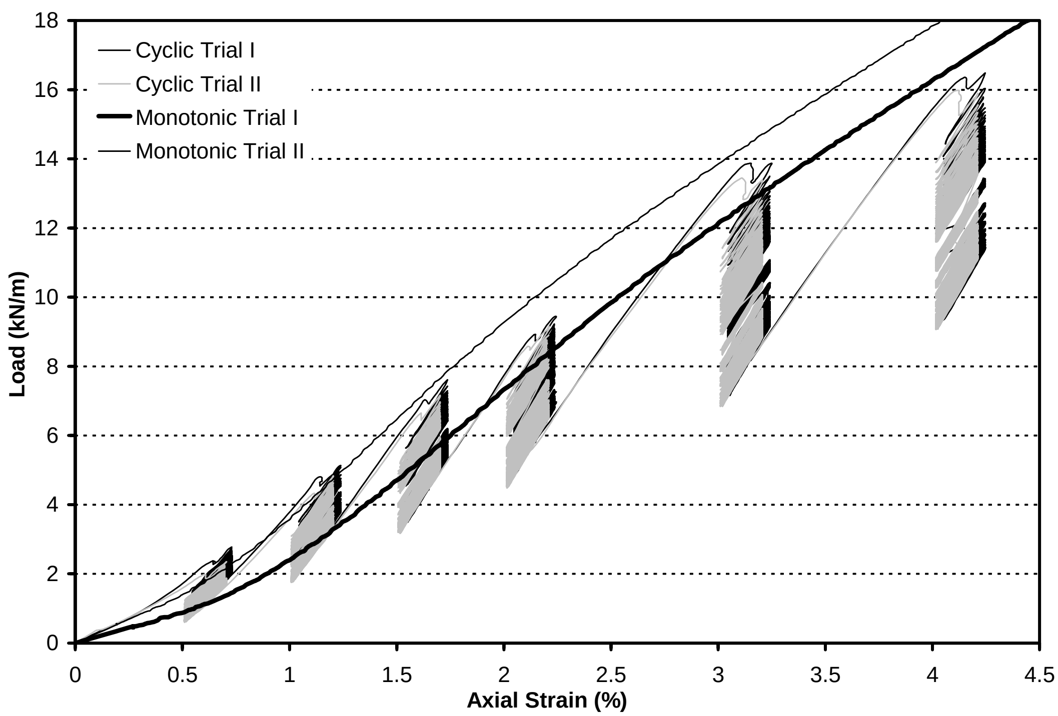

Figure E-4: Comparison of Load-Strain Curves for Synthetic Industries Geotex 3x3 Geotextile from Monotonic and Cyclic Tests in the Cross-Machine Direction

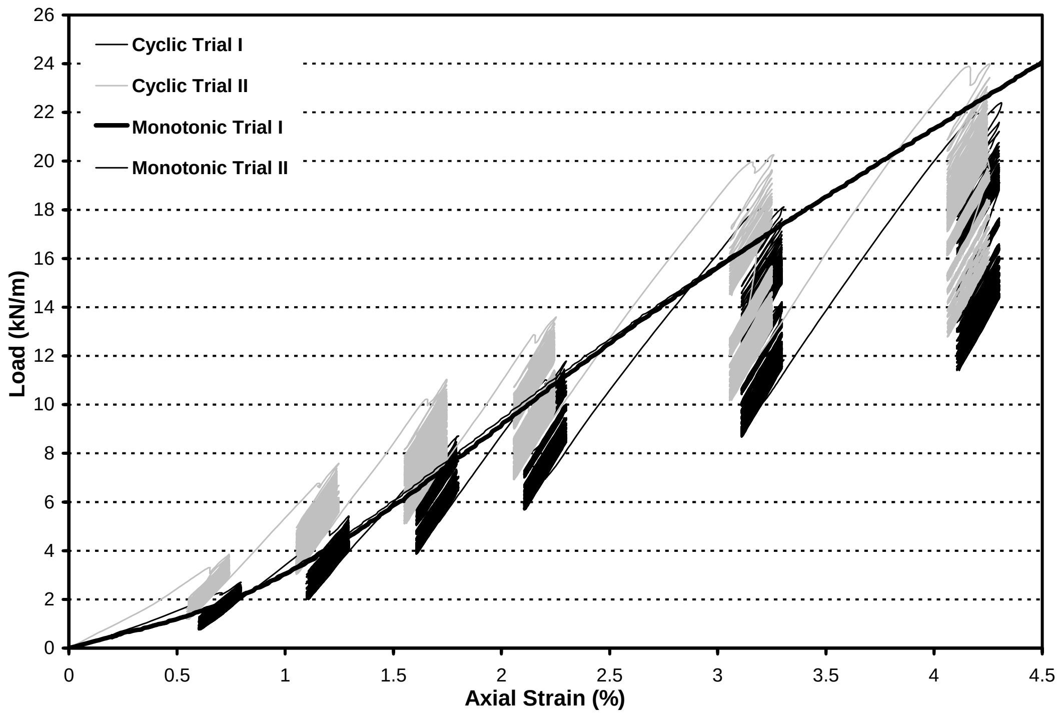

Figure E-5: Load-Strain Curves for Ten Cate Nicolon HP570 Geotextile from Monotonic and Cyclic Tests in the Machine Direction

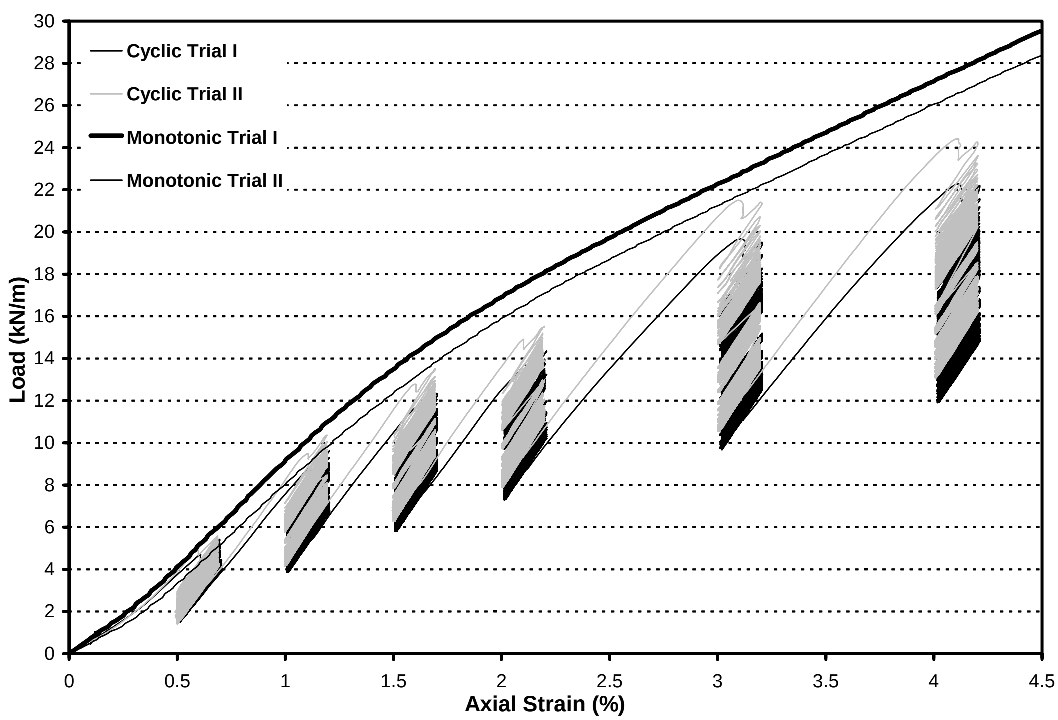

Figure E-6: Load-Strain Curves for Ten Cate Nicolon HP570 Geotextile from Monotonic and Cyclic Tests in the Cross-Machine Direction

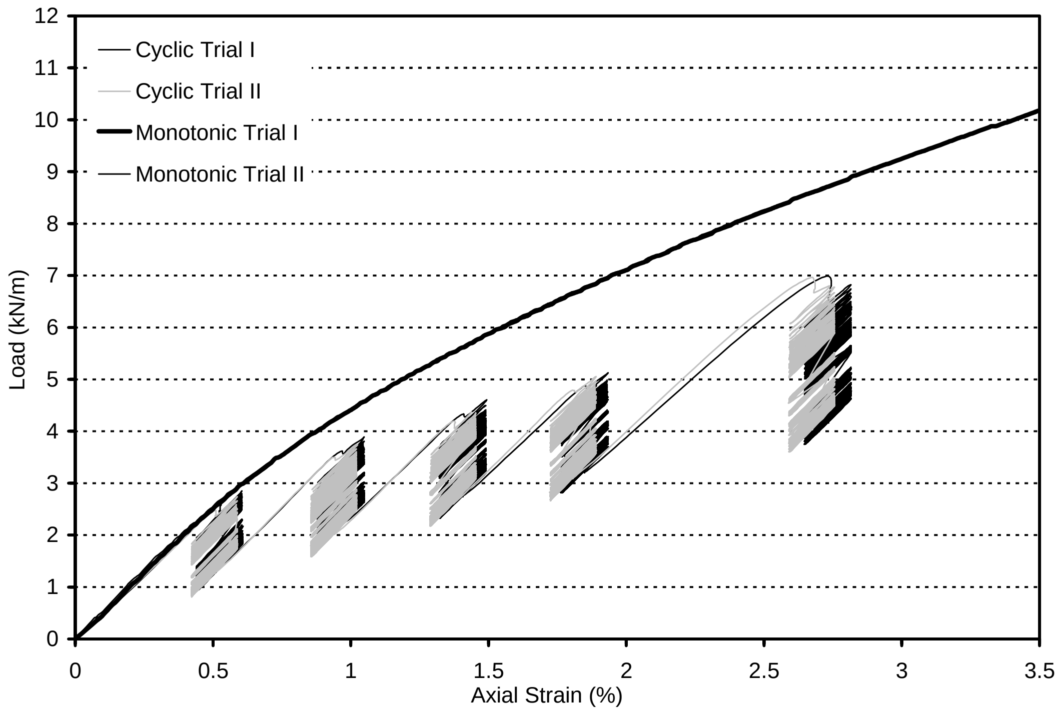

Figure E-7: Load-Strain Curves for Tensar BX 1100 Geogrid from Monotonic and Cyclic Tests in the Machine Direction

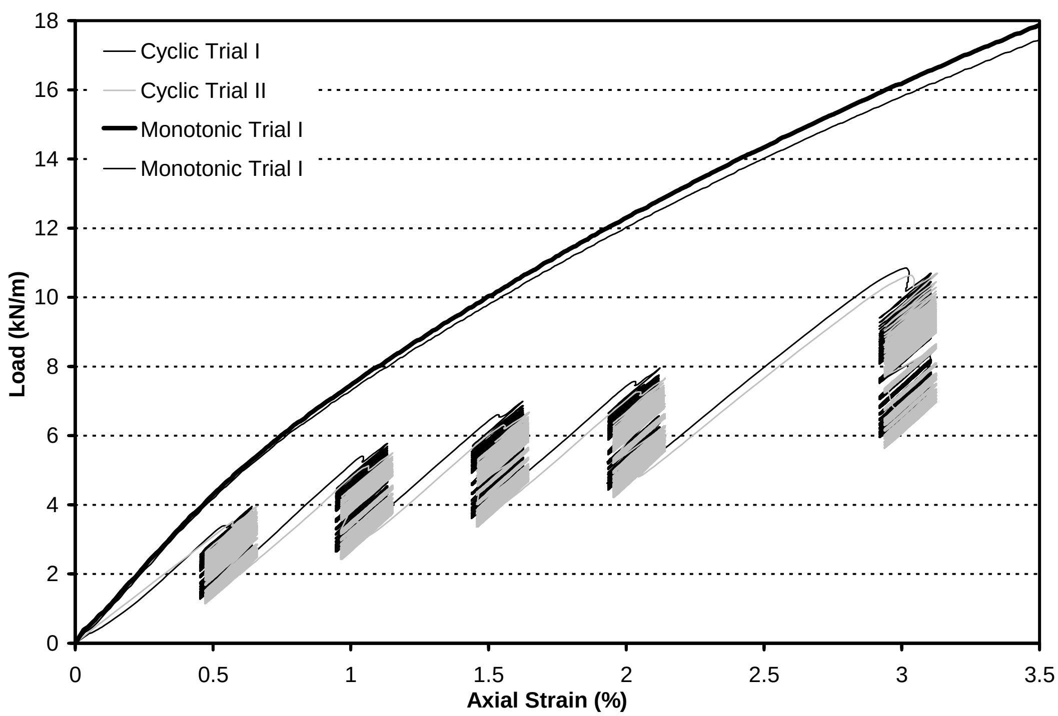

Figure E-8: Load-Strain Curves for Tensar BX 1100 Geogrid from Monotonic and Cyclic Tests in the Cross-Machine Direction

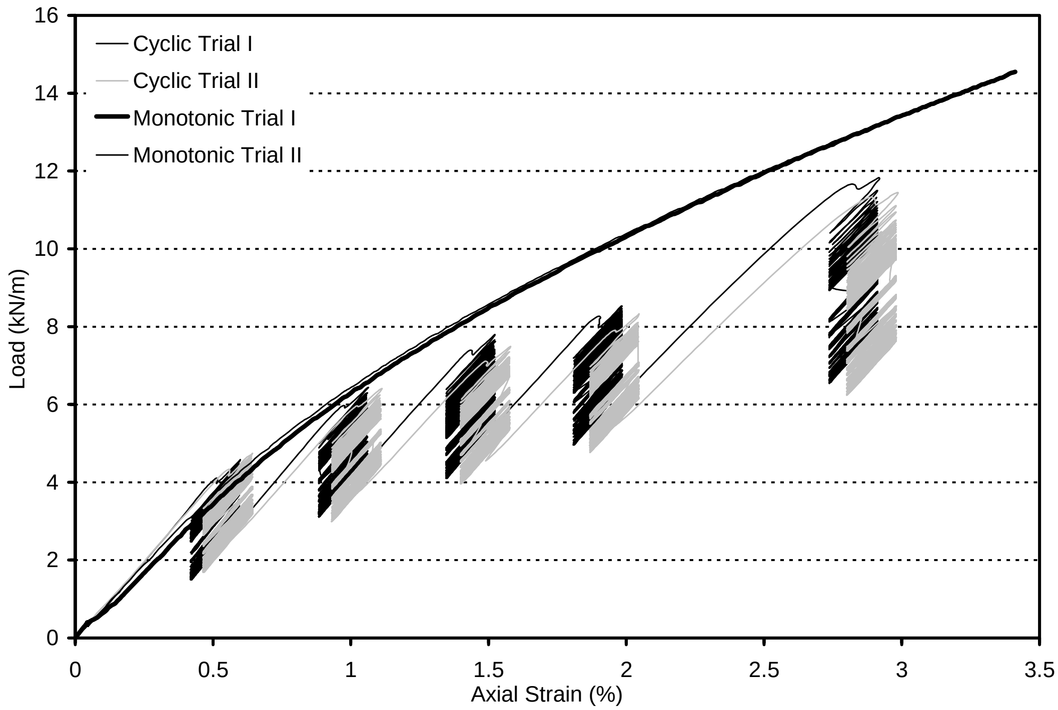

Figure E-9: Load-Strain Curves for Tensar BX 1200 Geogrid from Monotonic and Cyclic Tests in the Machine Direction

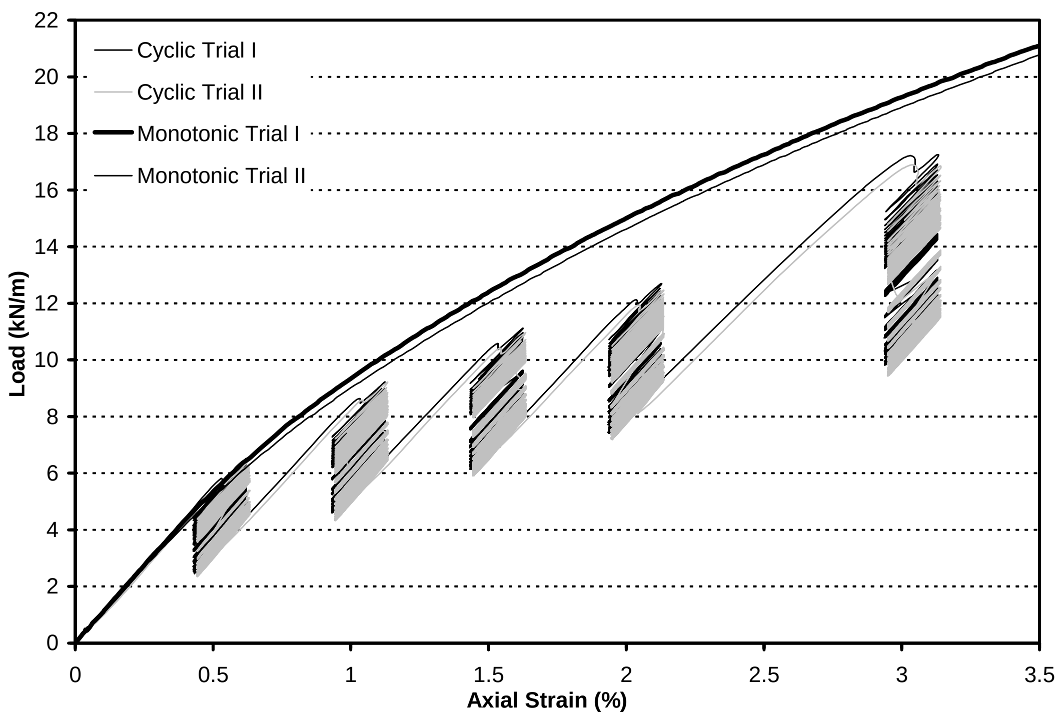

Figure E-10: Load-Strain Curves for Tensar BX 1200 Geogrid from Monotonic and Cyclic Tests in the Cross-Machine Direction

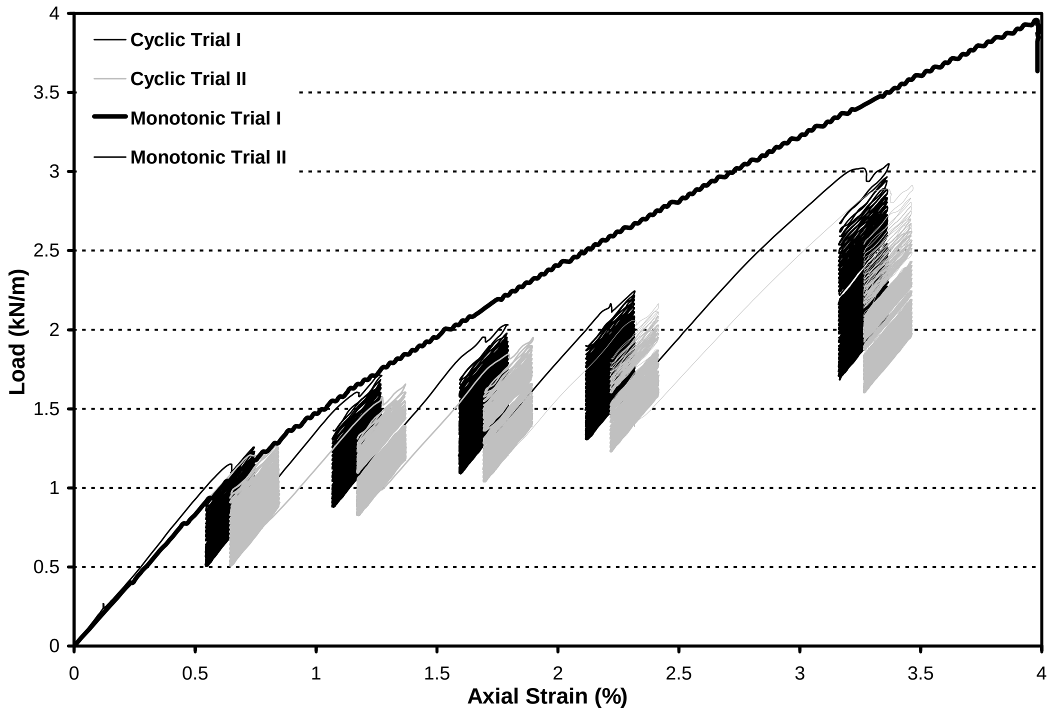

Figure E-11: Load-Strain Curves for Tenax MS220b Geogrid from Monotonic and Cyclic Tests in the Machine Direction

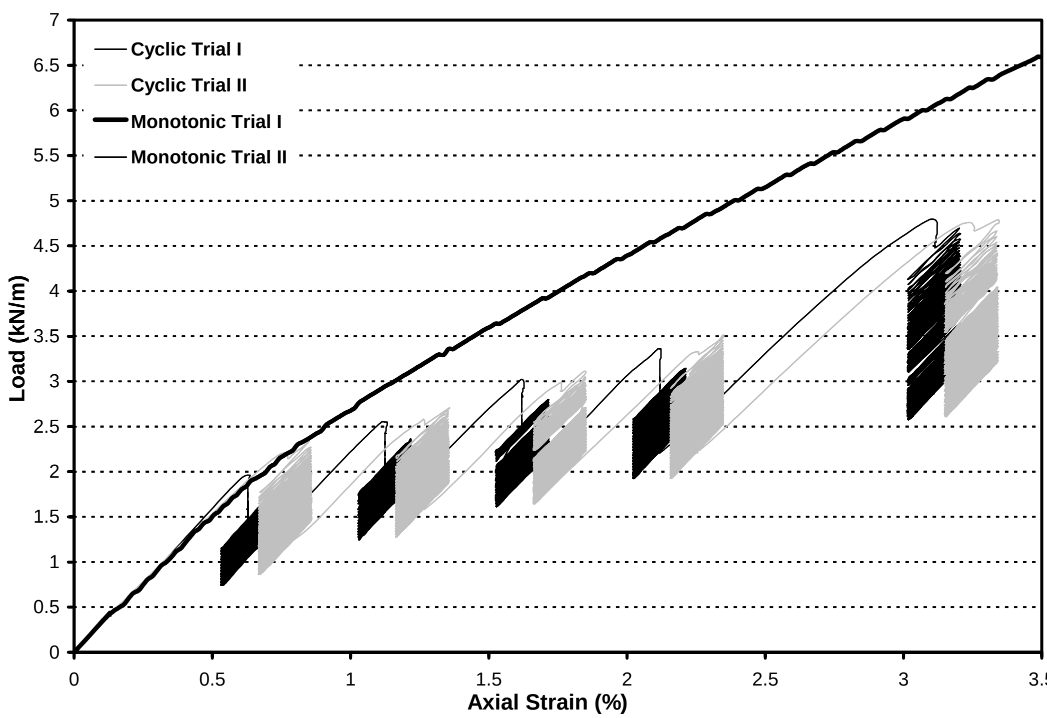

Figure E-12: Load-Strain Curves for Tenax MS220b Geogrid from Monotonic and Cyclic Tests in the Cross-Machine Direction

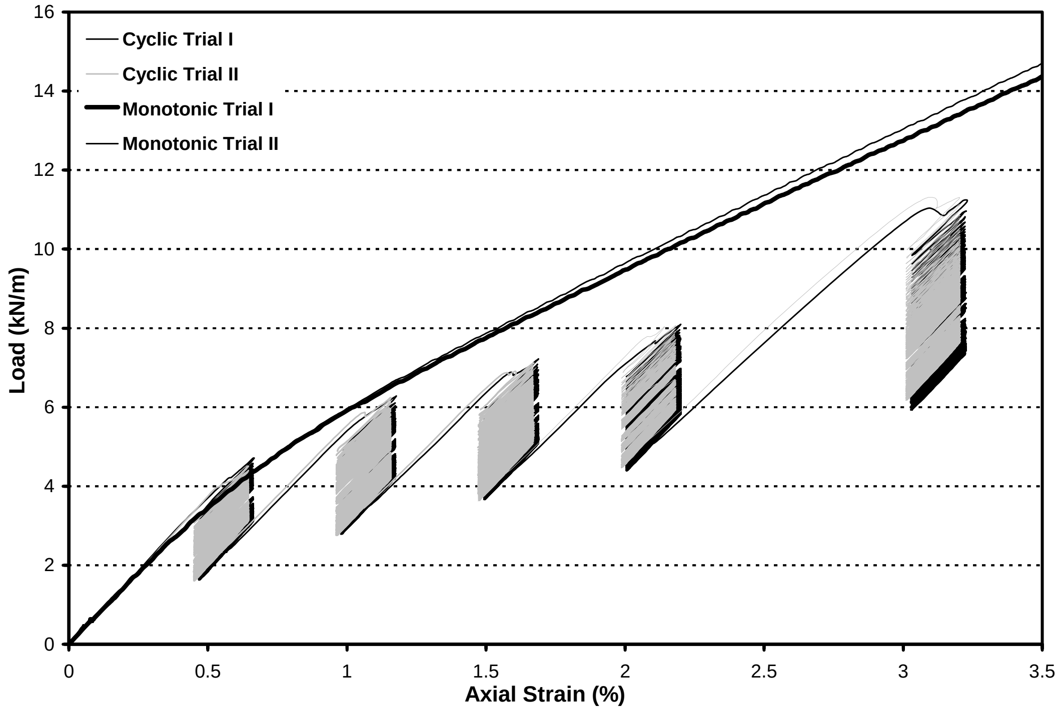

Figure E-13: Load-Strain Curves for Colbond Enkagrid Max 20 Geogrid from Monotonic and Cyclic Tests in the Machine Direction

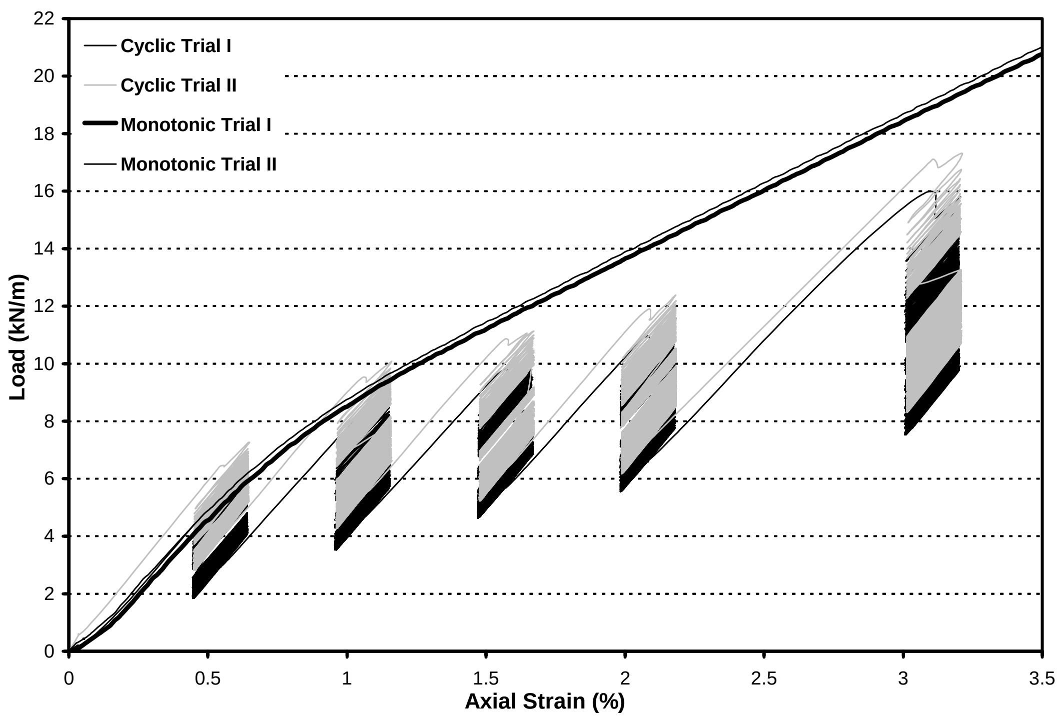

Figure E-14: Load-Strain Curves for Colbond Enkagrid Max 20 Geogrid from Monotonic and Cyclic Tests in the Cross-Machine Direction